Aston University

If you have discovered material in AURA which is unlawful e.g. breaches copyright, (either yours or that of a third party) or any other law, including but not limited to those relating to patent, trademark, confidentiality, data protection, obscenity, defamation, libel, then please read our Takedown Policy and contact the service immediately

POWDER PAINTING OF ALUMINIUM

by

P R SLIWINSKI MSc

Submitted for the Degree of
Doctor of Philosophy

The University of Aston in Birmingham

May 1985

THE UNIVERSITY OF ASTON IN BIRMINGHAM

POWDER PAINTING OF ALUMINIUM

PETER RICHARD SLIWINSKI

DOCTOR OF PHILOSOPHY

MAY 1985

Synopsis

The mechanisms involved in the production of chromate-phosphate conversion coatings on aluminium have been investigated. A sequence of coating nucleation and growth has been outlined and the principle roles of the constituent ingredients of the chromate-phosphate solution have been shown.

The effect of dissolved aluminium has been studied and its role in producing sound conversion coatings has been shown. Metallic contamination has been found to have a dramatic influence on chromate-phosphate coatings when particular levels have been exceeded. Coating formation was seen to be affected in proportion to the level of contaminaton; no evidence of sudden failure was noted.

The influence of substrate and the effect of an acidic cleaner prior to conversion coating have been studied and explained. It was found that the cleaner ages rapidly and that this must be allowed for when attempting to reproduce industrial conditions in the laboratory.

A study was carried out on the flowing characteristics of polyester powders of various size distributions as they melt using the hot-stage microscopy techniques developed at Aston. It was found that the condition of the substrate (ie extent of pretreatment), had a significant effect on particle flow. This was explained by considering the topography of the substrate surface.

A number of 'low-bake' polyester powders were developed and tested for mechanical, physical and chemical resistance. The best formulation had overall properties which were as good as the standard polyester in many respects. However chemical resistance was found to be slightly lower.

The charging characteristics of powder paints during application by means of electrostatic spraying was studied by measuring the charge per unit mass and relating this to the surface area. A high degree of correlation was found between charge carried and surface area, and the charge retained was related to the powder's formulation.

Keywords: Conversion Coating; Chromate-Phosphate; Aluminium; Powder Coating; Polyester

CONTENTS

LIST OF FIGURES

LIST OF TABLES

LIST OF PHOTOS

Page

Photo Numbers

1. POWDER COATING

1.1 Introduction

Powder coating can be defined as the technique of applying plastic materials to products where the coating materials are in powder form and contain no solvents. Since its conception in the USA in 1955(1) powder coating technology has progressively developed. The original thermoplastic formulations have been superseded by epoxy thermoset resins which have themselves been replaced by improved, specialised systems. Todays powders are designed to meet particular market demands based on cost, end-use, application technique and product specifications. Resin manufacturers are now responding to the needs of the powder coating industry. The race is on to find a low-cure energy resin capable of being processed and stored without reducing the high standards set by todays powder coating technology.

Initially only thermoplastic powders were produced for fluidised bed application, but by 1965 it was realised that improved performance could be obtained using thermosetting coatings(2) and a number of epoxy based powders were produced. However, the early powder coatings had major chalking and weathering problems and so despite their excellent mechancial properties they could not be used for outdoor products.

After much laboratory work new resins were developed; these included epoxy-polyester hybrid, urethane and polyester, glycidal or epoxy functional polyester and urethane-cured acrylics, all had some advantage over straight epoxy powders but unfortunately were more

expensive. The raw material cost has always been a contributing factor to the slow growth of powder coatings, but it is thought that as production increases, relative costs will become less, thus making powder coating more competitive. The use of powder coating increased from about 3% of the relevant surface coating markets in 1970 to approximately 4% in 1980 in the USA(3), this compares with 2.3% for 1980 in the EEC(4,5).

The main problems yet to be solved are;

(i) the production of thin film coatings free from holidays at which corrosion can start; and

(ii) colour change from one colour to another in production without contamination.

One development from powder-coating has been high-solids or powder-dispersive paints. As the name suggests these are paints of 80 to 90% solids made up by dispersing powder coating paints in water. It has been claimed(6) that fast colour change and thin film coatings are possible using this process. Expensive new application equipment is also unnecessary, liquid paint spraying guns may be used after some modification. However, high-solids paints have a high viscosity, this makes transportation through equipment more difficult, additional problems are often encountered; sagging or popping coatings, variation of colour, uniformity and film thickness are examples(3). In terms of growth high-solids paints are likely to be the main competitors against powder coatings in the same market areas. Both have plenty to offer in terms of performance,

economy and effluent control, but there are many problems to be solved before being accepted by industry at large.

The main advantage of powder coatings over wet paints is that no solvent is used. This reduces the bulk of storing paints by 50% (the approximate proportion of solvent in wet paint). Air pollution, fire hazards and health hazards are reduced during spraying because evaporation of solvent is eliminated.

There are no runs, sags or blisters in the final coating and due to the fact that powder and air mixtures behave as a liquid(7) powder coating is ideally suited to automation. Materials utilization can be as high as 99% if powder recovery and recyclng plant has been installed in the spraying booths(8). This compares with 50-80% utilization for wet paint systems in which recovery is not possible. Labour costs can be reduced as powder coating spraying requires less skill than wet paint spraying.

Colour change is often difficult especially on large automated plant. Powder paints cannot be tinted like liquid paints so colour must be carefully controlled during manufacture (extrusion). This means that should any particles of one colour find their way into another powder they will be seen as speckles in the finished coating. Thus if the colour being coated on a coating line is to be changed the line must be thoroughly cleaned to avoid contamination of the next coating. This is a very time consuming, costly and often difficult task. Colours are therefore usually kept separate from white application lines.

Some problems (such as pinholes) have been found to be due to contamination of one resin type with another (eg polyester and acrylic) so again care must always be taken to ensure that contamination does not occur.

Clearly the biggest incentive for any coater to change from wet paint to powder must be economic advantage. This has been one of the reasons for the slow growth rate of powder coatings. Old wet paint equipment cannot be adapted for powder application, and thus powder coating is usually considered only if a new plant is to be built.

Powder coating application equipment costs about 40% more than a liquid paint system[4] and the old equipment must be sold or scrapped. The higher cost of materials is a disadvantage, but its greater efficiency of application, reduction in material handling, increase in productivity and reduction in man-power, with eventual savings of about 10 to 45% compared with partially offset by wet paint systems[5].

In a report published by Frost & Sullivan[4,5] it was stated that forecasts made in 1970 predicted rapid growth for the powder coating industry, but this has not been the case. This is despite the technical advancement in thin film coatings, metallic finishes, coating complicated shapes, colour changes and advancements in efficient use of heat required to cure the coatings. It is believed that tough anti-pollution legislation, which was expected in the US and EEC, may have contributed to the over optimistic projections. The absence of any form of firm legislation required that powder coatings advance under the impetus of their own merits, and in this

respect there were too many negative factors to allow the level of acceptance earlier predicted by some forecastors(4).

A steady annual growth rate of some 10-11% is expected up to 1990 with increased usage by the automotive, domestic applicants, building and pipeline industries.

Future developments are likely to increase the available markets for powder coatings as special powders are developed and micro-processors employed for application and curing control.

Energy savings will be gained by the introduction of "low-bake" coatings, as calcu ations show that a reduction of temperature from 210°C to 170°C results with savings of 20% or more in fuel costs(7). Alternatively this saving could be translated into increased through-put by leaving the temperature at 210°C and raising the conveyor speed so that the same amount of energy is aquired by the coating. In an effort to produce thin film coatings on complicated shapes microprocessor controlled spray guns will be developed(8) to allow for the Farady Cage effect in which corners or recesses tend to attract less powder.

At present this means that if a coater has undertaken to produce a minimum coating thickness the process becomes extremely wasteful as he must coat most of the surface up to twice as thick as necessary to ensure minimum thickness at edges and corners.

Speciality finishes have been developed in many resin systems thus providing direct competition with wet paints. Hammertones, textures,

paints[9]. Recently resin manufacturers have recognised the demand for good "low-bake" coatings and have developed several polyester resins for this purpose, for example Emser Werke AG claim their polyester resin "Grilesta P7305" will be fully cured when stoved at 150°C within 17 minutes[8].

1.2 Production of Powder Coatings

There are three main ways to produce powder coating paints:- dry, melt, and wet processing. Of these, melt processing is favoured by industry as it is both economic and reliable.

Dry processing is the simplist and was the method initially employed by industry. The ingredients are dry blended in a ball mill for 12-18 hours which results in a mechanical mix. The constituents of the powder (resin, pigment, filler and additives) are chemically separated but well mixed into a fine powder. The coatings produced from dry mixed powders have low gloss and, due to problems with particle size control, recovery and recycling is difficult. However this process is inexpensive which makes it ideal for low performance coating applications.

Wet processing involves dispersing the ingredients in a solvent to form a homogeneous mixture. The solvent is then extracted by evaporation or freeze drying and the powder is finished by micro-pulverisation and screening. Alternatively the solvent can be extracted by spray drying, which removes the need for micro-pulverisation and screening. The spray drier is a large chamber in which the solution is atomised. This is followed by feeding in a volume of gas which is sufficient to evaporate the solvent completely and allows the resulting spherically shaped powder to be removed. The main advantage of wet-processing is that the particles are uniform in size and shape with ingredients that have been homogeneously mixed. The disadvantage is that the use of solvents negates some of the advantages (such as cost and safety) gained by eliminating

them from the process. In addition some solvent will remain in the powder and may cause problems such as agglomeration of the powder during use.

The third process, which almost all commercial manufacturers of powders use, is melt-processing. Initially it was used as a method to improve the quality of dry blend powders. It consists of softening the powder by heating, thorough mixing to produce a homogeneous powder, milling (or pulverising) and screening.

The skill required when using this method is in judging the process temperature; It must be above the glass transition temperature of the resin, but also well below the curing point. For epoxy or polyester resins a temperature of about 80°C is used[11].
Once the melt has softened it must be mixed. This was done in a Z-blender in the early days but it was soon recognised that this did not result in a homogeneous mix. Today powders are melted and mixed in an extruder which has the advantage of being a continuous operation and, if a cooling table is attached, several functions can be carried out in one operation[12]. There are usually four stages in a continuously operating single or twin screw extruder, namely, the mixing zone, melting zone, chopping zone and a back-flow mixing zone.

The back-flow mixing zone is designed to stop any layering that may take place after melting due to differences in specific gravity and which may cause one constituent to settle out before the others. The extrudate is then rolled into sheet between cooled rolls and conveyed on a cooled belt to a coarse grinder (kibbler).

Extrusion conditions are critical, many of the final coating properties are altered by this process alone. Temperature control is of prime importance. Heat is produced by the screws transferring work to the melt, hot-spots may occur and cause some resin to become partially cured within the melt.

Once the ingredients have been extruded and kibbled (the rolled extrudate is broken up into small chips) the resultant chips must be ground to the required size. The powder particle size distribution is important for two reasons. Firstly, the finished powder must possess fluid flow properties to assist the smooth transfer of the powder from the feed hopper to the electrostatic spraying device and then deposit uniformly on the workpiece. Secondly, in the subsequent stoving operation the powder coating melts and flows into a continuous film before curing occurs. A typical coating is 50-100 μm in thickness and therefore the particle size range must be chosen to comply with the requirements of good charge acceptance and optimum deposition efficiency to give uniform coverage. It has been found that powders with no particles of diameter less than 10 μm or more than about 70 μm will meet this condition[13].

Thermoset powder coatings are based on resins with a mean molecular weight of 2000-3000 and a glass-transition of above 55°C. Such resins are brittle and so comminution at 25°C requires little energy.

The design of modern milling machinery has been derived from the properties of the extruded flake which is to be comminuted.

There are two main methods used in industry for comminution, the

pin-disc mill and the cross-flow mill. As the name suggests the pin-disc mill consists of two sets of discs each with pins fixed into them; one rotates inside the other which remains stationary. The flake is introduced from the centre and is drawn outwards by the flow of air and centrifugal forces. Kinetic energy is imparted to the flakes by the rotating pins which cause fracture on impact. Particle size distribution can be controlled by altering the shape or number of pins, air intake, and speed of disc rotation.

The cross-flow mill is also an impacting machine. The term "cross-flow" is derived from the directional movement of the material within the grinding chamber between the rotor and the baffle. Reduction is achieved by impact of the flakes drawn in with the air-flow created by a high speed rotor which forces the flakes along a ribbed grinding track. Control is achieved by altering the feed rate, air-flow, rotor speed and grinding track geometry.

The main problem encountered with both types of mill is frictional heat which can raise the temperature of the powder above the glass-transition point. This causes tackiness which accelerates the heat build up to melting point and results in blocking of the mill. To avoid this problem mills are usually water cooled, but care must be taken to ensure that chip feed rates are not too high.

The next stage in production of powder paints is the classification of the milled powder. This is necessary as although good mills can prevent large particles from escaping it can not stop producing particles below 10 μm. In the past when hand-held spray guns were common this was only a minor inconvenience, but today with

the advent of automated plant and powder recovery systems the problem is magnified. In theory small particles would be expected to have a higher charge-to-mass ratio (when sprayed through an electrostatic gun) than larger particles and thus a higher proportion could be expected to deposit on an earthed workpiece. In practice this has been found not to be the case[14], as the movement of the larger particles is determined mainly by the depositing field while the fine particles are greatly affected by air flow and viscous drag. This causes a build-up of fines in recycled powder and thus may lower the quality of production.

Classification using a centrifugal air splitter can accurately remove fines from the main bulk of the powder. The fines usually amount to about 10% of the milled powder. A second benefit gained by classification is that powder flow is improved both through the equipment and in fluidised bed hoppers.

Finally the powder is sieved before packing. This is done to remove any large particles that may have been forced through the mill and cyclone classifier as well as bits of fluff from filter-bags or clothing from personnel. Most sieves used in the US and EEC are the vibratory type[15], which usually run at a high frequency to give a high output to keep up with the production line. Locating sieves under the rotary valve of a cyclone classifier allows the finished powder to be weighed and packed in a convenient and controlled manner. For powders with an average grain-size of 90 μm, a mesh with an aperture-size of between 105 to 125 μm will give a through-put of between 200 to 300 kilogrammes per hour. Thus a single sieve can match the production of a small mill. The through-put

depends on the specific gravity and pigment loading of the powder as well as the type of movement of the sieve. It has been found that a gyratory motion with a superimposed vertical component to bounce the powder gives the best results. The movement is gentle, allows the powder to roll about on the mesh and presents a number of different attitudes in quick succession. In the same way over-sized powder rolls about on the mesh without blocking the apertures.

1.3 Chemistry of Thermoset Powder Coatings

There are three main types of thermoset powder coatings, epoxies, polyesters and acrylics. Epoxies were the first thermosetting powder coating resins produced, and still retain the largest market share. However polyester resins have taken a large proportion of the epoxy market, and are likely to continue to do so as pricing becomes more competitive.

Sophistication in design of materials for thermoset powder coatings is reaching a level where it is difficult to distinguish between an epoxy and a polyester or acrylic. Co-blended and co-reacted systems are becoming common(2). Furthermore the tendency to design resins with a high crosslink density is changing, as resins with relatively low crosslink densities are being produced which have the properties of semi-thermoset/semi-thermoplastic resins.

Epoxies exhibit good friability in pigmented formulations thus contributing to their ease of manufacture. They store well with good physical and chemical package stability. They have a low melt viscosity which aids good flow-out and levelling prior to curing. The thermosetting reaction is not gradual: once a threshold temperature is reached, curing is rapid and complete. There are no volatiles from the crosslinking reaction, thus blistering, pinholing or bubbling are not problems with epoxy resins. These properties make epoxy resins almost ideal for powder coating systems, though, there are a few problems. Outdoor exposure resistance is poor and yellowing occurs quite rapidly, especially if cured at temperatures slightly above that recommended. Another problem is

chalking which occurs on exterior exposure. Thus the use of epoxies bright metallics and pewter finishes cannot be matched by wet has been somewhat limited despite their cost effectiveness, good chemical resistance and favourable physical properties.

The simplest epoxy compound of the type suitable for powder coatings is the diglycidyl ether of diphenylolpropane (bisphenol A). It is a low viscosity liquid of molecular weight 340. It is possible to increase the chain length of this basic epoxy compound by altering the ratio of the co-reactants and reaction conditions giving solid

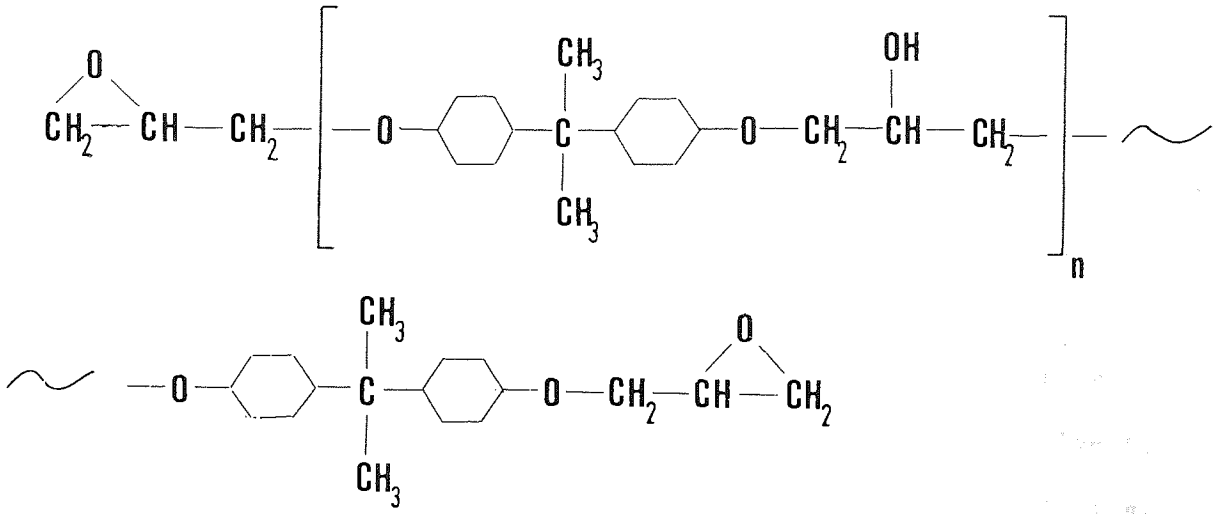

Figure 1.3.1 Epoxy resin structure (after Harris[16])

resins of higher molecular weight. A typical epoxy resin structure is shown in Fig 1.3.1 where 'n' may lie between 4 and 9 for powder coating products[16].

The excellent chemical resistance of epoxy powder coatings is due to the ether linkages (- O -). The small highly polar epoxy 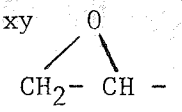 and hydroxyl groups give very good adhesive properties. The high aromatic content is responsible for reduced resistance to chalking and poor light and heat stability.

Techniques currently used to manufacture epoxy based powder coatings require resin melting points of 75-116°C and molecular weights in the range of 800 to 2,000.

The chemical reaction involved in the manufacture of epoxy resins is simple and of short duration. However, it is difficult to wash the resin free from salt formed during reaction which must be carefully controlled when increasing the chain length as failure to do so will result in jelled particles which will mar the appearance of the powder coating.

A compromise in the choice of resins must be made when formulating a powder coating. Low molecular weight resins show improved solvent, chemical and boiling water resistance with good flow characteristics. High molecular weight resins show improved impact resistance, flexibility and storage stability.

Crosslinking of the epoxy resin is achieved through epoxide or hydroxyl groups. Curing is normally an addition reaction without the formation of by-products, the reactions being exothermic and reaction rates increasing with increasing temperature. There are a large number of crosslinking agents available for use with epoxy resins; each has its own advantages and they are fully described by Harris(16).

The fastest growing thermoset powders in the US and EEC are thermosetting polyesters.

The polyester resins are polycondensation products of the reaction of polybasic acids with polyhydric alcohols. Where polyhydroxyl alcohols, particularly those containing three or more hydroxyls, are allowed to react with polycarboxyl acids, the esters formed are complicated because three dimensional interesterification and polymerisation occur(17). The polyester backbone can be formulated having free hydroxyl groups, free carboxyl groups, or both. Low molecular weight polyesters (2500 - 500 MW) with high aromatic content can be readily formulated to give friable solids with glass transition temperatures over 50°C. Polyesters being polar molecules, are noted for their excellent electrostatic spray properties.

The main advantage of polyesters over epoxies are their excellent weathering resistance and non-yellowing properties(18), as well as high reflectivity and gloss levels. Early systems used amino-plasthydroxyl polyester which exhibits good properties but requires long cure times at 180°C to achieve adhesion and flexibility to match that of epoxies.

They also suffered from poor storage stability, however this could be improved by additions to the resin. The coatings tend to bubble when the thickness exceeds 0.1 mm due to the slow cure profile which prevents complete release of the crosslinking volatiles.

Ester linkages do not contain the chemical inertness as compared with that of epoxy resins, but it is possible to obtain a high level of resistance to acid and alkaline conditions by the correct choice of reactants.

Taft[18] reports on a relatively new system used in Europe employing an epoxy/acid crosslinking mechanism between a non-yellowing epoxy and an acid terminated polyester. The polyepoxide is triglycidyl isocyanurate (TGIC) which cures in 15 minutes at 180°C and provides a non-yellowing, weather resistant finish in combination with the acid terminated polyester.

The cost and availability of polyester resins are probably responsible for the slow increase of the polyester powder coating market share in the past five years. However both price and availability are now on a par with epoxies for many applications and so should now expand rapidly.

The main advantages of polyester over epoxy systems are[16]:-

(i) Improved heat and light resistant
(ii) Better resistance to exterior weathering and chalking
(iii) Versatility to the resin formulator
(iv) Good gloss and improved levelling

The main disadvantages are;

(i) The wider molecular weight spread, giving a lower glass transition temperature and so causing lumping or blocking of the powder.

(ii) A tendency to hydrolyse which will result in coatings with lower chemical resistance.

Relatively new on the market are acrylic resins. As these are derived from chemicals found in the petrochemicals industry, they are likely to be subject to unstable raw materials prices. The main aim in this field is to produce a coating suitable for automobile top coats. The main formulating problem is to develop a polymer with a low glass-transition temperature to achieve enough flexibility. However the minimum T_g is about 40°C, below which storage stability is very poor. Should acrylics be successfully developed it is claimed that the advantages will include good light and heat stability, good detergent resistance, excellent physical properties, freedom from chalking, good stain resistance and high gloss with good levelling characteristics. These properties however are dependent on the make-up of the resin and a compromise amongst the most important properties will have to be reached.

1.4 Powder Additions

Additions can be made to powders to improve their performance. Caking resistance and exterior durability can be optimised by additions of cellulose acetate butyrate, whereas 0.1% silca improves fluidity and reduces caking. Ultra-violet screening agents can be added to improve resistance to breakdown by sunlight(19). Titanium dioxide is particularly good at absorbing ultra-violet radiation and thus a well dispersed pigment containing titanium dioxide will reduce photocatalytic degradation.

Powder coatings can be designed to give particular coating finishes such as textured, hammertoned, pewter, bright metallic and low gloss satin finishes.

Textured powders come in a wide range of finishes from sandpaper to a large pattern vinyl leather appearance. There are many methods used to produce textured finishes. The rough sandpaper type can be made by additions of particular extenders such as barium sulphate which will restrict the flow of the powder in a controlled way during curing. Alternatively the same effect can be achieved simply by having a high pigment loading. The degree of roughness can be controlled by adjusting the particle size distribution of the powder. However these coatings have reduced mechanical performance due to the high filler content of the powders.

The smoother 'vinyl-look' textures have a higher performance than the rough "sand-paper" textures. They are smooth to the hand and do not catch on materials. They are produced by additions of

special texturing agents and by careful formulation of the powder the pattern size is relatively insensitive to particle size making consistancy of appearance easy to achieve. The texturing agents take many forms but one method is to use a mix of two hardeners 'A' and 'B'. This gives a fine textured pattern by allowing a particle containing hardener 'B' to continue to flow when a particle containing hardener 'A' has gelled.

Metallic finish powders can be made to match that of wet paints. Metal pigment is mixed with a clear epoxy or epoxy-polyester powder so that the metal particles bond to the resin. This method avoids problems with reduction of deposition efficiency or shorting out of the guns(8).

A pewter finish is a texture coating with the background colour in the valleys and a metallic type colour along the ridges. The formulation and production of pewter coatings has brought together the technologies of textures, hammertones and metallics in one coating and can be designed in many textures to give manufactured products a novel appearance.

Gloss can be reduced by adding incompatible film formers such as ethyl cellulose, the reduction in gloss being proportional to the amount added. However, chemical and solvent resistance is reduced as a consequence of this addition. Techniques used to reduce the gloss of liquid systems cannot be applied to powder systems because these additions (eg stearates), cannot float to the surface of powder paints during curing (as they do with liquid) due to the vastly increased viscosity.

1.5 Powder Deposition

Powder deposition may be carried out in a number of ways depending on the shape and size of the object to be coated and the type of powder used(20,21,22,23,24,25,26).

The main techniques used are:- the fluidised bed, electrostatic fluidised bed, flock coating, flame spraying and electrostatic spraying.

A fluidised bed is a chamber in which powder is placed and gas is passed through, giving the appearance that the powder is boiling. The object to be coated is preheated to a temperature above the sintering range of the powder and immersed in the fluidised bed. The main problem with this technique is a limitation of product size; large objects cannot be coated in this way as fluidised beds become unstable and streaming occurs once a critical size has been passed. A second disadvantage is that coating thickness is difficult to control. However, there is no waste powder or recycled powder to deal with. The electrostatic fluidised bed was devised to overcome coating thickness problems; a fluidised bed similar to that above is used and the powder is electrostatically charged. The work piece is earthed thus powder is attracted to the work piece, but due to the mutual repulsion between the particles a limiting thickness is reached, so coating thickness control is improved.

To overcome constraints on work piece size various forms of powder spraying from hand held or mounted guns have been designed. The simplist form is known as flock spraying; powder is sprayed onto a

preheated substrate and subsequently cured. If preheating is a problem then flame spraying can be used where a gas-oxygen supply is arranged in such a way that the powder is heated as it is sprayed. The temperature is well above the degradation point of the powder but due to the velocity of the powder passing through the flame powder degradation does not occur.

Both methods have major disadvantages: finish is dependant upon the skill of the operator and recycling is difficult, especially in the latter case.

Electrostatic spraying was seen as the best way to overcome problems of size, finish and recycling. However, there are problems related to this technique. Thermoplastics cannot be readily sprayed as they tend to become sticky and form clusters causing a blockage in the gun assembly. Secondly, should a colour change be necessary, the complete assembly must be carefully cleaned as any remaining powder will cause a speckled appearance in the following coatings.

Electrostatic spraying has a lot to offer in terms of ease of application, good control and efficient powder deposition. As with the electrostatic fludised bed the mutual repulsion of the charged particles acts as a self-limiting mechanism controlling film thickness and the throwing-power is very good, enabling complicated shapes to be coated. Recycling the powder is also relatively easy: the overshot powder is simply collected, sized and re-used. Sizing is necessary as overshot powder tends to be particle size dependant but this is no problem using a balanced air-flow classifier. The adhesion of the particles is strong enough for the work piece to

be transfered to an oven for curing to give a thin continuous film. In recent years electrostatic spray equipment manufacturers have done much to find ways of charging up powders more efficiently in order to reduce the amount of recycled powder and to speed up colour change times. The most striking feature representing this effort is the introduction of non-conductive spraying booth s. A major problem with any powder handling system is the risk of fire or explosion. This is increased when combined with high voltages as in the case of powder coating where voltages as high as 60KV are often used to charge powders.

To combat this risk the spray booths were metallic and well earthed to prevent the build-up of charge and subsequent possibility of sparking. However, work carried out at Southampton University[27] has shown that some non-conductive materials such as Perspex cannot release sparks with sufficient energy to ignite a powder cloud. This is because the energy is released from only a small area as the resistance of the material is high, whereas an unearthed metallic booth releases all of its stored up energy at once causing a high energy spark.

The main advantage of electrically insulated booths is that once the walls have charged up they will repel electrical lines of force, and so concentrate them onto the work piece[28]. The charged powder particles will tend to follow the lines of force and therefore a cloud will form around the work piece improving deposition efficiency of the system.

This obviously helps overcome problems associated with colour change, as charged particles are repelled rather than attracted to booth walls so there will be less powder and it is easier to remove. Several manufacturers have taken up the challenge to produce a quick colour change coating system on a commercial scale, reducing change times from 6 hours to 5 minutes[29]. These improvements range from quick-release conveyor belts which run along the bottom of the spray booth, to a system in which the powder cloud is kept suspended by air jets and is charged by electrodes in the booth[30] as well as when entering the booth via spray guns.

The next big improvement achieved by the equipment manufacturers has been to improve the charging efficiency of the spray guns[28,30,31].

In 1962, a French company SAMES developed the first electrostatic powder spray gun[16] and for ten years or more most powder spray guns were based on a similar design. Powder is passed through the gun under the influence of an air-flow. At the exit of the gun is a needle electrode with a high surface field intensity (above 3 volts/micron) producing a corona discharge. The powder passes through the corona discharge and as it has a high resistivity the particle surface becomes highly charged. The two other less commonly used methods for charging powders are induction charging (used for low resistance powders which would be expected to lose their charge upon being deposited on an earthed substrate) and secondly, tribo-electric charging or static charging of the particles by rubbing within a low intensity electric field.

Recently powder spray guns have been designed with the needle electrode tucked away inside the gun[28,31]. These are run at relatively low-voltages (10KV) and use some form of Electro-Gas-Dynamic charging system. These have several advantages, for example, the corona discharge is withdrawn into the barrel so improving corona charge efficiency and the free ion density is reduced thus reducing the chances of back-ionisation occuring. A major problem appears to be that this type of gun becomes blocked due to charged powder attaching itself to part of the charging chamber after short operating times.

1.6 Electrostatic Charging and Behaviour of Powder Particles

In most commercial powder guns the powder is charged by a corona discharge mechanism. In the nozzle the powder stream is exposed to an ion cloud and becomes charged by ion bombardment. The ion bombardment charging theory for spherical particles was initially derived by Pauthenier(32). It was assumed that ions move along lines of force striking particles which in turn become charged. The theoretical charge q(t) acquired by a spherical particle by ion bombardment in time t is expressed by(33):-

$$q(t) = q(\infty)\left(\frac{t}{t+\tau}\right) \tag{6.1}$$

where the time constant $\tau = \frac{4\epsilon_o}{KN_e} = 4\epsilon_o \frac{E_c}{J}$ (6.2)

and the limiting charge $q(\infty) = 4\pi\epsilon_o E_c P a^2$ (6.3)

P is a constant given as $P = 1 + \frac{2(\epsilon-1)}{\epsilon+2} = \frac{3\epsilon}{\epsilon+2}$ (6.4)

Where a = Particle Radius
N_e = Electron density
E_c = Applied electric field
ϵ_o = Permittivity of free space
ϵ = Relative permittivity of the particle
J = Ion current density

by substituting equation (6.4) and (6.3) into equation (6.1), the maximum charge on a particle of radius 'a' in a time 't' will be given by

$$q(t)_{max} = 12\pi\epsilon_o\left(\frac{\epsilon}{\epsilon+2}\right) E_c a^2\left(\frac{t}{t+\tau}\right) \tag{6.5}$$

This equation shows the maximum charge on a particle is directly proportional to the electric field and to the square of the particle radius.

The above derivation is for conducting particles in a uniform electric field and in powder coating the particles are rarely spherical and they are charged in non-uniform fields. However Masuda and Akutsu[34] have found agreement with Pauthenier's theory using spinning non-conductive particles, where spinning is necessary to distribute the charge evenly over the particle surface. It appears that the shape of the particle gives a distribution of charge related to the average particle radius.

A similar approach can be used to find the theoretical maximum charge obtained by a particle in a non-uniform electric field as Pauthenier used for a uniform field. The final equation is extremely complex but a first order approximation may be obtained by averaging the electric field $E(r)_{ave}$ between the gun electrode and local earth. the equation then becomes:-

$$q(t) = 12\pi \epsilon_o \left(\frac{\epsilon}{\epsilon+2}\right) a^2 \left(\frac{t}{t+\tau}\right) E(r)_{ave}$$

Once the particles become charged they travel towards the work under the combined influence of aerodynamic and electrostatic forces. The air flow is derived from two sources; the air flow from the nozzle of the spray gun that was used to transport the powder from the hopper, and the extraction air passing through the booth to the recyling equipment. The net air-flow tends to carry the particles past the work piece and therefore it has been suggested that both air-flows should be minimised[35]. Air-flow induced by ion movement (corona wind) also has a significant influence[33,36].

It has been shown that the particle velocity relative to the air flow is proportional to the particle size, and that the particle

velocity increases rapidly with increasing air pressure of the spray gun. The increase in velocity due to electrostatic forces is very small until the particle is close to the work piece. When the particles approach the target electrostatic forces seem to have an increasing dominance influencing velocity and direction, creating a powder cloud around the work piece[37].

The adhesion of electrostatically deposited powder is the result of Coulomb, molecular, dipole and chemical forces, and has been studied in detail by Cross[38,39]. It is interesting to note that in general it has been found that techniques which give an improvement in surface finish can also lead to a reduction in adhesion forces for the unfused layer.

The corona discharges occurring in the deposited layer or in the gun can cause chemical changes in the polymer. Indeed many polymers are treated this way to increase the adhesion of glues[40,41]. The ultracentrifuge has been used by Cross[40] to study the adhesion of deposited layers and it was concluded that factors such as particle size, shape, and resistivity, ion current, magnitude and polarity of deposition field play an important part along with the above mentioned forces. It was also found that positive polarity gave greater adhesion than negative and that tribo-charging gives much lower adhesion, despite the fact that the powder charge per mass of tribo and conventional systems were similar[42].

A phenomenon known as back-ionisation has been a problem with powder sprayed coatings since their conception. When the coating has been cured this can be seen as pock-marks or craters in the film. The

mechanisms involved in back-ionisation have been the subject of many investigations and are extremely complex. The forces acting on the powder layers, which govern the stability and formation of the coating are determined principally by the electric field at the surface and current density through the layer. The condition for the onset of back ionisation assumes that the electric field intensity inside an electrostatically deposited layer E_d exceeds its breakdown limit E_{ds}. This can be formulated in the case of steady state conditions as

$$j_d \times E_d \geq E_{ds}$$

where j_d is the current density in the powder layer, and E_d is the apparent layer resistivity.

This condition has been confirmed[43] to hold for the resistivity range up to 10^{13} Ωcm, which is the range usually encountered in electrostatic precipitation. However, due to the self-limiting thickness mechanism known to exist in electrostatic powder coatings back-ionisation does not begin until a coating of about 100 μm is reached despite the higher resistivity of these powders[39].

A starting point has been described by Masuda et al[44] for a more general case, assuming Poisson's equation, continuity equation and Ohm's law to hold inside a powder layer formed at a constant velocity.

$$E_{max} = E_{ext} + (i_o \rho_d - E_{ext})\left(1 - e^{\frac{-X_o}{L_d}}\right) \geq E_{ds}$$

Where E_{max} = Maximum field strength
E_{ext} = External field strength
i_o = Total current density

ρ_d = apparent layer resistivity
x_o = limiting coating thickness
l_d = relaxation length
E_{ds} = Electric field intensity, breakdown limit

for the special case of ρ_d having an extremely high value ($>10^{13}\,\Omega cm$) then:-

$$Xo \ll L_d$$

where L_d, the relaxation length represents the penetration length of the external field into the coating. The field distribution becomes a linear function of the depth in the coating, the equation then simplifies to:-

$$E_{max} = E_{ext} + (i_o \rho_d - E_{ext})\,(X_o/L_d) \geqslant E_{ds}$$

The calculation of E_{max} at the onset of back ionisation agrees with the measured value of E_{ds} within an error of 20 - 30%.

It has been found that when particles charged by ion bombardment due to gaseous ions produced at the corona, only about 1% or less of the ions produced by the corona become attached to particles(40). The remaining ions form a free-ion current and have been shown to be the cause of back-ionisation(45). As coating proceeds, discharges occur in the layer creating a current of opposite sign to the corona ion current. These back ions tend to discharge the powder approaching the layer.

By carefully excluding the ion current Masuha et al(46) have shown back-ionisation can take place with the aid of an externally applied field. In more detailed investigations(36,39) it has been shown that not only was back ionisation giving rise to counter flow ions, which streamed out of the limiting powder layer, discharging

and turning away oncoming particles, but also powder particles were observed to be physically ejected from the powder coating after they had landed. This work was continued at Southampton University by Hughes and Ting[47] who found that the surface disruption caused by back-ionisation was dependent upon the polarity of the corona discharge. A negative corona gives rise to pin-hole damage in the powder coating. These pin-holes penetrate through the coating to the substrate and are therefore liable to become corrosion sites; however the coating is smooth and the pin-holes may flow-out during curing.

A positive corona produces a rough orange-peel type coating, but the craters do not penetrate the coating at any point therefore increasing corrosion resistance of the coating. It was also noted that tribo-charged coatings did not display any signs of disruption and it is suggested that this fact may be of some importance in the future design of powder spray guns. The onset of back-ionisation was noted after about 5 seconds of spraying for both positive and negative corona discharge.

Finally Singh et al[48] studied the transportation and deposition process of electrostatic powder coating. They found that the efficiency of powder transfer to an object and the velocity of transportation are dependent on the charge acquired by the powder particles by corona discharge. No transfer of powder could take place unless a charging level of 2×10^{-4} c/kg was reached. It was also found that transfer efficiency increased with increasing applied voltage, efficiencies of 80% were reported, although it is likely that severe back-ionisation would occur using high applied voltages.

1.7 The Curing Stage

The curing stage is the final process required to produce a finished powder coating. It is essential that curing is complete as this has a major influence on the final coating properties, yet on the other hand over-curing can cause problems, such as yellowing in epoxy coatings, and also markedly affects coating properties. In industry curing usually takes place in a large oven through which sprayed products are conveyed on an overhead track. The temperature of the substrate must be periodically monitored and the oven temperature adjusted along the complete length of the track, watching out for any hot spots that may develop.

During the curing process the powder softens when its temperature reaches the glass transition point, then melts and flows, each particle merging with adjacent particles to form a thin continuous film. Typically the temperature of aluminium sheet increases at a rate of 30°C per minute until about 200°C is reached. The substrate is then kept at this temperature for about ten minutes, although this may be much shorter for 'low-bake' coatings.

The rate of flow of the molten particles decreases with time as cross-linking reactions occur at the onset of cure and viscosity increases. At the end of the curing cycle the cross-linking reactions are complete and the physical and mechanical properties are fully developed[49]. This point emphasises the problems encountered by polymer chemists developing low-bake resins for powder coating. As time and temperature of cure are decreased, so the particle fusion and cure temperatures become closer allowing

little time for flow. Attempts to formulate a resin with a lower glass transition temperature, lower melt visocity, and lower molecular weight spread, which extend the possible flow time during cure result in a reduction of physical properties and unstable storage properties(50).

The two main techniques used to study the cure of thermosetting powder coatings are the measurement of melt viscosities using the Weissenberg Rheogonometer, and the measurement of kinetics and thermodynamics of cure using Differential Thermal Analysis (DTA) or Differential Scanning Calorimetery (DSC). Klaren(51) and others(52,53) have found that the cure peak maximum (the cure temperature) increases for increasing heating rates using viscosity/time profiles. This shows that the thermoset cure mechanism is both time and temperature dependent, and has a practical use as higher cure temperatures have lower melt viscosities and therefore better levelling properites.

Work carried out by Smith(54) on thermoplastics have shown that flow is also dependent upon molecular weight, good flow being obtained from low molecular weight resins. However it has also been noted that the reduction of molecular weight produces coatings with poor mechanical properties(55), thus formulators must compromise on this point. The effect of relatively small modifications has been found to profoundly alter melt viscosity(56). Usually additions are made which reduce the reactivity of the resin and lower the melting point. Nix and Dodge(57) studying the cause of orange-peel have shown that poor levelling is not aways due to high melt visocity. They stated that orange-peel was the result of an agglomeration of

powder due to low molecular weight powders sticking to one another or by electrostatic attraction between the particles. Thus low molecular weight powders can have poor levelling characteristics. They also studied the effect of particle size on powder flow and claim that smaller particles flow better than large powders and powders with a large size distribution flow better than those with a narrow distribution band. Further work studying flow using hot-stage microscopy[58] has shown that stale powders do not flow as well as fresh powders and that moisture up-take by the powder is partially responsible for the lack of flow in stale powders. It was also found that although surface-tension of the molten powder does have a great effect on the flow characteristics[57] these are also dependent upon the substrate surface characteristics such as roughness or pretreatment[59]. Theoretical studies have been carried out by Freshwater[60] on particle size and shape but further work is necessary on particle packing, incidence of porosity, coating density and the number of point contacts.

Differential Scanning Calorimetery (DSC) has been used to study the state of cure on bond performance on an epoxy resin[61]. It was found that bond strength increased with degree of cure, bond failure being cohesive in the range 70-90% cure and adhesive in the range 90-100% cure.

A method of studying the non-isothermal viscosity change during the cure cycle was developed by Nakamichi[62]. A small ball was embedded in a coating on an inclined substrate and the velocity of the ball was measured against time. The final stage of cure obviously cannot be studied using this technique. An alternative is the use

of a torsion pendulum[64] which has been successfully used to obtain temperature-time-transformation diagrams (TTT) and continuous heating transformation diagrams (CHT) for thermosetting epoxies. Figure 1.7.1 shows the TTT diagram for an epoxy resin produced by Shell Chemicals, Epon 834/DDS. Figure 1.7.2 shows the CHT diagram for the same resin. The resin is liquid at the start and has a glass-transition temperature at 185°C. Both diagrams would be considerably different for solid powder coating resins.

Another method used to study the last stages of cure for thermosetting resins monitors changes in the modulus of elasticity[63]. This technique measures the amount of bend that takes place for a standard panel as it is heated or cooled. A fully cured coated panel displays a closed hysteresis loop whereas a partially cured coated panel displays an open hysteresis curve. Adhesion is crucial for this method to work properly as the amount of bending depends on the difference between coefficients of thermal expansion of the coating and the substrate.

L Simpson[65] reports the use of dielectric analysis to determine the degree of cure of a coating. The dielectric loss tangent is a measure of the relaxation process associated with the dipoles in the sample responding to a changing electric field. The temperature at which a peak occurs is related to the glass transition temperature. As the degree of cure in a coating increases the temperature at which the peak occurs also increases. By using this technique it is possible to correlate the extent of cure with a coatings mechanical and physical performance.

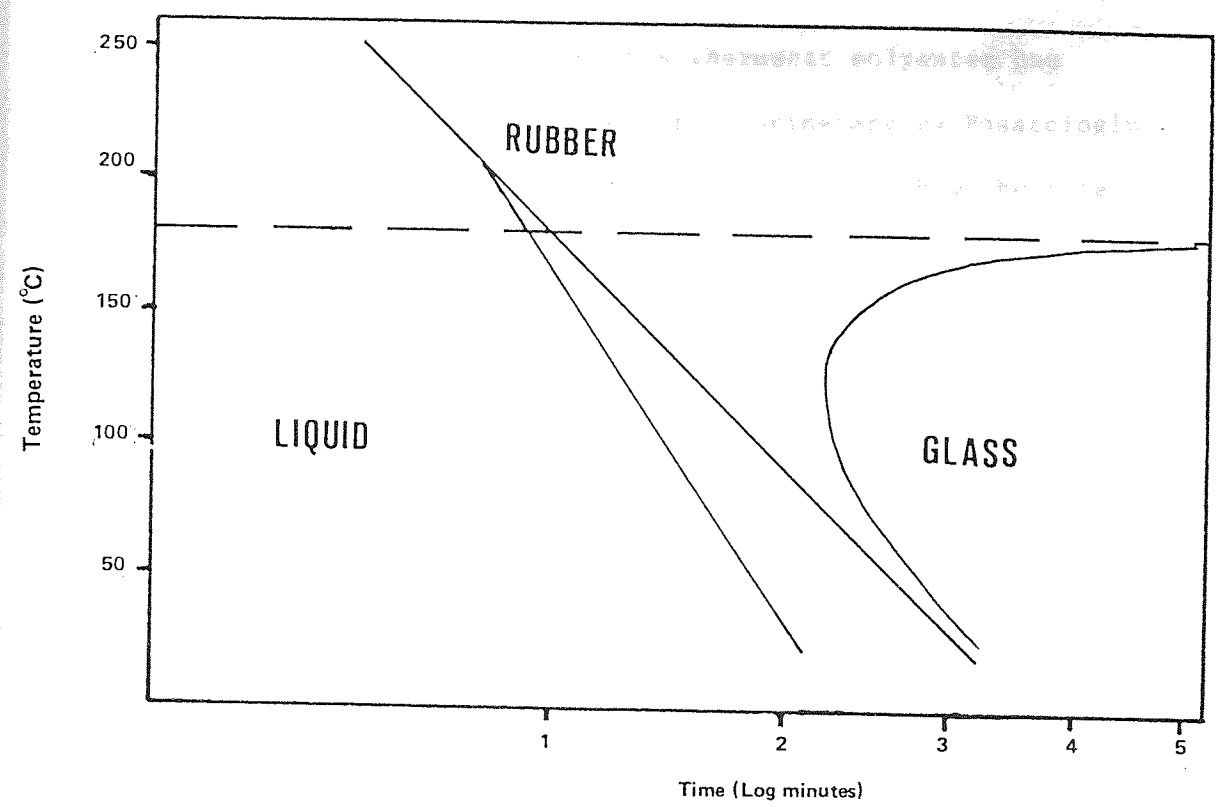

Figure 1.7.1 TTT Diagram for epoxy resin Epon 834/DDS (after Enns, Gillham and Doyle [64])

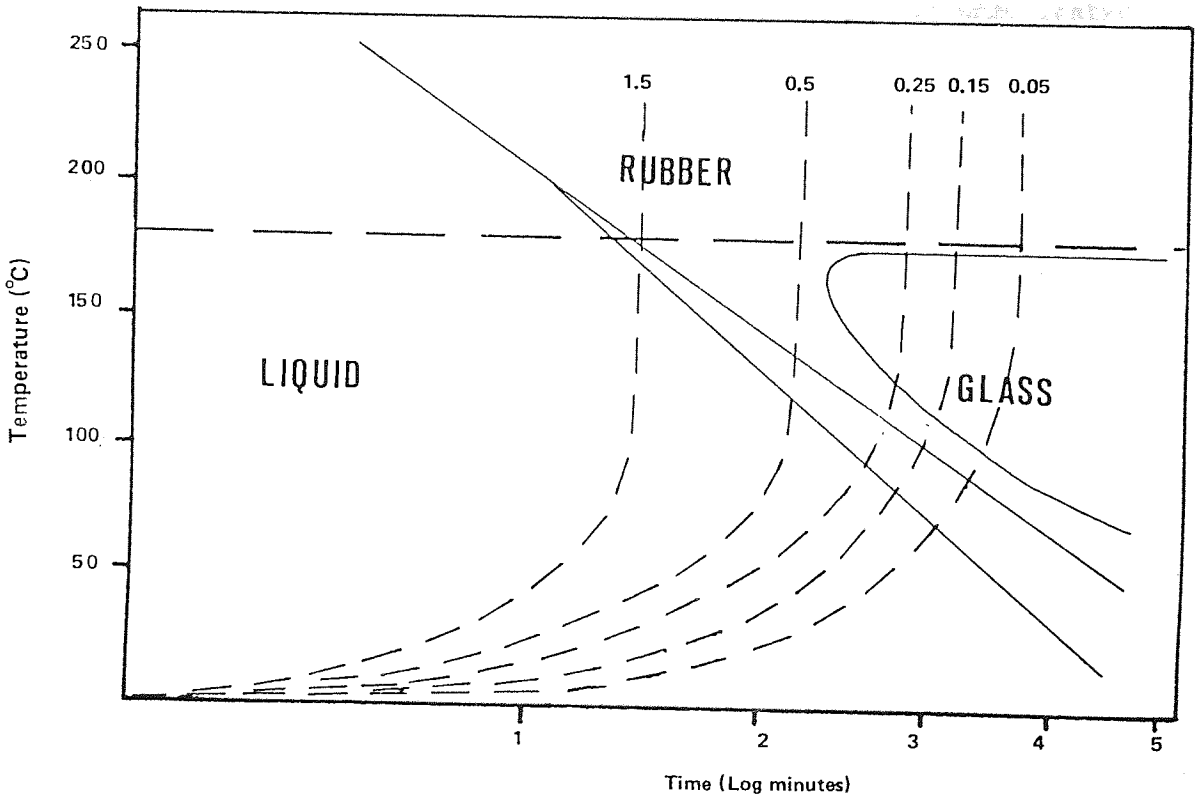

Figure 1.7.2 CHT Diagram for epoxy resin Epon 834/DDS; heating rates:- 1.5, 0.5, 0.25. 0.15 and 0.05°C/min (after Enns, Gillham and Doyle [64])

The heats of reaction and kinetics of a thermoset polyester has been studied using Differential Scanning Calorimetery by Pusatcioglu and co-workers[66]. A model has been constructed to show the rate of cure for thermosetting polyester resins:-

$$\frac{dP}{dt} = A \exp(-E_a/RT)\, P^a\, (1-P)^b$$

where P= relative degree of cure
E_a = activation energy

$A \exp(-E_a/RT) = k$ = rate constant

and a,b = constants independent of temperature.

This has been based upon the fact that the exothermic heat of cure comes from the following reactions[67]:-

(i) the propagation reaction of free radical crosslinking of the styrene monomer with an active double bond of unsaturated polyester

(ii) the decomposition reaction of the peroxide initiator

where heat liberated from (ii) is negligible compared with (i). Good agreement between the model and experiment results have been reported.

In a subsequent paper by the same authors[68] the variation of thermal conductivity and specific heat during cure of thermoset polyesters was found using DSC. It was reported that both thermal conductivity and specific heat increase linearly with increasing temperature.

1.8 Degradation of Powder Coatings

As application of powder coatings become move diverse, the environments in which coatings are expected to perform become harsher. When exposed outdoors the coatings must withstand the combined effects of moisture, oxygen, heat, ultraviolet light and micro-organisms in order to meet the required standards.

It is recognised that progressive loss of gloss, chalking and mass loss that occur on exterior weathering is due to the effect of ultraviolet light in the presence of oxygen and moisture[69]. Two different mechanisms can be proposed to explain this[2]:-

i) direct photodegradation of the binder

ii) degradation by hydroxyl radical formation, due also to the photocatalytic activity of the titanium dioxide in white pigments.

The photochemical degradation of the binder is mainly due to an oxidation process with oxygen absorbed from the atmosphere. Energy must also be absorbed for this process to start and has been found to come from ultraviolet radiation.

The molecular bonds in the binder are broken by UV quanta or protons which collide with electrons the rate of breakdown being dependent upon the energy absorbed. The shorter the wavelength of the incident ultraviolet light the greater the energy but the intensity of the radiation and absorption characteristics of the binder also effect the total energy absorbed. This is of great importance when conducting exposure tests.

Most of the ultraviolet radiation absorbed by a paint film pigmented with titanium oxide is absorbed by the pigment[19] and this is also expected to be the case for other types of pigment[2].

Absorption may be expected to reduce the amount of damage done by ultraviolet radiation. However, titanium oxide and other pigments are photoactive, and as a result can catalyse the breakdown in the binder. Thus the presence of a pigment can accelerate or retard degradation depending on the photoactivity of the pigment.

When pigment crystals are irradiated with sufficient energy, electrons are excited from valancy bands to conductive bands thus allowing both the electrons and the holes created by missing electrons to move about within the crystal lattice. Some electrons and holes reach the surface where they are capable of initiating chemical reactions in the surrounding medium. The positive holes react with hydroxyl groups to form adsorbed hydroxyl radicals.

$$\text{hole} + OH^- \longrightarrow OH^- \text{ (ads)}$$

The electrons react with absorbed oxygen to form the O_2^- radical ion which then reacts with water to form the perhydroxy radical.

$$e + O_2 \longrightarrow O_2^- \text{ (ads)}$$

$$O_2^- \text{ (ads)} + H_2O \longrightarrow OH^- + .HO_2$$

both radicals can initiate breakdown of organic compounds and hence the process of paint film degradation is started.

Photocatalytic activity can be controlled by coating the pigment with various hydrous oxides which eliminate most of the hydroxy

radicals. These coatings are often hydrous oxides of silicon, aluminium, titanium or zirconium and are in the order of 5-10% of the total pigment weight. Unfortunately these coatings may also have an adverse effect on opacity and colour, and in addition, the presence of relatively high levels of silica has a detrimental effect on dispersion properties resulting in low gloss[19]. Another method for reducing the photocatalytic effect of pigments is by judicious additions of zinc or aluminium oxide which act as recombination centres and reduce the number of electrons and holes that reach the surface.

A microenvironment is created by erosion and microfracture of the polymer surface which is conductive to moisture and dirt accumulation. Photoxidation causes a build up of a variety of carbonyl groups which can make the surface very hydrophilic. This allows the polymer to swell and results in additional cracking and allows mildew growth. Gabriele et al[70] have found that additions of benzothiazole UV absorbers such as 2(2' - hydroxy - 5' - methylphenyl) benzothiazole (LSII) and hindered amine light stabilizers (HALS), typically bis [2,2,6,6 tetramethyl - 4 - piperidone] sebaccate (LS1) extend the life of paint films exposed to severe atmospheric conditions. This is claimed as a better approach to coating formulation as it reduces the complexity of formulation and therefore reduces the possibility of incompatibility.

Before any coating system can be accepted for use in a production line it must first be tested for its weathering characteristics. As previously stated sunlight and its intensity are extremely important factors controlling degradation but there are other variables that

also have an important role. The amount of sunlight reaching any particular point on the earth's surface varies according to the ozone level, water vapour, water droplets, dust, thickness of atmosphere and angular height of the sun above the horizon. It is for this reason that terms such as "hours of sunshine" or "Kilo Langley's exposure" are recorded during exterior exposure tests. Surface temperature is also important; unfortunately this will vary with wind speed and air temperature and is therefore difficult to quantify. Surfaces are much better at absorbing radiant heat than air so they become much hotter. The ability of a surface to absorb radiant heat depends on its colour and finish. Thus pigments have a physical role as well as a chemical role(71).

Moisture is also important for weathering. Physical processes such as leaching, diffusion and swelling are dependent upon the length of time the surface stays wet. Much data on rainfall around the world is available but unfortunately very little information exists on the duration of wetness for different locations. This will be dependent upon such factors as relative humidity, surface temperature, angle of slope, wind, surface wetting and deposition of dew. The chalking of paints is most dependent upon relative humidity and temperature, increasing rapidly at temperatures over 60°C(72).

Thus a formidable array of variables must be taken into account when using accelerated weathering tests. Many testing devices have been produced and used. However, it is basically impossible to accelerate the influence of time(73), and therefore care must be taken when considering accelerated weathering results.

The only reliable data available can be obtained by carrying out a full exposure program at a recognised testing station. Obviously the siting of such a station is of vital importance. It was recognised as early as 1927 that that south east Florida has a unique and relatively constant climate[74].

The combination of high daily relative humidity, heavy dew, heavy annual rainfall, warm temperature all year round and high values of solar radiation produce a type of weathering failure which is very similar to that observed on surface coatings exposed in more temperate climates, but occurs very much faster. Thus Florida is a suitable place to base weathering test results and to which accelerated tests can be compared.

2. ALUMINIUM PRETREATMENT

2.1 Introduction

The oxide film that forms spontaneously on an aluminium surface exposed to air has poor corrosion resistance and paint bonding characteristics. It is therefore essential to pretreat any aluminium product that requires an organic finish. Chromate conversion coatings have been found to be particularly good pretreatments, and have become widely used in industry. However, research on the fundamental aspects of these conversion coatings has been limited and so in the basic mechanisms of coating growth corrosion resistance and paint bonding are not understood.

Environmental concern has encouraged the development of a chromium-free process and numerous attempts have been made to formulate such a system. It appears that none have attained the high standards set by chromate pretreatments, this failure is partly due to a lack of understanding of current technology.

Five minimum requirements necessary to produce a true reaction system forming conversion coatings have been described by Ayres(76).

1. The metal must be surrounded by a fluid such as a mild acid which will render its surface reactive.

2. The medium must contain soluble anions or anion formers.

3. The character of the medium at the interface must be so changed by the anion - cation interaction that it does not dissolve the reaction product.

4. The insoluble chemical compound formed must precipitate sufficiently close to the substrate so that it remains an integral part of the surface.

5. A transition layer must develop, across which the binding forces holding the coating to the metal can be exerted.

Chemical conversion coatings have been developed relatively recently, despite the existence of some forms of conversion coatings that have been known for sometime. There are basically two groups of chemical conversion coatings, those that thicken the naturally occurring oxide film and those that produce phosphate or chromate coatings. Of the latter there are again many types, the one chosen will depend upon the alloy and its application[77]. Chemical conversion coating solutions are based on zinc, aluminium, chromate-phosphate, or chromium-chromate solutions or a "chrome-free" solution designed to produce a chromate type coating or coating properties. The chromium-chromate bath which has been recently developed from the chromate-phosphate bath has the best uncoated corrosion resistance[78] and is widely used by industry. However, chromate-phosphate coatings have outstanding paint bonding characteristics[79] and when coupled with its non-toxicity, good corrosion resistance and pleasant olive-green appearance it is not difficult to appreciate this system's continued popularity.

A description of the ideal conversion coating was listed in five points by Edwards as long ago as 1942[80], these were:-

1. It should be continuous or substantially so, and should be impervious to gases or liquids.
2. It should be inert or almost insoluble in its environment.
3. It should not electrolytically accelerate the attack on the base metal.
4. It should be resistant to mechanical injury such as abrasion or scratching or should be self repairing.
5. It should bond readily with paints and other organic finishing materials.

Chemical conversion coatings were originally introduced to industry as a substitute for anodic coatings and were originally used as such. It soon became apparent that these coatings have unique properties and caused several new specifications to be written around them.

All continuous organic films are permeable to some degree by moisture[81] and paint coatings either have defects or acquire them in service. Consequently, it is general practice to supplement the physical protective properties of coatings with provision for electrochemical activity, and this is usually done by chemical conversion coating.

A good example illustrating the wide range of useful properties displayed by conversion coatings is the finish of the Echo II satellite. In order to establish passive temperature control a chemical conversion coating was used to alter the thermal radiation

properties of the metal surfaces. A chromate-phosphate coating with a weight of 215 mg/dm^2 provided a ratio of solar absorptivity to emissivity such that the temperature would not rise to the point of weakening the aluminium laminate structure(82).

2.2 Early Conversion Coatings

The function of a conversion coating is to replace the naturally occurring oxide film found on aluminium with a corrosion resistant film to which organic coatings will bond well. This was once done by anodising which is acknowledged as the best corrosion-resistant treatment available for aluminium. However anodising has several disadvantages, including cost and production time. Painted articles do not generally require such good corrosion resistance, but they do need a surface to which adhesion is strong.

The first conversion coating was developed in Germany by Bauer and Vogel in 1915 although the idea was first suggested in 1857 by Buff[83] The original solution was an alkaline bath in which pure aluminium required treatment time of 2 to 4 hours at temperatures of 90 to 95°C. It was further developed and then patented in 1923[84].

The treatment time for the improved solution was still very long when compared to modern processes. The addition of an aluminium compound to act as a catalyst reduced the process time to between 30 and 60 minutes. The coating formed having been rinsed and dried was light-grey but would appear darker with longer treatments. It was claimed to adhere well even if it was subsequently bent and to have good corrosion resistance to neutral salt spray and sea water. The registration of this patent signalled the start of much work to find a solution that would produce a protective coating in much shorter times.

A process based on the original solution was developed in 1930 by Eckert[85,86] and is known as the Modified Bauer-Vogel (MBV) process.

The solution contained sodium carbonate and sodium chromate in a ratio of about 3 to 1 and operated at a temperature of 90-100°C. This process produced a light grey to dark grey coating depending on the processing time and was found suitable for the application of paint or could be sealed for additional corrosion resistance. Further, this process was found to work for aluminium and aluminium alloys low in copper and required treatments times of 3 to 5 minutes.

The coating formed was described as a chemically thickened oxide film. The precise mechanisms are not known but the following have been suggested.

Aluminium is known to form hydrous oxides in water according to [87]:-

$$Al \longrightarrow Al^{3+} + 3e$$

$$3H_2O + 3e \longrightarrow 3HO^- + 2/3\ H_2$$

$$2Al^{3+} + 6OH^- \longrightarrow Al_2O_3\ nH_2O + (3 - n)\ H_2O$$

where n lies between 0 and 3

To prevent the oxide film from completely stifling further reaction the coating solution must contain an attacking agent; in alkaline solutions this is the OH^- ion. Thus the balance of ingredients in operating solutions is of prime importance. Many chemical oxide thickening solutions contain chromium and Schenk[88] suggests the production of aluminium oxide as well as chromic oxide due to secondary reactions of the chromate on aluminium

$$2Al + 2Na_2CrO_4 \longrightarrow Al_2O_3 + 2Na_2O + Cr_2O_3 \qquad -(1)$$

This is only a secondary reaction however, the main reaction agent in the MBV solution is thought to be sodium carbonate (89):-

$$2Al + Na_2CO_3 + 3H_2O \longrightarrow 2\ Na\ AlO_2 + CO_2 + 6H \qquad -(2)$$

$$2\ Na\ AlO_2 + H_2O \longrightarrow Al_2O_3 + 2NaOH \qquad -(3)$$

and the reduction of sodium chromate takes place by the action of the hydrogen ions produced in reaction (1) by

$$2Na_2\ CrO_4 + 6H \longrightarrow Cr_2O_3 + 2Na_2O + 3H_2O \qquad -(4)$$

It is not known to what degree reaction (1) and (4) take place, but it is known that the chromate in solution tends to inhibit to some extent the attack of the alkaline solution on the metal. Coating characteristics such as thickness, porosity, physical and mechancial properties will largely depend on the nature of the inhibitor, solution temperature and substrate.

A modification of the MBV process which produces a nearly colourless coating is the Erftwerk (EW) process (90,91). Additions of silicates or fluorides are used to slow down the attack of the chromate, decreasing the chromate content of the coating and reducing colouring. The corrosion resistance is somewhat better than that of the MBV process even though the coatings are thinner. As a result of sodium silicate forming in the coating the pore spacing is decreased, thus the rate of formation is reduced. As a consequence EW coatings are not suitable as a paint base and are rather more expensive to produce than MBV coatings. The EW process can be used on alloys, such as Duralumin or high-strength alloys, which the MBV process is not easily applied. Further advantages of EW coatings are

that they do not fingerprint, may be dyed, have improved abrasion resistance and a smooth finish.

Another modified version of the MBV process is known as the LW process developed by the Vereingte Aluminium Werke AG (92). In this version disodium phosphate is added to the MBV solution. LW coatings like EW coatings are colourless and have improved corrosion resistance over MBV coatings. Unlike EW coatings LW coatings can be painted successfully but again are thinner and more expensive than MBV coatings.

By this time a number of systems were being developed in the UK and US. Alrok is an example of a American process similar to MBV which uses a solution of 2 - 3 percent sodium carbonate as the dissolving constituent and 0.1 - 0.5 percent alkali dichromate as a film forming agent. In the UK the Pyrene Co Ltd developed a process that employs additions of carbonate of a heavy metal to the MBV solution. This was known as the Pylumin process, and had two distinct advantages over the MBV process.

i) It is a long lasting bath able to be kept at optimum conditions by regular chemical additions.

ii) Gives a good covering on alloys containing heavy metals.

2.3 Chromate-Phosphate Coating Solutions

The single most important development in conversion coating technology was announced in 1945 when F P Spruance Jr of the American Chemical Paint Company registered a patent[93] that described the production of chromate-phosphate coatings. This process was known as the Alodine process in the US and was introduced in the UK by ICI Ltd as the Alocrom 100 process.

In contrast to the early chemical conversion processes the Alocrom process is acidic and can not be described as a 'chemical oxidation process'. In fact it has been described as the intermediate stage between chemical oxidation and phosphating[75]. It differs from phosphated coatings in that the Alocrom 100 coatings are compact and amorphous rather than the crystalline structure typical of phosphated coatings.

The basic components of the chromate-phosphate bath are

1. Chromium trioxide as chromic acid
2. Phosphoric acid
3. Hydrofluoric acid

These constituents may be successfully used within a relatively large range of compositions. The original patent included a diagram showing this range and the optimum composition line.

This diagram is very useful as not only does it clearly show the region of optimum conditions but it also indicates the expected result of operating a bath which is out of balance.

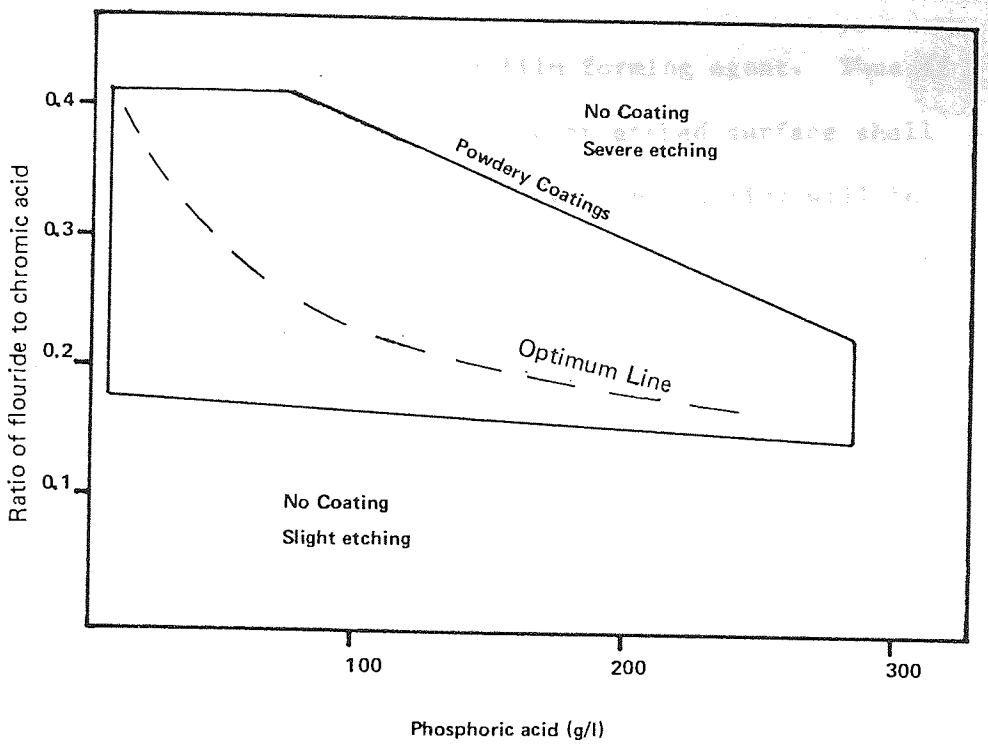

Figure 2.3.1 Operating range of Alocrom 100 process (after Spruance [93])

The optimum range of the solution is

PO_4^{---}	20 to 100 g/l
F^-	2 to 6 g/l
CrO_3	6 to 20 g/l

with the ratio of fluoride to chromic acid (F^-/CrO_3) between 0.18 and 0.36 with an optimum value of 0.27.

The phosphate ion content is important as it has a sensitivity effect on the fluoride to chromic acid ratio. Should the phosphate ion concentration fall below 6 g/l then solution control is difficult as the F^-/CrO_3 ratio must be kept within a narrow range in order to get a coating on the metal.

The ratio of fluoride to chromic acid, is basically the ratio between

oxide film attacking agent and the film forming agent. Thus if this ratio is too high a loose coating or etched surface shall result; if it is too low a thin coating or no coating will be produced. Another factor greatly influencing the coating is the acidity of the solution. Spruance states that the total acidity must not exceed that corresponding to 3.0 normal acid(93). Acidity is usually measured in terms of pH, but unfortunately no accurate means of measuring pH in these solutions has been found. pH indicators are unreliable because the dichromate ion present in solution oxidizes them. Similarly the hydrogen and quinhydrone electrodes can not be used because of the oxidizing effect of the dichromate. The electrical pH meter is also unreliable as the glass electrode is attacked by the fluoride present in the solution. Spruance(93) has recognised this problem and suggests that pH is best measured with a glass electrode. He found that although the readings obtained exhibit a "curious excursion with time", going from a low value to a higher value then back to an even lower value, the final nearly - steady pH reading or the lowest value indicated within the first 10 minutes has some significance. Using this technique the pH should remain within the range of 1.6 to 2.2 and preferably within 1.7 to 1.9. If the acidity is too low a thin coating or no coating is formed. If the acidity is too high, loose powdery coatings form, or badly etched surfaces result if the acidity is much too high.

The state of the coating itself may be used to gauge any adjustments necessary to the bath in the absence of a suitable pH meter. The rates of consumption of the ingredients are approximately:-

F^- = 1.1 g/dm^2 (of aluminium surface area)

CrO_3 = 0.75 - 1.5 g/dm^2

$PO_4 3-$ = 0.54 - 1.1 g/dm^2

Acid = 0.065 - 0.15 g/dm^2 (g equivalent replaceable hydrogen)

Another major advantage of this process over the numerous chemical oxide thickening solutions is that the operating temperature covers a wide range. At room temperature the optimum coating thickness is produced in five minutes, but at increased temperatures processing times are greatly reduced as shown in figure 2.3.2. Further reductions in processing times can be achieved by using a spray-technique instead of dipping. Process times in the order of 20 seconds can be obtained this way, these coatings tend to be thinner and more compact than dip coatings.

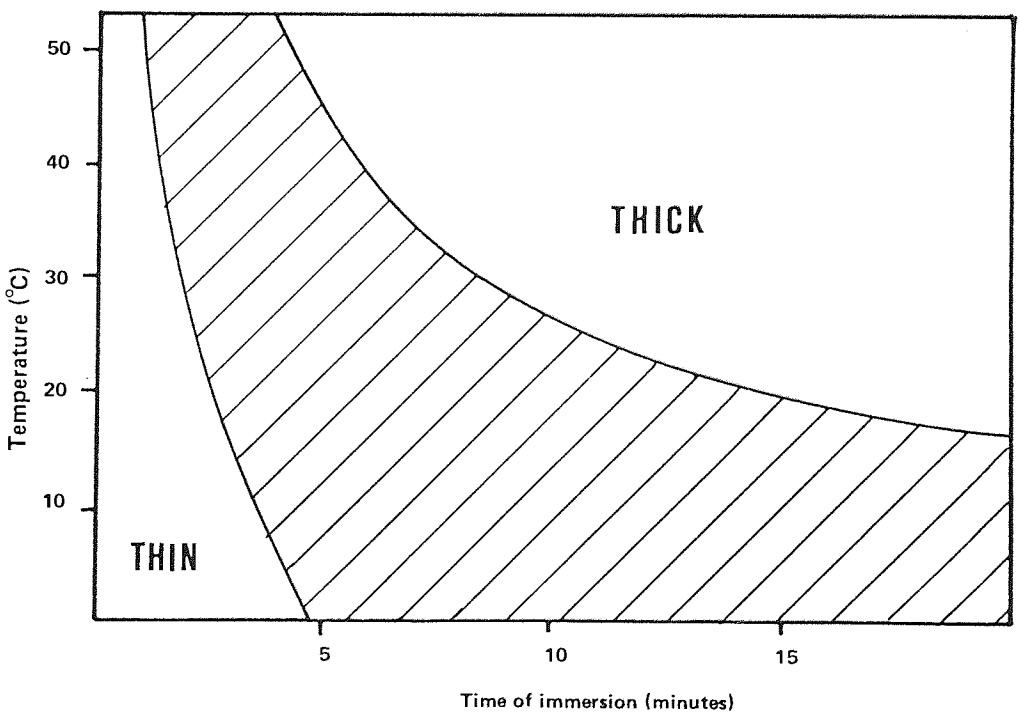

Figure 2.3.2 Effect of operating time and temperature on coating thickness (Alocrom process) (after Wernick and Pinner [75])

It has been reported that a reversal in the rate of growth exists between 55°C and 60°C[75]. The reason for this is not known although it does correspond to a decrease in the rate of dissolution of aluminium in the solution.

Another great advantage of this type of bath is that the original bath can be used for many years simply by replacing the ingredients lost in the coatings produced. The level of dissolved aluminium in the bath is controlled by precipitation. Salts such as cryolite (Na_3AlF_6) or elpasolite (NaK_2 AlF_6) occur depending on the cations introduced.

The build-up of aluminium in the bath would result in coatings becoming whiter and powdery. Therefore the precipitation mechanism is of vital importance for the day to day maintenance of the bath.

2.4 Chromium-Chromate Solutions

The most widely used aluminium pretreatment used in industry today is known as chromium-chromate. Introduced about 25 years ago it has been used extensively in coil-coating and extrusion painting of aluminium. Chromium-Chromate coatings provide considerably more corrosion resistance than chromate-phosphate coatings when unpainted. However chromate-phosphate solutions do have two advantages over chromium-chromate[94]; firstly, they are considered to be non-toxic and secondly they aid cleaning. The cleaning stage is of vital importance when chromium-chromate coatings are produced.

A wide range of coating weights can be produced, from 5 mg/dm^2 which is colourless to 200 mg/dm^2 which has a dark brown appearance. The coatings are also influenced by 'ageing' the solution. Contaminated solutions produce darker coatings. Leaching fresh coatings in hot water reduces the colour but also reduced the corrosion resistance, more so if high purity water is not used.

The basic ingredients are as follows:-

Chromium trioxide	CrO_3
Hydrofluoric acid	HF
Potassium ferricyanide	$K_3Fe(CN)_6$

Potassium ferricyanide was not used in the first chromium-chromate solutions developed in the early forties, but they became popular because of their low cost, simplicity and excellent unpainted

corrosion resistance. The coating weight produced by these unaccelerated solutions ranges from 5 to 80 mg/dm^2 and are golden in colour.

It was soon found that the rate of coating build-up would be increased dramatically by the addition of potassium ferricyanide. Solutions with this addition are known as accelerated chromium-chromate. They have become popular throughout industry because of the short treatment times required as well as the properties found in the unaccelerated solutions.

Newhard found that these coatings suffer from thermal degradation when heated above 70°C [79,94], the corrosion resistance to salt spray drops off proportionally to the rise in temperature. Complete breakdown was noted at a temperature of 300 - 320°C, however it is not clear how much of this was due to degradation of the coating and how much due to a breakdown in the metallurgical structure of the substrate.

The film thickness for a coating weight of 100 mg/dm^2 has been calculated to be 600Å. Freeman and Triggle [95] studied the variation of coating weight and colour with immersion time and temperature for a chromium-chromate solution, shown in figure 2.4.1. They found a reversal in the rate of coating growth similar to that found in chromate-phosphate solutions. The immersion time at which this reversal was seen decreased with increasing temperature.

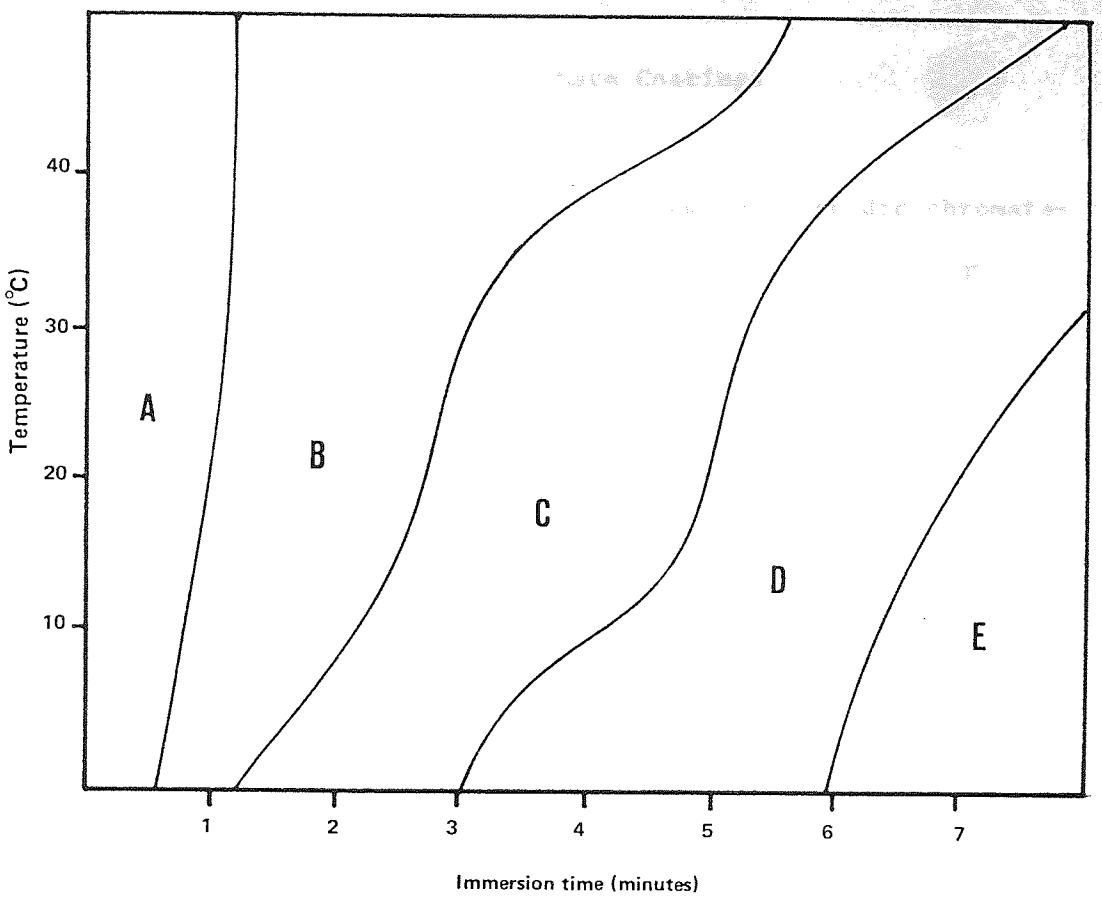

Figure 2.4.1 Variation of weight and colour of coating produced in an acid chromium-chromate solution with time of immersion and temperature (after Freeman and Triggle [95])

A No Coating

B Irridescent Coating 5.4 mg/dm^2

C Yellow Coating 8 mg/dm^2

D Golden-Yellow Coating 10.3 mg/dm^2

E Brown Coating

2.5 Composition of Chromate-Phosphate Coatings

The coating produced by immersion of aluminium in an acidic chromate-phosphate or chromium-chromate solution is formed as a gel. The gel is weak and can easily be damaged before it is dried. The coating loses about 40 percent of its weight on drying and becomes increasingly corrosion resistant(75).

Before drying the coating can be removed by immersion in 70% nitric acid. However, once the dry coating has formed, nitric acid cannot easily remove it.

Early analysis of chromate-phosphate coatings involved wet analysis of stripped coatings(79). The postulated composition of the coating based on wet analysis was:-

$$Al_2O_3 \cdot 2CrPO_4 \cdot 8H_2O$$

This result was tested by Newhard(79) using thermogravimetric analysis. He found that a total weight loss of 26.1% occurred when the dried coating was heated from 80°C to 800°C, this is in near agreement with the expected result if all the water of hydration was removed from the above formula.

Nimon and Korpi(96), who were working on chromate-phosphate coatings at about the same time, came to the conclusion that fresh coatings consisted essentially of hydrated chromium phosphate. However, they also stated that the dried coating consisted of both hydrated chromium-phosphate and hydrated aluminium-phosphate with trace amounts of

Al_2O_3. The hydrated chromium and aluminium phosphate were said to exist in roughly the same relative amounts. However, this result is inconsistent. If before heating, the coating is hydrated chromium-phosphate and after heating half hydrated chromium-phosphate and half hydrated aluminium-phosphate, then either extra phosphate appears from somewhere or some chromium is lost somewhere. This is necessary to account for the phosphate required to produce hydrated aluminium-phosphate. Obviously this is not possible.

In a more recent paper by Treverton and Davies[97] modern surface analysis techniques were used to investigate aluminium pretreatment coatings. X-ray photoelectron spectroscopy (XPS) was used in conjunction with ion etching in order to obtain detailed depth profiles of the various coatings. They found that the major elements present in the coating were chromium, phosphorus and oxygen. Only relatively small amounts of fluorine and aluminium were found. In the early stages of analysis of the surface layers of the coating, the percentages of chromium and phosphorus were equal. This suggests that one of the major components in the top part of the coating was chromium-phosphate.

The ratio of oxygen to either chromium or phosphorus was 5.1, suggesting that some water of crystallisation remained in the coating. As analysis of the coating continued the chromium content rose slightly whereas the phosphorus and oxygen levels decreased as shown in Figure 2.5.1. This indicated that not all of the chromium can be accounted for as its phosphate salt. This can be explained if the excess chromium is present as the oxide $Cr_2O_3.xH_2O$ which increased in concentration in the regions close to the metal

interface. The other observed element was fluorine which remained at an almost constant level throughout the coating, and only began to decrease when a significant amount of aluminium has appeared. At this stage both chromium and phosphorus were decreasing rapidly in concentration thus aluminium fluorates were concentrated at the metal/coating interface.

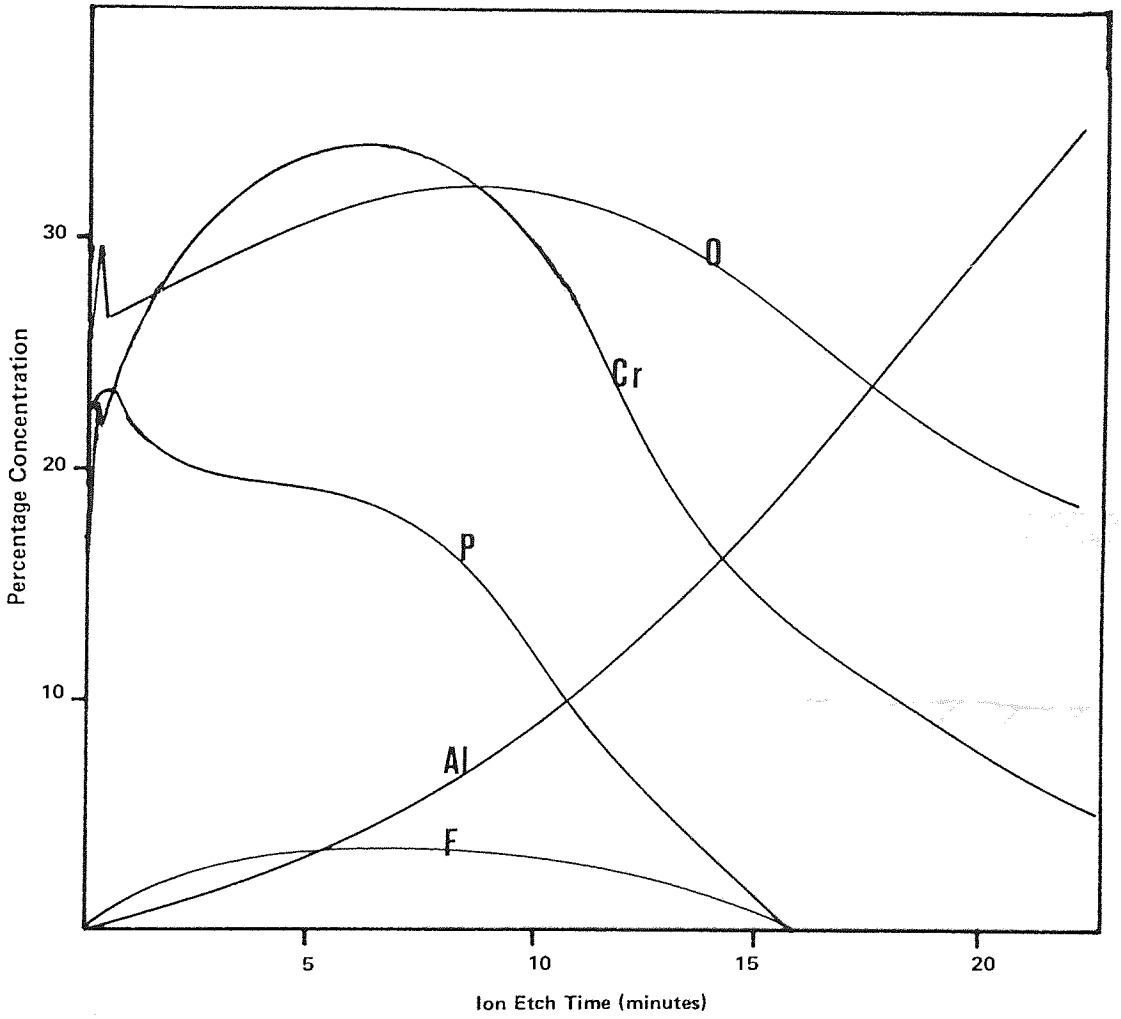

Figure 2.5.1 Variation of percentage of element present in chromate-phosphate coatings during ion etching (after Treverton and Davies[97])

Treverton and Davies also noted that the decrease in oxygen concentration near the coating interface is not as rapid as both the chromium or phosphorus. This suggests the presence of aluminium oxide or oxyfluorides at the interface.

They therefore concluded that the main component in the coating was a hydrated form of chromium-phosphate, and the principle minor component was chromium oxide which was found in regions near the coating/metal interface.

At the interface small amounts of aluminium oxides and fluorides were found. These results were summarised as a sketch, shown in Figure 2.5.2.

The possibility, that aluminium phosphate was present in chromate-phosphate coatings has been ruled out by Treverton and Davies, who suggest that since the phosphorus and aluminium profiles were completely independent aluminium phosphate is totally absent from the film.

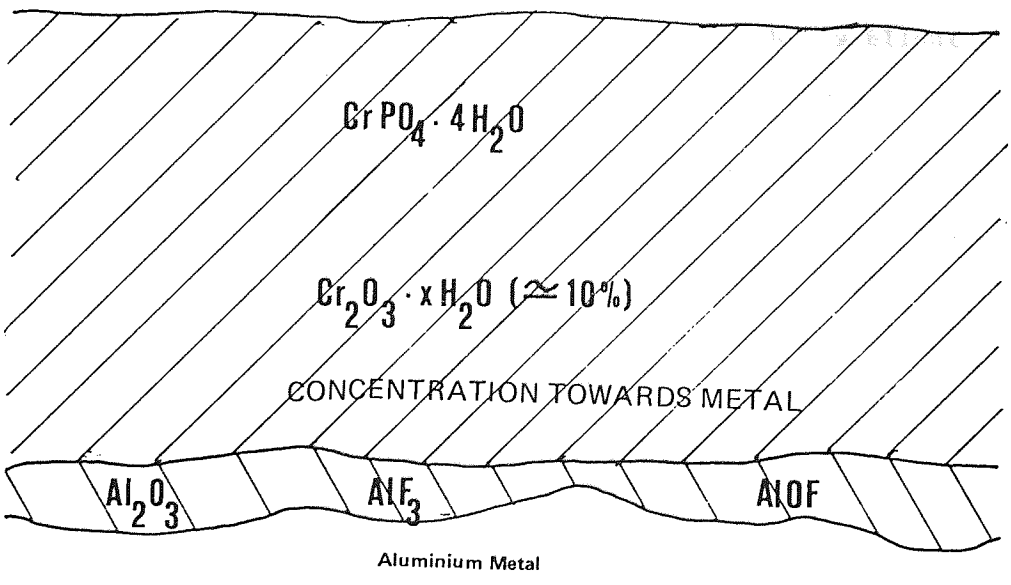

Figure 2.5.2 Structure of Chromate-phosphate conversion coating. (after Treverton and Davies[97])

2.6 Composition of Chromium-Chromate Coatings

Chromium-chromate coatings have a similar gel-like appearance to chromate-phosphate coatings before heating. The main visible difference between the two coatings is colour, obviously chromium-chromate coatings contain no phosphorus. Early wet analysis together with TGA and Infa-Red(IR) spectral analysis indicated an empirical formula[79] for:-

i) Unaccelerated

$$Cr(OH)_2\ HCrO_4\ .\ Al\ (OH)_3\ .\ 2H_2O$$

ii) accelerated

$$CrFe\ (CN)_6\ 6Cr\ (OH)_3.\ H_2CrO_4\ .\ 4Al_2O_3\ .\ 8H_2O$$

It was thought that hexavalent chromium was present in fresh coatings, and that this was in someway responsible for the excellent corrosion resistance obtained from these coatings. Zelley[98] concluded in a report on "improved conversion coatings on aluminium" that hexavalent chromium acts as an anodic inhibitor in the coating. He further stated that thermal treatment decreases the corrosion resistance by rendering the hexavalent chromium less soluble and thus preventing it from being leached in a sufficient amount to serve as an inhibitor.

This idea was supported by other workers[99,100] who believed that hexavalent chromium was present in fresh coatings and available for leaching into scratched or damaged areas.

However, Sunderland[101] suggested that the corrosion resistance of chromium-chromate coatings was due to the amorphous insoluble gel-like film that acts as a barrier to a corrosive medium, the hexavalent chromium inhibits corrosion should the barrier become penetrated. Sunderland used Auger Electron Spectroscopy (AES) Secondary Ion Mass Spectroscopy (SIMS) and Ion Scattering Spectrometery (ISS) in his investigations. He concluded that the aluminium oxide was largely converted to the chromium oxide Cr_2O_3 as the photoelectron spectrum showed chromium to be in the trivalent state.

Treverton and Davies studied accelerated chromium-chromate coatings alongside their study of chromate-phosphate coatings using XPS[97]. An analysis of the surface showed that it contained carbon, nitrogen iron, chromium and oxygen. It was thought that ferricyanide occurs as its chromium salt, $CrFe(CN)_6$, since an atomic ratio of nitrogen to iron of 6:1 was found and chromium is the only element in the solution likely to be a suitable cation. However this does not account for all of the chromium present on the surface thus it was concluded that the surface consists of chromium ferricyanide and chromium oxide in a molar ratio of 2:1.

Ion etching produced marked changes in the spectra, which were plotted as atomic percentage against ion-etch time, shown in Figure 2.6.1. It is noticeable that concentrations of iron, carbon and nitrogen fall rapidly as the film is etched away. This suggests that chromium ferricyanide is present mainly at the surface and not in the bulk coating.

The major coating components are chromium and oxygen with a concentration ratio of between 1:1.5 and 1:2. This points to the major component of the coating being a hydrated form of chromic oxide, $Cr_2O_3 . xH_2O$, where x = 1 or 2.

Hexavalent chromium compounds were not found in the coating and this was not thought to be due to any reduction effect caused by the ion etch beam. Fluorine was found as a minor constituent throughout the film but was seen to increase in concentration at the coating/metal interface.

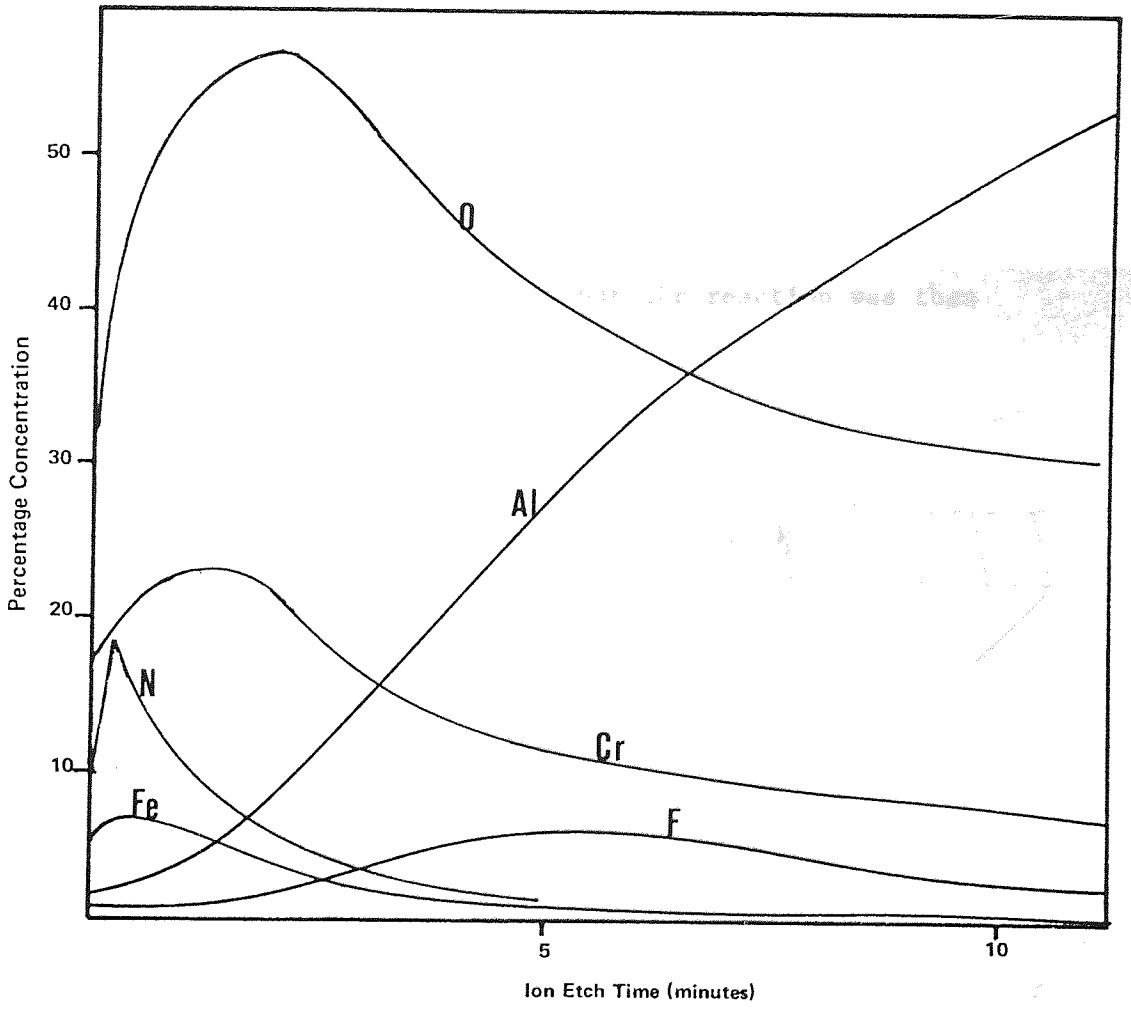

Figure 2.6.1 Variation in percentage of constituents in chromium-chromate coatings during ion etching (after Treverton and Davies[97])

The dependence of the fluorine concentration upon the aluminium concentration suggests that fluoride is present as an aluminium fluoride. Aluminium oxide was also shown to be present at the coating/metal interface since there is a divergence betweeen the chromium and oxygen profiles at this point.

These results have been summarised as a sketch shown in Figure 2.6.2. Treverton and Davies[102] suggest that the reason that no hexavalent chromium was found, in contrast to other workers[79,98,99,100,101], was that all the coatings they studied were more than 24 hours old. The previous results were obtained from freshly formed coatings that may not have completely reacted with the surface. This suggestion is supported by Reeves and Newhard[103] who found that hexavalent chromium was no longer leachable from the coating after 24 hours, which could indicate that the reaction was then complete.

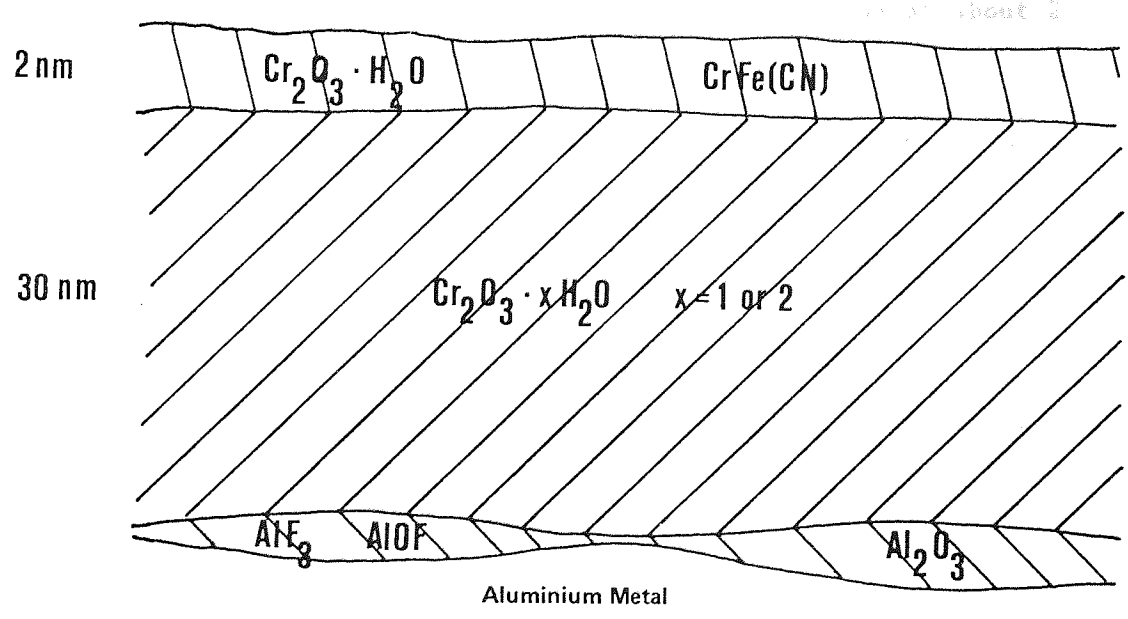

Figure 2.6.2 Structure of chromium-chromate conversion coating (after Treverton and Davies [97])

2.7 Mechanisms of Coating formation: Chromate-Phosphate

The results obtained by Treverton and Davies[97] for chromate-phosphate coatings are of great interest because it is possible to deduce a general mechanism for coating growth. The following was suggested[97]:-

The reduction of the hexavalent chromium during coating formation is consistent with the appearance of trivalent chromium in the coating. This must have occurred at the aluminium metal surface since this is the only reducing agent available.

$$Cr^{VI} + 3e \longrightarrow Cr^{III}$$

$$Al(Metal) \longrightarrow Al^{3+} - 3e$$

This redox reaction cannot occur without the naturally occurring oxide film being penetrated or removed. The predominant fluoride species at a pH of about 1.5 and fluoride concentration of about 2 x 10^{-2}M is HF[104]. Traces of fluorine were found at the metal/film interface suggesting that HF present in the solution was attacking or removing the oxide film.

$$Al_2O_3 + 6HF \longrightarrow 2AlF_3 + 3H_2O$$

A reduction of chromate ions then occurs at the metal surface which can be shown as the following overall reaction:

$$8H^+ + 2HCrO_4 + 2Al\ (Metal) \longrightarrow 2Al^{3+} + Cr_2O_3 \cdot 3H_2O + 2H_2O$$

The occurrence of chromium-chromate has been reported in fresh

coatings[79,103], and more recently hexavalent chromium has been found on the coating surface[94]. This suggests that there is an intermediate stage in the above reaction such as:-

$$Al\ (metal) + 5H^{+} + 2HCrO_4 \longrightarrow Al^{3+} + Cr(OH)_2\ HCrO_4 + H_2O$$

and

$$Al\ (metal) + 3H^{+} + Cr(OH)_2\ HCrO_4 \longrightarrow Cr_2O_3 \cdot 3H_2O + Al^{3+}$$

Once the coating is removed from the solution a similiar type of reaction must occur since no hexavalent chromium has been found on coatings more than 24 hours old. The reaction is:-

$$Al\ (metal) + Cr(OH)_2\ HCrO_4 + 2H_2O \longrightarrow Cr_2O_3 \cdot 3H_2O + AlOOH$$

The final proposed reaction concerns the formation of the major component of the coating, chromium-phosphate, which was found above the chromium oxide in the film. This could be formed by:-

$$Cr_2O_3 \cdot 3H_2O + 2H_3PO_4 \longrightarrow 2CrPO_4 + 6H_2O$$

These reactions successfully account for most components found in the coating, and may also be found in chromium-chromate film growth mechanisms (except for the last reaction).

2.8 Mechanisms of Coating Formation: Chromium-Chromate

Chromium-chromate coatings can be produced from either accelerated or unaccelerated solutions. The difference is mainly the addition of ferricyanide ions to the accelerated solution. Thus both types of solution depend on a balance between fluorine and chromium ions and so probably have similar mechanisms of coating growth.

Early work using modern techniques of analysis was done by Abd Rabbo et al(105) using secondary ion mass spectrometry to examine the coating surface.

Super purity aluminium was anodized to give a barrier coating of 72 nm which was then immersed in an unaccelerated chromium-chromate solution. Coating profiles were obtained from samples with increased immersion times to show the action of the solution on the oxide film against time.

In the first minute the film was attacked by fluorine ions shown by a peak at the solution/oxide interface for F^+ concentration. At this time a second peak was observed at the oxide/metal interface despite little or no evidence of penetration of the oxide film. It was thought that access to the oxide/metal interface was gained via flaws in the coating. The presence of F^- at the oxide/metal interface caused undermining of the anodic film.

The Cr^+ ion was also present at the coating surface, some of this was as a result of plugging of the flaws by hydrated chromium oxide produced by reduction at cathodic sites, but some are due to

chromate/dichromate ions that have penetrated the intercrystallite regions of the film. After 6 minutes immersion the oxide film has been thinned considerably, however, the three profiles are basically the same as before except for the Cr^+ profile which had increased.

After 15 minutes of immersion the oxide film had been completely removed and replaced by a conversion coating of normal thicknesss (about 150 nm). The F^- ion was concentrated at the metal/coating interface but was also present at a lower concentration throughout the coating. The Cr^+ ion concentration was relatively constant throughout the coating, as was the Al^+ concentration. Ion images however showed some interesting results.

The chromium distribution was found to be laterally uniform, yet the aluminium and fluoride distributions were seen to have a local lateral distribution. This was explained as showing that the bulk of the coating consists mainly of hydrated chromic oxide. This was essentially amorphous but contains a cellular-like structure, aluminium and fluoride being concentrated in the inter-cellular regions, probably as a complex oxyfluoride.

In a subsequent paper[106] a similar technique was used with ultramicrotome and transmission electron microscopy (TEM) to study the development of chromium-chromate coatings. It was suggested that the aluminium oxide film was removed by the formation of soluble aluminium complexes with fluoride which prevent the repassivation of the surface. The metal/coating interface was seen to be relatively flat, since the coating mechanism is electro-chemical, involving local anodes and cathodes this points to

continuously shifting active sites.

The ultramicrotomed section showed fine "pathways" through the coating. Thus it was suggested that:-

The coating precipitates as a gel-like substance. Through this gel fine pathways are formed which provide access to the substrate for the solution. However at these sites anodic dissolution may occur and cathodic activity rapidly results in the production of conversion coating which will block the pathways. New pathways are opened up due to the complexing action of the fluorine ions and further reaction results. In this way the flat metal/coating interface may be maintained without excessive chemical conversion occurring at any site.

In a paper presented by Treverton[107] the mechanisms of coating growth were outlined and the influence of the ferricyanide ion in accelarated coatings was considered. Treverton agrees with previous work[105,106] that has shown the role of the fluorine ion in chromium-chromate solutions and shows this as:-

$$Al_2O_3 + HF \longrightarrow AlF_3 \text{ (or AlOF)} + H_2O$$

He also agrees that the role of the chromium ions was to react with the aluminium metal to form hydrated chromic acid, and states that the reaction for this is:-

$$Al + 4H+ + Cr_4^{2-} \longrightarrow Al3+ + Cr(OH)_3 + OH-$$

Of course in addition to this reaction aluminium atoms could react

with water to form aluminium oxide or the aluminium ions produced by the above reaction could precipitate out as aluminium hydroxide. Treverton states that an additional role of the fluorides in the process is to continually remove these oxides as they are formed.

In essence this is in agreement with Furneaux et al[106] when they describe the production of fine pathways through the coating as it is formed. In a previous paper[97] Treverton and Davies found that that ferricyanide could be detected only on the surface of accelerated chromium-chromate coatings. Treverton[108] explained that this was due to the nature of the ferricyanide in its role as an accelerator. The absorption of ferricyanide on the coating surface prevents the adsorption of chromates on the same sites, so increasing the chromate concentration in the solution at the coating/metal interface and the rate of reduction to form the coating. In a paper by Treverton and Davies[102] published at the same time, a more detailed study using XPS was presented of the location of the ferricyanide. It was found that the bulk of the ferricyanide was absorbed on the surface of the growing coating. However, it was also found that ferricyanide was also present throughout the coating, and further, that the results were consistent for elements found in thin layers of spherically shaped particles.

These findings support the idea that coating growth occurs by reduction of hexavalent chromium at the metal surface (after the oxide film has been removed by the action of fluoride), chromium oxide precipitates on the surface as spherical particles onto which ferricyanide is absorbed. This causes an acceleration in the rate of hexavalent chromium reduction, so the coating is formed at an increases rate of growth.

The coating thickness itself is self-limiting[94] possibly due to the electronic resistance of the coating, which increased in proportion to the coating thickness, screening the metal from the oxidizing potential of the solution. An alternative possibility is that after the initial formation of the coating, the chromium oxide being deposited on the surface is being dissolved at the same rate at which it is produced.

The effect of pretreatment time was also reported by Treverton[107] who did not comment on any self-limiting mechanism, possibly as this effect may not be obvious on accelerated coatings. However for short periods of pretreatment an oxide layer was present between the pretreatment coating and the metal. Longer periods of pretreatment lead to a decrease in the amount of oxide remaining at the film/metal interface. This shows that much of the oxide film removed occurs from beneath the growing chromate coating.

It was also stated that solutions contaminated with more than 600 ppm of metallic magnesium resulted in almost total inhibition of film formation.

This may be due to magnesium precipitating the fluorides from solution inhibiting the removal of the oxide film. This is an important factor when considering pretreatment failures in industry. When processing aluminium alloys containing magnesium the amount of magnesium in the solution may build up to a level of about 600 ppm, sudden failure of the pretreatment could then result.

The effect of contamination of chromium-chromate solutions by aluminium metal is less critical, however an increase of aluminium and fluoride levels in the coating were noted[107] in coatings produced in aluminium metal contaminated solutions.

Fluoride concentration was altered to study its effect on conversion coatings[107]. An increase in fluoride concentration had a marked effect on the levels of both aluminium and fluoride in conversion coatings of similar thickness, increasing proportionally to the increased fluoride in the solution. When the fluoride content was reduced from the optimum level the composition profile was not much altered, although coating growth was slower.

This result is consistent with the general mechanism for coating production whereby competing reaction for the aluminium surface by fluorides, water and chromates was suggested. When the concentration of fluoride is high, a large amount of aluminium fluoride is formed and becomes trapped in the coating. It is generally accepted that excess fluoride in the pretreatment solution leads to embrittling of the film.

Unaccelerated chromium-chromate coatings were studied independently by Katzman et al[94] in 1979. They used XPS in conjunction with ion beam sputtering to study coatings both before and after exposure in a salt-spray cabinet. Two types of chromium-chromate coating were studied, an alkaline MBV solution (as previously described in section

2.2) and the acidic STC solution which is made up of:-

CrO_3	4 g/l
$Na_2\ Cr_2O_7\ 2H_2O$	3 g/l
NaF	0.8 g/l

This is a similar solution to that used by Treverton and Davies(97) but without any ferricyanide accelerator.

Auger analysis of the MBV and STC coatings resulted in depth profiles which were very similar, except that the MBV depth profile had no fluoride present and was three times as thick as the STC coating. It is stated that the thickness of the STC coating does not increase after 30 seconds immersion in the solution, although the amount of aluminium found in the solution does increase with time.

It was also noted that STC coatings become thicker at lower solution temperatures, but no change in corrosion protection was observed. Varying the F^- concentration by a factor of 10 in either direction resulted in thin coatings with very poor corrosion resistance.

Using the results obtained by Auger and XPS a general mechanism of growth was proposed for both types of coating, only the STC coating shall be reported here, however both coatings had very similar mechanisms. Agreement is found here with mechanisms proposed by Treverton and Davies(97) for accelerated chromium chromate coatings. However the reactions have been changed slightly.

The first step is penetration of the oxide film on the surface. HF is the predominant fluoride species in the solution, so

$$AlOOH + 3HF \longrightarrow AlF_3 \text{ (soluble)} + 2H_2O$$

Valand and Nilsson[109] have suggested that fluoride ions incorporated into aluminium oxide coatings increase the rate of both cathodic and anodic reactions. They explain this effect by assuming that the F^- ions replace some of the O^- ions in the oxide since the ionic radii are similar. The change in charge distribution will increase both ionic and electronic conductivity, and hence, increases the rates of the electrode reactions.

An interesting experiment was conducted on the role of fluoride after the removal, or penetration of the oxide film[94]. An aluminium specimen was immersed in the STC solution for 5 seconds, then quickly transferred without rinsing to a similar solution free from fluoride. A thin coating with poor corrosion resistance resulted, showing that fluoride plays an important role throughout the production of the coating.

The reaction for reduction of hexavalent chromium was shown as:-

$$Cr_2O^{2-} + 2Al + 2H^+ + H_2O \longrightarrow 2CrOOH + 2AlOOH$$

The precipitation of hydrated mixed oxide on the aluminium metal surface begins the coating growth.

The AlOOH in the mixed oxide is then dissolved by the hydrogen fluoride, leaving the less soluble CrOOH on the surface. Any weak spots in the coating provide access to the aluminium surface for the

solution, as coating growth continues these weak spots become clogged with impervious hydrated chromium oxide.

$$2Al + Cr_2O^{2-} + 2H^+ + 6HF \longrightarrow 2AlF^3 \text{ (soluble)} + 2CrOOH + 3H_2O \quad (1)$$

Some of the weak spots may be created by the fluoride ions that become incorporated into the coating.

The CrOOH that is deposited on the surface is somewhat soluble in the STC solution, so:-

$$CrOOH + 3HF \longrightarrow CrF_3(\text{soluble}) + H_2O \quad (2)$$

This indicates that a continuous process of coating deposition and dissolution is taking place. This can be represented as the sum of equations (1) and (2):

$$2Al + Cr_2O^{2-} + 2H^+ + 12HF \longrightarrow 2AlF_3 + 2CrF_3 + 7H_2O$$

Katzman et al also state that as the coating begins growth aluminium metal is oxidised at the metal/oxide interface, as electrons are being drawn through the oxide film by the oxidising action of the chromate ions adsorbed on the surface. A concentration gradient develops across the oxide film since Al ions are dissolved by the solution at the oxide surface. This process is shown schematically in Figure 2.8.1.

This is in direct agreement with observations noted by Treverton(107) for accelerated chromium-chromate coatings, in which the oxide film was seen to be present beneath a layer of hydrated chromium oxide for

short pretreatment times. Further, it is in agreement with results reported by workers at UMIST[95,106] studying unaccelerated chromium-

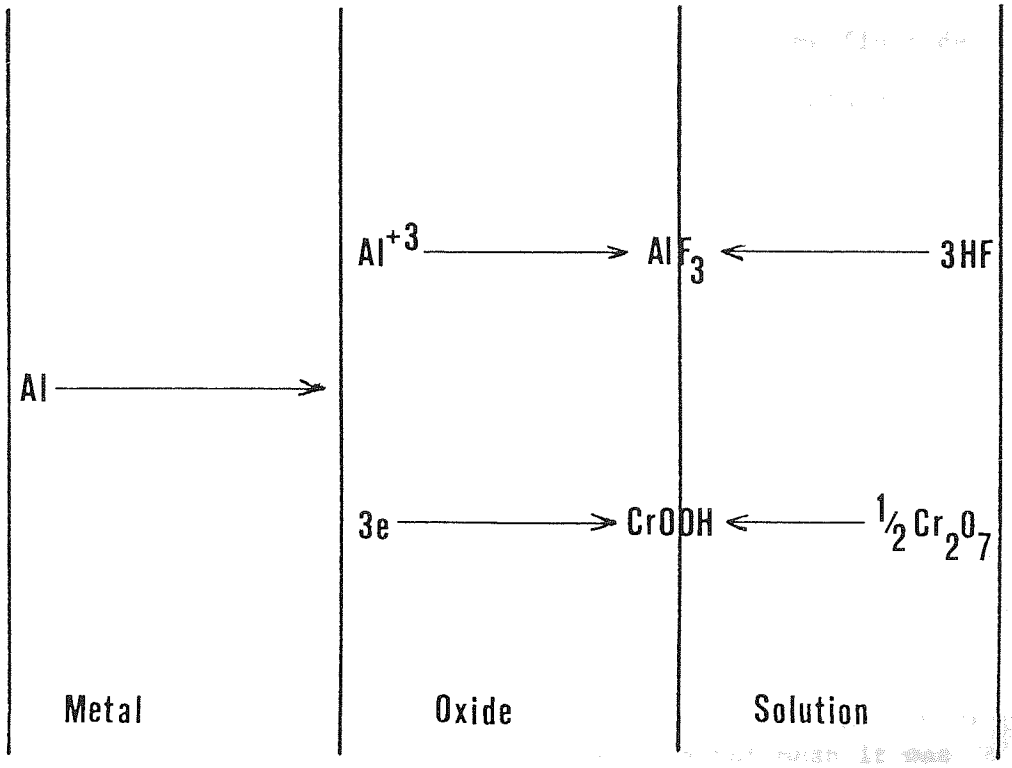

Figure 2.8.1 Mechanism of Coating growth (after Katzman et al [94])

chromate coatings formed on anodized aluminium.

The model of film formation and dissolution satisfies the requirement for self limiting coating thickness reported by Katzman et al[94], it also explains the observation of thinner coatings when produced at increased solution temperatures. At increased solution temperatures the rate of equation (2), CrOOH dissolution, may increase more than the rate of equation (1), CrOOH formation. This would shift the kinetic equilibrium between coating formation and dissolution toward dissolution and therefore produce thinner coatings.

The corrosion mechanism of chromium-chromate coatings was also studied

studied by Kaztman et al[94]. They observed three stages associated with coating breakdown using Auger depth profiles. After 80 hours in a salt-spray cabinet the coatings were uniformly thinned by about 200 Å, no visible corrosion could be seen and some fluoride had been lost. This indicates that fluorine may have helped dissolution of the coating. After 175 hours exposure there was still no visible sign of change on the coating surface. The depth profile however, showed that some of the chromium had been leached out from the coating. It is interesting to note that despite Treverton's earlier conclusions that hexavalent chromium was not found in chromium-chromate coatings[97] other workers[98,99, 100,101] have suggested that some of the chromium in the coating is in the form of hexavalent chromium. In later papers Treverton[102,107] states that because of the nature of hexavalent chromium, the fact that he could not detect it in the coatings does not mean it was not present before ion etching. In fact Treverton[102] calculated that as much as 15% in atomic percentage of the coating could have been hexavalent chromium.

Katzman et al[94] claim that after 175 hours exposure to salt-spray, chromium-chromate coatings still contain some hexavalent chromium (10% of the remaining chromium); and further, state that it is mostly hexavalent chromium that has been leached away and replaced by aluminium from the substrate.

Finally the third stage of corrosion occurred after 225 hours, slight visible corrosion was present on the coating. The corrosion product was aluminium oxide. The state of the remaining coating was not described. Tests carried out on samples with various

coating thicknesses (produced in solutions at various temperatures) all showed these three stages of corrosion. The time taken to begin each stage was similar for all the samples. Thus corrosion protection is not strongly dependent upon the coating thickness, but due to the insolubility and impervious nature of the coating.

In a recent paper presented by Treverton and Amor(108) the mechanisms promoting very good adhesion to organic coatings by chromium-chromate coatings were investigated. The microtopography developed by accelerated chromium-chromate coatings were studied using an SEM with a second stage situated between the objective and condenser lenses, within the objective lens field. This set up reduced spherical aberration to a minimum and resulted in a maximum resolution of 3nm as compared with 5nm of a conventionally placed stage.

At this resolution it could be seen that the chromium-chromate coatings had a layered structure, each layer was about 30 to 50 nm thick. It was found that a coating produced by immersion for two minutes could be partially removed by "adhesive-taping". This revealed that the coating structure had an array of circularly shaped particles 0.3 to 0.5 μm in diameter. This corresponds to close-packed spherically-shaped particles where the contact zones were not visible.

When studying the flakes that had been removed by the adhesive tape a similar structure could be seen but the particles were smaller, with diameters of about 70nm. However in some areas flakes comprising of only a single layer were removed from the surface of the coating, the structure of these flakes could not be resolved implying that

the surface particles were either much larger or smaller than particles within the coating.

On coatings formed by 30 seconds immersion, "adhesive taping" ie removal of part of the coating, was not possible. However a similar structure of circular particles could be resolved, the largest were 34nm in diameter and the smallest were below that of maximum resolution.

XPS studies of the 2 minute coating have shown that ferricyanide is present on the hydrated chromium particles throughout the coating, despite the difference in particle size between particles on the surface and that in the bulk coating.

It was clear that the original caustic etched topography was not enhanced by the chromium-chromate coating. It was also seen that no small topographical features such as aluminium oxide whiskers (formed by phosphoric acid anodizing(110)) were present on the surface and cracking, noted on thicker coatings is generally accepted as a cause of poor adhesion. Thus mechanical keying is not likely to be a major factor contributing to adhesion.

In the absence of any other visible bonding mechanism Treverton and Amor suggest that the spherical particles themselves promote adhesion. They further suggest that the bonding mechanism could be influenced by surface area, obviously spherical particles would increase surface area. This would increase the number of surface sites available for interaction with polymers of organic coatings so the number of interactions may also increase. If the breakdown

of adhesion is dependant upon breakdown of the interactive bonds, the greater the number of bonds there are the better adhesion will be.

A mismatch of the spherical particles may cause weakness within the coating, thus it was suggested that the mismatch between the large particles within the bulk of the 2 minute coating and the particles on the surface of the coating caused the loss of adhesion that resulted when pulled off by adhesion tape.

A general critism against Treverton and Amor's findings is that most of the results have been produced on coatings that have failed. It could therefore be said that the significance of this work is mainly in establishing the cause of such failures and that adhesion is not due to these spherical particles. However in support for their arguments is the fact that in a previous paper[102] Treverton had suspected that chromium-chromate coatings were composed of spherical particles in thin layers, as well as the fact that Treverton and Amor state that spherical particles were found on the surface of coatings that did not fail.

3. EXPERIMENTAL PROCEDURE AND RESULTS

The two main topics covered by this work were

i) Chromate-phosphate pretreatment of aluminium

ii) Powder coating

A proprietary chromate-phosphate solution (Alocrom 100*) was studied and simulated in the laboratory. The role of each constituent part of the formulation was then carefully investigated. The influence of the substrate, cleaner, surface oxide film and contamination on the conversion coating formed were also studied.

The work carried out on powder coatings was split into two main parts:

i) Investigation of powder particle flow

ii) Development of a 'low-bake' polyester powder

The first part used a technique developed at Aston[58,59] to study the influence of particle size and substrate condition on flow characteristics of melting polyester powders.

The second part covers a detailed investigation on the viability of the new 'low-bake' polyester resins recently developed by the resin manufacturers for the powder coating industry.

---

*ICI Paints Division, Slough

3.1 Standard Techniques and Procedures

3.1.1 Materials

Test panels were guillotined from rolled sheet approximately 1mm thick to the required size, typically 10mm x 70mm. These were then degreased by scrubbing in acetone with cotton wool, and allowed to dry in air. The panels were then kept in a desiccator containing silica-gel to ensure a consistant dry storage environment. The panels were usually used in the "as received" surface condition. However, where necessary, the appropriate treatment, such as chemical polishing, electropolishing, mechanical polishing etc was carried out before being processed. Two compositions were used, these being:-

i) anodising quality super purity aluminium supplied as bright rolled annealed sheet 0.9mm thick, with the following composition:-

Al	$\geq$ 99.98%
Mg	0.0005%
Cu	0.0020%
Si	0.0055%
Fe	0.0060%
Mn	0.0015%

ii) E4S rolled sheet 1.0mm thick, specified as follows:

Al	balance
Cu	0.3% maximum
Mg	0.2 - 0.8%
Si	0.6% Maximum
Fe	0.7% Maximum
Mn	0.3 - 0.8%
Zn	0.4% Maximum
Cr	0.2% Maximum
Ti	0.1% Maximum

E4S is the Alcan GB specification for the international standard alloy 3105, nominally 0.5% Mn, 0.5% Mg.

3.1.2 Proprietary chromate-phosphate solution preparation

Alocrom 100 solution was used at the standard strength as recommended by ICI[111]. The solution was made by diluting 'Alocrom 100 make-up solution' to 10% with de-ionised water, to which was added 22 grammes per litre of 'Alocrom 100 make-up powder' and 5 grammes per litre of 'Alocrom 100 replenishing powder'. This was then vigorously stirred and heated to about 45°C to ensure complete dissolution of the powder.

The tank used was built from stainless steel, glass being unacceptable due to fluoride ions attacking sodium in the glass, reducing the ratio of fluoride to chromic acid to a level where the solution became inactive. A waterbath with a thermostatically controlled heater and water circulator was used to heat the solution to the required temperature.

A freshly made up Alocrom 100 solution must be aged by immersion of scrap aluminium with a suitable surface area[111]. Solutions were used in both aged and fresh conditions, ageing was standardised as follows: 99.99% aluminium sheet with a surface measuring $0.5dm^2$ per litre of solution was immersed for 45 minutes at room temperature. The Alocrom 100 solution strength was then checked before any work was carried out. The solution strength was checked at regular intervals during its use, following the procedure outlined in the ICI information sheet [111].

5 cm3 of the working solution was measured into a beaker containing 200 cm3 of distilled water, 12 drops of indicator (0.1% bromo-cresol

green in denatured alcohol) was then added, and mixed well. This was then titrated with 0.5N solution of sodium hydroxide until an end point (orange to green) was observed. The bath was then adjusted by adding 10ml of 'Alocrom 100 make-up solution' and 10 grammes of 'replenishing powder' per litre of working solution for every 1 cm^3 below $8cm^3$ of 0.5N sodium hydroxide titrated. This check was carried out every time the working level of the bath was adjusted, compensating for water loss due to evaporation, especially when an elevated bath temperature was used.

3.1.3 Proprietary cleaning solution preparation

A phosphoric acid based aluminium cleaner known as AC51 manufactured by 'Robertsons Chemicals Limited' of Norfolk was used extensively throughout this work. AC51 has a pH of about 0.6 and a working temperature range from room temperature to a maximum of 60°C. Chemical degradation occurs at temperatures greater than 60°C. Preparation of the working solution involved simple dilution of the stock solution to 10%, with de-ionised water. A thermostatically controlled water bath was employed to heat the solution to 50°C $\pm$ 2°C. The solution was usually made-up in 1 litre batches and was used in a wide range of conditions from fresh to aged. Problems resulting from evaporation were overcome by ensuring the working solution was covered at all times by a 'watchglass'. Almost all of the water vapour lost from the solution condensed on the watchglass and returned to the solution.

3.1.4 Conversion coating procedure

Aluminium coupons were cut to size and cleaned as outlined in section 3.1.1 followed by surface preparation as necessary. Before treatment all coupons were numbered using a sharp scribe. Panels were jigged by attaching to stiff wire via crocodile clips with which they were held fully immersed in hot cleaner for five minutes followed by thorough rinsing in water. The cleaning procedure must be carried out properly - failure to do so will result in poor conversion coatings. After thorough rinsing the panels were transferred without dejigging to the conversion coating bath. The panel was then left for the appropriate time depending on the coating weight required.

It was often necessary to know the weight of the coupon before it was treated in the chromate solution. In this case the coupon was dried with a hot air blower immediately after it had been cleaned and rinsed, it was then weighed, re-jigged and finally immersed in the conversion coating bath.

To avoid problems associated with galvanic coupling between the aluminium coupon and the mild steel crocodile clip great care was taken to ensure the crocodile clip never entered the chromate solution. After the appropriate treatment time the coupon was removed from the bath and rinsed carefully for about 60 seconds. Care must be taken at this stage to avoid damaging the coating which is mechanically weak when wet. Finally the coupon was dried by holding over a hot air blower. The hot air must not exceed 60°C as the coating may be damaged by an excessively high baking

temperature. The coating was then strong enough for handling but care was still necessary to avoid damage.

Treated coupons were kept for future reference. Specimens were catalogued as appropriate on loose file paper and then held in a ring binder. Double-sided tape was found suitable for this purpose; the tape was only placed on the untreated area left due to the position of the jigging clip.

3.1.5 Coating examination

All conversion coatings produced were examined using a Cambridge Instruments Model 150 scanning electron microscope (SEM) and analysed with an energy dispersive X-ray analysis (EDXA) attachment. Early work used a 'Kevex series 7000' EDXA attachment. Peaks were identified manually using peak energy indexes or alternatively they could be identified semi-automatically using a numbered 'window' system. The 'Kevex' attachment was replaced at the beginning of 1983 with a 'Link Systems series 2' EDXA attachment which had an improved peak identification and semi-quantitative analysis programme.

Samples measuring approximately 10mm x 10mm were cut from the treated coupons. Each one was mounted on a small SEM stub using double-sided pressure sensitive tape. Aluminium conversion coatings have very high electrical resistance. To avoid electrical charging in the SEM, all samples were covered with a thin conductive coating of either gold or carbon and were electrically connected to the SEM stud with colloidal silver. Gold coatings were used when high resolution work was required or when the surface was

particularly uneven or porous. Carbon was preferred however, as this coating had no effect upon the EDXA results. EDXA was usually carried out using a large spot size as this increased 'dead-time' and therefore improved accuracy; dead-time was standardized to 30%. All high resolution work was done using the smallest practical spot size.

The stage tilt-angle (ta) normal to the electron beam was standardised to an angle of 30° to facilitate comparison between each other. It was found that a very high tilt-angle (approaching 90°) could be used to highlight surface features which were otherwise difficult to observe. For example, pits on a polished aluminium surface can only be seen using this technique. On some samples coating thickness could also be estimated this way.

EDXA analysis was usually carried out under standard conditions, viz:- spot size set to 1.2 amps (final lens current) ta = 30°, level set to normal, scan to TV, dt = 30% and time of analysis set to 100 seconds. Occasionally these conditions were not used (eg for spot analysis) and care must be used when considering such results.

3.1.6 Coupon weight change procedure

Coupon weight change has been used extensively throughout this work in order to study the rate of film formation or removal. In many cases the change in weight was very small, so a standard procedure giving results with 95% confidence was devised.

A 'Stanton Instruments' balance (model CL5D) was used, capable of weighing with recorded readings of $\pm$ 0.00001g. It was found by repeated weighing of an untreated coupon that this balance had a standard deviation of 0.00004. By using Students T-test and assuming that the standard deviation does not change then;

$$\frac{S}{N} \times t^{\gamma}_{(N-1)} = 0.00005$$

This implies an accuracy of $\pm$ 0.0005g with 95% confidence.

where S = Population standard deviation

γ = Confidence limits = 0.0025 for a twin tailed test

N = Number of samples

Using the above conditions and standard Students T-test tables, it was found that each coupon must be weighed 5 times and the mean found in order to get the result to within $\pm$ 0.00005g with 95% confidence.

All weight change experiments were conducted as follows:-

A coupon was cleaned in AC51 as specified, rinsed, dried and the mean taken from 5 weighings. The coupon was then treated, dried, and again weighed 5 times and the mean calculated, so the change in mass was found. The treated surface area of each coupon was calculated by measuring the width and height of the treated area using the expression:-

$$Sa = 2(w + t)l + wt$$

where Sa = Surface Area
w = Width
l = Length
t = Thickness

The result can now be expressed as a change in weight per unit surface area (mg/dm^2). Note that both sides and all edges (except the top edge which was not immersed) are included in this calculation.

3.2 Initial Observations

3.2.1 The effect of AC51 on aluminium

To study the effect of the acidic cleaner on the surface of 99.99% aluminium and E4S aluminium alloy a time series was produced for each substrate. Immersion times where varied roughly logarithmically between 30 seconds and 20 minutes. The cleaner was in the fresh condition and kept at 50 $\pm$ 2°C without any agitation. All samples produced were examined carefully under the SEM and electron photomicrographs recorded as necessary in order to show the etching characteristics of the cleaner.

Photo 1 and 2 show the observed time series obtained by immersing 99.99% and E4S alloy respectively in fresh AC51 cleaning solution for up to 20 minutes. It can be seen that despite being described as a non-etch aluminium cleaner, AC51 caused pitting in both substrates. The etch pits on E4S were more severe and evenly distributed than on the 99.99%. Areas of intense dissolution were noted on the 99.99% which were not present on E4S.

It was noticed that for long immersion times for both substrates various sized particles formed on the surface. This can be seen most clearly in Photo 1E. A large number of these particles were studied with EDXA and found to contain mainly copper with various amounts of iron, sulphur, chloride and phosphorus.

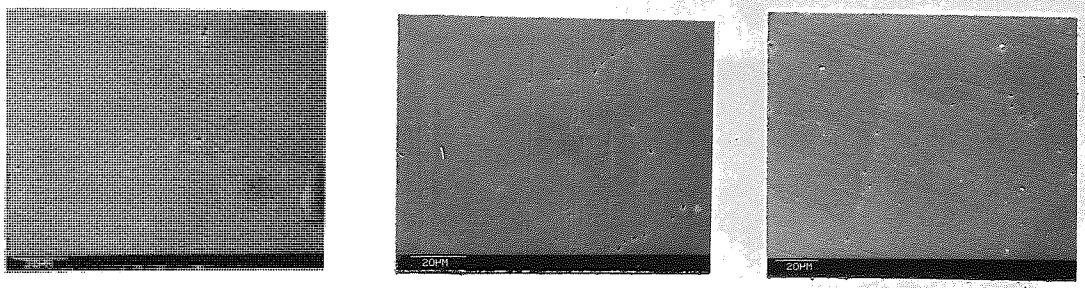

A

1 minute

B

2 minutes

C

5 minutes

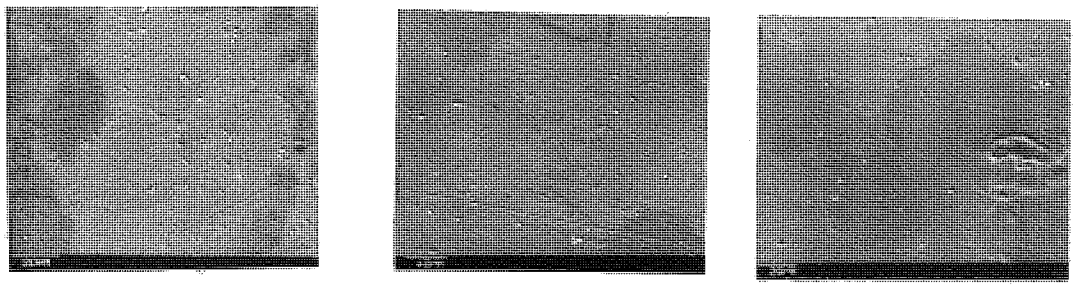

D

11 minutes

E

15 minutes

F

20 minutes

Photo 1 Time series of 99.99% aluminium immersed in AC51 (fresh) at 50°C (Ta = 30° in all frames).

Frame A, Mag. = x1K : Pitting in grain boundaries.

Frame B, Mag. = x1K : Etch pits slightly larger.

Frame C, Mag. = x1k : Optimum immersion time; preferential dissolution can be detected by lighter appearance of some grain on surface.

Frame D, Mag. = x1K : Preferential dissolution more apparent.

Frame E, Mag. = x500: Surface roughened by etch pits.

Frame F, Mag. = x1K : Lighter areas can be seen to have many etch pits compared to darker areas. However, the dark areas suffer from intense of etching.

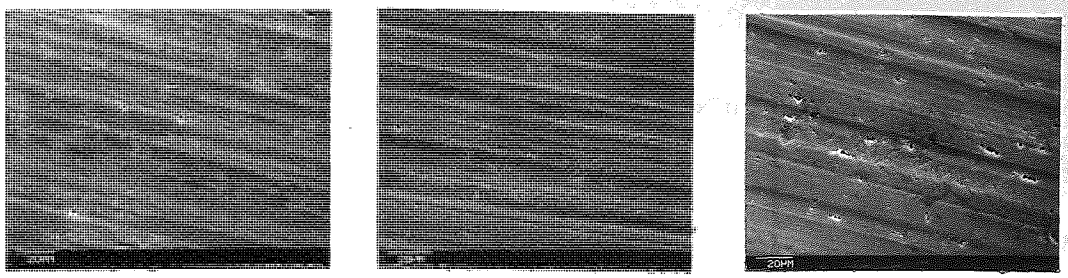

A 1 minute

B 2 minutes

C 5 minutes

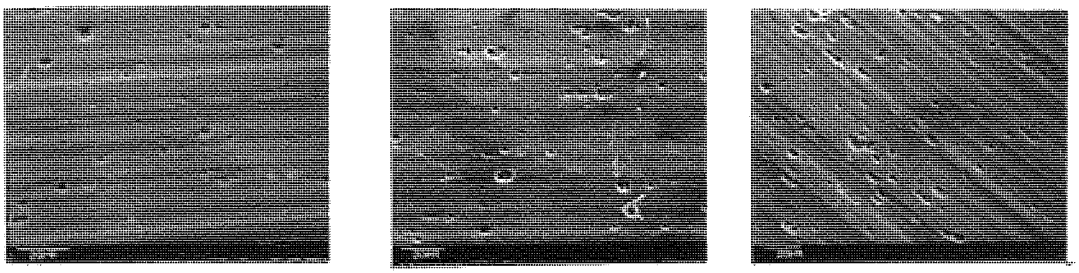

D 10 minutes

E 15 minutes

F 20 minutes

Photo 2 Time series of E4S aluminium alloy immersed in AC51 (fresh) at 50°C (Ta = 30° in all frames).

Frame A, Mag. = x1K : Slight pitting of surface.

Frame B, Mag. = x1K : Pitting becoming more severe.

Frame C, Mag. = x1K : Optimum immersion time; increasing number of pits formed randomly over the surface.

Frames D-F, Mag. = x1K (all frames) : Severity of pitting increasing proportionally with time. No preferential dissolution can be seen.

3.2.2 Coating growth in an Alocrom 100 solution

The coating growth characteristics on aluminium immersed in an Alocrom 100 solution were studied under the SEM. It is not possible to observe coating growth directly, since this only occurs during immersion, so a time series was produced. Coatings formed on 99.99% aluminium and E4S aluminium alloy between 30 seconds and 20 minutes at room temperature and at 45°C on a roughly logarithmic time scale were studied. All coupons used for this work were given identical treatment before coating formation, ie in the 'as-received' condition following 5 minutes immersion in AC51.

A coupon weight change study was also carried out for each substrate in Alocrom 100 at room temperature.

Photos 3-6 show the time series obtained by immersing 99.99% aluminium and E4S in Alocrom 100 solution at room temperature and 45°C. The sequence of coating growth is similar in all cases. However, substrate composition and solution temperature have a significant effect on the rate of coating formation. The coupon weight change against immersion time has been plotted out in Figure 3.2.2. This shows the rate of weight gain increasing with time, and that 99.99% aluminium has a higher rate of weight gain than E4S. The coating analysis results conducted by EDXA are presented in Table 3.2.3. In all cases the only peaks detected were for aluminium, phosphorus and chromium.

EDXA analyses a volume of material rather than just the atoms at the surface, resulting in high aluminium readings for low coating

weights. The coating weight for E4S after 10 minutes immersion is less than the corresponding coating weight for 99.99% aluminium. The proportion of phosphorus detected in the coating increases slightly with immersion time.

Aluminium dissolution is more rapid on 99.99% aluminium than E4S and is shown by an initial decrease in weight of the coupon weight change curve for 99.99% aluminium (Figure 3.2.3). This is in agreement with the topographical observations of 99.99% aluminium and E4S immersed in AC51, in which large areas of the 99.99% aluminium were attacked.

Light coloured patches were visible on conversion coatings inspected by eye but were not easily detectable under the SEM. Photo 3E (Centre) shows a patch of coating slightly standing proud of the surface, whereas Photo 4C clearly shows an area of coating below the surface of the surrounding surface. It is possible that this variation in rate of coating growth is due to varying local rate of aluminium dissolution.

It has been suggested that the mud-cracked appearance of these chromate-phosphate coatings was caused by the conditions inside the SEM chamber, ie low pressure and electron beam bombardment. Several freshly made coatings were examined under an optical microscope at magnifications of approximately 1000 times. It was apparent that a similar cracked topography was present. It was concluded that the mud-cracked surface characteristic of chromate-phosphate coatings was not due to exposure to low pressures or bombardment by an electron beam.

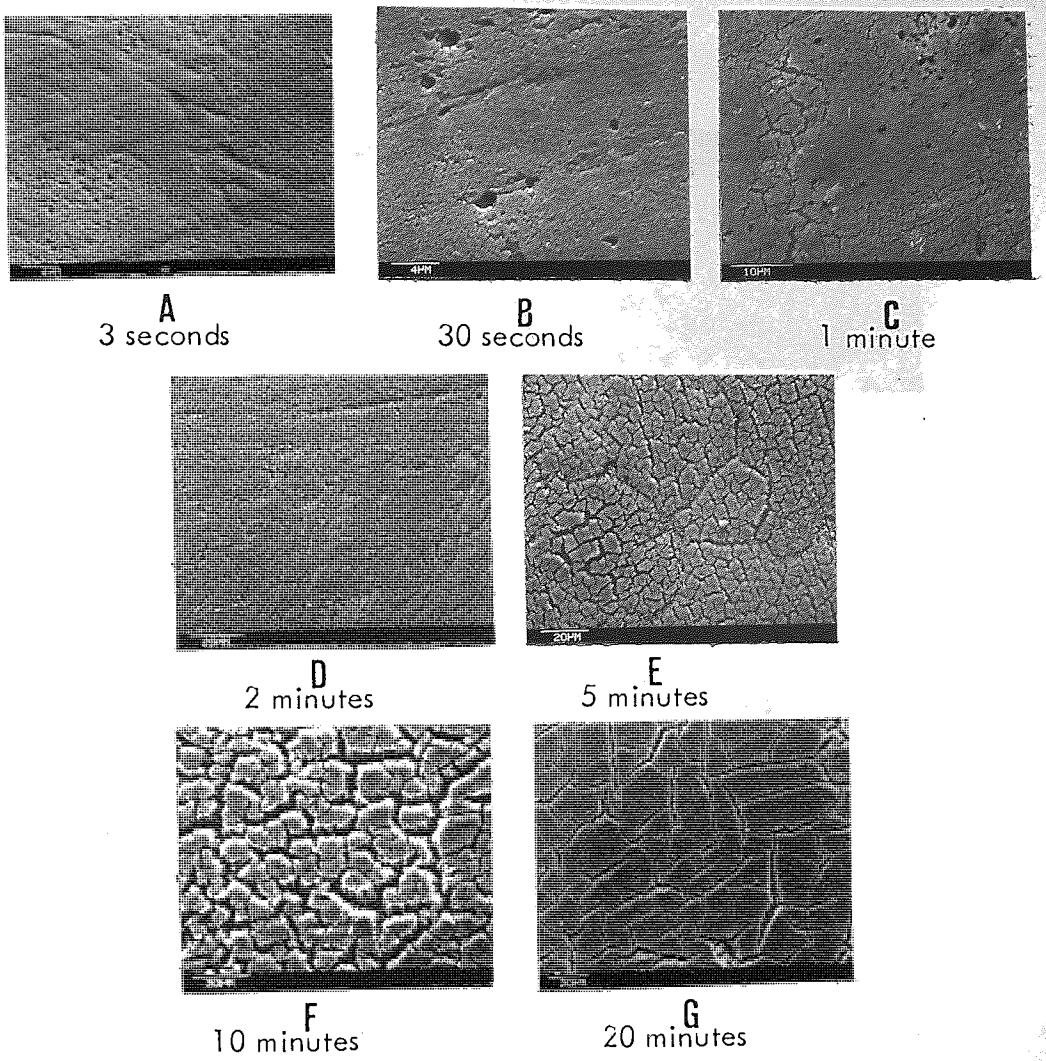

Photo 3 Time series of Alocrom 100 coating formation on 99.99% aluminium at room temperature (Ta = 30° in all frames).

Frame A, Mag. = x5K : Coating formation begins on etched surface.

Frame B, Mag. = x5K : Coating covers surface as small 'islands' gassing defects visible.

Frame C, Mag. = x2K : Mud cracked appearance, typical of chromate-phosphate coatings, takes form.

Frame D, Mag. = x1K : Mud cracked appearance complete. Gassing pits evident.

Frame E, Mag. = x1K : Optimum coating weights; few defects in coating. Clusters of 'islands' seem to slightly protrude above others (centre).

Frame F, Mag. = x1K : Coating weight beyond optimum; severe cracking and increased island size apparent.

Frame G, Mag. = x1K : Island size increased further; some island edges were seen to be lifting (top and bottom of frame).

A

30 seconds

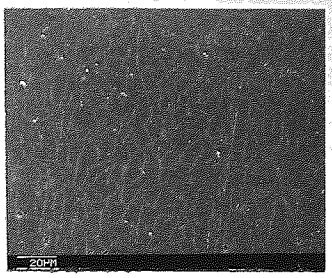

B

90 seconds

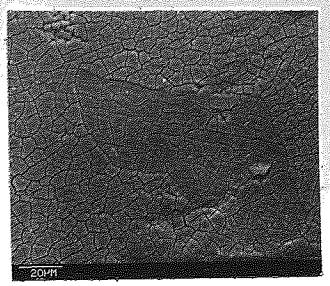

C

3 minutes

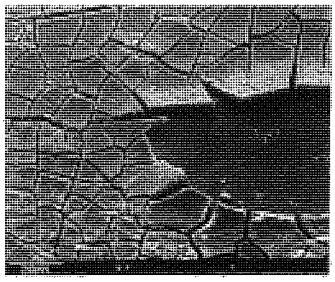

D

6 minutes

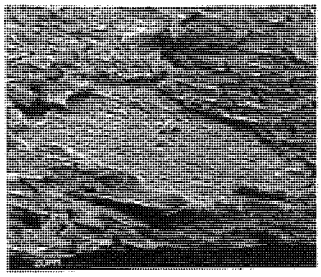

E

20 minutes

Photo 4 Time series of Alocrom 100 coating formation on 99.99% aluminium at 45°C. (Ta = 30° except frame E = 63°).

Frame A, Mag. = x2K : Coating formation and some cracking already clearly visible.

Frame B, Mag. = x1K : Defect free coherent coating with fine cracking

Frame C, Mag. = x1K : Optimum coating weight; some clusters of 'islands' appear to have slightly different growth rates to the majority of the film.

Frame D, Mag. = x1K : Islands and crack widths grow with time. Part of this coating has blistered and fallen off leaving the substrate exposed, the coating is about 2.2 μm thick at this point.

Frame E, Mag. = x1K : Island edges lift on drying leaving a rough surface. Some patches of coating have fallen off exposing a second layer of coating below. The top coating was approximately 2.1 μm thick.

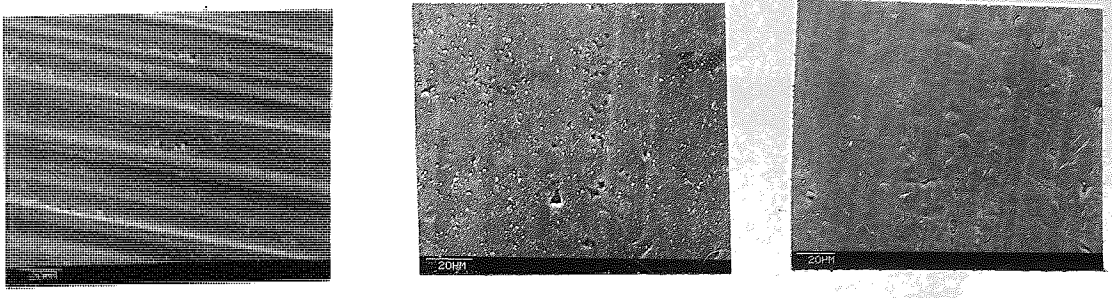

A

30 seconds

B

1 minute

C

2 minutes

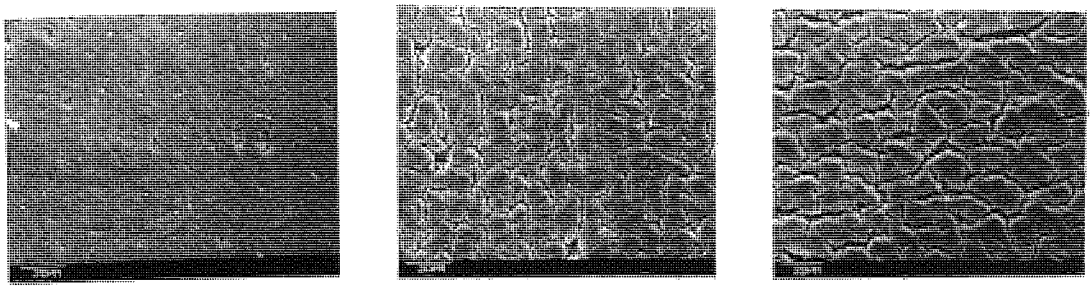

D

5 minutes

E

9 minutes

F

20 minutes

Photo 5 Time series of Alocrom 100 coating formation on E4S aluminium alloy at room temperature (Ta = 30° in all frames).

Frame A, Mag. = x1K : 'As received' surface after cleaning visible. Coating detected by EDXA.

Frame B, Mag. = x1K : Thin coating now visible under SEM, with pits running along the direction of extrusion.

Frame C, Mag. = x1K : 'Mud-cracked' surface forms independently to direction of extrusion; pitting still evident.

Frame D, Mag. = x1K : Optimum coating weight; good coverage, few defects.

Frame E, Mag. = x1K : 'Island' size and crack width both increased as coating goes beyond optimum weight.

Frame F, Mag. = x1K : Further enlargement of islands and lifting of island edges.

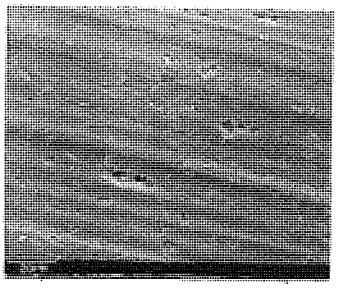

A

30 seconds

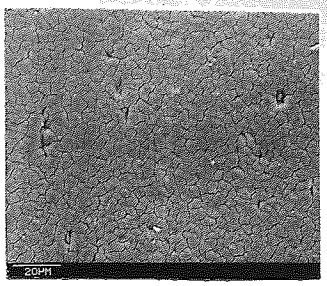

B

2 minutes

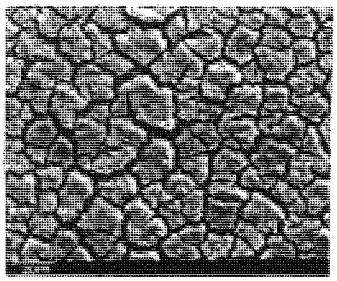

C

6 minutes

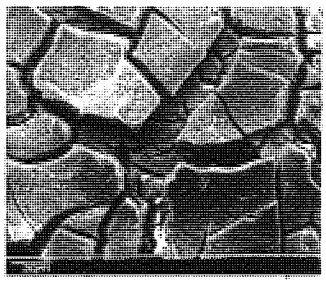

D

20 minutes

Photo 6 Time series of Alocrom 100 coating formation on E4S aluminium alloy at 45°C (Ta = 30° in all frames).

Frame A, Mag. = x1K : Coating and 'mud-cracking' visible; extrusion lines still evident.

Frame B, Mag. = x1K : Coating weight just below optimum; some gassing defects still visible.

Frame C, Mag. = x1K : 'Islands' and cracks have enlarged, second layer just visible between cracks.

Frame D, Mag. = x1K : Continued growth of top layer islands which are beginning to lift at the edges, and the bottom layer islands which are now clearly visible.

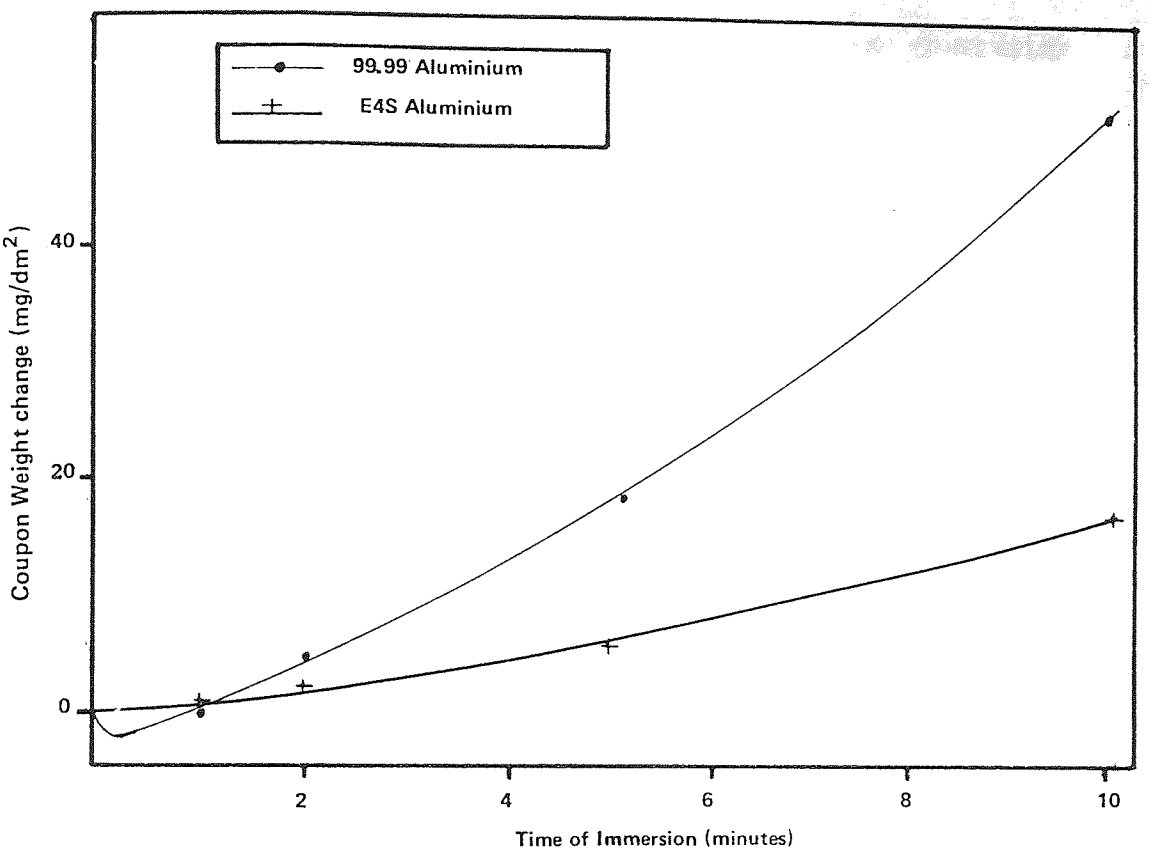

Figure 3.2.2 Coupon Weight change against immersion time for 99.99% aluminium and E4S alloy in fresh Alocrom-100 solution at room temperature

Table 3.2.2 EDXA Results for Alocrom 100 Coatings Formed on Aluminium at Room Temperature

Substrate	Time of Immersion (mins)	Peak Areas			Ratio of P:Cr
		Aluminium %	Phosphorus %	Chromium %	
99.99%	0.5	99.39	0.33	0.28	1.18
"	1	96.99	1.86	1.15	1.62
"	2	89.68	6.54	3.77	1.73
"	5	50.78	30.82	18.40	1.68
"	10	12.74	54.72	31.18	1.76
E4S	10	71.28	19.98	8.74	2.29

4. THE INFLUENCE OF THE SURFACE OXIDE ON CLEANING AND CONVERSION COATINGS

4.1 Introduction to Experimental Work

It is known that the surface oxide film on aluminium plays an important role in many electrochemical reactions that occur during finishing processes for aluminium, such as electro or chemical polishing and electroplating. The effect of increasing the thickness of the oxide on the aluminium surface was studied both on etching in the acid cleaner and upon film formation in the chromate-phosphate bath.

The influence of aluminium additions to the cleaning solution was also studied in order to simulate industrial conditions and find the effect of ageing the cleaner.

4.1.1 Production of thick surface oxide films

99.99% aluminium coupons were used throughout this work. Coupons that had previously been cut to size and degreased were treated by heating in air or by hard anodising in order to increase the surface oxide film in a controlled manner.

Thick air-formed oxide films were produced by heat treatment in a thermostatically controlled muffle furnace. Two samples were produced at each temperature and treatment time. Untreated coupons were used as control samples. A special jig was designed to ensure ready access by the hot air to the entire surface of all treated coupons.

The first batch of treated coupons was used to study the influence of the surface oxide on the cleaner (AC51). A second batch was produced to study the influence of the surface oxide on the production of conversion coatings.

Much thicker oxide coatings can be formed by anodising. For this purpose coupons were anodised using the set-up shown in Figure 4.1.1. A "Farnell" stabilised power supply (model H60/25) programmed to provide an output of 0.5A, and 1 litre of 10% (V/V) sulphuric acid agitated by nitrogen gas released via a sintered glass filter were used. The anodising temperature was controlled by a 'Grant' refrigeration unit circulating 30% glycol ethylene at temperatures down to -10°C. The cathode was lead sheet positioned 5 cm away from the anode. Anodic film thickness was controlled by altering immersion times. The conditions used were those required to give a hard anodised finish, ie solution temperature -8°C and current density 5 A/dm^2. Two samples were produced at each of the immersion times; one was used for oxide thickness measurement and the other to study the influence of anodic films in AC51. A second set of anodised samples was produced using the same conditions except for solution temperature which was maintained at 20°C. The anodic film weight was found using the coupon weight change procedure (Section 3.1.6) and was converted to anodic film thickness assuming an anodic oxide density of 2.5(120). The oxide film was stripped using a chromic acid solution that does not attack the substrate:-

2% Cr_3O (w/v)
3.5% H_3PO_4 (v/v)
heated to boiling point

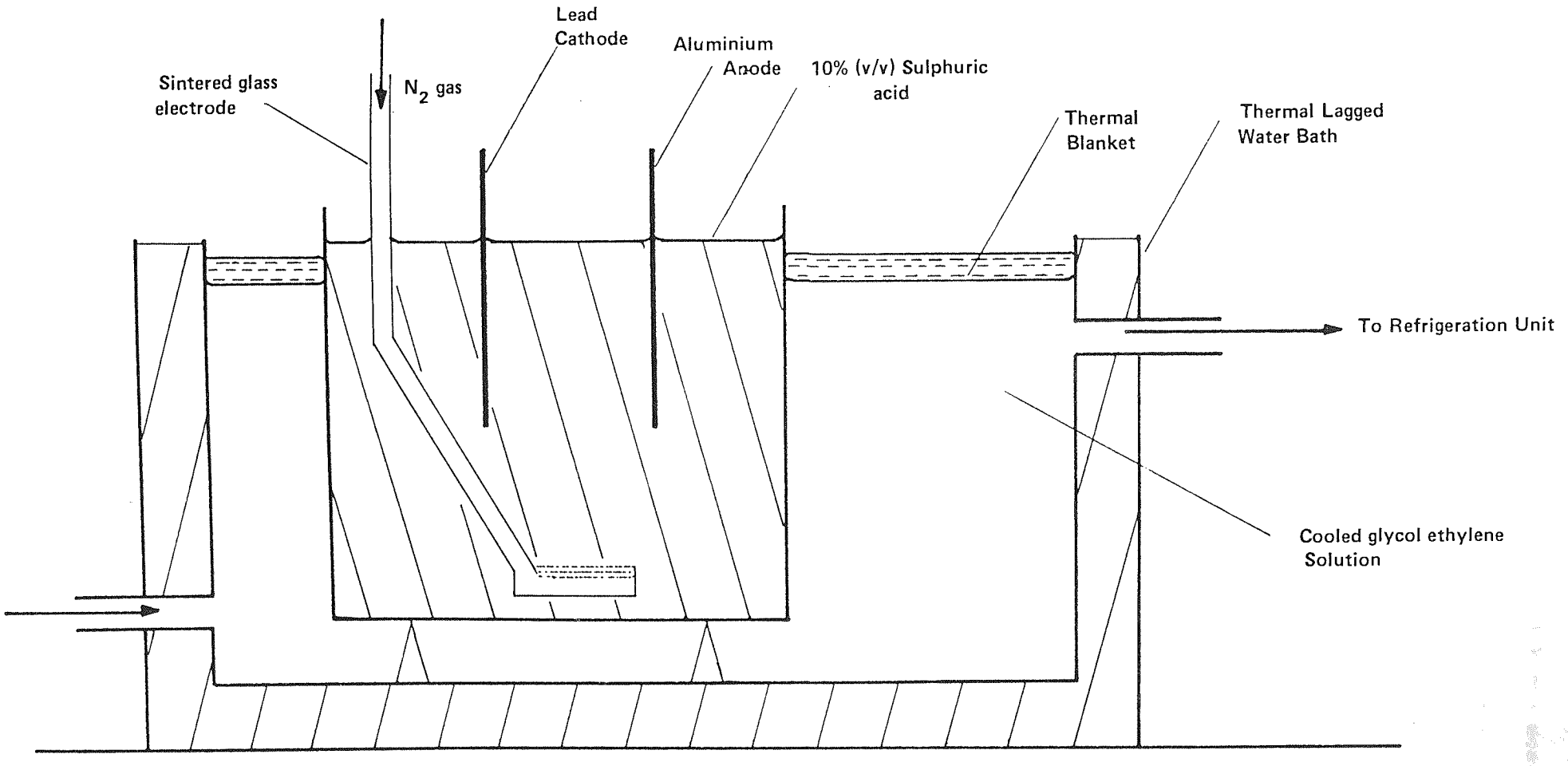

Figure 4.1.1 Anodizing Equipment Set-up

Each anodically treated coupon used for oxide thickness measurement was first weighed then boiled in the above solution for 10 minutes, rinsed, dried and re-weighed. The coupon was again boiled for a further 5 minutes and re-weighed in order to check that the oxide was completely stripped. A graph of anodic treatment time against anodic oxide thickness was then plotted for both anodic solution temperatures. Potential-time curves could then be related directly to oxide thickness and oxide structure.

4.1.2 Effect of surface oxide cleaning

The effect of increasing surface oxide thickness on treatment in AC51 was initially studied using the air-formed oxide samples. Potential-time curves were produced for each sample in both still and moderately agitated solutions. The calomel electrode was isolated to avoid any effect caused by the chlorine ions in the KCl solution. Ionic contact was maintained through a pair of salt bridges, the first connected the electrode to a dump, and the second from the test solution to the dump. In this case the test solution is AC51. However, potential-time curves were also obtained during growth of conversion coatings, in which case the test solution would be a chromate solution. It was found that the potential recorded was dependent upon the type of solution resident in each salt bridge. To keep this constant the solution levels were adjusted as shown in Figure 4.1.2. Both the KCl solution and the test solution levels were kept a few millimetres above the dump solution level. This ensured that KCl solution remained in the electrode/dump salt bridge and test solution was retained in the test bath/dump salt bridge.

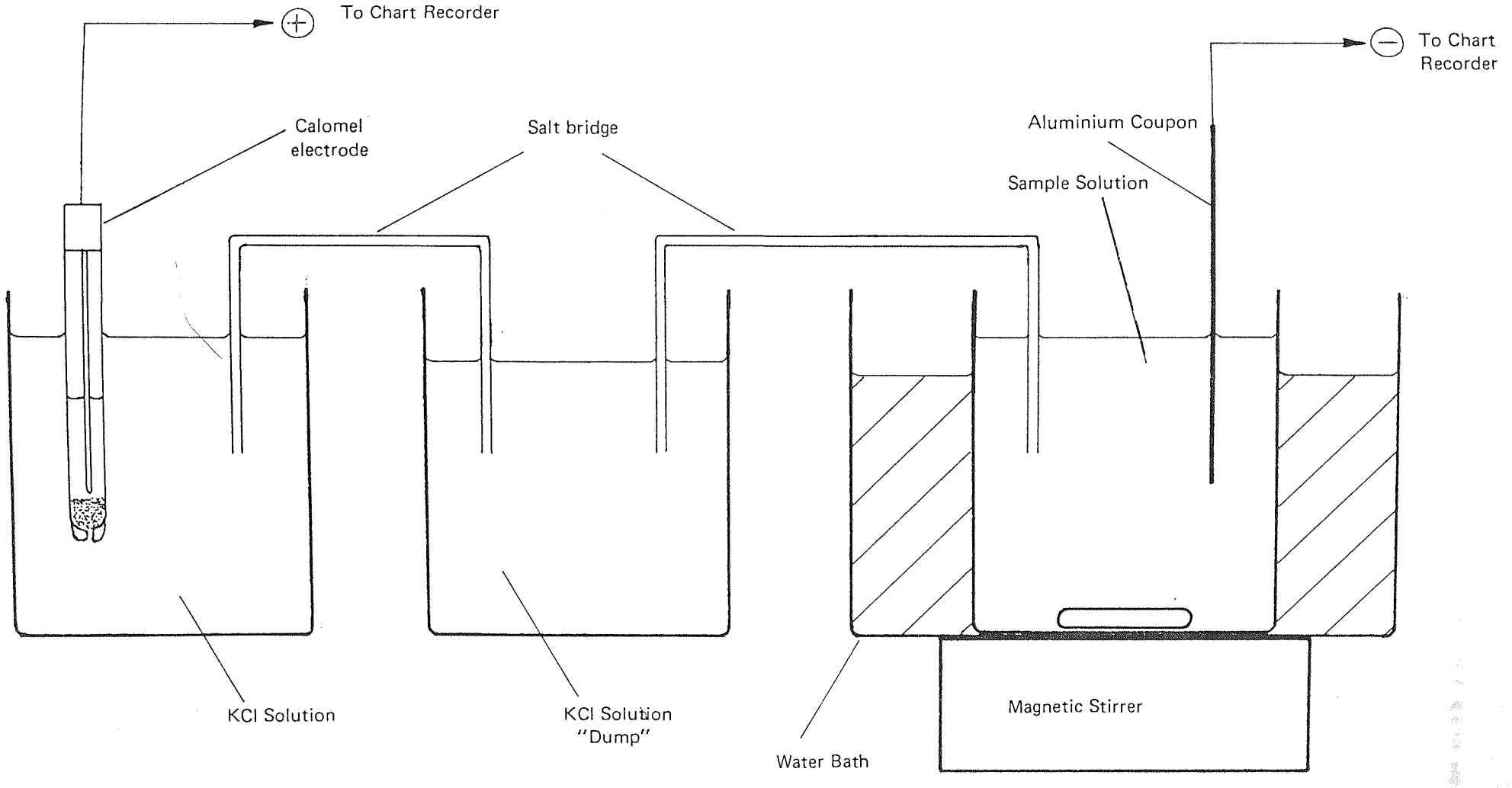

Figure 4.1.2 Potential-time Equipment Set-up

It was also found that the composition of the dump solution was not critical, therefore contamination of the initial fresh KCl solution in the dump had little effect on the recorded potential. However, to avoid any possible error due to test solution draining into the dump solution it was changed frequently.

The potential was recorded continuously on a 'Tekman' chart recorder (model TE200) with variable speed and full scale deflection settings. The full scale deflection was usually set at 1 volt, whereas the speed setting depended upon the time taken for the test. In all cases the recorder was allowed to warm up for at least 30 minutes before being used, and was frequently calibrated against a 'Farnell' stabilised power supply (model L10-3C).

A 1 litre beaker containing AC51 solution was used and changed periodically throughout the study. The cleaning solution was heated to 50°C in a thermostatically controlled waterbath and held at that temperature for about 30 minutes before the start of any test run. The potential of a 99.99% heat treated coupon immersed in AC51 was recorded for approximately 60 minutes for each run. This procedure was then repeated using the two sets of anodized samples; agitation was not used.

Finally the efficiency of AC51 in removing a thick oxide film from the surface of aluminium was investigated. All of the coupons used for the potential-time study were weighed individually and boiled in the oxide stripping solution for 10 minutes. Each specimen then being rinsed, dried and re-weighed.

The amount of aluminium which had dissolved into each solution was measured by atomic absorption at suitable time intervals using the procedure outlined below. At various stages of the test programme immediately following determination of the aluminium content, a potential-time curve was plotted using 99.99% aluminium immersed in the test solution. These were plotted as a family of potential-time curves which related to the state of the aged cleaning solution.

4.1.2.1 Determination of aluminium in solution

Aluminium concentration was found using a 'Perkin-Elmer' Atomic Absorption Spectro-photometer (AA), model No. 560, with a burner control unit to enable analysis using a nitrous-oxide/acetylene flame.

The linear range for detecting aluminium is between 0-50 ppm using the nitrous oxide/acetylene flame set to burn with a rich (red) flame. Test solutions were diluted sufficiently to fall within this range (starting by trial and error), so maintaining maximum accuracy. At first problems were encountered due to contamination of either the sample solutions, the standards and/or glassware used to prepare solutions. This was overcome by using a systematic procedure whereby all glassware and equipment was constantly rinsed in diluted nitric acid (1:24) and then distilled water. This was found to be time consuming but essential if reliable results were to be consistently produced.

It was found that one standard of 50 ppm was sufficient as the linear range was not to be exceeded. The standard was produced by

diluting fresh test solution (containing no dissolved aluminium) the same amount as the test solution, then pipetteing 5 ml of aluminium nitrate (1000 ppm Al) into a 100 ml flask and making up to 100 ml with the diluted fresh test solution. A blank solution (0 ppm Al) was also required and this was simply produced by diluting fresh test solution 20 times. Atomic aluminium tends to become ionised in the spectrophotometer flame. To inhibit this behaviour, which would markedly affect the results, the solutions were 'spiked' by the addition of 1,500 ppm KCl (0.286 g KCl per 100 ml of solution). To ensure consistent conditions, all solutions were 'spiked' regardless as to whether or not they contained any aluminium.

The position of the burner head and the flame settings were found to be critical when analysing for aluminium. If these were set incorrectly, then aluminium tended to build up on the burner head and caused the baseline to drift, giving increasingly inaccurate analysis results.

In all cases the analysis procedure was as follows:-

The aluminium lamp was installed, the lamp current set, the gain increased, the absorption wavelength adjusted and the diffraction grating slit width set. The burner head was cleaned, installed, and its height adjusted. The acetylene-air flame was then lit and once the head was warm, nitrous oxide was introduced as the oxidant. Maximum absorbance was found by adjusting the burner head position (in relation to the beam from the aluminium lamp), and the fuel/ oxidant settings, while aspirating a 50 ppm aluminium standard.

Sampling time was set for 5 seconds (found to be optimum when used for aluminium analysis) and the standard set to 50.00 ppm. The instrument was then ready for use. A blank (ie zero ppm Al) was introduced to the nebulizer and the zero level set. This was followed by aspirating the 50 ppm standard, then finally by aspirating the sample solution and noting the concentration of aluminium.

Distilled water was passed through the nebulizer between each setting. Each reading was repeated as a check on accuracy. The standard and zero had to be reset between every reading because of a slight background drift which was difficult to avoid during analysis of aluminium. An accuracy of within 1 ppm could be achieved using this technique.

4.1.3 Effect of surface oxide on Alocrom 100

The second batch of air-formed oxide films described in section 4.1.1 was used to study the effect of increasing oxide film thickness on the formation of chromate-phosphate films in Alocrom 100.

Each heat-treated aluminium coupon was immersed in a moderately agitated, aged Alocrom 100 solution at room temperature. A family of potential-time curves relating to various surface oxide thicknesses was obtained. Two samples were produced for each temperature during heat-treatment, one was used to produce a 10 minute potential-time curve whereas the other was used to produce

a 1 minute potential-time curve. The chart speed was set to 20 mm/minute for the 10 minute run and 200 mm/min for the 1 minute run. This was done in order to determine the potential accurately for the first few seconds of immersion.

4.1.4 Effect of ageing the cleaning solution

Atomic Absorption Spectroscopy and potential-time determinations were used to study the influence of increasing aluminium content in AC51 on its effect on aluminium surfaces immersed in it.

Two 1 litre solutions of AC51 were made up and held at 50°C. A 99.99% aluminium coupon with a surface area of 0.1544 dm^2 was placed in solution 1, and a similar coupon with a surface area of 0.7720 dm^2 was placed in solution 2.

Aluminium concentration was determined in each solution at intervals ranging between 5 minutes to 350 hours on a logarithmic scale. A potential-time curve was also recorded at each interval.

4.2 Results

4.2.1 Thickness of Surface Oxide Films

The air-formed surface oxide films were too thin to be measured gravimetrically, so an arbitrary system using the heat treatment temperature as an indication of oxide thickness was employed.

The thickness of anodically produced oxide films, which are much thicker than air-formed oxide films, can be determined by direct gravimetric analysis. The results of such determinations are shown in Table 4.2.1 and show that anodising temperature had little effect upon the anodic film thickness.

Table 4.2.1 Anodic Film Thickness Measurement

Anodising Temperature (°C)	Time (min)	Weight Change (mg)	Surface Area (dm^2)	Anodic Film Thickness (μm)
-8	1	4.57	0.0854	2.14
-8	2	9.21	0.0868	4.24
-8	4	18.16	0.0826	8.79
-8	6	26.52	0.0865	12.26
-8	8	35.71	0.0857	16.67
20	1	5.00	0.0802	2.53
20	2	8.53	0.0839	4.24
20	6	24.81	0.0791	12.37

Figure 4.2.1 shows the relationship between treatment time and anodic film thickness. If it is assumed that the temperature of the anodising solution has little effect upon the density of the anodic film produced, then any difference in the behaviour of the treated samples in subsequent tests must be due to differing anodic film structure.

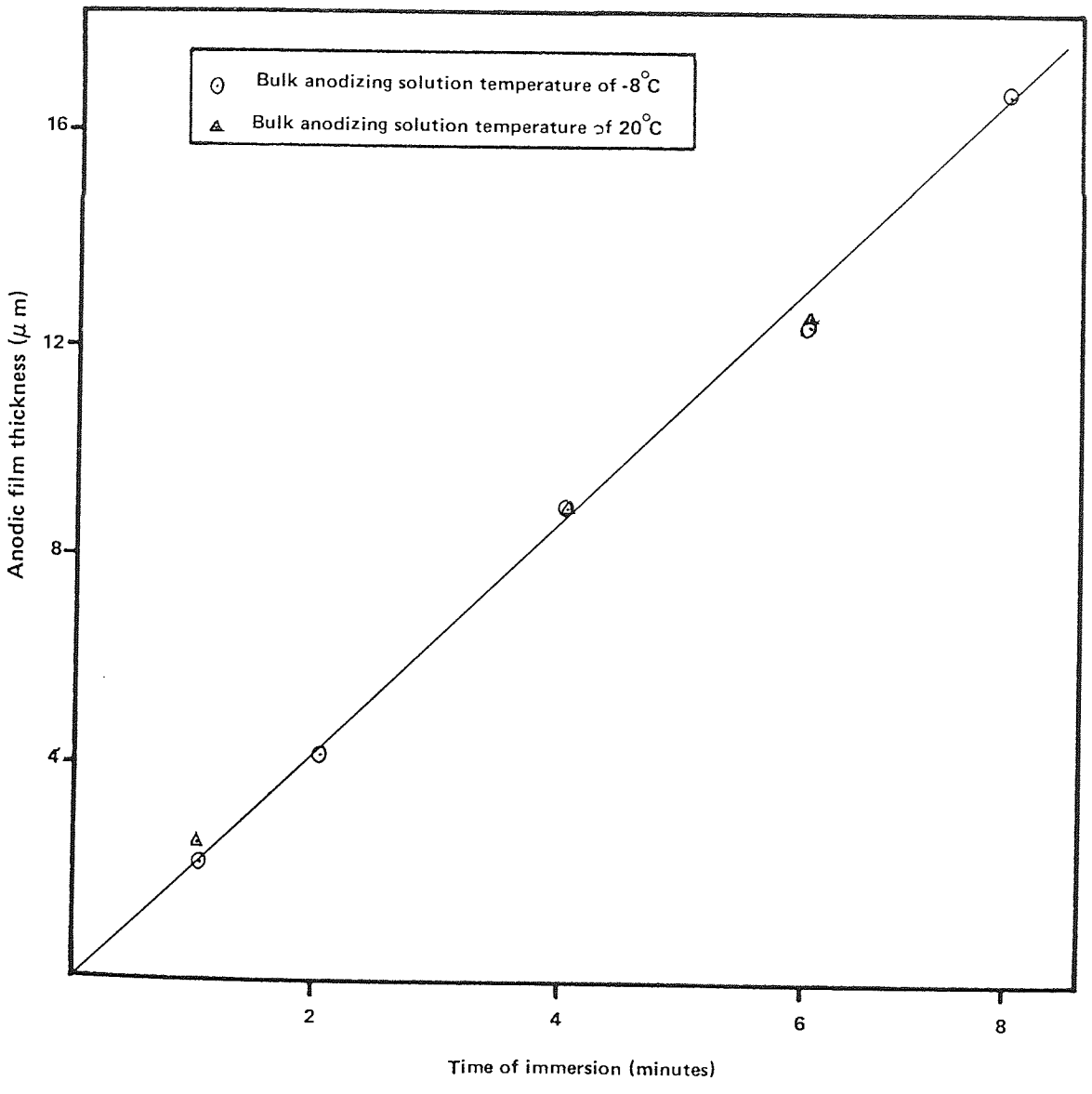

Figure 4.2.1 Anodic film thickness against immersion time

4.2.2 Effect of surface oxide on cleaning

The potential-time curve for 99.99% aluminium immersed in AC51 had a characteristic shape which was not affected by the initial surface oxide thickness.

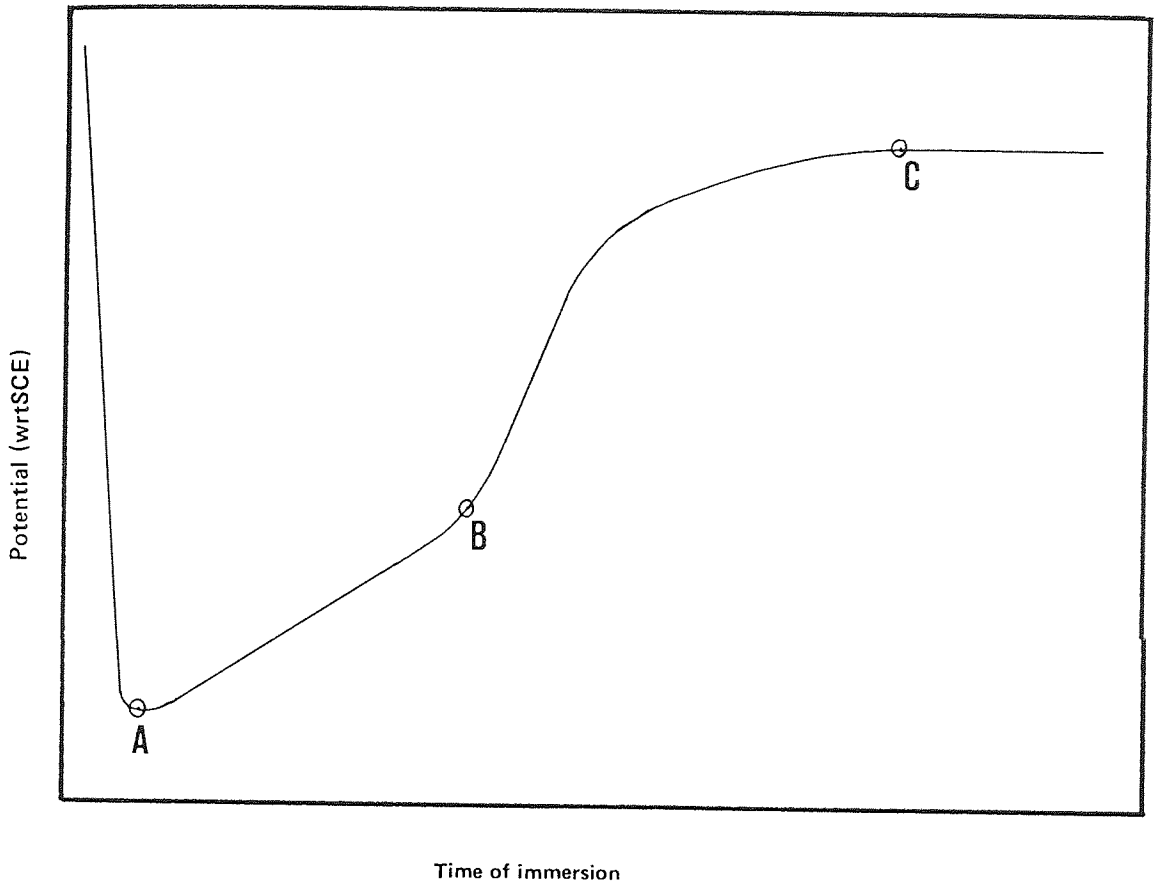

Figure 4.2.2.1 Typical potential-time relationship for 99.99% aluminium immersed in AC51

In all cases the potential dropped rapidly to its most active state upon immersion of the coupon, shown as point A in Figure 4.2.2.1. This was then followed by a steady increase in potential (becoming more noble) until after some time (point B) the rate of increase became more rapid. The potential levelled out some time later and reached a steady state at (point C) onwards.

Tables 4.2.2.1. - 2 show the time taken for the potential to reach points A and C for heat treated samples immersed in unagitated

and agitated solutions respectively. In Figure 4.2.2.2 these results have been plotted as the time taken to reach the most active state (point A of Figure 4.2.2.1) against heat treatment temperature.

Table 4.2.2.1 Tabulated Results from Potential-Time Determinations in Unagitated AC51

Heat Treatment		Solution Age	Time to most Active Potential	Time to Steady State Potential
Temperature °C	Time Mins	Mins	Mins	Mins
75	30	Fresh	1.3	-
	30	-	-	-
	60	30	1.1	23.6
	60	60	-	22.1
	90	90	1.2	25.0
120	30	120	1.4	27.3
	60	155	1.3	31.1
	90	190	1.6	44.9
160	30	240	2.1	59.6
	60	25	1.4	25.5
	90	60	1.8	29.8
210	30	100	2.1	25.5
	60	135	2.2	29.4
	90	Fresh	1.2	23.4
250	30	30	1.7	22.5
	60	60	1.5	26.4
	90	90	1.8	27.0
Room Temp Control		170	2.1	37.8

Figure 4.2.2.3 shows the time taken to reach the steady state potential against the heat treatment temperature. Clearly there is no apparant correlation between heat treatment temperature and the potential-time results. Figures 4.2.2.4 - 5 show the time taken to reach the most active and steady state potentials respectively against the total processing time (usage) of the solution. The correlation for time to the steady-state potential

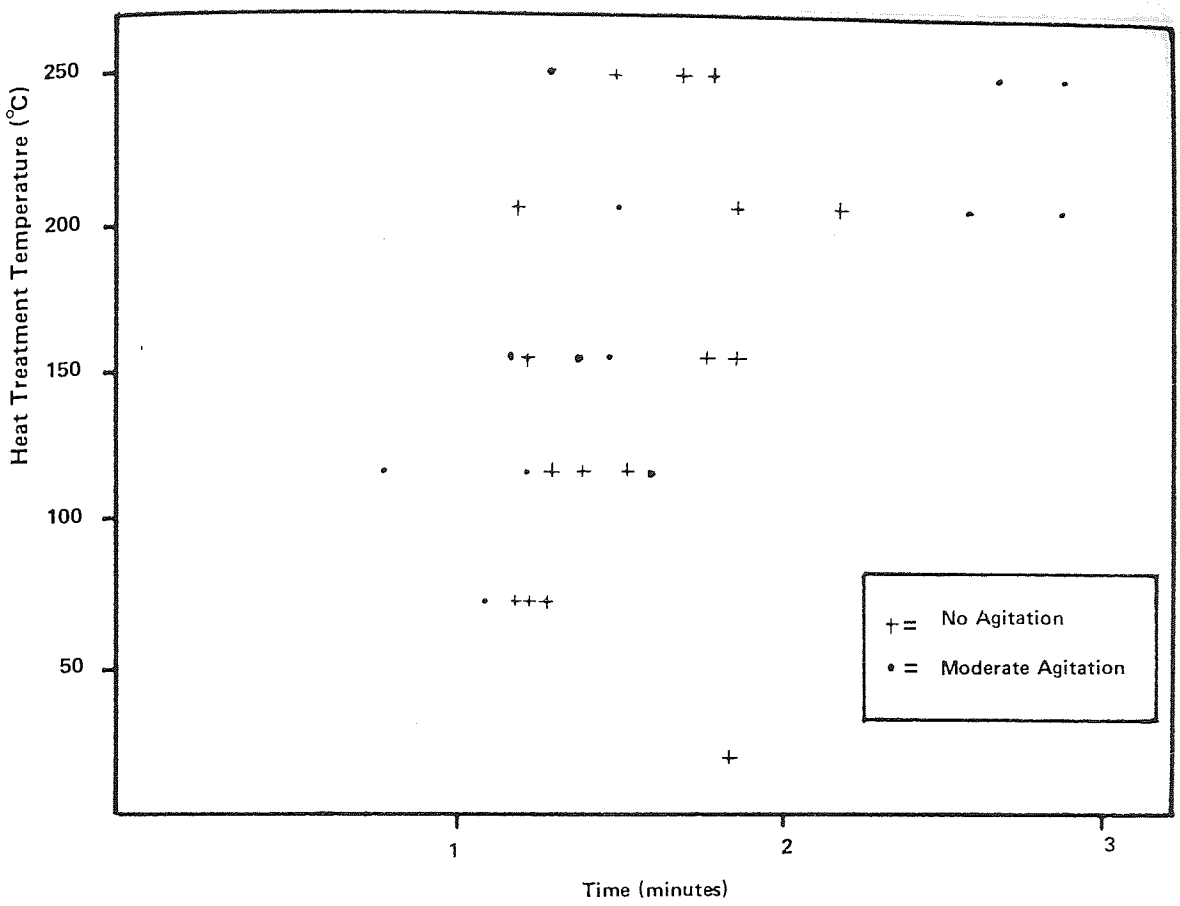

Figure 4.2.2.2 Time to the most active potential against heat treatment temperature for 99.99% aluminium in AC51

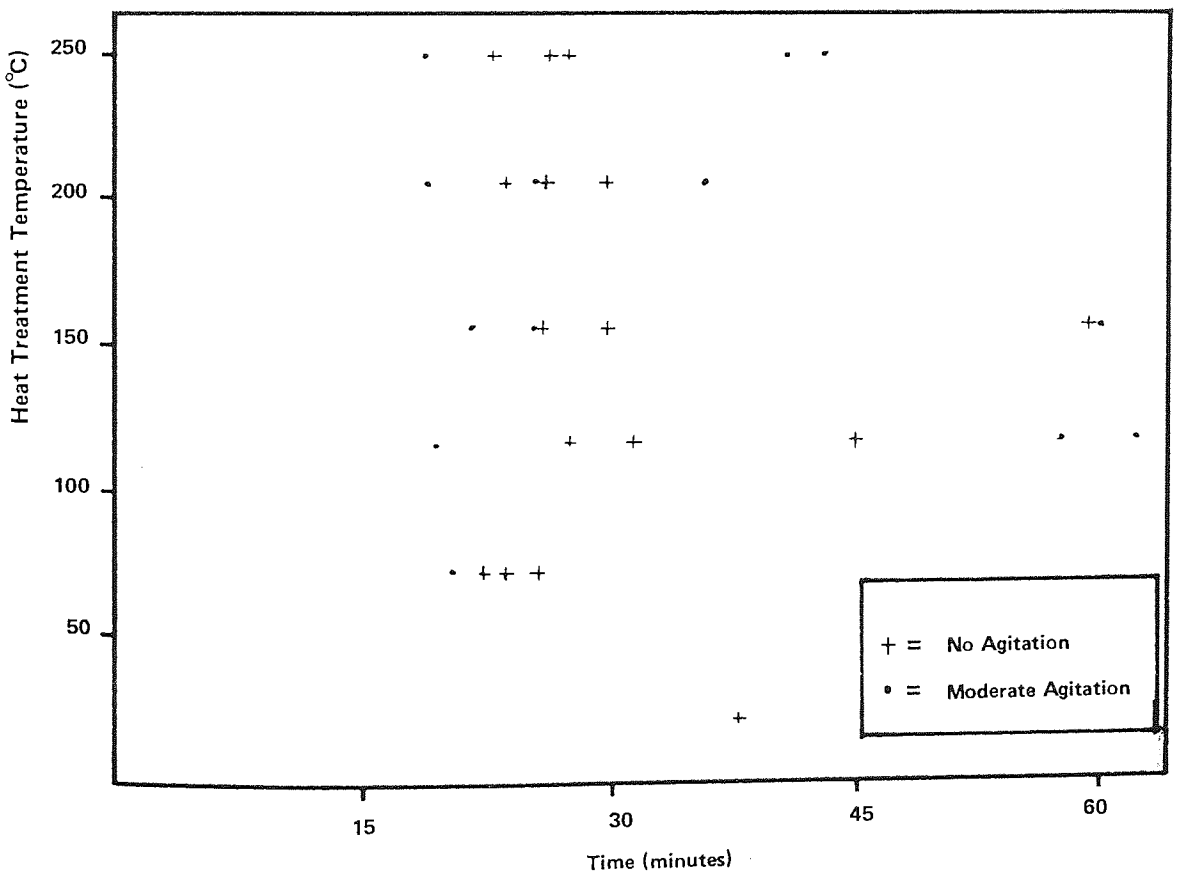

Figure 4.2.2.3 Time to steady-state potential against heat treatment temperature for 99.99% aluminium in AC51

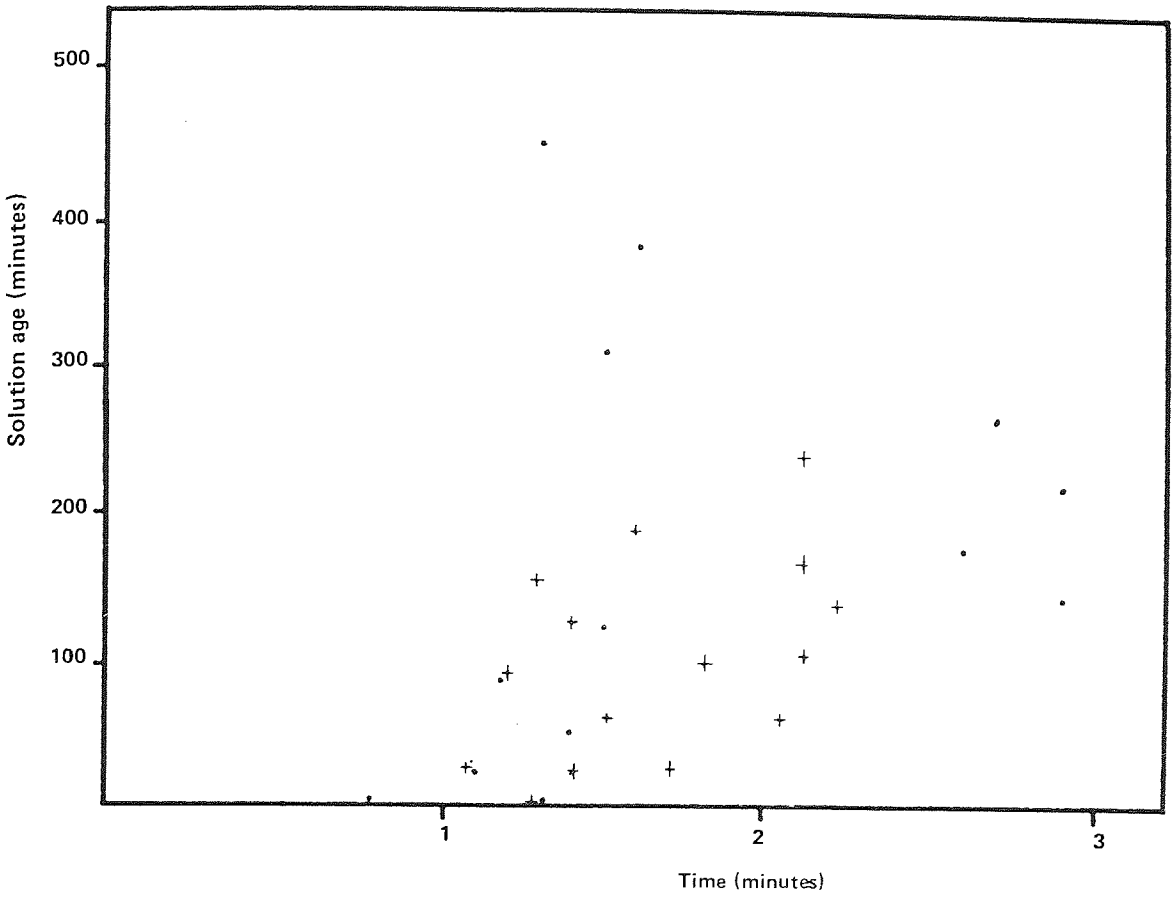

Figure 4.2.2.4 Time to most active potential against heat treatment for 99.99% aluminium in AC51

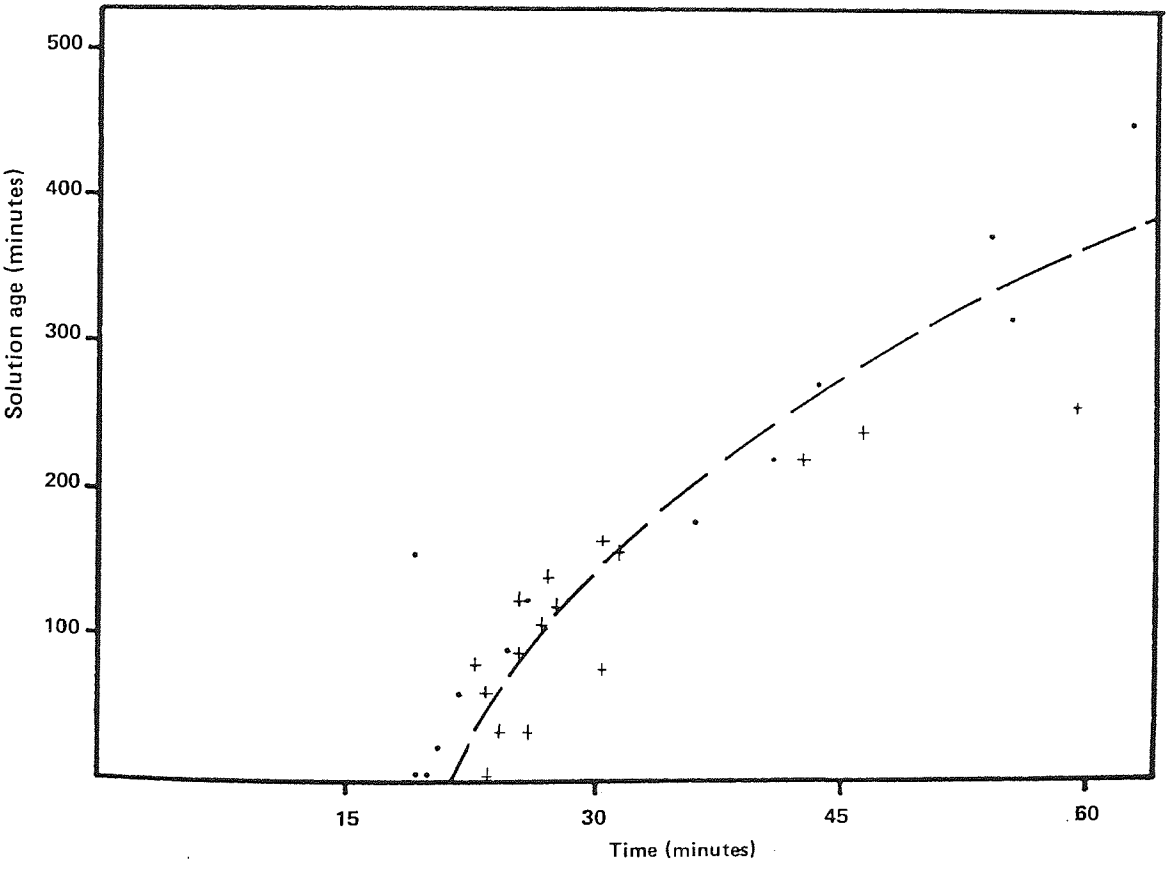

Figure 4.2.2.5 Time to steady-state potential against heat treatment temperature for 99.99% aluminium in AC51

is high, showing that the 'solution age' is an important factor and that AC51 ages rapidly.

Table 4.2.2.2 Tabulated Results from Potential-Time Determinations in Moderately Agitated AC51

Heat Treatment		Solution Age	Time to most active Potential	Time to Steady State Potential
Temperature °C	Time Mins	Mins	Mins	Mins
75	90	25	1.1	20.4
120	30	Fresh	0.8	19.7
	60	450	1.3	62.7
	90	380	1.6	54.1
160	30	310	1.5	55.7
	60	55	1.4	21.5
	90	85	1.2	25.0
210	30	120	1.5	25.5
	60	150	2.9	18.8
	90	175	2.6	36.0
240	30	220	2.9	40.5
	60	270	2.7	43.2
	90	Fresh	1.3	18.6

The potential-time curves obtained by immersing samples anodised at -8°C in fresh AC51 are shown in Figure 4.2.2.6. A clear relationship between the potential-time curves and measured anodic oxide film thickness can be seen. It was noted that the most active potential reached within the first few minutes of immersion increased (became less active), and that the potential became increasingly more errattic as the anodic film became thicker. This was thought to be caused by:-

i) increasing barrier layer thickness

ii) undermining of the anodic film by AC51

iii) gassing

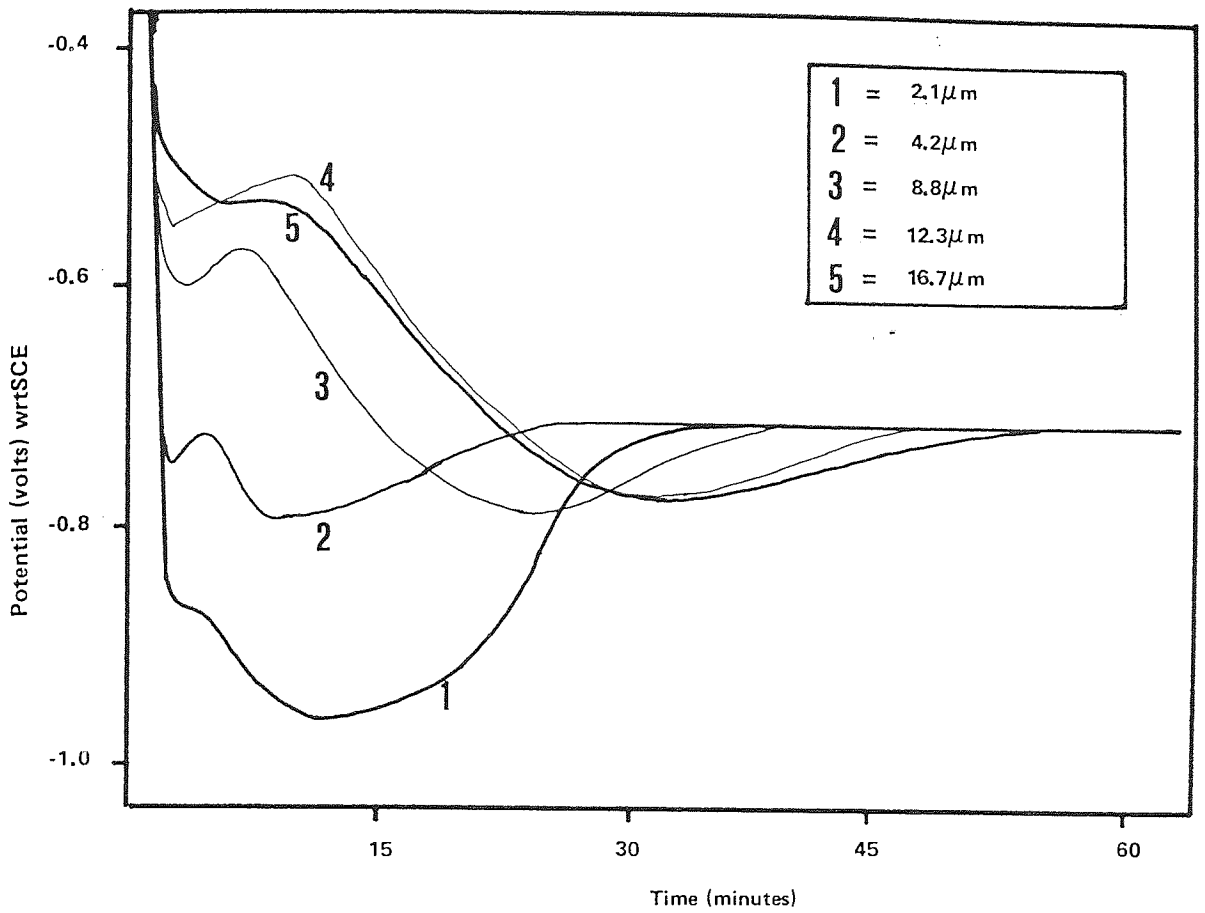

F igure 4.2.2.6 Potential-time family for 99.99% aluminium immersed in AC51 after anodic treatment at -8°C for various times

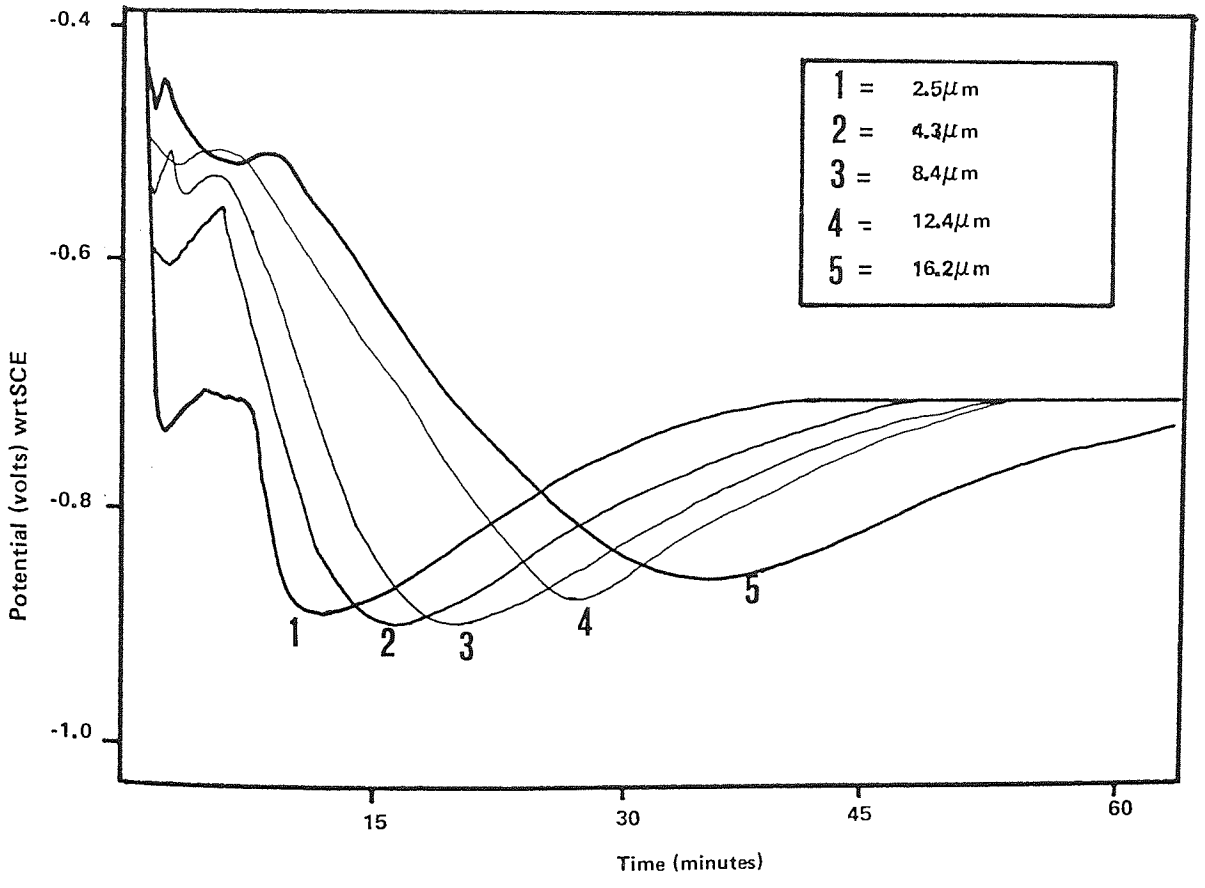

Figure 4.2.2.7 Potential-time family for 99.99% aluminium immersed in AC51 after anodic treatment at 20°C for various times

In order to test this theory the anodic oxide film structure was altered by increasing the anodising solution temperature. It has been shown that the anodising solution temperature did not markedly affect the anodic film thickness (section 4.2.1). Mason and Shinder[112] found that increased solution temperature lead to increased ion mobility, the aluminium dissolution rate increased and the anodic film structure became more porous with an increased pore size. Therefore any change in potential-time behaviour is likely to be due to a change in the anodic film structure rather than the thickness.

Figure 4.2.2.7 shows that the potential-time curves obtained from samples anodised at a room temperature have different characteristics. The potential reached within the first few minutes of immersion are, in general, more noble and erratic than the potentials reached by corresponding samples anodised at -8°C. The most active potential reached is very consistent and has a definite point. The most active potential reached by the -8°C samples do not display such consistent behaviour. However, the final steady-state potential are similar in all cases.

Figure 4.2.2.8 shows the relationship between the time taken to reach the most active potential and the measured anodic film thickness for both sets of anodised samples.

The efficiency with which AC51 removed thick anodic films was checked by measuring the weight of any oxide left on the samples surface after immersion in AC51. Table 4.2.2.3 shows the thickness of any remaining oxide along with the original anodic film

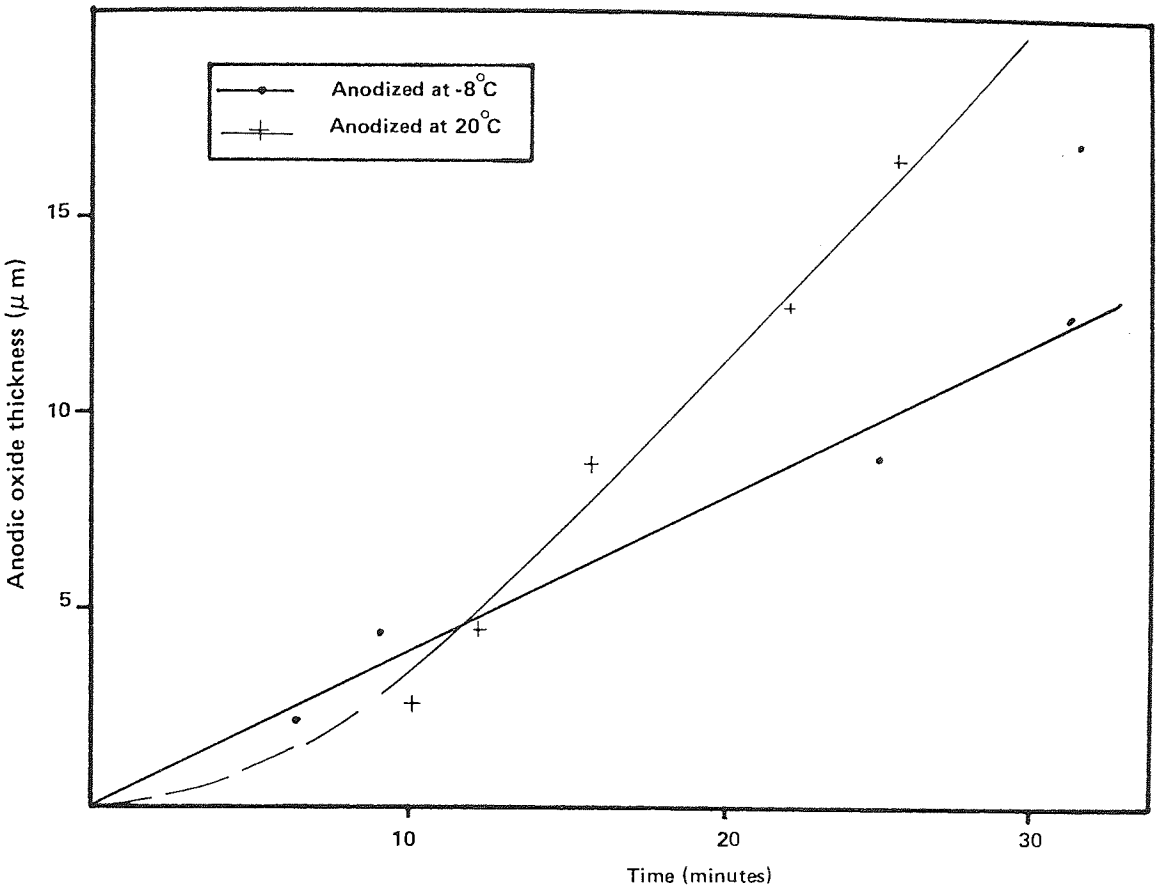

Figure 4.2.2.8 The relationship between anodic oxide thickness and time to reach the most active potential for 99.99% aluminium in AC51

Table 4.2.2.3 Time of Immersion of Anodised Samples in AC51 and Average Thickness of Remaining Oxide.

Anodising Temperature (°C)	Anodic Film Thickness (μm)	Time of Immersion in AC51 (Mins)	Average Remaining Oxide Thickness (μm)
-8	2.1	38	0.13
-8	4.2	60	0.06
-8	8.8	46	-
-8	12.3	94	0.21
-8	16.7	51	0.16
20	2.5	32	0.05
20	4.2	44	0.03
20	8.8	38	0.06
20	12.3	102	0.06
20	16.7	62	0.07

thickness and time of immersion in AC51. The anodic film has been efficiently removed by the AC51 solution. The cause for the slight positive readings may be that small islands of oxide remained on the surface after immersion in AC51 or that the stripping solution slightly etched the substrate.

4.2.3 Effect of the Surface Oxide on Alocrom 100

The potential-time determinations obtained by immersing heat treated coupons in Alocrom 100 are shown in Figure 4.2.3. It can be seen that increasing heat treatment temperature resulted in a

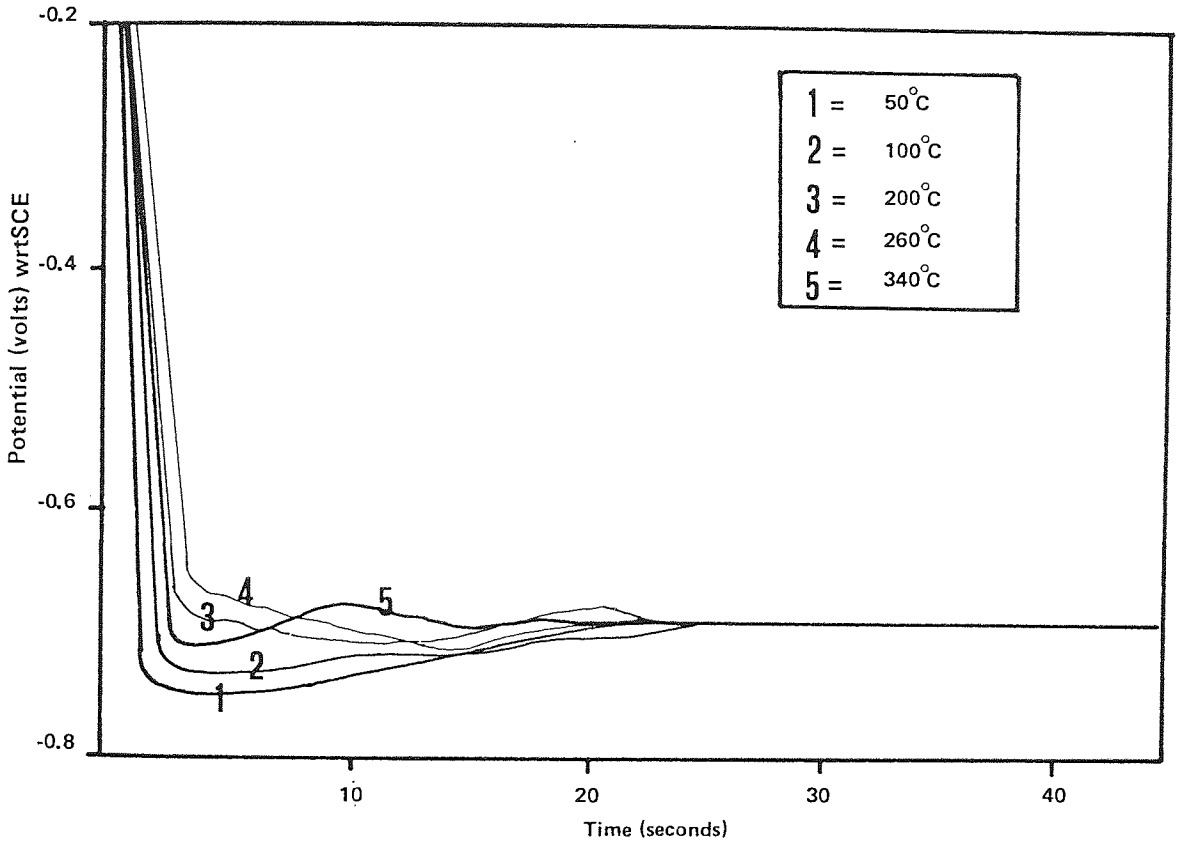

Figure 4.2.3 Potential-time family for 99.99% aluminium annealed for 1 hour at various temperatures prior to immersion in standard Alocrom 100.

less active initial potential. However steady-state potentials were achieved within 25 seconds in all cases.

4.2.4 Effect of ageing the cleaning solution

It was found that the rate of aluminium dissolution in AC51 cleaner solution, at operating temperature of 50°C, was dependent

upon the surface area of the immersed aluminium sheet. Table 4.2.4.1 shows the amount of aluminium detected in the AC51 solutions. Solution 1 (initially 1 litre of fresh AC51) had super pure aluminium sheet with a surface area of 0.1544 dm^2 immersed in it. Solution 2 (initially as solution 1) had 99.99% aluminium sheet with a surfae area of 0.7720 dm^2 immersed in it.

Table 4.2.4.1 Showing Aluminium Detected in Ageing AC51

Immersion time (Mins)	Aluminium detected in solution	
	Solution 1 (ppm)	Solution 2 (ppm)
5	4	8
10	5	16
20	9	32
30	13	46
50	16	55
80	22	75
100	27	96
150	44	141
200	53	179
300	76	241
450	112	322
600	135	287
900	192	515
1860	340	884
4500	824	1872
8460	1268	2736

The data was found to fit a curve described by

$$Al_{conc} = K\ t^{0.7886}$$

where Al_{conc} = aluminium in soluton after time t
K = surface area constant

The surface area constant (K) was found to be 0.87 and 2.6 for solutions 1 and 2 respectively. Further, it was thought that

$$K = Sa \times D$$

where Sa = Surface area
D = rate of aluminium dissolution per unit surface area.

However, the true surface area of the solution/metal substrate was not known and so this cannot be shown to be correct.

Figure 4.2.4 shows the computed curves for solutions 1 and 2 with the recorded results plotted over them as individual points. Very good correlation exists between the model and the observed results. A sample of used cleaning solution (AC51) was obtained from a commercially used bath (Metallic Protectives Ltd). This solution was worked under typical conditions, including loss from drag-out and solution replenishment. It was found to have an aluminium content of 0.14 g/l (1,400 ppm).

The potential-time curves produced by immersion of 99.99% aluminium in AC51 at various stages of 'ageing' had the same characteristic shape as fresh solutions (Figure 4.2.2.1). Table 4.2.4.2 shows that the time taken for the initial fall of potential was greatly increased for aged solutions.

Table 4.2.4.2 Tabulated Potential-Time Results for 99.99% Aluminium in AC51 at Various Stages of 'Ageing'

Aluminium Content (g/l)	Time to Active Potential (Mins)	Time to Steady State potential (Mins)
0	2	9
0.34	7	27
0.88	15	54
1.27	26	52
2.74	73	160

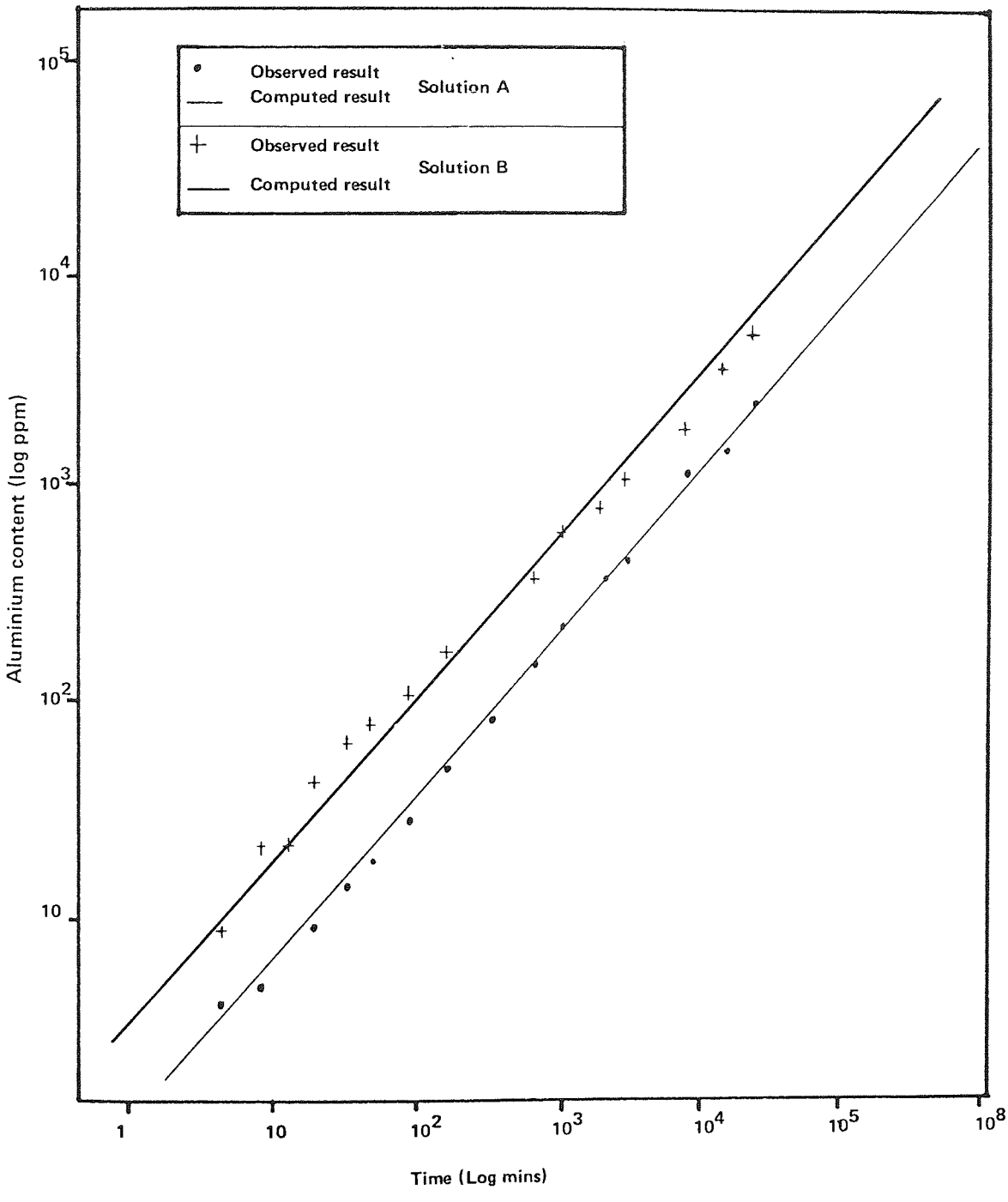

Figure 4.2.4 Log Log plot of aluminium concentration against time 99.99% aluminium in AC51 solution

SEM observations of the surface of 99.99% aluminium, degreased and cleaned in AC51 for 5 minutes for both fresh and aged solutions are shown in Photo 7. It is possible to see that the fresh solution caused more etching along grain boundaries than the aged solution. Photo 7D shows an area of intense pitting caused by local anodic dissolution of aluminium in fresh AC51.

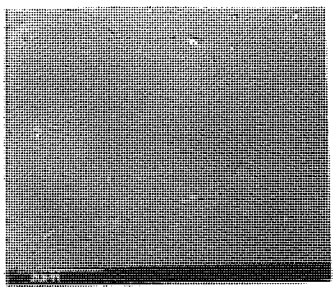

A

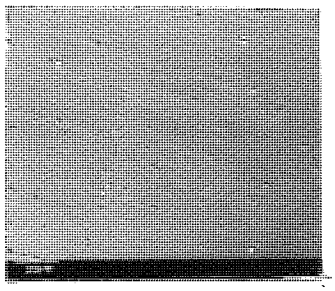

B

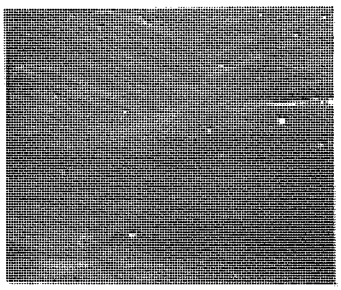

C

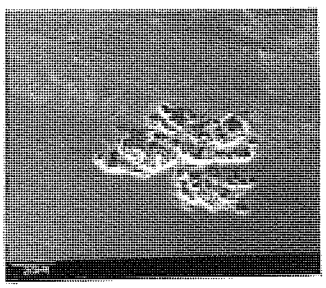

D

Photo (7) 99.99% aluminium treated by

Mag = x 1K Ta = 30°

A Degreased by acetone swab
B Degreased and cleaned in fresh AC51 for 5 minutes
C Degreased and cleaned in aged AC51 (1270 ppm Al) for 5 minutes
D Intense pitting after 5 minutes in fresh AC51 on 99.99% aluminium

5. INVESTIGATION INTO THE ROLE OF CONSTITUENT INGREDIENTS OF A CHROMATE-PHOSPHATE SOLUTION

5.1 Introduction to Experimental Work

The original Alocrom 100 patent[93] was examined in order to produce a similar type of solution under laboratory conditions. Total control of the solution make-up could be gained in this way allowing fundemental research upon the role of the main constituents.

The effect of the fluoride to chromic acid ratio and overall concentration was studied, initially by producing coatings from various solutions on 99.99% aluminium. Potential-time, weight change and SEM studies were made of coatings formed.

The role of phosphoric acid was studied using a number of solutions with identical fluoride and chromic acid ratios but with varying phosphoric acid concentration.

5.1.1 Patent solution make-up and use

The initial solution made up used the mid-point optimum values suggested in the patent[93]. The fluoride ion to chromic acid ratio was taken to be 0.27 and the chromic acid concentration was 13 g/l. From this the fluoride ion concentration required was calculated to be 3.51 g/l which was equivalent to 7.76 g/l of sodium fluoride (NaF). To bring this solution into the optimum operating range (as suggested in the patent) 82 ml/l phosphoric acid (140 g/l H_3PO_4) was added.

The solution was made up to 1 litre with distilled water and

thoroughly stirred. The pH of this solution was found to be 1.9, just within the pH range stated in the patent. The mid-point solution make-up was:-

Chromic acid (CrO_3)	13 g/l
Sodium fluoride (NaF)	7.76 g/l
Phosphoric acid (H_3PO_4)	140 g/l (or 82 ml/l)

A 99.99% aluminium coupon was cleaned in AC51 followed by immersion in the above solution for 5 minutes then rinsed and dried. This test sample seemed to indicate that the solution was overactive, since a powdery deposit had formed. Therefore a series of tests were made on solutions with the same ratio of ingredients but with reduced overall concentrations.

5.1.2 Effect of reducing the solution concentration

The laboratory made solution taken from the patent[93] described in the previous section was used in various concentrations shown in Table 5.1.2 to find the effect of reducing the activity of the solution.

A series of samples were produced with increasing immersion times for each solution prepared; all solutions were tested both fresh and in the aged condition. Potential-time determinations and coupon weight change/time curves were found for each solution.

Table 5.1.2 Solution Ingredients in Grammes per Litre

Ingredients \ Solution No.	1	1B	1C	1D	1E
Chromic acid (CrO_3)	13.00	10.40	8.67	6.50	4.33
Sodium fluoride (NaF)	7.76	6.21	5.17	3.88	2.59
Phosphoric acid (H_3PO_4)	140.0	112.0	93.0	70.0	47.0
Effective dilution (%)	0.0	20.0	33.30	50.0	66.7

99.99% aluminium coupons were cleaned in aged AC51 for 5 minutes then immersed in 100 ml of solution at room temperature, with moderate agitation provided by a magnetic stirrer. All solutions were discarded immediately after use in order to avoid any problems with changing solution composition. After immersion the samples were carefully rinsed and dried using a cold air blower. Each specimen was logged carefully and examined under the SEM as soon as possible following a visual inspection of the surface film formed.

5.1.3 Effect of changing the concentration of constitutent ingredients

The effect of changing the fluoride ion to chromic acid ratio ($F^-:CrO_3$) was studied in order to ensure that the mid-point of the range suggested in the patent[93] was in fact the optimum for this solution. The effect of the phosphate ion concentration in the solution was studied by altering the phosphoric acid content. Table 5.1.3 shows the composition of the solutions studied. Solutions 3A, 4A and 4B were made up by additions of extra chromic acid or sodium fluoride to samples of solutions 3 and 4 respectively.

A time series was produced on 99.99% aluminium for each solution prepared. Potential-time and weight change/time curves were found using the techniques and conditions described previously. All samples were examined visually before logging; SEM examination was carried out as required.

Table 5.1.3 Solution Composition

Solution No.	Chromic Acid (g/l)	Sodium Fluoride (g/l)	Phosphoric Acid (g/l)	F^-: CrO_3 ratio
2	13.0	7.8	70	0.27
3	6.5	3.9	140	0.27
3A	8.5	3.9	140	0.21
4	13.0	7.8	0	0.27
4A	20.5	7.8	0	0.17
4B	13.0	10.4	0	0.36
5	19.0	7.8	0	0.18

5.1.4 Investigation into the role of phosphoric acid

The role of the phosphate ion in the coating formation mechanism was investigated. A series of solutions with identical chromic acid and fluorine ion content, but increasing phosphoric acid content was produced. Coupon weight change, potential-time, SEM, and AAS studies were then carried out for each solution.

Each solution was made-up as follows:-

i) 6.5 g/l of chromic acid and 3.88 g/l of sodium fluoride were weighed out.

ii) phosphoric acid ranging from 0 to 1275 g/l as in Table 5.1.4 was measured out and made up to 1 litre with distilled water.

iii) all ingredients were mixed together until completely dissolved.

Table 5.1.4 Shows the Composition of the Solutions Made-Up

Solution	Phosphoric Acid content (g/l)	Volume of Phosphoric acid (ml/l)
A	0	0
B	35	22
C	70	41
D	140	82
E	200	118
F	250	147
G	300	176
H	350	206
J	560	329
K	1275	750

The potential-time and coupon weight change studies were carried out using the standard procedure outlined previously. Immersion times ranged from 1 minute to 200 minutes on a roughly logarithmic scale. 99.99% aluminium coupons cleaned in an aged AC51 solution for 5 minutes were used throughout this work. 100 ml of fresh solution was used at room temperature with moderate agitation for each test. A sample of the used solution was saved after each test in a small air tight polypropylene container ready for future analysis.

It was found that prolonged time (more than 24 hours) between the cleaning of a coupon in AC51 and conversion coating had a detrimental effect on the adhesion of the coating formed.

Finally each solution was analysed for aluminium content as a function of coupon immersion time using the solutions saved from the coupon weight change programme. Atomic absorption spectrophotometry (AAS) was used to determine the amount of aluminium present in each solution. Solution A was found to have very low aluminium content levels and so a standard 5 ppm was prepared from the aluminium nitrate stock solution. All standards and blanks were prepared using fresh 20% solutions of each solution under test ie A - K, the sample solution was also diluted to 20%. All solutions used including blanks and standards were spiked with 1500 ppm KCl.

5.2 Results

5.2.1 'Mid-point' solution observations

The sequence of formation and growth of a conversion coating produced by the 'mid-point' solution is shown in Photo 8. Spherical particles 0.25 μm in diameter cover the surface after 45 seconds immersion. By 90 seconds these particles have become column shaped and covered by a second compact layer, clearly shown in Photo 8B. The powdery appearance noted by visual examination of the specimens was caused by the formation of a third layer (Photo 8C) of spherical particles, which had poor adhesion to the lower layer of the coating. EDXA showed that the coating was formed from phosphorus and chromium only. A large aluminium peak was also noted, but was probably due to the porous nature of the coating rather than showing the presence of aluminium in the coating itself. Ageing this solution had very little effect on the coating structure or composition.
Table 5.2.1 shows the EDXA results for coatings with increasing film weight.

5.2.2 Effect of reducing the soluton concentration

A visual assessment of the conversion coatings formed showed that reducing the concentration of the 'mid-point' solution taken from the patent(93) improved the uniformity and adhesion of the coatings at all stages of development. The colour of the coatings became darker with increased immersion time. Solution 1 produced a dark green conversion coating with 6 minutes immersion whereas

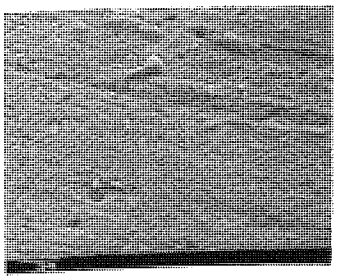

A
45 seconds

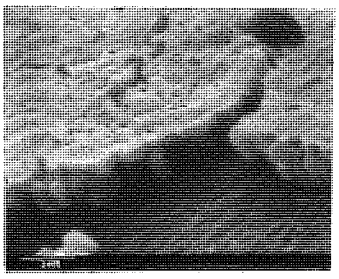

B
90 seconds

C
360 seconds

Photo 8 The 'mid-point' solution on 99.99% aluminium at room temperature.

Frame A; Mag = x 10K, Ta = 60°C: Surface covered with spherical particles about 0.25 μm in diameter

Frame B; Mag = x 20K, Ta = 60°: Two layers visible; lower coating made up of individual particles 0.5 μm high. Upper coating is continuous and gives a 'mud-cracked appearance', about 0.25 μm thick.

Frame C; Mag = x 1K, Ta = 30°: Large groups of particles between 1 to 2 μm in diameter on a typical mud-cracked film. The top layer is very powdery and non-uniform in appearance.

Table 5.2.1 EDXA Results on Coatings Formed in an Aged 'Mid-point' Solution.

Time of Immersion (Mins)	Detected peaks			P: Cr ratio
	Al (%)	P (%)	Cr (%)	
1	85.8	13.7	0.5	26.8
2	80.7	17.4	1.9	9.2
3	54.2	40.6	5.2	7.8
4	50.9	43.2	5.9	7.3

solution 1E (See Table 5.1.2) produced a translucent light-green coating. The optimum solution producing fast-growing cohesive coatings was represented by solutions 1D-E; both produced coatings that were very similar to Alocrom 100. In all cases, ageing the solution had the effect of increasing the coating colour and reflectivity (judged by eye).

SEM examination of the coatings showed that the multi-layered structure of coatings produced in the 'mid-point' solution are not formed by less concentrated solutions. Photo 9 shows that coatings become less porous as the concentration of the solution decreases. All the coatings were produced by 6 minutes immersion, Photo 9A shows the solution B coating thickness is 4-5 μm, the porous structure clearly visible. Solution 1C produced a more coherent coating, but hair-line cracks (not the deep mud-cracks) and pits can be seen on the surface. Solution 1D (50% solution 1) has no porosity visible on the coating's surface.

Potential-time measurements recorded an instantaneous steady-state potential for all solutions, fresh and aged. The potential became slightly less active as the solution concentration was reduced and became 0.2 v more active upon ageing.

The colour of the coating appeared to give some sort of guide as to the coating thickness. This suggested that dilute solutions produced coatings which had a lower coating weight. The weight change/time curves are plotted in Figure 5.2.2.

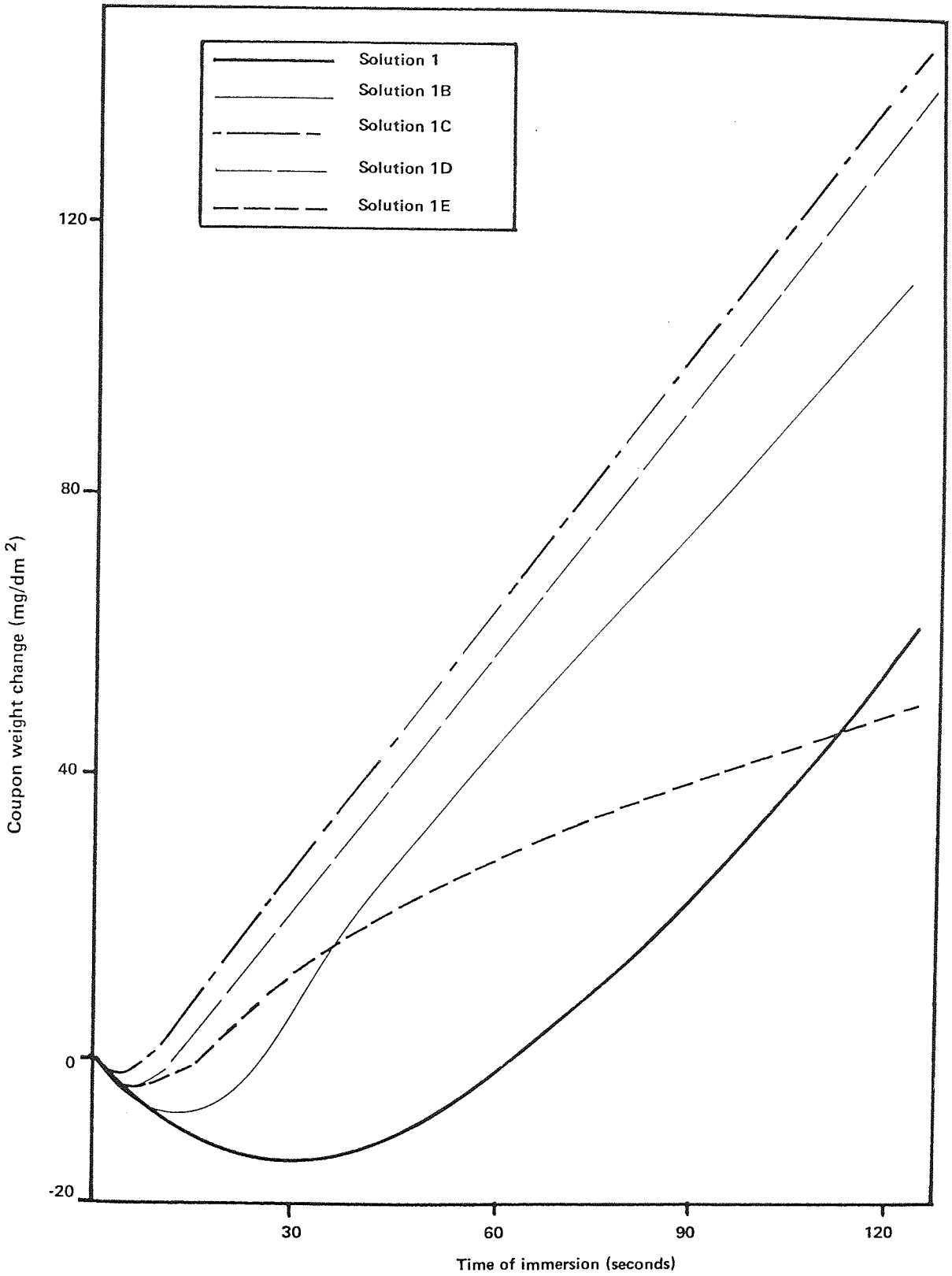

Figure 5.2.2 The effect of reducing the concentration of solution 1 (see Table 5.1.2) on coupon weight change.

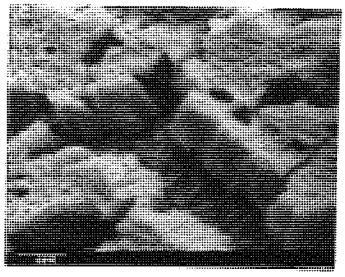

A

Solution 1B

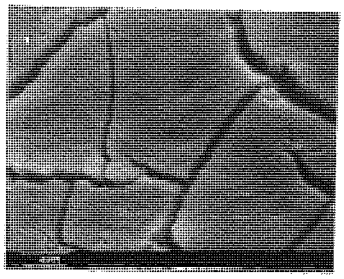

B

Solution 1C

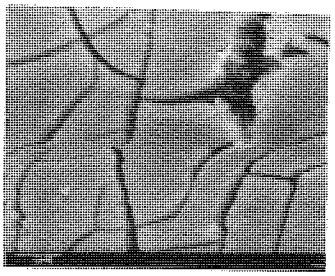

C

Solution 1D

Photo 9 Various coatings formed on 99.99% aluminium at room temperature with 6 minutes immersion.

(Mag = x 5K Ta = 30°)

Frame A; The porous nature of this coating is clearly visible as pits in the surface and the 'island' edge structure.

Frame B; Porosity is shown by fine cracking on islands surfaces and small pits.

Frame C; No porosity visible at all. This coating has adhered well enough to withstand an inward bend halfway up the frame.

During the first 30 seconds of immersion, aluminium dissolution was greater than coating formation resulting in the observed negative weight change. The 'mid-point' solution (solution 1) had the highest rate of aluminium dissolution; reduced concentration lead to reduced dissolution. The weight change curves appear to show that solution 1C has the highest rate of coating formation. However, if the rate of aluminium dissolution were taken into account, it would probably reflect the order suggested by the colour of the coatings.

5.2.3 Effect of changing the levels of constituent ingredients

The effect of reducing phosphoric acid content in the solution by 50% (solution 2) on the conversion coatings it produced was not easy to detect. Coatings produced were very similar in appearance to coatings formed in solution 1 (the 'mid-point' solution). It was therefore concluded that the formation of the powdery coatings seen in solution 1 was either due to the solution being over active or out of balance.

Solution 3 had half the chromic acid and fluoride content of solution 1 but the same level of phosphoric acid. This produced very good light coatings, but thicker coatings again became matt and had poor adhesion. Increased fluoride content (solution 3A) produced compact coatings (visibly) when the solution was aged, but was very slow and required long immersion times to produce a reasonable coating weight.

A phosphoric acid free solution (solution 4) with the same chromate and fluoride levels as solution 1 was found to produce coatings with a powdery, olive-green appearance. The potential-time curve obtained from this solution is shown in Figure 5.2.3.1. No explanation can be given for this cyclic behaviour.

It was noted that agitation had a significant effect upon the period of the cycling, increasing the time for cycling to commence and increasing the period of oscillation. Large gas bubbles could be seen on the surface of the coupon, but no obvious connection between the bubbles and the cycling was noted.

The coupon weight change/time curve is shown in Figure 5.2.3.2. The down-turn in weight gain corresponds to the beginning of potential cycling.

SEM examination of these coatings could not adequately resolve any surface features of the topography. However, it was thought that the coatings were made up from very small spherical particles up to 200 nm in diameter. EDXA showed the presence of chromium and sodium in the coatings formed, which did not change in structure

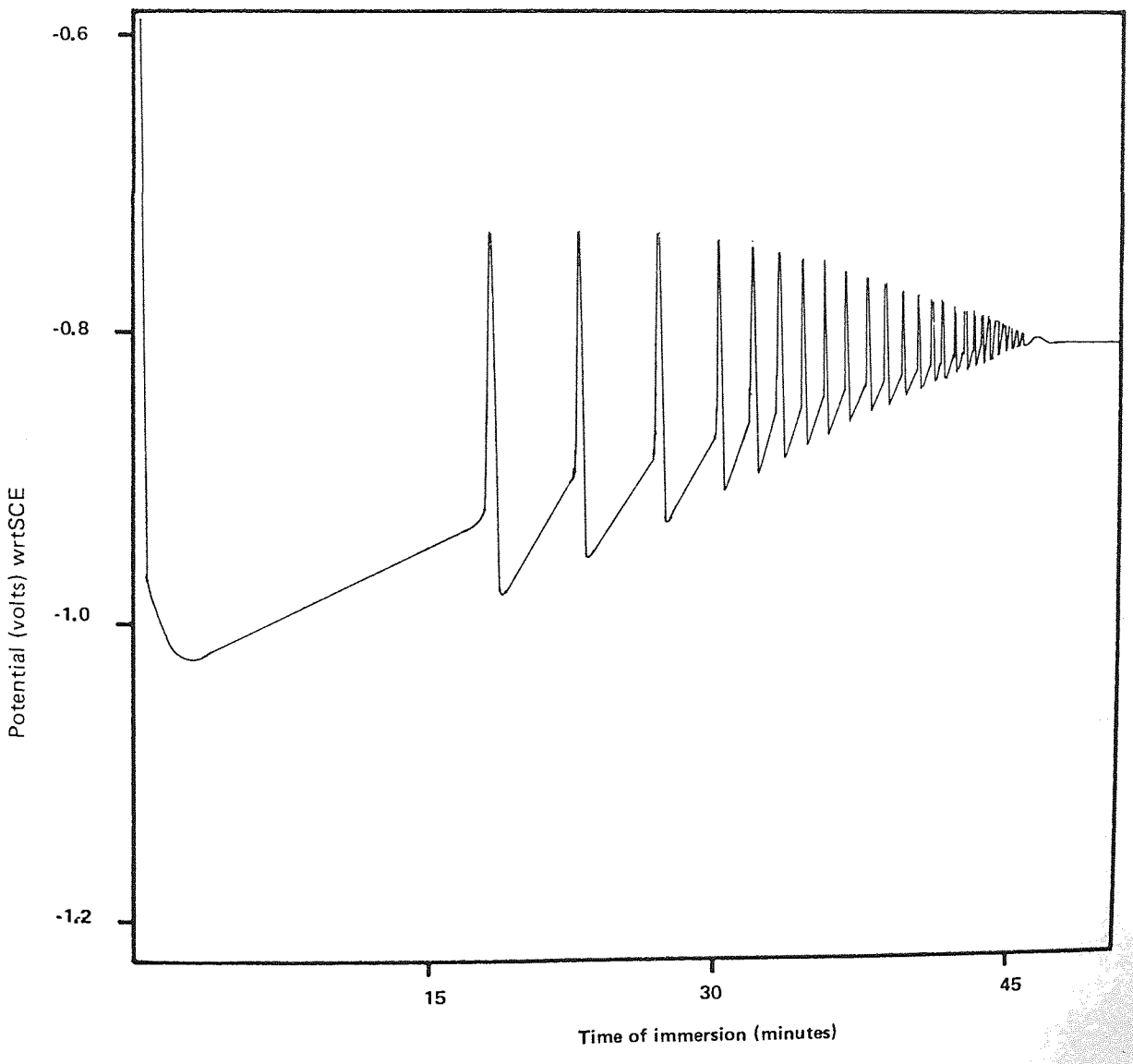

Figure 5.2.3.1 Potential-time curve of 99.99% aluminium in a phosphorus free chromate solution

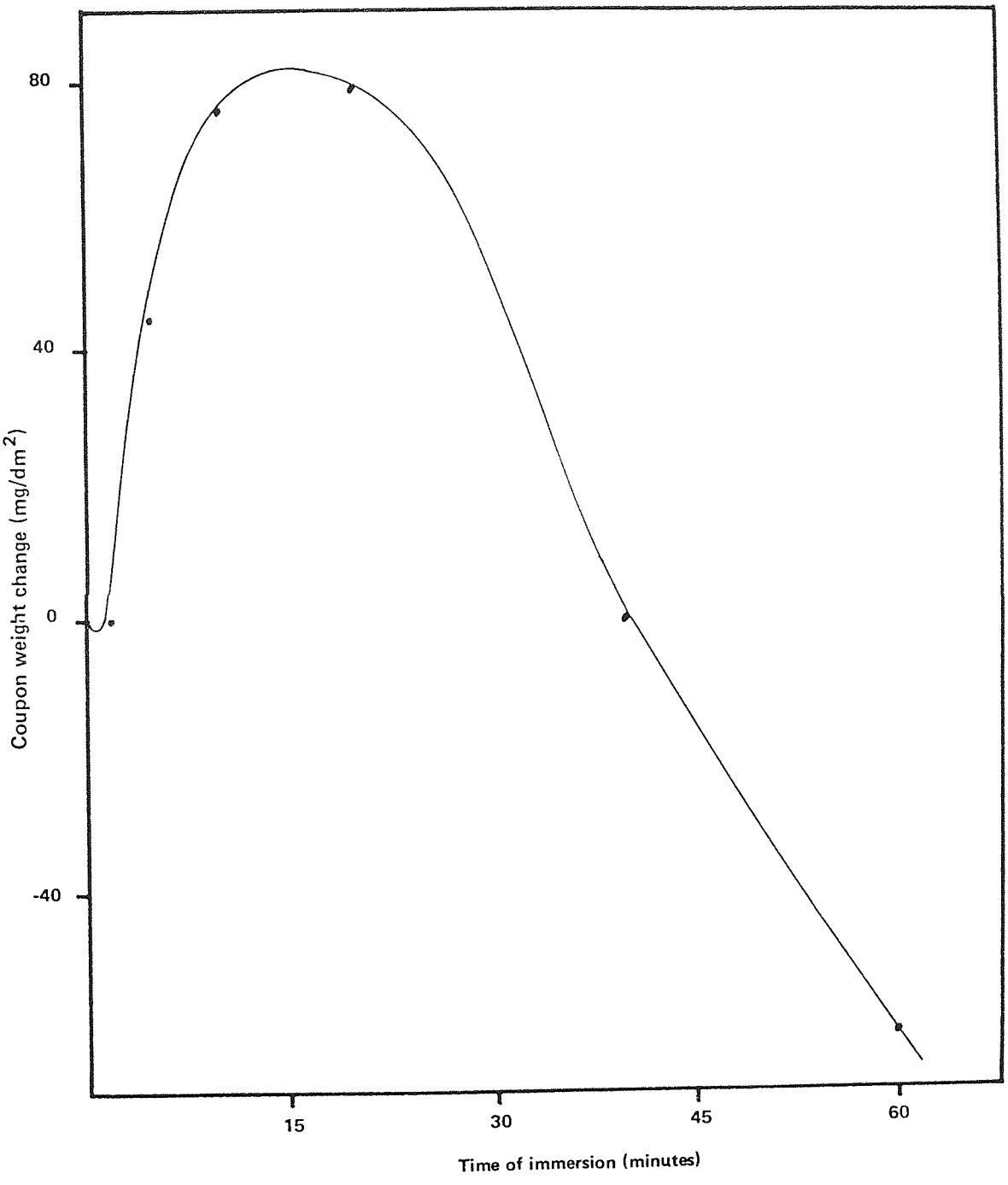

Figure 5.2.3.2 Coupon weight change against time for 99.99% aluminium in solution 4 (see 5.1.3) at room temperature.

or composition after 15 minutes. Increasing the fluoride content (solution 4B) resulted in severe etching of the substrate with no coating formed at all. Increasing the level of chromic acid (solution 4A and 5) produced a matt yellow-gold colour coating. Photo 10 shows the coating observed under the SEM, EDXA detected aluminium (from the substrate), chromium and sodium in the upper layer. However, the lower layer was devoid of sodium.

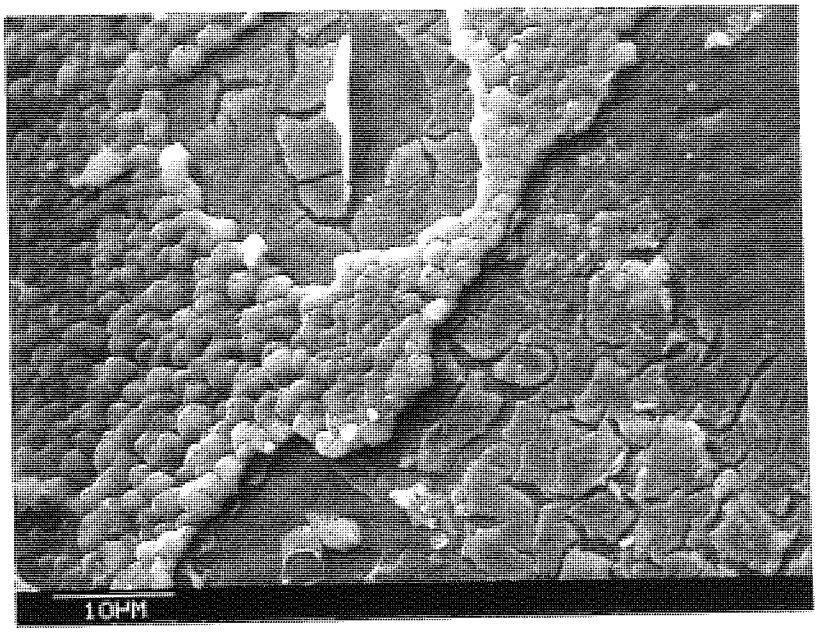

Photo 10 Shows the structure of a phosphorus free coating produced from solution 5 (F^-: CrO_3 = 0.18)

Mag = x 2K Ta = 30°

The potential-time curves obtained from solution 4A and 5 did not display any signs of cycling, a potential of -0.76 wrt SCE was achieved within 1½ minutes of immersion which slowly increased to a steady-state voltage of - 0.68 volts wrt SCE by 24 minutes immersion.

5.2.4 The role of phosphoric acid

Ten solutions were prepared using the optimum levels of chromic acid and fluoride ions as found from the previous section (ie 6.5 g/l CrO_3, 3.88 g/l NaF). The amount of phosphoric acid in each solution varied from 0 to 1275 g/l covering the complete range possible.

All specimens produced were examined using the SEM. However despite apparent visual differences, many samples displayed a similar mud-cracked pattern.

Solution A, 0 H_3PO_4

Visual examination: up to 20 minutes immersion, coatings formed were light green, and non-uniform. After 20 minutes, light green powdery coatings where formed covered with yellow-gold colour spots and had poor adhesion.

SEM study: The sequence of growth of the coating is clearly visible in the series of electron micrographs shown in Photo 11. After 1 minute immersion about 40% of the original surface was covered with precipitated particles, approximately spherical in shape and up to 2 μm in diameter (Photo 11A). Rolling lines and a few pits that developed in the acid cleaner were clearly visible on the original surface not covered by the spherical particles. After 2 minutes immersion the spherical particles had grown to about 4 μm in diameter and had merged due to lateral growth (Photo 11B) to form a monolayer covering about 95% of the original surface (Photo 11C). By 5 minutes immersion a second set of spherical particles also about 4 μm in diameter could be seen to

have formed on top of the monolayer of merged spheres formed in the initial 2 minutes (Photo 11D). The topography of the original surface can be seen in the upper left hand corner of Photo 11D where some of the coating has flaked off (possibly due to preparation of SEM examination when dry). The rolling lines and a few pits that developed in the cleaner, which were visible in Photo 11A, can still be seen but were slightly rougher due to acid attack on the aluminium.

After 60 minutes immersion at least two successive layers had been built up, shown in a glancing view in Photo 11E. Crack paths in the coating can be seen along the boundary between merged spheres (Photo 11D, E and most clearly in F), mechanically the weakest part of the coating. Photo 11G shows the substrate/coating interface, where part of the coating had flaked off, has a typical mud-crack pattern, characteristic of vitreous and brittle materials. The circular holes in the coating were gassing sites, the continuous production of bubbles maintaining the circular shape during immersion. Channels for solution transport to the metal interface and for escaping gas bubbles can be seen between some of the merged spherical particles (Frame H).

EXDA was carried out for each coating while in the SEM. Table 5.2.4.1 shows these results both for a large area of each coating and for selected regions such as individual particles. Direct comparison can be made between coating results since analysis conditions were similar in all cases. However, conditions were changed for selected region analysis and must therefore not be used for direct comparison but is useful as a guide to part of an overall picture.

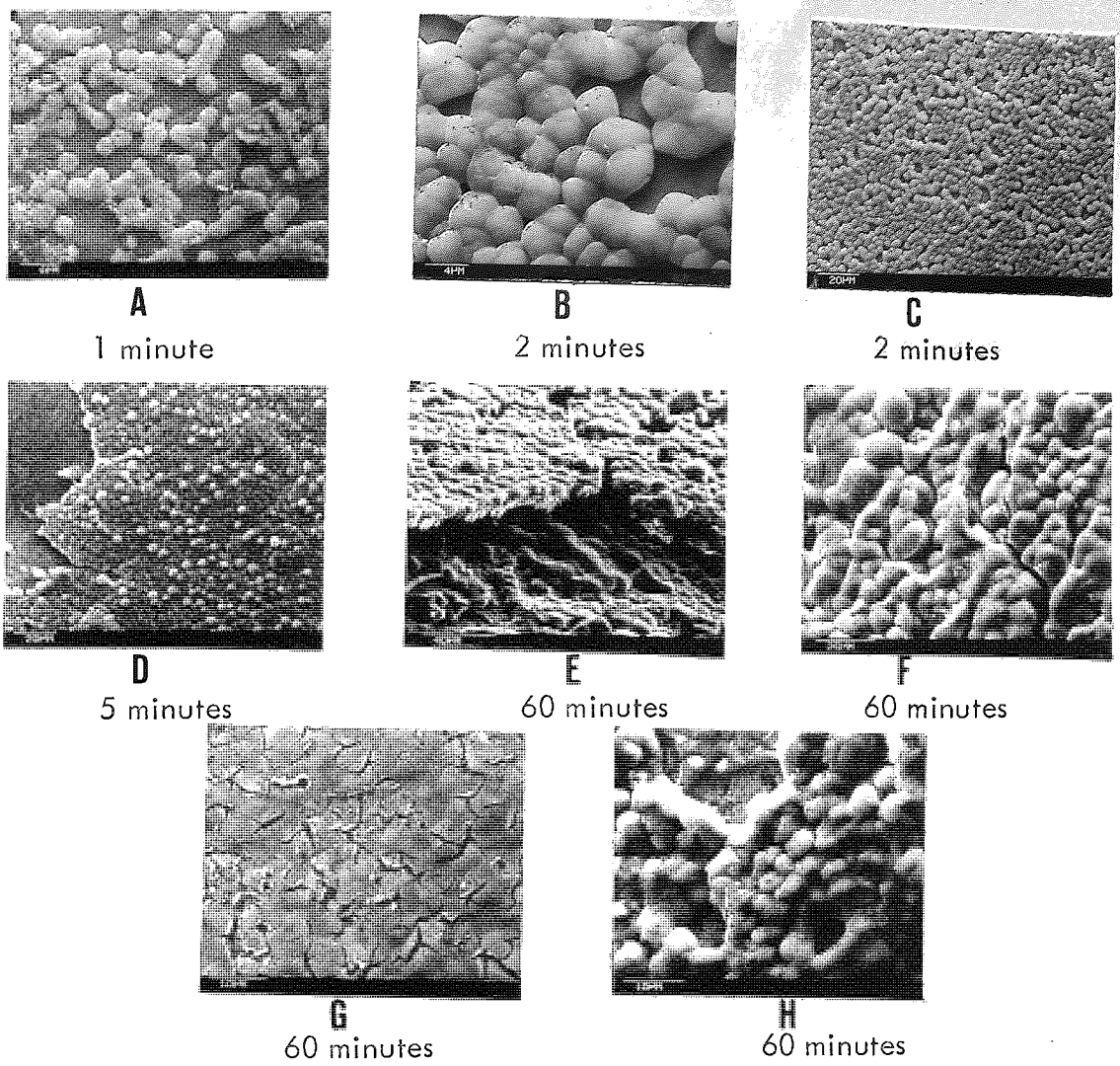

Photo 11 Time series of coating formed on 99.99% aluminium from solution A (zero H_3PO_4) (Ta = 30°, except E=57°).

Frame A; Mag = x 5K; Spherical particles nucleate on surface after 1 minute of immersion.

Frame B; Mag = x 5K; Particles begin to merge together after 2 minutes.

Frame C; Mag = x 1K; Surface almost completely covered after 2 minutes.

Frame D; Mag = x 1K; A second set of spherical particles formed on the monolayer produced in the initial 2 minutes. The original surface is also visible on the top left hand corner.

Frame E; Mag = x 500; Glancing view of coating showing two successive layers of merged spherical particles.

Frame F; Mag = x 1K; Crack path can be seen running between merged particles.

Frame G; Mag = x 2K; Substrate/coating interface where part of the coating had flaked off.

Frame H; Mag = x 2K; Channels for solution transport and gas escape between merged particles.

Table 5.2.4.1 EDXA Results of Coatings Produced from Solution A (H_3PO_4 free)

Time of Immersion (Mins)	Major Peaks (%)			Comments
	Na	Al	Cr	
1	0.3	98.4	1.1	general coating
2	21.9	75.0	3.1	
5	16.6	82.5	0.9	
20	31.9	64.9	3.3	
60	51.5	42.4	5.9	
120	67.4	28.2	4.4	
1	0.4	97.5	1.8	individual particles
2	30.8	65.1	4.1	
5	46.4	51.4	2.2	
20	64.7	30.0	4.5	
60	59.7	36.0	4.2	

This shows that the major coating constituents were sodium and chromium. Aluminium may also be present in the coating, but its presence could also be due to penetration of the substrate by the electron beam. The Na:Cr ratio was consistently higher for the analysis of individual particles than for the coating, possibly indicating that the particles were richer in sodium than the surrounding areas.

Solution B, 35 g/l H_3PO_4

Visual examination: The shortest immersion times produced films with complete coverage. Colour ranged from a translucent green tinge to a dark green powdery surface. Adhesion was good up to 5 minutes but then becames poor as the surface became "powdery" in structure.

SEM Study: Photo 12 shows the development of this coating. It is clear that the spherical particles that were seen to develop in the phosphorus free coating are not visible at any stage. The first indication of film formation occurred after two minutes immersion. The surface appears roughened and 'crows-foot' type defects became visible (Photo 12A). By five minutes a typical mud cracked film had developed, the islands continue to increase in size with increasing time of immersion (Photo 12B) and increasing film weight. After 60 minutes immersion the coating surface shows evidence of dissolution. Etch pits and ridges form on the surface (Photo 12C). One ridge seen on the middle right of Photo 12C had been split by a crack in the coating. This may be attributed to the mud cracking occurring upon drying after the ridge had been formed. After 195 minutes immersion the coating had become about 30 μm in thickness. Photo 12D shows that lateral cracking has taken place at various depths in the coating, giving the film a layered appearance when viewed from above. The edges of each 'island' can be seen to have risen up from the substrate with just the mid part adhering to the substrate. EDXA results show that sodium was not present in this coating. Table 5.2.4.2 shows the results obtained together with the P:Cr ratio which was found to be similar for all coatings analysed. It was noted that the P:Cr ratio had a similar upward trend and value to that found for Alocrom 100 on 99.99% aluminium (Table 3.2.1).

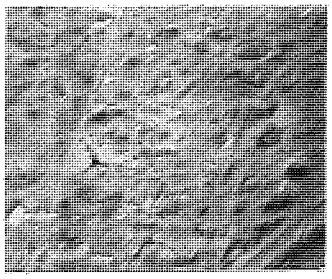

A
2 minutes

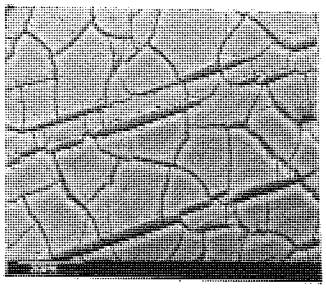

B
10 minutes

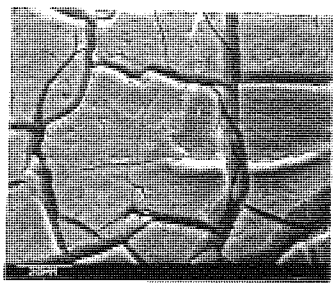

C
60 minutes

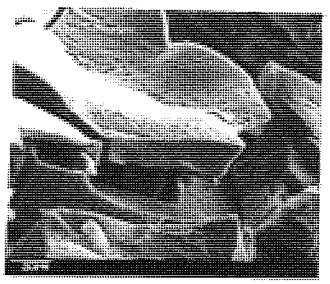

D
195 minutes

Photo 12 Time series of coating formed on 99.99% aluminium in solution B (35 g/l H_3PO_4) (Ta = 30° except D = 82°).

Frame A; Mag = x 2.3K; First sign of film formation, small cracks visible in the coating.

Frame B; Mag = x 1K; Typical 'mud-cracked' appearance. The film was approximately 2 μm thick at this stage.

Frame C; Mag = x 1K; 'Islands' have grown in size and are themselves cracked. The surface shows signs of dissolution, with pits and ridges.

Frame D; Mag = x 1K; Glancing angle shows island edges lifting away from the substrate surface. The coating was up to 30 μm thick. Lateral cracking produces layers much thinner than this.

Table 5.2.4.2 EDXA Results for Coating Formed on 99.99% Aluminium in Solution B (35 g/l H_3PO_4)

Time of Immersion (Mins)	Major Peaks			P:Cr ratio
	P %	Al %	Cr %	
10	5.5	54.7	39.3	1.4
20	3.0	58.6	38.5	1.5
40	8.4	54.7	36.8	1.5
60	0.8	60.6	38.4	1.6
120	3.8	59.5	36.7	1.6

Solution C 70 g/l H_3PO_4

Visual examination: Short immersion times gave full coverage. Coatings were similar in colour to those produced in solution B but they had a "grainy" structure. This coating had much better cohesion, having a shiny rather than powdery appearance. Adhesion was excellent.

SEM Study: Observation made under the SEM showed that this coating has a very similar sequence of growth to coatings produced in Solution B. A thin film was observed on the coupon after 1 minute of immersion, which is visible in Photo 13A. By 2 minutes immersion a fine network of cracks can be seen (Photo 13B). Islands were less than 4 μm square at this stage. The adhesion of the coating was very good. A coupon was bent double before being mounted and viewed in the SEM. This showed no sign of any coating becoming detached from the substrate (Photo 13C). The coating was about 1.6 μm thick after 5 minutes. Photo 13D shows the surface of an 'ideal' conversion coating. The crack density was even over the entire specimen surface and there were no

signs of any defects such as blisters, lifting island edges or coarse cracking. By 10 minutes immersion a few defects were visible mainly due to lifting island edges. As the film thickened so lateral cracking worsened. By 20 minutes immersion a few islands had become detached from the substrate. The coating was measured to be about 4 μm thick at these places. Photo 13E shows a rough surface had developed by 60 minutes immersion. As in the 60 minute sample of Solution B (35 g/l H_3PO_4) [Photo 12C], the ridge had been produced before the onset of cracking. Photo 13F shows that large blisters form in the top layers of very thick coatings. Bent samples showed that lateral cracking occurred at various depths in the coating. Adhesion was very good, despite areas where the heavy coating had failed due to lateral cracking. Very few areas were found with the substrate exposed.

The EDXA results are shown in Table 5.2.4.3. This shows that the P:Cr ratio is higher than for similar measurements taken from coatings produced in Solution B (shown in Table 5.2.4.2). An upward trend is again noted for the P:Cr ratio after the initial 2 minutes immersion.

Table 5.2.4.3 EDXA Results for Coatings formed on 99.99% Aluminium in Solution C (70 g/l H_3PO_4)

Time of Immersion (Mins)	Major Peaks			P:Cr ratio
	P %	Al %	Cr %	
1	91.0	7.1	1.9	3.7
2	81.6	14.2	4.2	3.4
5	46.2	40.1	13.7	2.9
20	2.6	73.6	23.8	3.1
60	1.3	76.7	22.0	3.5
120	1.0	79.1	19.9	4.0

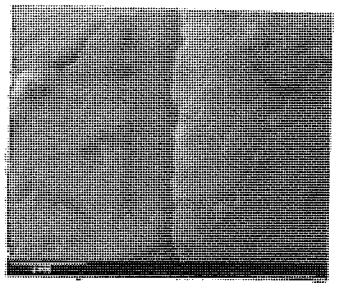

A

1 minute

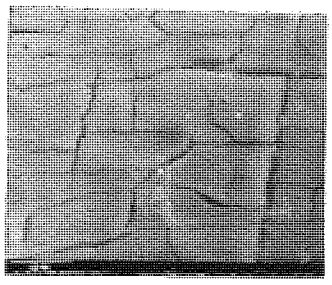

B

2 minutes

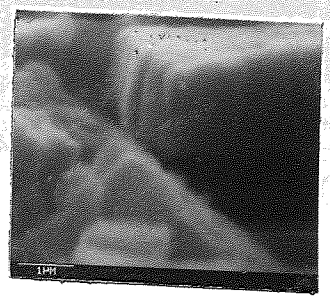

C

5 minutes

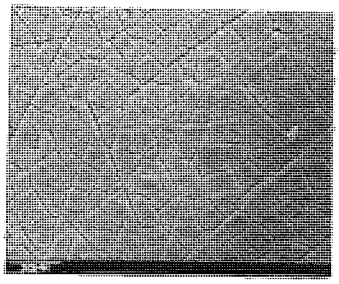

D

5 minutes

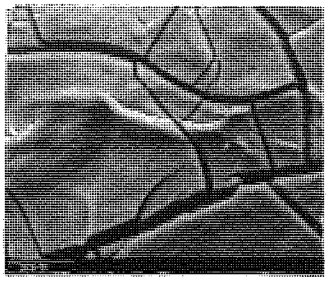

E

60 minutes

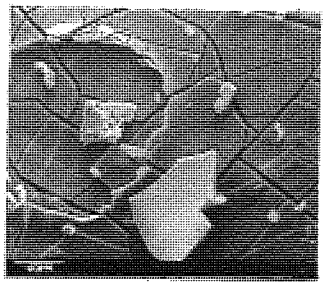

F

120 minutes

Photo 13 Time series of coating formed on 99.99% aluminium in solution C (70 g/1 H_3PO_4) (Ta = 30°, except C = 83°).

Frame A; Mag = x 20K; Coating present within 1 minute of immersion.

Frame B; Mag = x 5K; Mud-cracked appearance already clear.

Frame C; Mag = x 20K; Glancing view of a bent coupon. Adhesion was very good; no coating was dislodged. Coating was about 1.6 μm thick at this point.

Frame D; Mag = x 1K; Optimum conditions; no defects in coating. Very even crack density over entire specimen surface.

Frame E; Mag = 1K; Surface has been roughened due to dissolution by the solution. Cracking occurred after ridges had formed.

Frame F; Mag = x 500; Coating weight continued to increase with time, resulting in lateral cracking within the coating and blistering.

Solution D 140 g/l H_3PO_4

Visual examination: Very thin transparent coatings were formed the first minute. These coatings were lighter in colour than similar coatings produced in Solution C, but otherwise very alike. The film had good adhesion and mechanical properties.

SEM Study: A coating was found on the 1 minute specimen and was seen to have developed a fine crack structure similar to that shown in Photo 13A. However, by 2 minutes immersion, pits were seen to have developed at 'crack junctions' in the film (Photo 14A). The number of pits forming along crack lines increased with time of immersion, until after 5 minutes the cracks were very coarse and rough (Photo 14B). Crack density continued to decrease with increasing film weight as seen for coatings produced in Solutions B and C. Photo 14C shows the coating after 20 minutes immersion. The cracks have become well defined with no sign of pitting between islands. The coating surface had become covered by small indentations or shallow pits approximately 4 μm in diameter. Blistering was again present on heavy coatings. Photo 14D shows a low magnification shot of the coating formed in 120 minutes immersion.

Several blisters can be seen, three of which have collapsed, leaving a small portion of the top layer of the coating sticking upwards. These blisters were probably caused by entrapment of hydrogen gas during film formation or by water vapour produced during drying.

The EDXA results are shown in Table 5.2.4.4

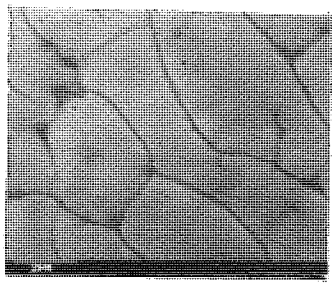

A
2 minutes

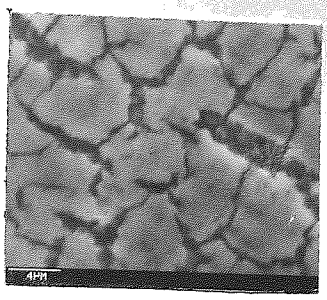

B
5 minutes

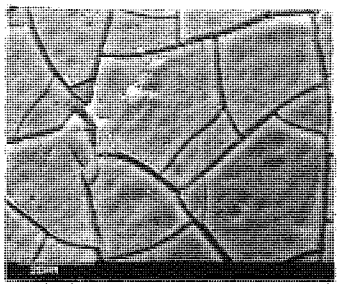

C
20 minutes

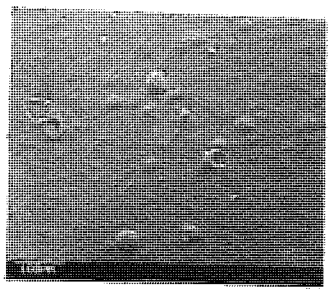

D
120 minutes

Photo 14 Time series of coating formed on 99.99% aluminium in solution D (140 g/l H_3PO_4) (Ta = 30° for all frames).

Frame A; Mag = x 10K; The film formed by 2 minutes immersion has typical mud-cracks; pits can also be seen at 'crack junctions'.

Frame B; Mag = x 5K; Coating has coarse cracking around 'islands' and rough crack edges due to pitting between the islands.

Frame C; Mag = x 1K; Cracks have become sharper and the coating surface is covered with shallow pits.

Frame D; Mag = x 200; Blisters formed on thick coatings.

Table 5.2.4.4 EDXA Results for Coatings Formed on 99.99% Aluminium in Solution D (140 g/l H_3PO_4)

Time of Immersion (Mins)	Major Peaks			P:Cr ratio
	P %	Al %	Cr %	
1	94.2	4.2	1.6	2.6
2	88.5	8.0	3.5	2.3
5	64.0	25.1	10.9	2.3
20	1.1	68.3	30.6	2.2
60	1.0	72.5	26.5	2.7
120	0	79.7	20.3	3.9

Solution E 200 g/l H_3PO_4

Visual examination: For the first 40 minutes the film had a non-uniform coverage and appeared to be powdery or dull. After 40 minutes immersion the coverage was uniform and the coating became more cohesive (ie fairly glossy). The colour of the coating was lighter than for similar coatings produced in solution D.

SEM Study: Immersion for 1 minute resulted in the production of roughly spherical particles approximately 500 nm in diameter. Photo 15A shows an area covered with these particles. Coverage was about 75% over the entire coupon. Increased immersion time caused the particles to increase in size and merge together in a similar way to solution A (Photo 11A-C). These particles were much smaller in size than those produced in solution A, and tended to nucleate along regions of high activity such as rolling lines or scratches. Photo 15B shows an area with two lines of merged particles (diagonally crossing the frame). Coverage had increased to about 85% over the specimen by 2 minutes immersion. Photo 15C shows the onset of a second layer developing over the initial layer of particles. At this stage the initial layer covered about 90% of the surface and the top layer covered about 50%. The top layer was itself formed from particles which were of a similar size to those in the initial layer. Further increases in immersion time lead to increased coverage by the top layer. By 10 minutes immersion, the bottom layer had about 95% coverage where visible, and the top layer covered 80% of the sample surface. The top layer continued to develop with increasing time of immersion

until complete coverage was attained after 10 minutes immersion.

Photo 15E shows the coating after 40 minutes immersion and a typical mud-cracked topography was evident. The surface of this coating was roughened by small pits similar to those seen on thich coatings of solution D (140 g/l H_3PO_4)). Prolonged immersion increases the amount and depth of these pits further. However blistering did not occur at any stage.

Table 5.2.4.5 EDXA Results of Coatings Formed on 99.99% Aluminium in Solution E (200 g/l H_3PO_4).

Time of Immersion (Mins)	Major Peaks			P:Cr ratio
	P %	Al %	Cr %	
1	98.0	1.4	0.6	2.3
2	97.3	2.1	0.6	3.5
	91.2	6.9	1.9	3.6
10	92.6	5.8	1.6	3.6
40	15.2	67.0	17.8	3.7
120	2.4	75.3	22.3	3.4

The EDXA results shown in Table 5.2.4.5 show that the coating had very poor coverage (or was very thin) until 40 minutes immersion, the time taken for complete coverage of the second layer. Even after 120 minutes the aluminium peak was still higher than for 20 minute coatings of previous solutions. This was probably due to the formation of a thin coating, since coverage was complete at this stage and no large cracks were observed exposing the substrate.

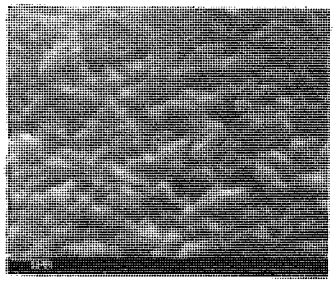

A

1 minute

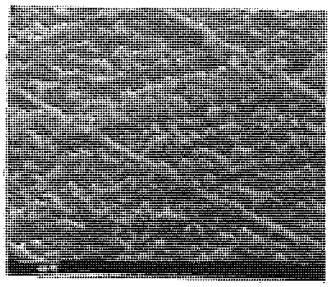

B

2 minutes

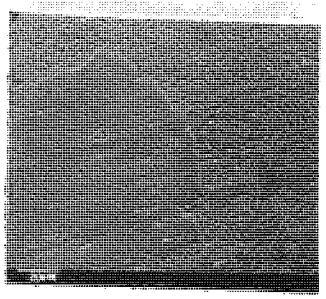

C

5 minutes

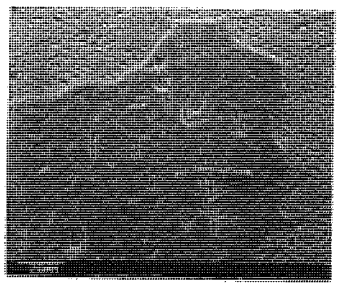

D

10 minutes

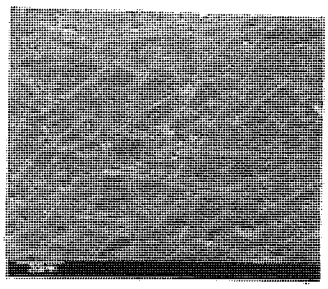

E

40 minutes

Photo 15 Time series of coatings formed on 99.99% aluminium in solution E (200 g/l H_3PO_4) (Ta = 30° in all frames).

Frame A; Mag = x 20K: Roughly spherical particles cover the surface.

Frame B; Mag = x 5K: Particles beginning to merge together.

Frame C; Mag = x 1K: The initial coating has been partially covered by a second layer.

Frame D; Mag = x1K: The second layer has expanded and now covers over 50% of the specimen surface.

Frame E; Mag= x 1K: Coverage is complete. The surface now has a typical mud-crack structure, but is covered with small pits.

Solution F 250 g/l H_3PO_4

Visual examination: A very thin white coating was produced within the first minute. Increasing immersion time etched this coating, removing it completely by 40 minutes immersion. The original white film was replaced by a dull light green coating which started to form after about 20 minutes immersion and covered the specimen within 60 minutes. This final coating did not develop further after 90-120 minutes.

SEM Study: The 1 minute sample, Photo 16A, was found to have been covered by a thin uniform film about 400nm thick. The surface was completely covered, except for gassing sites and rolling lines. After a further minute of immersion this coating had full coverage.

Photo 16B shows an island that had a much more compact structure had grown on top of the initial film within 5 minutes of immersion. By 20 minutes immersion much of the initial coating had gone. The 'islands' covered about 10% of the sample surface and were deeply pitted. Photo 16C shows the edge of an island. It borders three distinct areas. It is likely that these areas correspond to the grain structure of the substrate. After a further 40 minutes immersion, the islands can be seen to have become rougher in appearance due to severe etching or gassing. The surrounding coating has now completely covered the sample. Photo 16E shows that the islands remain clearly definable after very long immersion times (240 minutes).

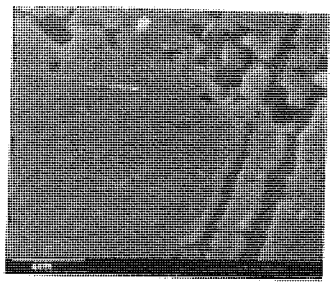

A
1 minute

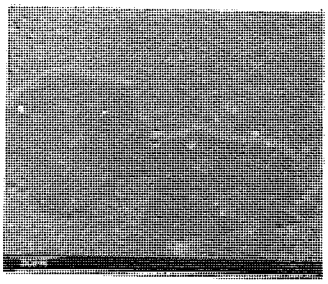

B
5 minutes

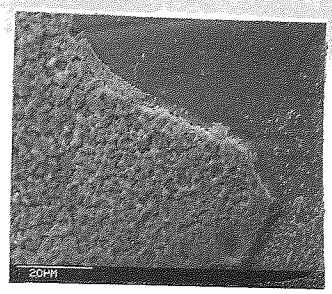

C
20 minutes

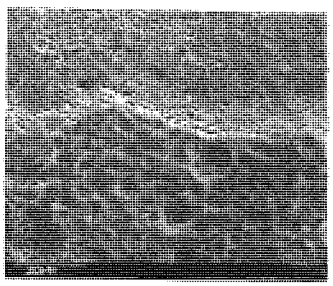

D
60 minutes

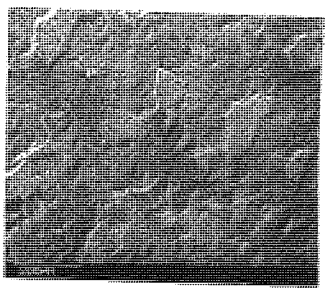

E
240 minutes

Photo 16 Time series of coatings formed on 99.99% aluminium in solution F (250 g/l H_3PO_4) (Ta = 30° for all frames).

Frame A; Mag = x 5K: A thin uniform film formed over the surface within 1 minute of immersion.

Frame B; Mag = x 1K: By 5 minutes immersion small 'islands' of coating had formed over the initial film.

Frame C; Mag = x 1K: Shows edge of an island on the left joining on to three regions; top has no particles or film formation; top right has a few particles on it and the bottom right hand corner is covered with small particles.

Frame D; Mag = x 1K: After a further 40 minutes immersion the islands have not increased in size or height above the surrounding coating, which has now formed a film with complete coverage.

Frame E; Mag = x 100: Low magnification shot showing the islands were still very clear after 240 minutes immersion.

Table 5.2.4.6 EDXA of Coatings Formed on 99.99% Aluminium in Solution F (250 g/l H_3PO_4)

Time of Immersion (Mins)	Major Peaks			P:Cr ratio
	P %	Al %	Cr %	
1	97.4	2.0	0.6	3.3
2	96.9	2.2	0.9	2.4
5	97.4	2.0	0.6	3.3
20	68.2	21.9	9.9	2.2
40	72.7	21.2	6.1	3.5
60	73.3	18.5	8.3	2.2
120	18.9	55.2	25.9	2.1
240	27.8	47.6	24.6	1.9

The EDXA results obtained from each coating are shown in Table 5.2.4.6. All readings shown were obtained between islands. Results of analysis of the islands themselves were very similar but had reduced aluminium peaks due to the increased thickness of the film.

Solution G 300 g/l H_3PO_4

Visual examination: This solution had a similar coating sequence to the previous solution (solution F), except the rate of aluminium dissolution had increased. This resulted in the first thin white film being completely removed by 20 minutes, and the second film not beginning formation until 40 minutes immersion. By 240 minutes particles were formed with an even distribution over the coupon's surface. However, the percentage coverage was very low. The aluminium surface had become very bright and reflective.

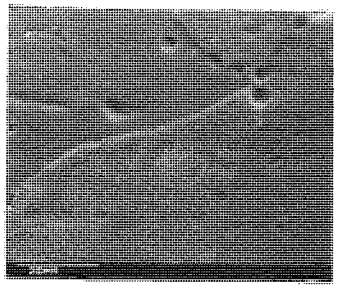

A

20 minutes

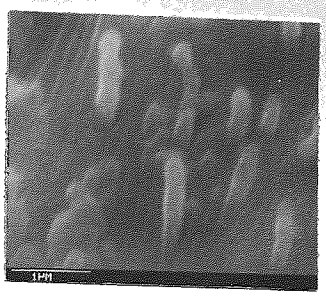

B

20 minutes

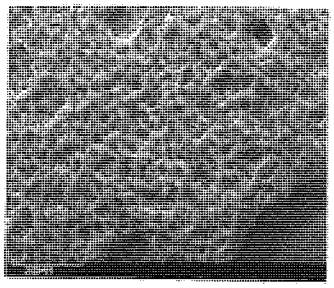

C

60 minutes

D

60 minutes

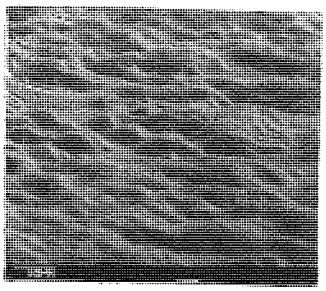

E

240 minutes

Photo 17 Time series of coating formed on 99.99% aluminium in solution G (300 g/l H_3PO_4) (Ta = 30° except E = 80°).

Frame A; Mag = x 1K: Grains of aluminium stand proud from the surface.

Frame B; Mag = x 20K: Whiskers growing out from raised areas.

Frame C; Mag = x 1K: Detail of Islands.

Frame D; Mag = x 100K: Low magnification shot showing islands.

Frame E; Mag = x 2K: Glancing angle showing roughened aluminium surface.

SEM Study: The main feature observed was the formation of 'whiskers' after 20 minutes immersion (Photo 17B). These were growing out from the surface of the substrate in areas possibly determined by the underlying grain structure of the substrate. By 60 minutes of immersion, patches of porous coating had formed (Photo 17C-D). EDXA indicated that the whiskers and precipitated coating were formed from chromium and phosphate with no aluminium present.

Solution H 350 g/l H_3PO_4

Visual examination. No film formed at all. The aluminium surface became lightly etched within 1 minute and became brighter (ie increased reflectivity) after 60 minutes. Severe etching could be seen after 60 minutes immersion.

SEM Study: SEM and EDXA confirmed the observed result that no coating formed. Photo 18 clearly shows the removal of the active surface layer of the substrate followed by general etching. Some areas have slower dissolution rates leaving islands proud of the surrounding surface.

Solution J 560 g/l H_3PO_4

The surface of 99.99% aluminium immersed in this solution was very similar to the topography seen on samples immersed in Solution H, with the exception that reflectivity did not increase at any stage.

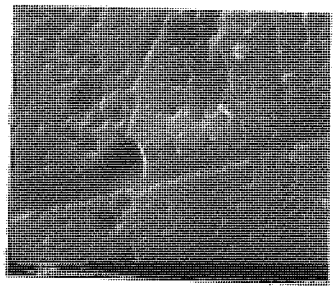

A

1 minute

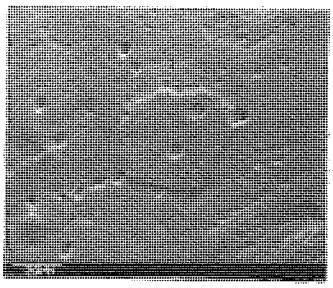

B

40 minutes

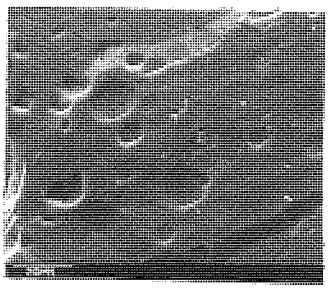

C

120 minutes

Photo 18 Time series of 99.99% aluminium immersed in solution H (350 g/l H_3PO_4) (Ta = 30° for all frames).

Frame A; Mag = x 10K; Small etch pits cover the surface.

Frame B; Mag = x 1K; Etching has become more intense, some areas standing proud of the surface (up to 10% of surface area).

Frame C; Mag = x 1K; Large etch pits now cover the surface. The areas still standing proud of surface are also badly etched.

SEM Study: Photo 19 A-C shows that aluminium dissolution was no more severe than that of the previous solution. The formation of many small etch pits may have reduced reflectivity. These etch pits were not seen on the surface of samples treated in Solution H.

Solution K 1275 g/l H_3PO_4

This solution was approaching that of an electropolishing solution [¾ phosphoric acid (vol/vol)]. Severe etching did not occur. However, brightening did not occur either. This was because polishing conditions were not obtained, although the lack of severe etching suggests that this solution could be developed for that purpose.

SEM Study: Photo 19 D-F shows light etching occurs on the surface of the substrate. No severe dissolution took place, as seen with samples immersed in previous solutions.

Figure 5.2.4.1 shows the weight-change/time curves obtained from solutions A-K. It can be seen that the rate of coating formation increases, or aluminium dissolution decreases (or both), as phosphoric acid content is increased. A maximum weight gain rate is reached by 35 g/l phosphoric acid after which dissolution of the coating and substrate increase and the rate of coating formation decreases as seen during SEM observations. A low rate of aluminium dissolution is achieved by Solution K, supporting observed results. The potential-time curves recorded are shown in Figure 5.2.4.2. Potentials become more active with increasing phosphoric acid content, implying increased aluminium dissolution and/or the formation of less protective coatings. The most active potentials

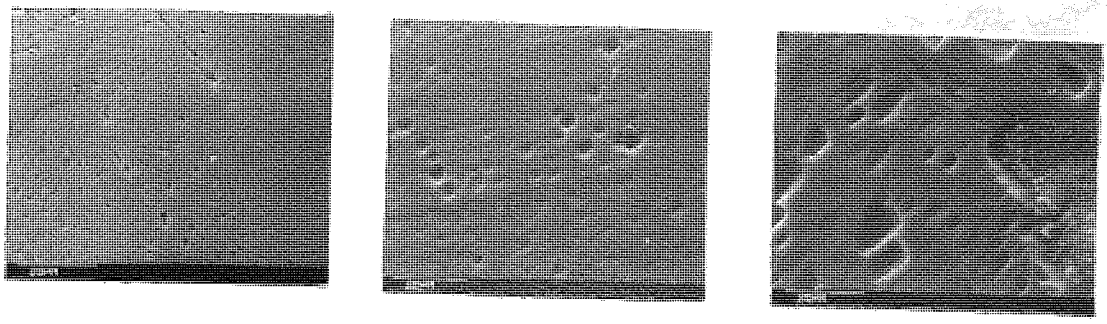

A
1 minute

B
20 minutes

C
120 minutes

Solution J

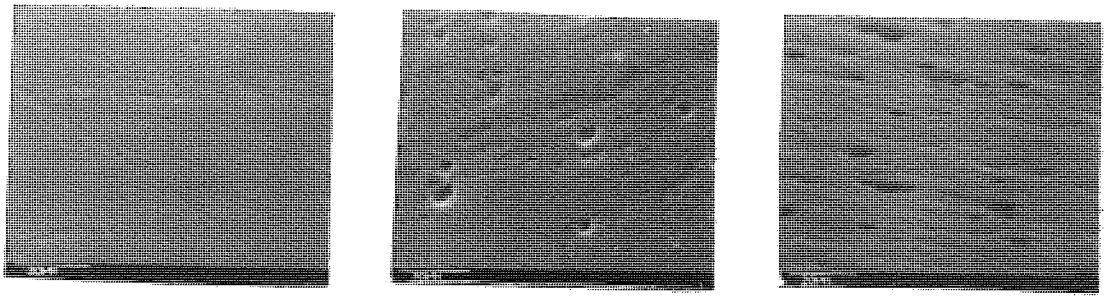

D
5 minutes

E
60 minutes

F
120 minutes

Solution K

Photo 19 Time series of 99.99% aluminium immersed in solution J (560 g/l H_3PO_4) and solution K (1275 g/l H_3PO_4) (Ta = 30° except frame F = 81°).

Frame A; Mag = x 1K: Light etching of surface.

Frame B; Mag = x 1K: Etching becoming more severe.

Frame C; Mag = x 1K: Large etch pits cover surface.

Frames D - F; Mag = x 1K: Etching was less severe than for corresponding immersion times in soluton J. No coating formed.

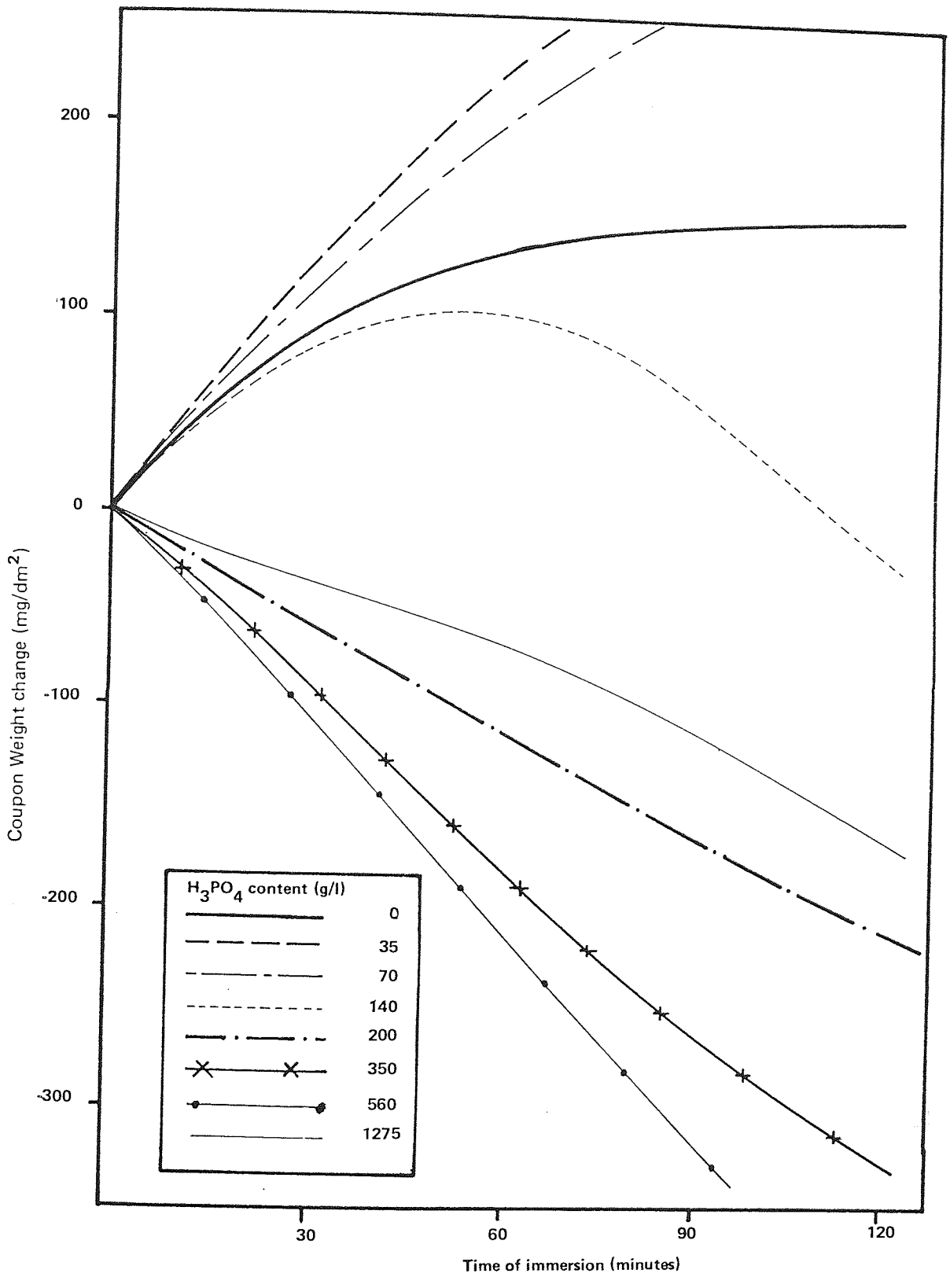

Figure 5.2.4.1 The effect of increasing phosphoric acid concentration in a chromate solution on the weight change relationship for 99.99% aluminium.

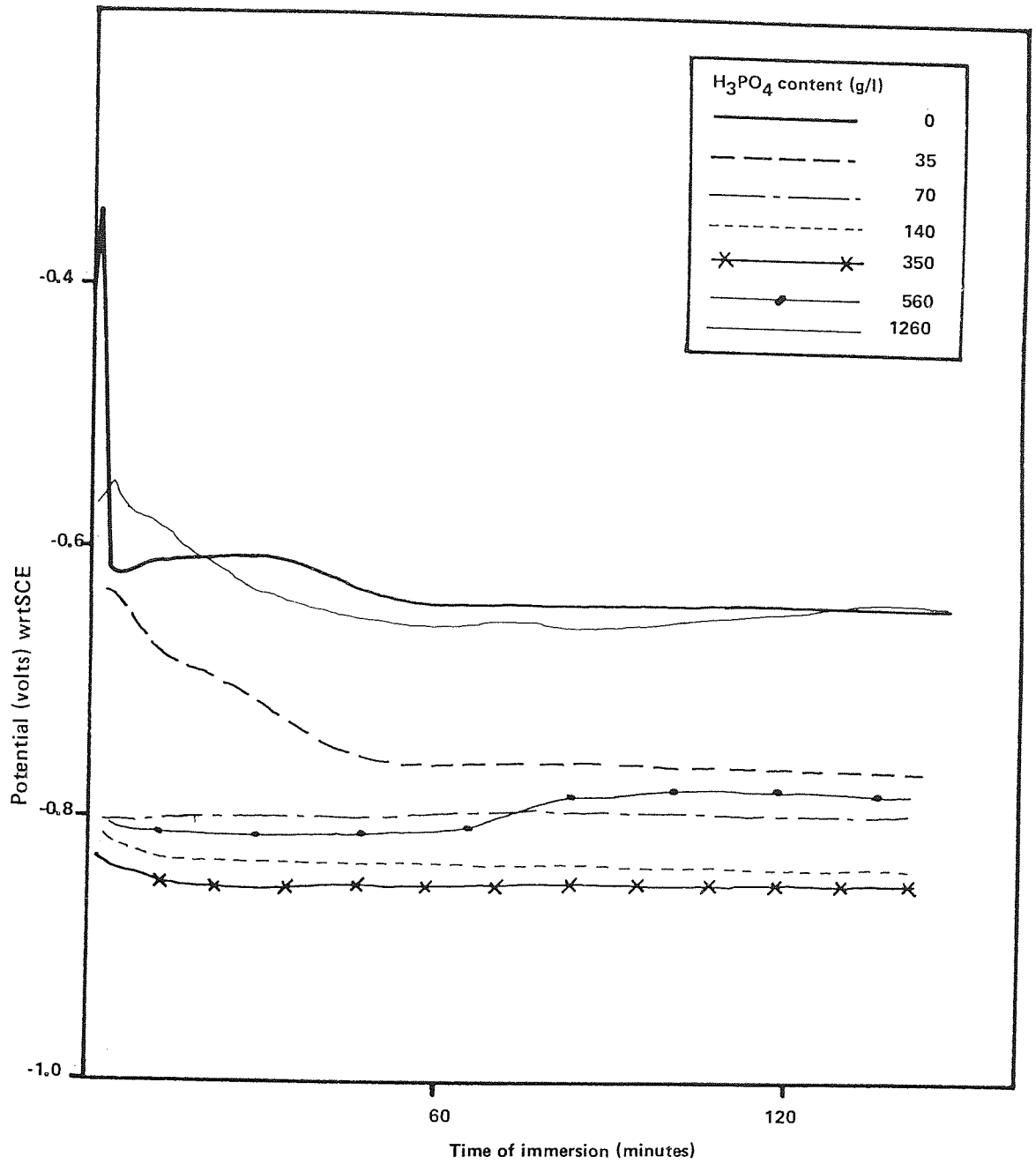

Figure 5.2.4.2 The effect of increasing phosphoric acid concentration in a chromate solution on the potential-time relationship for 99.99% aluminium.

were recorded for solutions containing 350 g/l phosphoric acid (Solution E). Further additions approach polishing conditions and the potential becomes more noble.

The effect of phosphoric acid on the rate of aluminium dissolution was studied by analysis of spent solutions. Solution A (zero phosphoric acid) did not have a build up of aluminium ions in solution. This was despite evidence of electrochemical reactions occurring on the aluminium surface, of which the anodic reaction was the dissolution of aluminium. Figure 5.2.4.3 shows the relationship between aluminium concentration and time of immersion for Solution A, and this can be split into four main parts:

1. Aluminium ions going from the surface into solution (at time = 0, no aluminium in solution, therefore this reaction rate was rapid).

2. The coating which had formed on the substrate inhibits the anodic reaction and absorbs much of the aluminium ions in solution back into the film.

3. A steady-state of reaction was found between aluminium ions going into solution and aluminium ions becoming absorbed into the film.

4. A steady-state is reached.

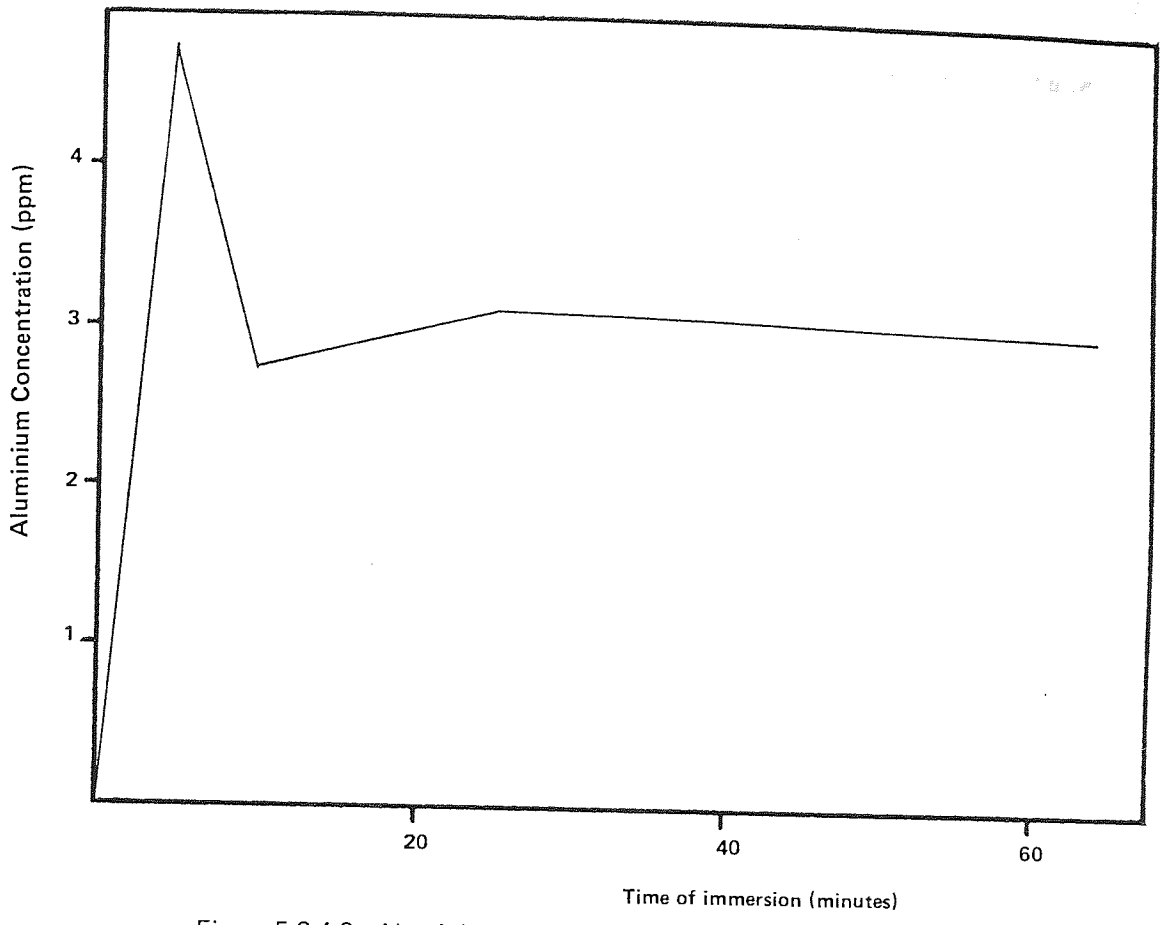

Figure 5.2.4.3 Aluminium concentration in solution A (Zero H_3PO_4) as a function of coupon immersion time

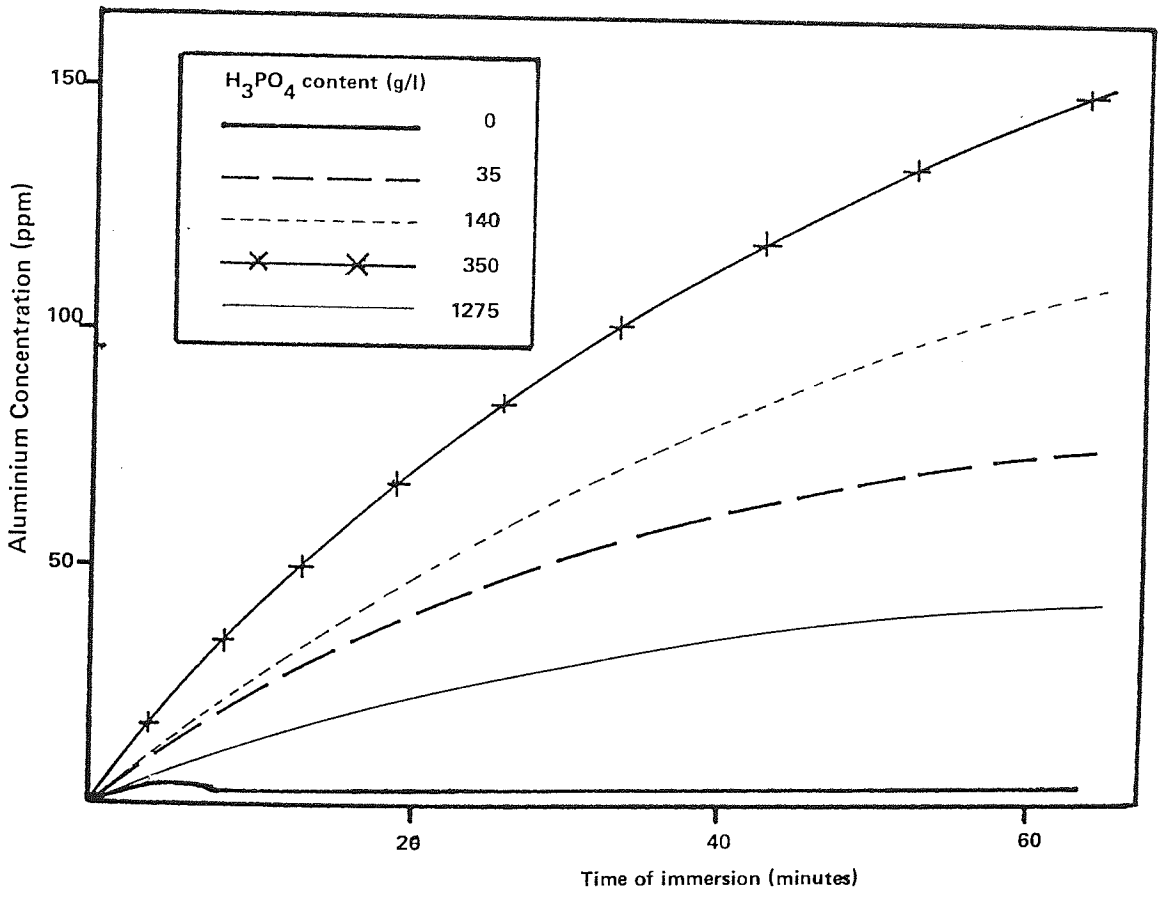

Figure 5.2.4.4 The effect of phosphoric acid content on aluminium concentration found in solution as a function of coupon immersion time

The introduction of phosphoric acid had a marked effect on the rate of dissolution of aluminium into solution, possibly due to phosphates going into the coating which reduced or stopped re-absorption of aluminium ions back into the coating. Figure 5.2.4.4 shows the relationship between aluminium in solution against coupon immersion time for each increase in phosphoric acid content. It can be seen that increasing the phosphoric acid content increased the rate of aluminium dissolution up to additions of 350 g/l H_3PO_4. At 1275 g/l H_3PO_4, the rate of aluminium dissolution is markedly decreased, showing that conditions favouring polishing rather than aggressive etching had been achieved.

6. INFLUENCE OF METALLIC CONTAMINATION OF SOLUTIONS ON CONVERSION COATINGS

6.1 Introduction to the Experimental Work

Spruance[93] states in his patent specification for chromate-phosphate conversion coatings that metallic cations may be present in the solution without any deleterious effect on coatings formed. However, Treverton and Davies[97] have shown that contamination of the solution by certain metals alter both the thickness and structure of coatings formed.

The manufacturers of Alocrom 100 recommend ageing a freshly made solution before use[111] as failure to do so results in the formation of thin, powdery coatings. Thus the influence of aluminium ions in solution is important with regard to coating formation mechanisms.

The influence of zinc contamination in chromate-phosphate solutions on the formation of conversion coatings was of interest as it is common practice for some industrial metal finishers to process galvanised steel products in the same Alocrom bath that is used for aluminium products. Magnesium and copper contamination was also studied. Contamination of industrial chromate baths by these metals is likely due to treatment of aluminium alloys.

6.1.1 Ageing a proprietary conversion coating solution

The effect of ageing Alocrom 100 solution on coating formation was studied using potential-time, weight change/time, SEM and EDXA. A series of Alocrom 100 solutions containing an increasing amount

of dissolved aluminium was produced. Aluminium additions ranged from 0 to 1.0 g/l in increments of 1.0 g/l. Aluminium does not readily dissolve in Alocrom 100 as it is protected by the formation of a chromate-phosphate coating. Aluminium was therefore first dissolved in a 25% solution of phosphoric acid which is a constituent ingredient of Alocrom 100. A large quantity of Alocrom 100 was made up and small additions of the phosphoric acid - aluminium solution were made. In this way aluminium could be introduced into the solution without markedly affecting the balance, ie free acid content of the solution. Table 6.1.1 shows the addition made at each increment. Initially 15 litres of Alocrom 100 were made up and the concentration checked. Solution B consisted of 200 ml of 25% H_3PO_4 into which 9.5g of 99.99% aluminium powder was added gradually and dissolved. At each step 1000 ml of solution was drawn off from the bulk solution.

Table 6.1.1 Tabulation of Aluminium Additions for Artificially Ageing Alocrom 100

Bulk Solution Volume (l)	Aluminium Metal additions (g)	Solution Concentration (g/l)		Solution B Addition (ml)
		Cummulative Effect	TOTAL	
15	0	0	0	0
14	1.4	0.1+0	0.1	29.47
13	1.3	0.1+0.1	0.2	27.37
12	1.2	0.1+0.2	0.3	25.26
11	1.1	0.1+0.3	0.4	23.16
10	1.0	0.1+0.4	0.5	21.05
9	0.9	0.1+0.5	0.6	18.95
8	0.8	0.1+0.6	0.7	16.84
7	0.7	0.1+0.7	0.8	14.74
6	0.6	0.1+0.8	0 9	12.63
5	0.5	0.1+0.9	1.0	10.53
	9.5			200.0

The formula for converting metallic aluminium additions to additions of solution B is as follows:

$$\text{unit weight of aluminium} = \frac{\text{Total volume of solution B}}{\text{Total weight of dissolved aluminium}}$$

or

$$1 \text{ gram of Al} = \frac{200 \text{ ml}}{9.5 \text{ g}} = 21.053 \text{ ml}$$

The aged solutions were stored in air-tight polypropylene containers until required for use. Contact with glass was kept to an absolute minimum at all times to ensure that the fluoride in solution was not lost.

While preparing the Alocrom 100 solution for artificial ageing, an insoluble powder was noted to have settled at the bottom of the tank. A sample of this powder was obtained and carefully washed for several days in distilled water. The cleaned powder was dried on filter paper and analysed by EDXA and X-ray diffraction.

Potential-time determinations were made for each of the solutions described with 99.99% aluminium coupons cleaned in aged AC51 for 5 minutes at 50°C. The chromate-phosphate conversion coating solution was used at room temperature with moderate agitation provided by a magnetic stirrer. 100 ml of fresh solution with various aluminium additions was used for each run and was discarded immediately following the test. The equipment used was set-up as described in Section 4.1.2, the chart speed was set to 20mm/minute, and each run lasted for 10 minutes.

The coupon weight-change versus time of immersion was studied for each solution using similar conditions to the potential-time study. Prepared and weighed 99.99% aluminium coupons were immersed in the artificially aged solutions for 1,2,5 and 10 minutes respectively. They were then carefully rinsed, dried, re-weighed and the coupon weight change per unit area calculated. The results were plotted against time of immersion to show the coupon weight-change relationship for increasing aluminium additions to the solution.

Each of the specimens produced was catalogued and later studied under the SEM and EDXA in order to find any structural or bulk composition change due to the increasing aluminium content of the chromate-phosphate solution.

6.1.2 Depth-profiles of coatings formed in aged Alocrom 100 solutions

The effect of aluminium additions to Alocrom 100 solution on the structure and composition of the film grown on 99.99% aluminium was studied by a combination of Auger spectroscopy and ion milling. The result of this combined technique was the production of a depth-profile of the coating.

Specimens were prepared using the same solutions and conditions as outlined in the previous section. Two coating thicknesses were produced; one by immersion for 3 seconds and the other by immersion for 30 seconds.

Solutions with aluminium additions of 0.1, 0.4, 0.7 and 1.0 g/l were chosen to represent the range of conditions found during

ageing of a commercial conversion coating solution. Samples measuring 8 x 8mm were cut from the prepared specimens, into these 3mm diameter holes were bored to provide anchorage points for the samples on the Auger stage. The instrument used was a 'Kratos XSAM 800' Scanning Auger Microscope (SAM) with an SEM and ion beam miller attachment.

A suitable area was selected using the SEM attachment on the SAM, (trying to avoid any cracked regions) and was then analysed. The spatial resolution of Scanning Auger Microscopy is poor and it was not possible to resolve the very small particles present in the film. However depth penetration is very low (one or two atomic layers) so true surface analysis can be achieved. The atomic layers analyised were then removed by ion milling and the process repeated until the aluminium content rose to more than 60% indicating the substrate metal had been reached. The spectra from Auger Electron Spectroscopy take the form of a series of peaks which correspond to particular elements.

The peaks were measured and fed into a computer program to calculate the percentage concentration for each element and to plot a depth-concentration profile.

6.1.3 Accelerated corrosion study of conversion coatings produced in aged solutions

In order to establish the effect of aluminium contamination in Alocrom 100 on the corrosion resistance of the coatings formed, two sets of 99.99% aluminium panels 90 x 10 mm in size were produced and exposed to a natural salt fog for 250 hours. Each set of

panels covered the complete range of artificially aged solutions (aluminium additions of 0 - 1.0 g/l), with treatment times of 3 and 30 seconds respectively. All panels were cleaned in aged AC51 for 5 minutes prior to treatment.

A standard Canning salt spray corrosion cabinet was used. A 5% salt solution with pH of 7 was prepared and placed in the salt spray cabinet reservoir. The water jacket surrounding the cabinet was maintained at 40°C. The treated panels were placed in a random sequence on the specimen rack which was located centrally in the salt-spray cabinet. The air pressure for the spray was set to 1 bar. Frequent checks were made to ensure the spray jet did not become blocked. The test was run for a total of 250 hours with one break for 70 hours.

Upon removal from the salt spray cabinet the panels were first layed out in the same order as they were in the specimen rack. Their respective positions were noted along with a visual assessment to check that corrosion damage was not related to position in the cabinet.

Panels were then arranged in order of corrosion resistance performance as judged by eye and their positions noted. Each panel was cleaned with distilled water which removed all loose debris from the surface. Again the panels were arranged in order of corrosion resistance performance and noted.

6.1.4 Conversion coating formation on zinc

The treatment of zinc, in the form of galvanised products, is of great interest to commerical applicators. Various claims are made about the effectiveness of such pretreatment but little published work on the subject has been found. It was therefore thought appropriate to spend some time on studying the action of Alocrom 100 on a zinc surface.

Pure zinc sheet 0.5 mm thick was cut into twelve coupons measuring 10 x 70 mm. These were then marked, cleaned, rinsed and dried before being weighed. Two samples were immersed in fresh Alocrom 100 solution for various times from 1 to 60 minutes. Following immersion one sample was carefully rinsed in still de-ionized water and dried. The other sample was blasted with a jet of water before being dried, removing any coating present. Each sample was then re-weighed and the sample weight change calculated. These results were plotted as sample weight change against time both for stripped and coated samples. Thus the coating weight could be estimated for any immersion time up to 60 minutes.

6.1.5 The influence of zinc contamination in Alocrom 100 on the formation of conversion coatings

The main side effect of treating galvanised products in a chromate-phosphate bath is that the bath will become contamined with zinc. The degree of zinc contamination would depend upon the number of galvanised products treated in the bath relative to the amount of aluminium processed and the amount of drag-out. Clearly the level of contamination would be constantly changing.

To study the effect of zinc contamination on chromate-phosphate coatings a number of coatings were produced in Alocrom 100 solution with various zinc additions.

Three 1 litre solutions of Alocrom 100 were made up. Solution A was used in the fresh condition. Solutions B and C had 1 and 5 grammes of pure zinc dissolved in them followed by a solution concentration check and adjustment as necessary. Potential-time determinations were found for each solution using 99.99% aluminium coupons in two conditions;

(i) degreased only and

(ii) cleaned in aged AC51

This was repeated using degreased E4S aluminium alloy coupons with and without treatment in aged AC51 for 5 minutes.

The effect of zinc contamination on coupon weight change was also studied using the above solutions. E45 aluminium alloy coupons were degreased, cleaned in aged AC51 for 5 minutes, dried and weighed. They were then immersed in each solution for times between 1 and 20 minutes. Following treatment they were carefully rinsed, dried and re-weighed. The coupon weight change per unit area was calculated and plotted as a function of immersion time.

The topography of the coatings formed on both substrates in the cleaned and degreased only conditions were studied using the SEM and EDXA attachment.

6.1.6 Effect of metallic contamination of chromate-phosphate solution on the formation of conversion coatings

The effect of contamination of chromate-phosphate solutions by zinc, magnesium and copper on the formation of conversion coatings was studied by SEM and EDXA. In addition, coupon weight change verus time and the potential-time relationships were determined. It was found that the metal oxides could be dissolved readily in chromate-phosphate solutions, the limit of solubility depending upon the level of phosphoric acid in solution.

The standard chromate-phosphate solution into which metallic additions were made was as follows:-

Chromic acid (CrO_3)	6.50 g/l
Sodium fluoride (NaF)	3.88 g/l
Phosphoric acid (H_3PO_4)	70 g/l

made up with distilled water.

Each test used 100 ml of prepared solution with additions of zinc, magnesium or copper as shown in Tables 6.1.6.1-3. Conditions used were as before: moderate agitation at room temperature. Potential-time determinations were made for each solution using 99.99% aluminium coupons that had been cleaned in aged AC51 solution for 5 minutes. Coupon weight change versus time studies were also conducted using cleaned 99.99% aluminium for each solution for immersion times up to 10 minutes. SEM and EDXA studies of the coatings formed were made as soon as possible after each test in order to avoid damaging the coatings during storage.

Table 6.1.6.1 Zinc Additions to the Standard Chromate-Phosphate Solution

Solution Code	Zinc Oxide Addition (g/l)	Zinc equivalent (g/l)
Zn.1	1.2009	1
Zn.2	2.4018	2
Zn.5	6.0046	5
Zn.10	12.0091	10
Zn.15	18.0135	15

The solubility limit for magnesium oxide in the standard chromate-phosphate solution was found to be between 7-8 g/l at room temperature. Therefore magnesium contamination was studied only up to 4 g/l.

Table 6.1.6.2 Magnesium Additions to the Standard Chromate-Phosphate Solution

Solution Code	Magnesium Oxide Addition (g/l)	Magnesium Equivalent (g/l)
Mg.1	1.658	1
Mg.2	3.316	2
Mg.3	4.974	3
Mg.4	6.632	4

A test was conducted to find the solubility limit of copper oxide in the standard chromate-phosphate solution. This revealed that cupric oxide had a very low solubility point in this solution at room temperature: less than 1 g/l Cu. Cuprous oxide was tried

and found to have a solubility limit of just over 11.26 g/l (Cu equivalent of 10 g/l). Additions of cuprous oxide (Cu_2O) were made to standard chromate-phosphate solution as shown in Table 6.1.6.3. Great care was necessary when handling the copper contamination specimens; the coating produced was extremely soft and loose and could therefore become damaged easily.

Table 6.1.6.3 Copper Additions to the Standard Chromate-Phosphate Solution

Solution Code	Cuprous Oxide Addition (g/l)	Copper Equivalent (g/l)
Cu.1	1.126	1
Cu.2	2.252	2
Cu.3	3.378	3
Cu.5	5.640	5
Cu.10	11.260	10

To assess the level of metallic ion contamination of commercial solutions, samples of AC51 cleaning solution and Alocrom 100 conversion coating solution were taken from the processing tanks of Metallic Protectives Ltd of Warwick and the zinc and aluminium content determined by Atomic Absorption Spectroscopy.

6.2 Results

6.2.1 Effect of ageing a proprietary chromate-phosphate solution

The topography of coatings formed on 99.99% aluminium in Alocrom 100 solutions with increasing aluminium content are shown in Photo 20 and 21. Characteristic circular defects can be seen on the thicker coatings (Photo 20 B-C) the size of which seem to be dependent upon the aluminium content of the conversion coating solution. The 2 minute coating formed in Alocrom 100 solution with a 0.6 g/l aluminium addition has fewer gas pits and defects than corresponding coatings produced in solutions with less aluminium additions.

Photo 21 shows a similar trend; increasing aluminium content results in a lower coating weight. All coatings were compact rather than porous. The EDXA results are shown plotted against time of immersion in Figure 6.2.1.1-3 for aluminium, phosphorus, and chromium content respectively. These show that the coating weight increases in solutions containing up to 0.3 g/l aluminium additions. Further additions of aluminium result in reduced coating formation as seen in Photo 21.

The potential-time curves obtained by immersion of 99.99% aluminium in Alocrom 100 solution with various aluminium additions are shown in Figure 6.2.1.4. There appear to be two groups of curves. The first includes the solutions with 0 - 0.5 g/l aluminium, the remainder form the second.

Coupon weight change was recorded for each solution for various immersion times up to 10 minutes and plotted on one graph shown in Figure 6.2.1.5. The weight change versus time curves for solutions with 0 - 0.3 g/l aluminium additions show increasing weight gain with time. Further aluminium additions result in both reduced

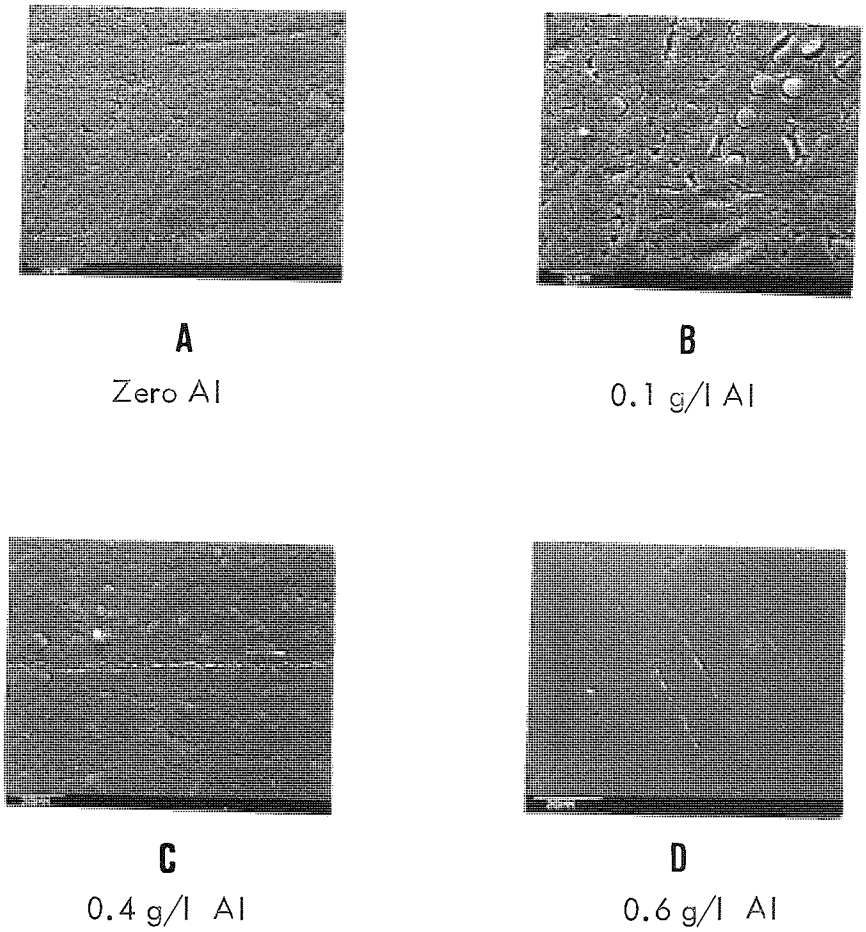

Photo 20

2 minute coatings formed in Alocrom 100 solution with various aluminium additions at room temperature on 99.99% aluminium.

(Mag = x 1K Ta = 30° for all frames)

Frame A-D; Coating thickness decreasing with increasing aluminium content in solution. The number of gassing pits and circular defects reduce with increase aluminium content.

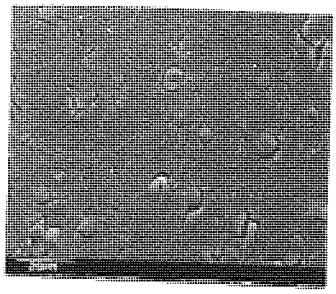

A

0.6 g/l Al

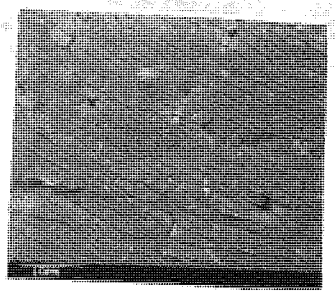

B

0.7 g/l Al

C

0.8 g/l Al

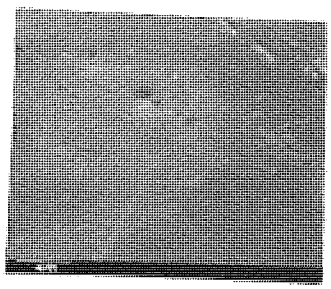

D

0.9 g/l Al

Photo 21

5 minute coatings formed in Alocrom 100 with various aluminium additions at room temperature on 99.99% aluminium.

(Ta = 30° for all frames)

Frame A; Mag = x 1K: Typical area showing circular defects formed after 2 minutes immersion (Photo 20B).

Frame B; Mag = x 2k: Mud-cracking and small defects clearly visible but coating weight visibly reduced.

Frame C-D; Mag = x 5K: Coating weight clearly reduced as aluminium content in solution is increased.

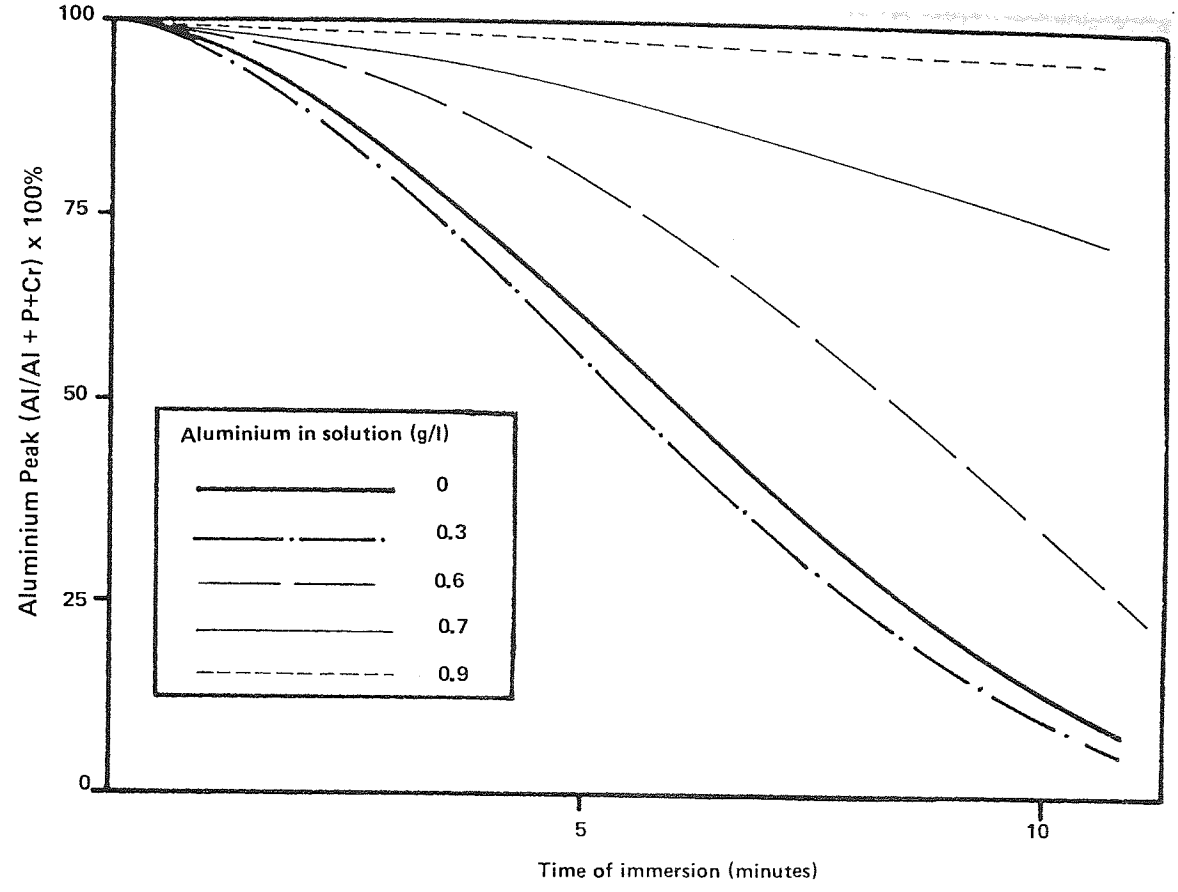

Figure 6.2.1.1 Aluminium content of coatings formed on 99.99% aluminium in Alocrom 100 solutions with various aluminium additions

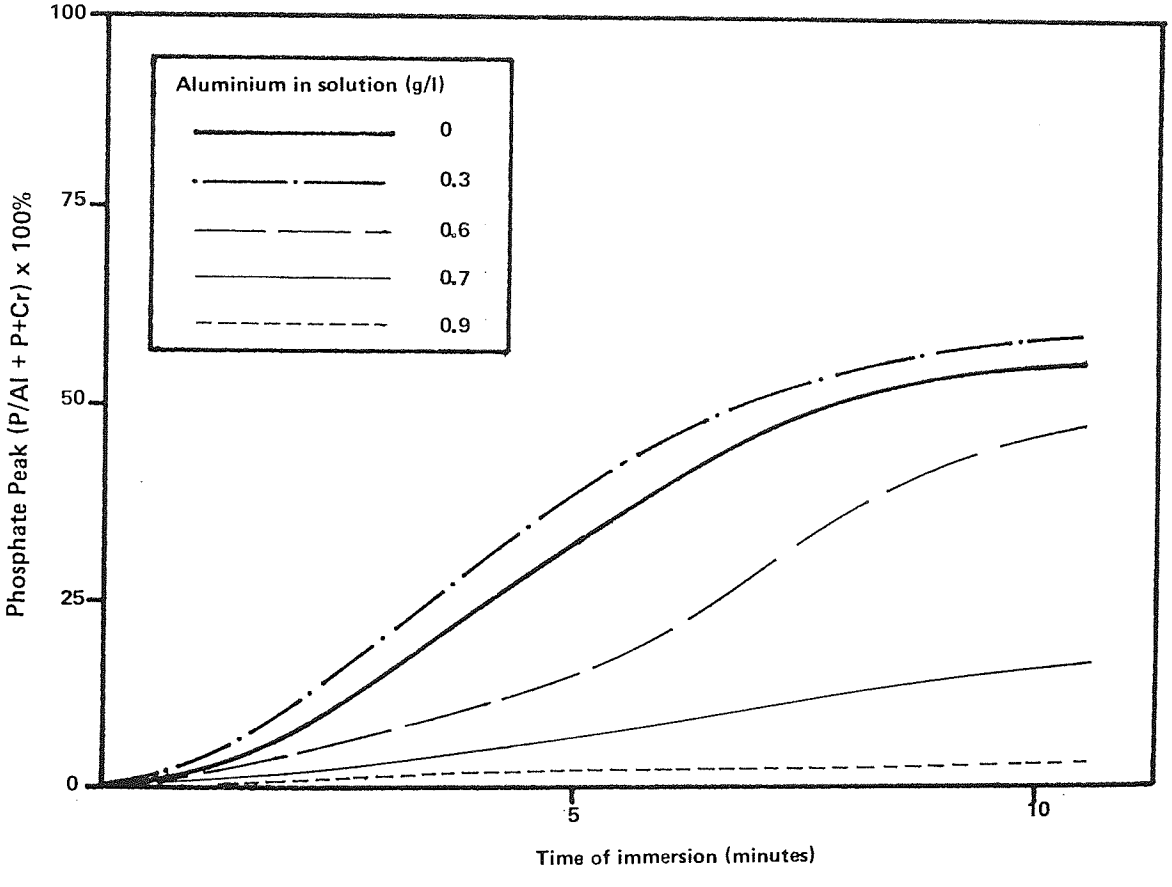

Figure 6.2.1.2 Phosphorus content of coatings formed on 99.99% aluminium in Alocrom 100 solution containing various aluminium additions

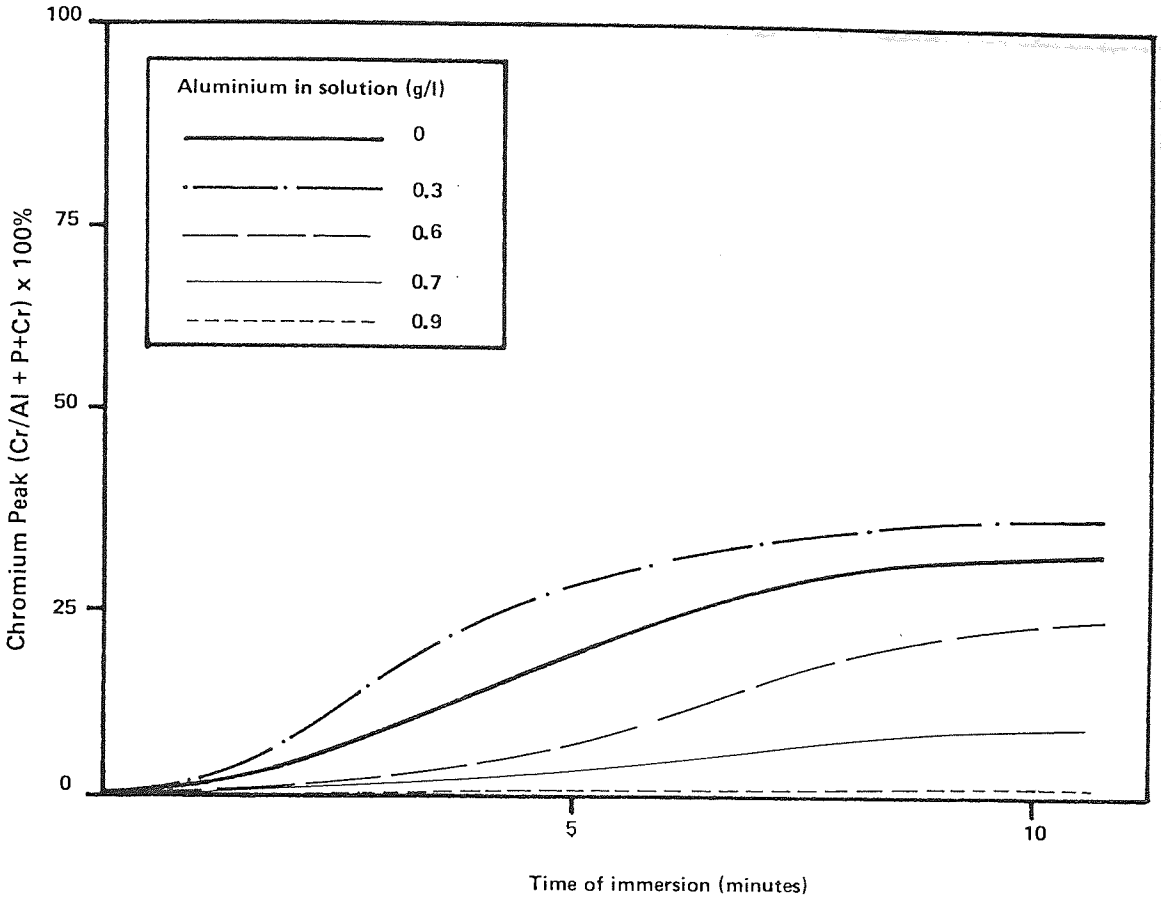

Figure 6.2.1.3 Chromium content of coatings formed on 99.99% aluminium in Alocrom 100 solutions containing various amounts of aluminium additions

coupon weight gain and decreasing weight gain with time. The coupon weight loss seen within the first minute of immersion decreases with increasing aluminium additions.

The white powder that was found at the bottom of the tank of freshly made Alocrom 100 was found to contain potassuim, aluminium, sodium, fluorine, silicon, chromium and calcium by EDXA analysis. X-ray diffraction revealed that the majority of this substance was $K_2Na\ AlF_6$ (Elpasolite). The identity of the remaining portion of the substance could not be found.

A small sample of freshly made Alocrom 100 solution was analysed for aluminium content by AAS. This was found to contain 0.16 g/l

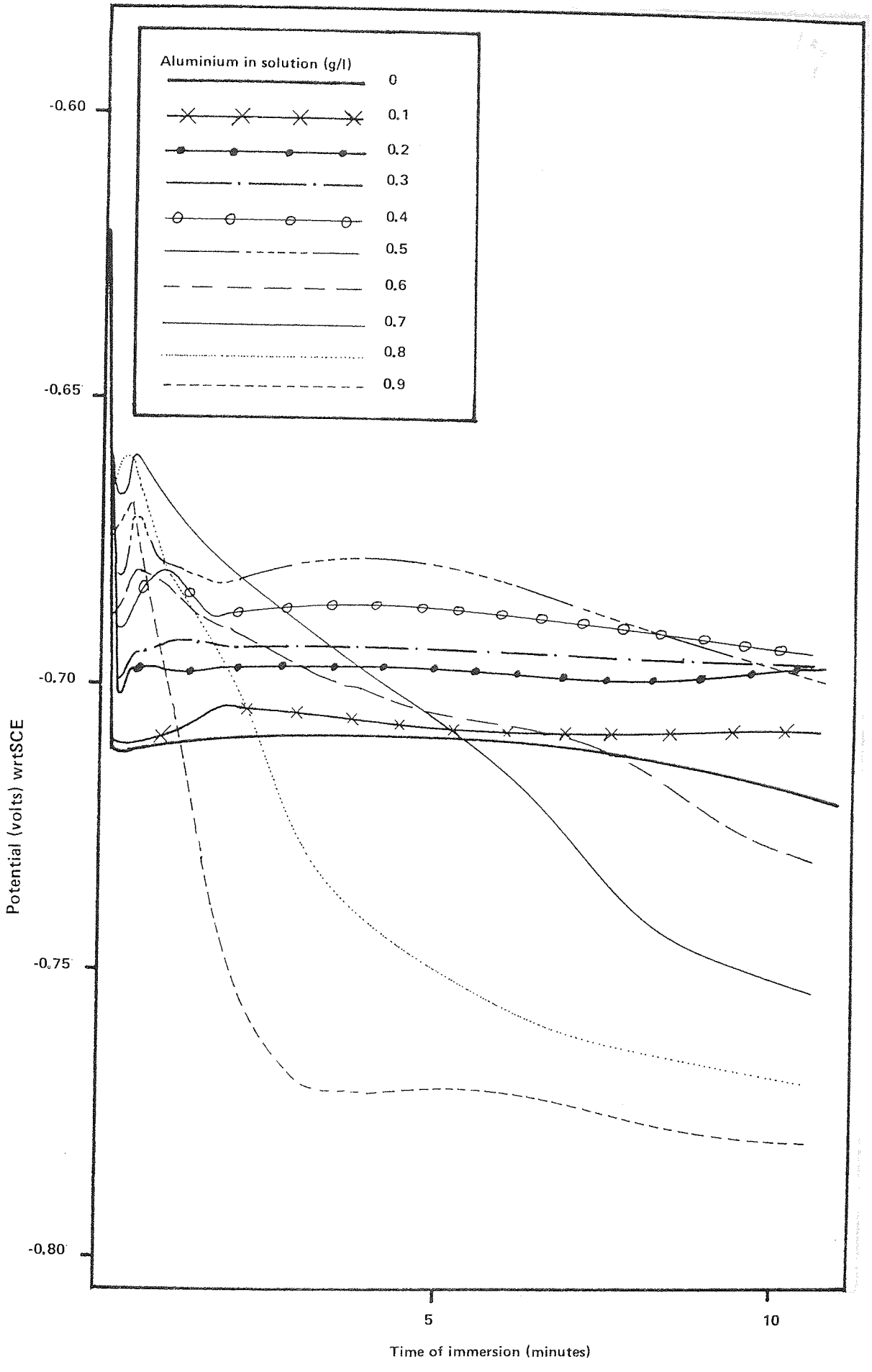

Figure 6.2.1.4 Potential-time curves for 99.99% aluminium in Alocrom 100 with various aluminium additions

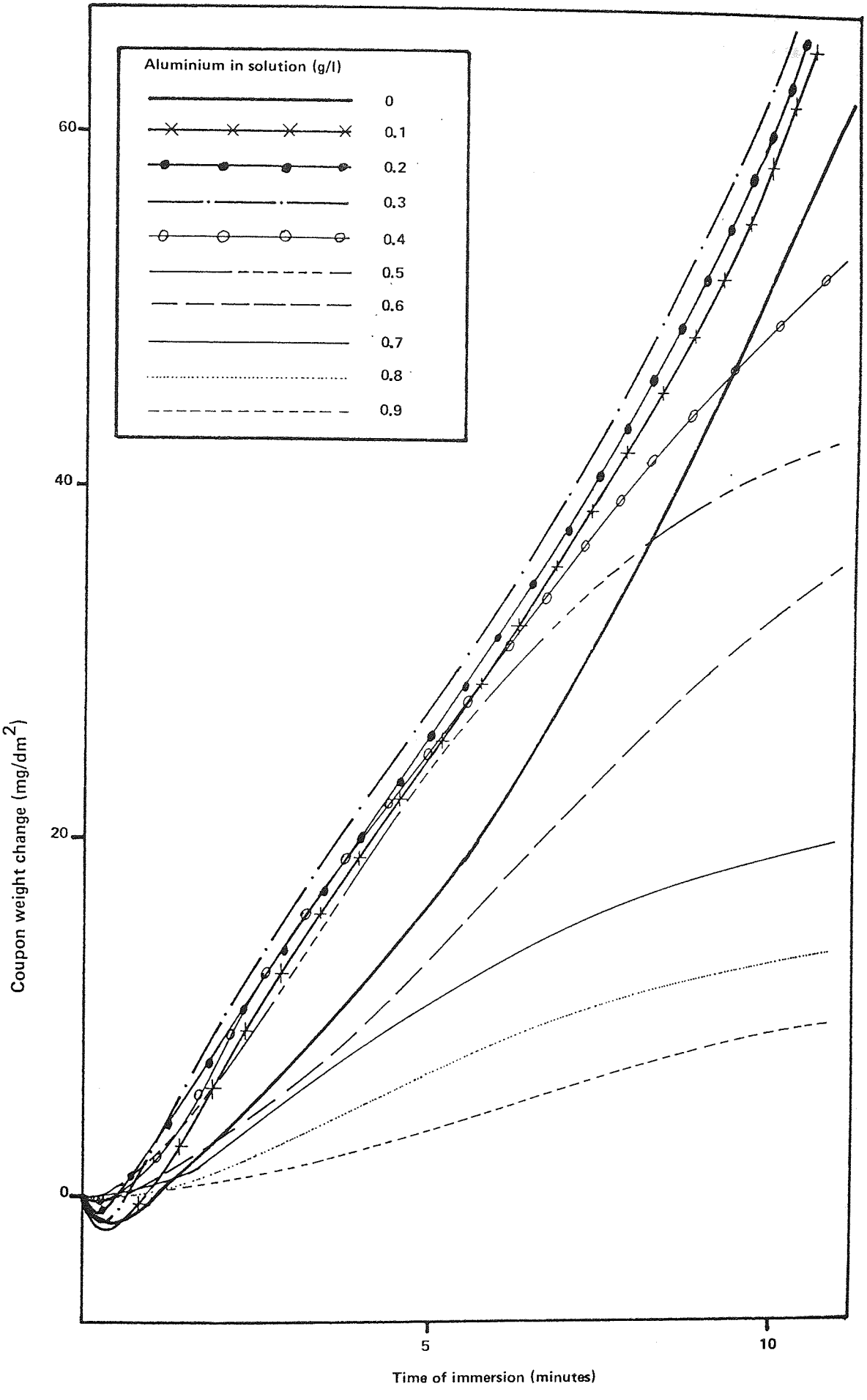

Figure 6.2.1.5 Coupon weight change against time of immersion of 99.99% aluminium in Alocrom 100 with various aluminium additions

aluminium. Therefore the total aluminium content of the solutions used in this section is the sum of the addition made and the 0.16 g/l already present.

6.2.2 Depth-profiles of coatings formed in aged Alocrom 100 solutions

The resulting depth profiles are shown in Figure 6.2.2.1-4 and correspond to aluminium additions of 0.1, 0.4, 0.7, and 1.0 g/l respectively. All were immersed for 30 seconds. It was found that the 3 second coatings were not suitable for study, probably due to insufficient coating material on the surface. The depth scale (mins ion etch) has been drawn to the same scale in all figures to show the extent that the coating weight falls as the aluminium content in solution increases.

It can be seen for the solution with 0.1% aluminium additions that phosphorus is present from the top to the middle of the coating whereas chromium is present from the top to the coating/metal interface. Fluorine can be detected in the coating near the coating /metal interface which supports the view that fluoride is responsible for removing the oxide film when the sample is first placed in the Alocrom 100 solution.

It was also noted that aluminium was not detected near the coating surface, but was found one third of the way through the coating. The final curve is that for carbon which was due to natural carbon pick up at the surface of the film and contamination by the vacuum system.

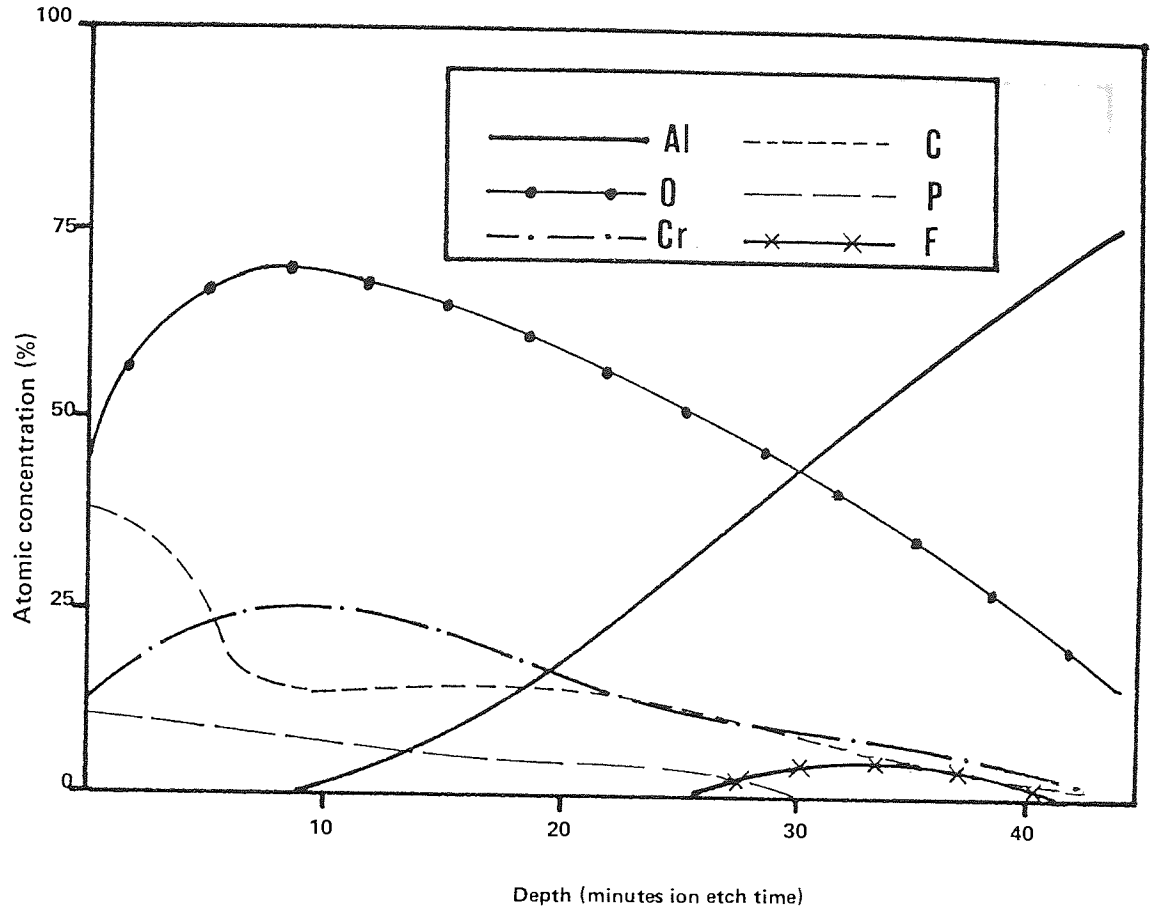

Figure 6.2.2.1 Depth profile of coating formed on 99.99% aluminium immersed in Alocrom 100 containing 0.1 g/l aluminium for 30 seconds

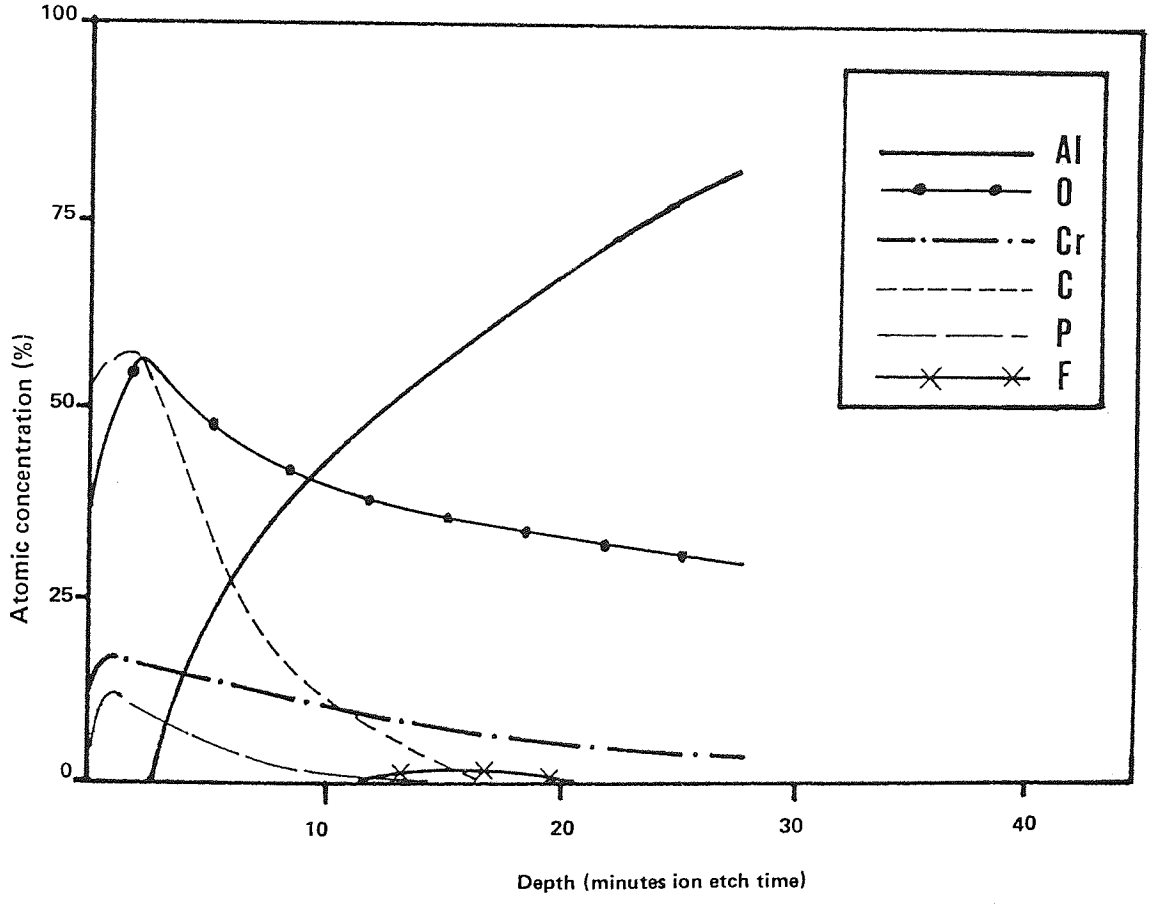

Figure 6.2.2.2 Depth profile of coating formed on 99.99% aluminium immersed in Alocrom 100 containing 0.4 g/l aluminium for 30 seconds

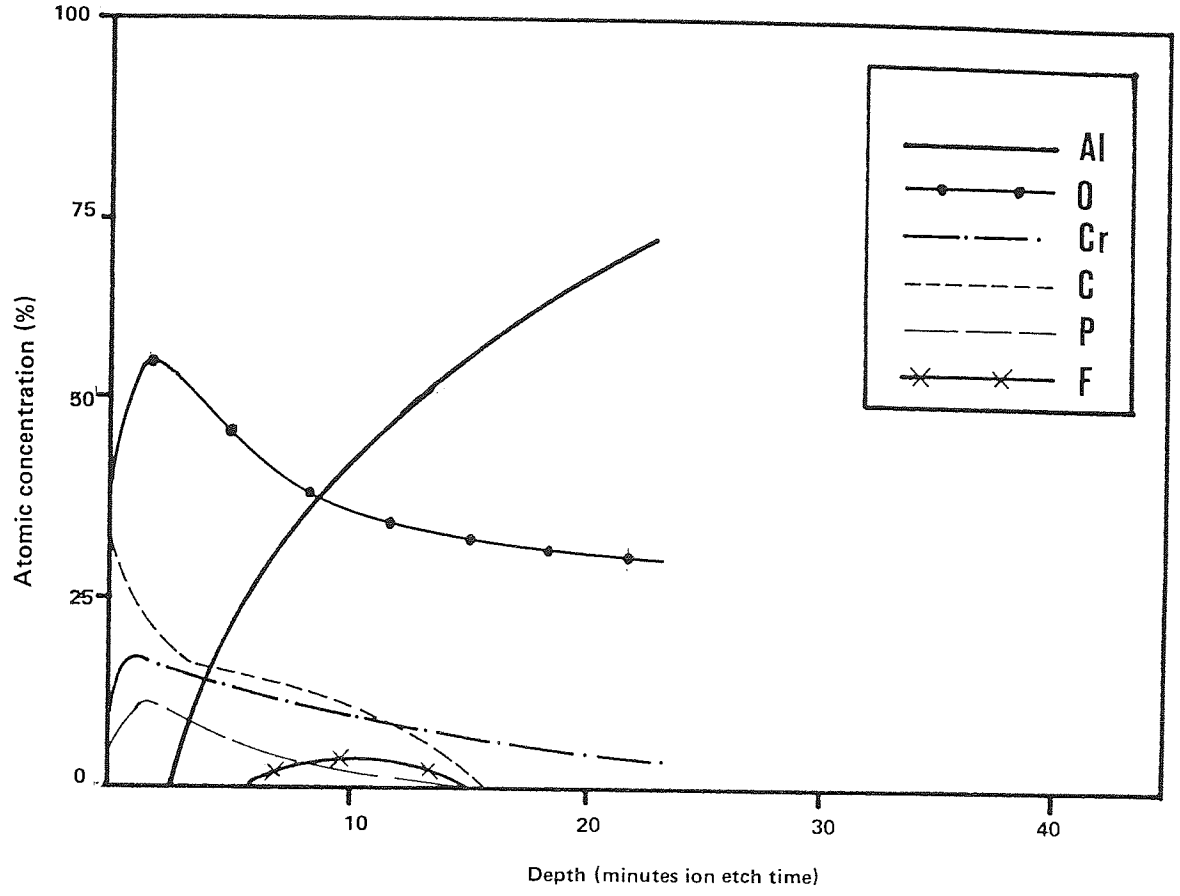

Figure 6.2.2.3 Depth profile of coating formed on 99.99% aluminium immersed in Alocrom 100 containing 0.7 g/l aluminium for 30 seconds

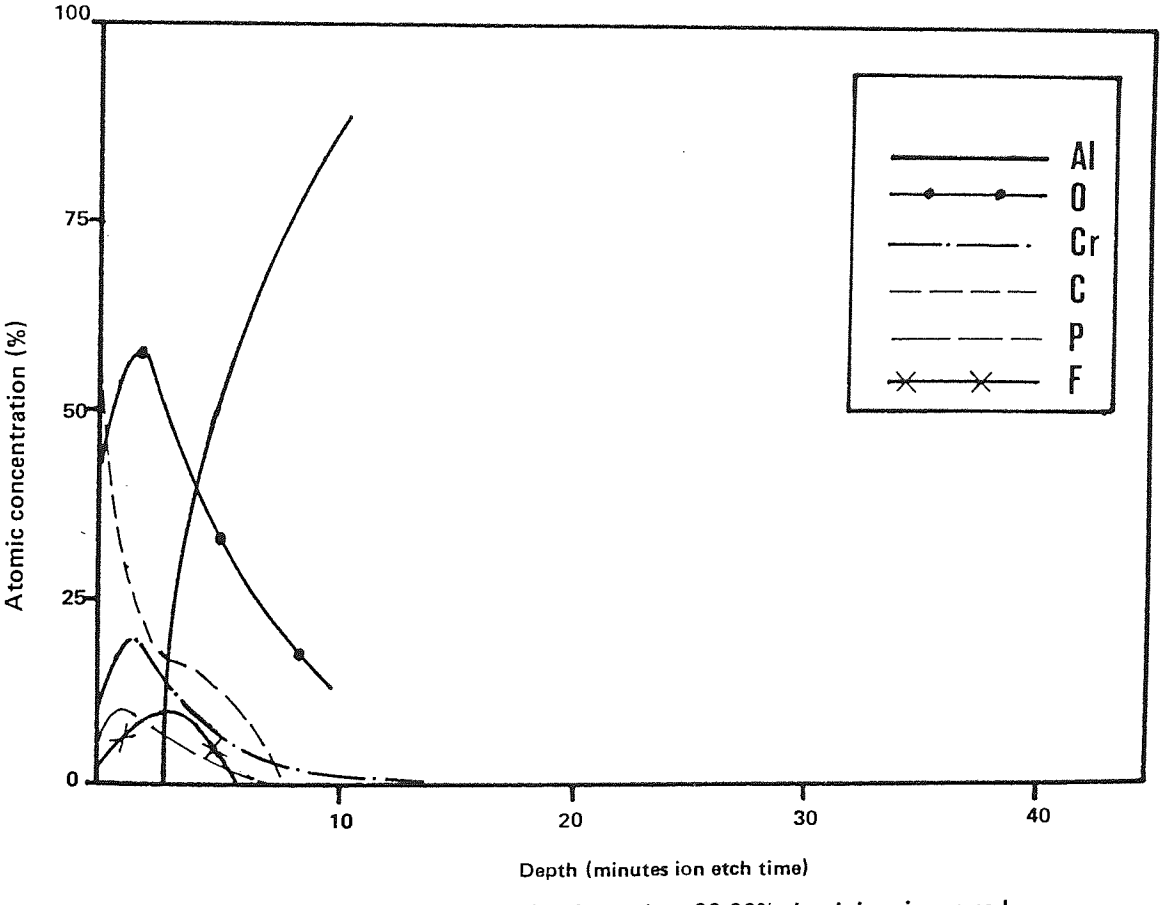

Figure 6.2.2.4 Depth profile of coating formed on 99.99% aluminium immersed in Alocrom 100 containing 1 g/l aluminium for 30 seconds

The remaining profiles ie those with aluminium additions, are very similar except that the fluorine trace does not appear to be at the film/substrate interface. Fluorine can be seen to appear in the second third of the coatings produced in solution with 0.4 and 0.7 g/l aluminium additions and the top two thirds in the sample from the 1.0 g/l solution. However the most striking result of increasing aluminium additions to Alocrom 100 is that the coating weight is markedly reduced.

The shift of the fluorine trace may be due to analysis of an area which was not flat or that had a variation in film thickness. Alternatively, it may be due to changing film formation mechanisms.

6.2.3 Accelerated corrosion study of conversion coatings produced in aged solutions

The position of the panel in the salt-spray cabinet did not have a marked effect on the corrosion performance of the coatings (placed in a random order on the cabinet rack). The 30 second coatings had fewer corrosion products on the surface than the 3 second coatings which were covered with a black powdery substance. Before the panels were cleaned they were sorted into the order of corrosion resistance. The panels were washed in distilled water and arranged as before. The results of this 250 hour salt-spray test are shown in Table 6.2.3.

Since judging the relative performance of each sample was subjective, only the best and worst of each set has been included.

Table 6.2.3 Salt-Spray Corrosion Results

Pretreatment Time (seconds)	Corrosion Resistance (Al content g/l)		Sample Condition
	Best	Worst	
3	0	0.9	Unwashed
30	0.2	0.6	Unwashed
3	0	0.9	Washed
30	0.1	0.8	Washed

6.2.4 Conversion coating formation on zinc

Scanning Electron Microscopy was used to study the surface of zinc sheet immersed in Alocrom 100 for times between 1 minute and 60 minutes. Photo 22 shows the surface after 5 minutes, it is clear that a thick continuous film has not formed. Small platelets of chromate-phosphate coating (confirmed by EDXA analysis) can be seen. Crystallographic etching can be seen between these platelets.

As time of immersion increased beyond 5 minutes, fewer platelets were detected and the corresponding crystallographic etching became more severe. The data obtained by coupon weight-change measurement was plotted as weight loss against time of immersion (Figure 6.2.4). Dissolution of zinc immersed in Alocrom 100 slows down markedly after 30 minutes. If the weight difference between the two curves is due to the removal of any chromate-phosphate coating from the zinc surface by the water jet treatment then it can be seen that the coating weight increases up to about 20 minutes. After this time the coating weight remains constant and the rate of zinc dissolution is reduced.

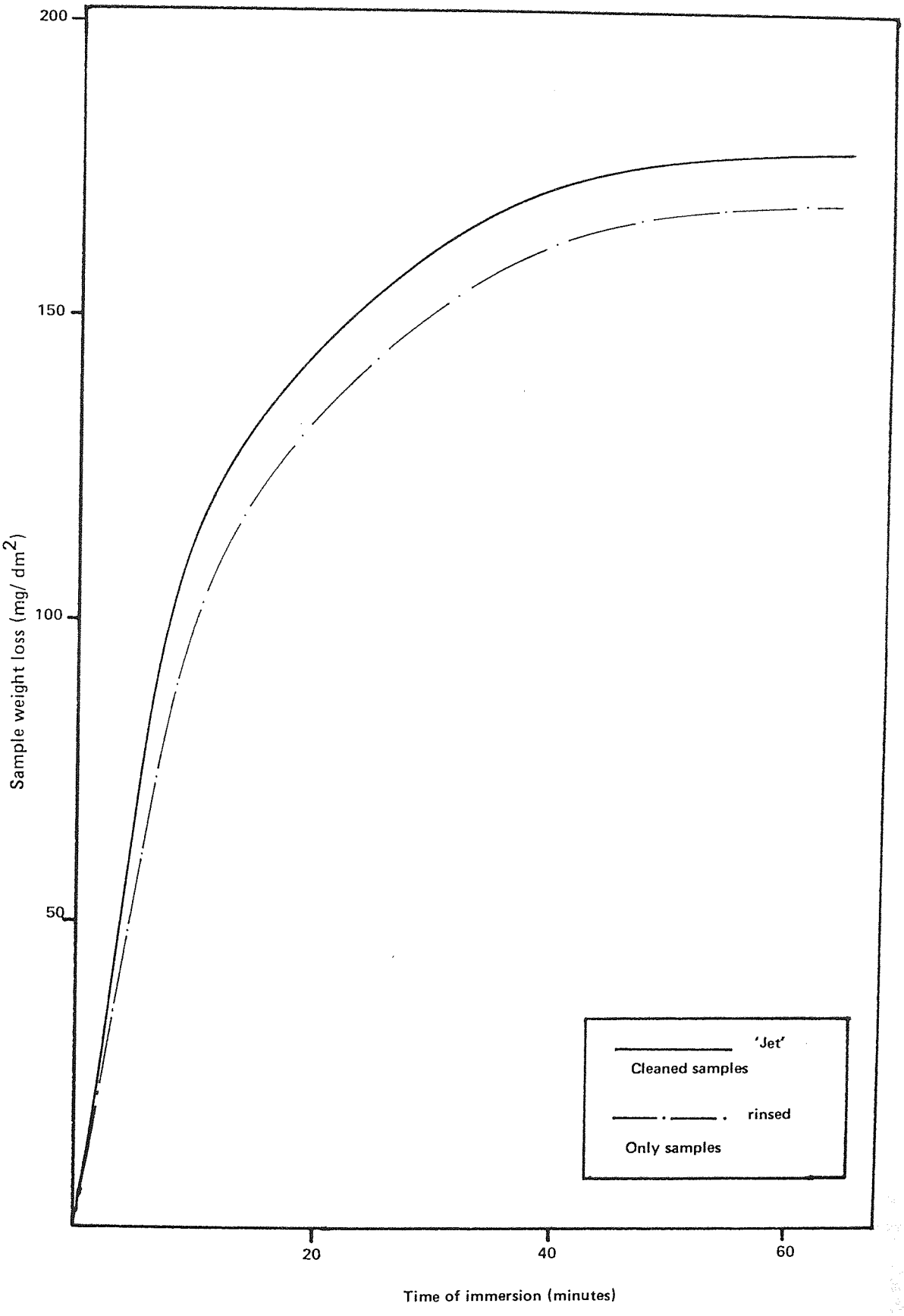

Figure 6.2.4 Weight loss curve for pure zinc in standard Alocrom 100 solution, with and without a 'Jet' water wash

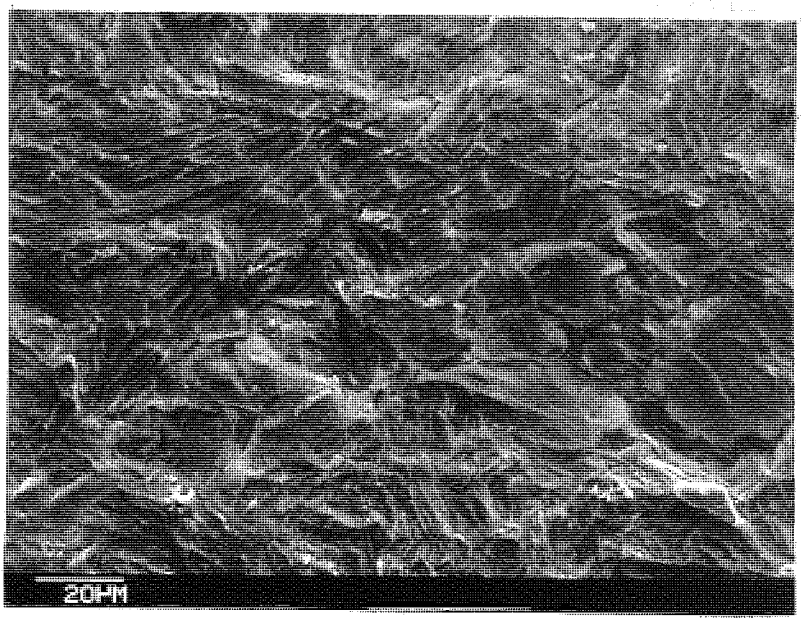

Photo 22

Pure zinc immersed in Alocrom 100 for 5 minutes at room temperature

(Mag x 1K Ta = 30°)

6.2.5 The influence of zinc contamination in Alocrom 100 on the formation of conversion coatings.

The effect of zinc contamination of Alocrom 100 on chromate-phosphate coatings formed on aluminium is shown by Photo 23 and 24. Photo 23 shows the coatings formed on 99.99% aluminium in the cleaned and uncleaned condition after 10 minutes immersion in Alocrom 100 solutions containing an addition of 0.1 and 5 g/l zinc respectively. A similar set of micrographs showing the coating formed on E4S aluminium alloy sheet is shown in Photo 24. It can be seen from both sets of photos that the cleaner has a significant effect upon the subsequent coating.

The coupon weight change versus time for E4S immersed in Alocrom 100 with various zinc additions is shown in Figure 6.2.5.1. Coupon weight gain decreases with a small zinc addition, but increases with further zinc additions. Figure 6.2.5.2 shows the potential-

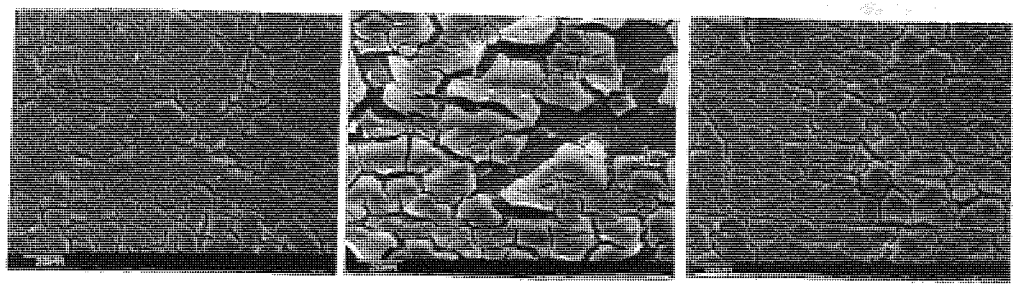

degreased only

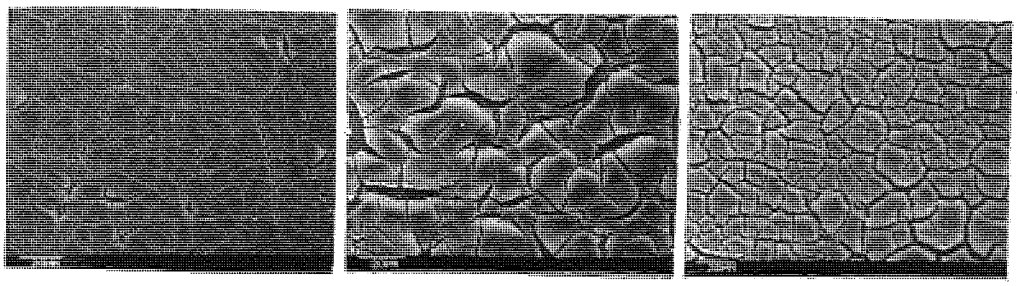

degreased and cleaned

0 g/l 1 g/l 5 g/l

Photo 23

99.99% aluminium sheet immersed in Alocrom 100 with various additions of zinc for 10 minutes.

(Mag. = x1K Ta = 30° for all frames)

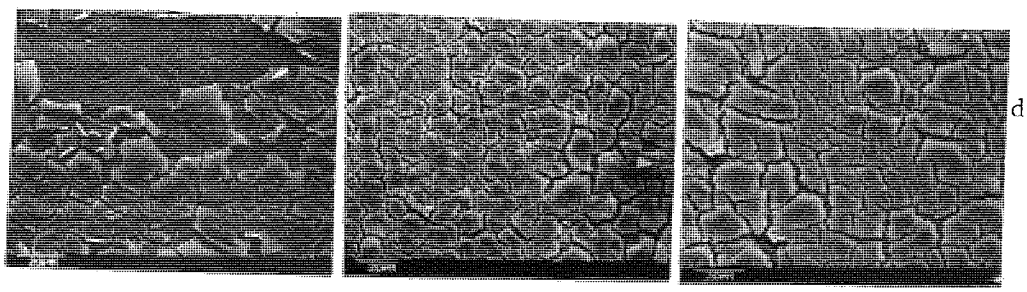

degreased only

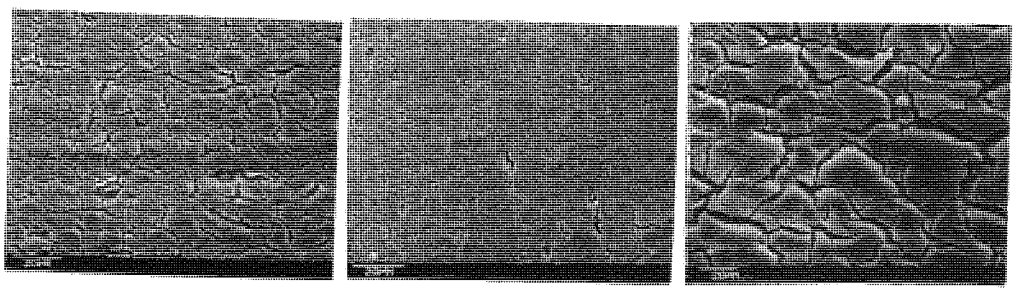

degreased and cleaned

0 g/l 1 g/l 5 g/l

Photo 24

E4S aluminium alloy sheet immersed in Alocrom 100 with various additions of zinc for 10 minutes.

(Mag. = x1K Ta = 30° for all frames)

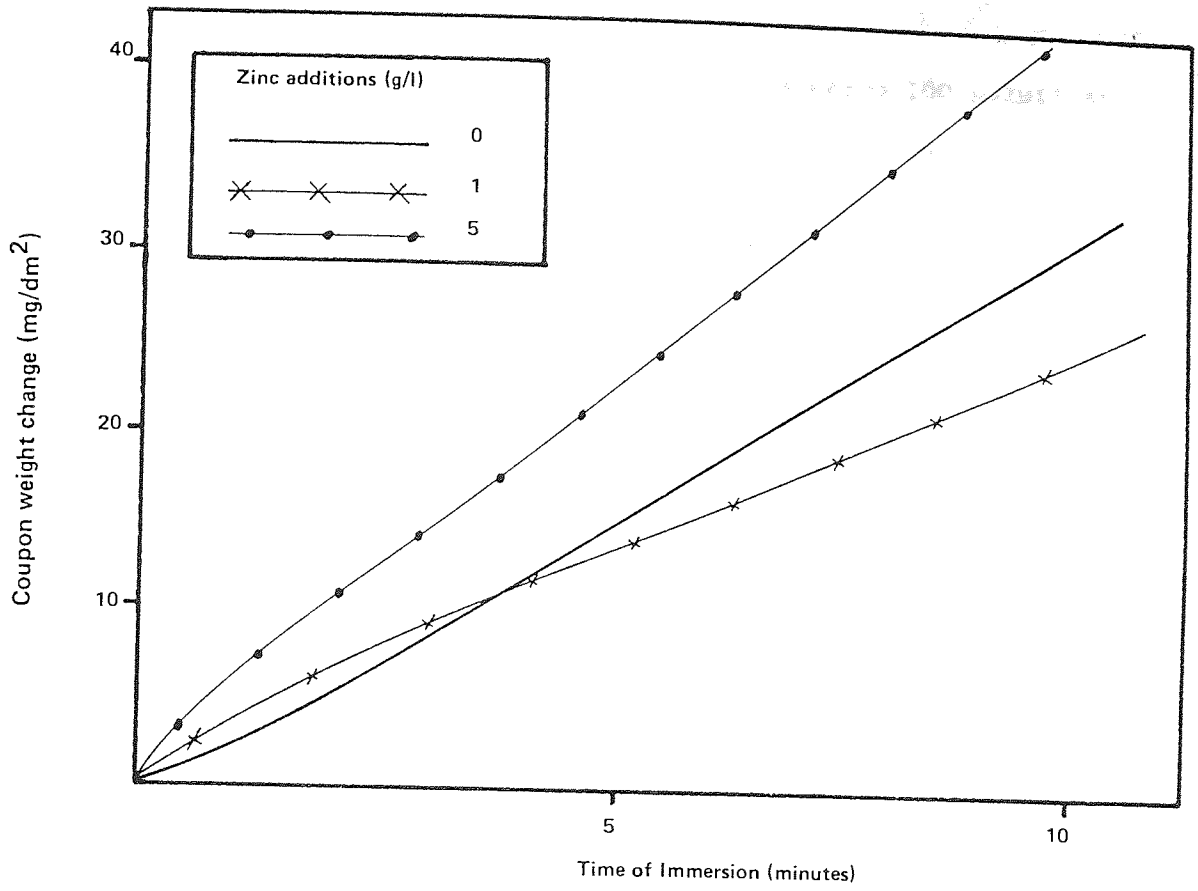

Figure 6.2.5.1 Coupon weight change curves for E4S alloy immersed in Alocrom 100 with various zinc additions (at room temperature)

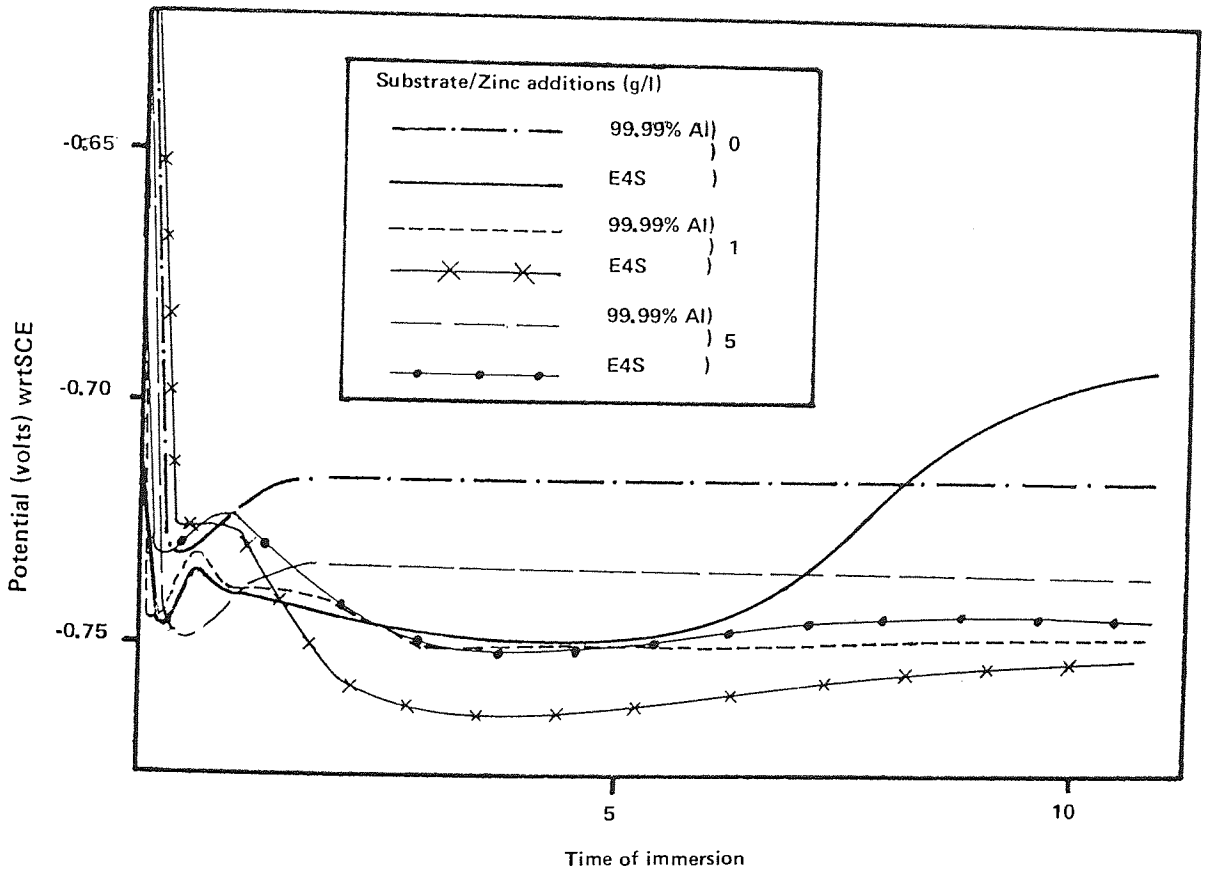

Figure 6.2.5.2 Potential-time curves for 99.99% aluminium and E4S alloy in Alocrom 100 with various zinc addition (at room temperature)

time results for 99.99% aluminium and E4S in Alocrom 100 solutions with various zinc additions. These plots were produced during formation of the coatings seen in Photo 23 and 24 and so are directly comparable. If the relative position of each curve is examined it will be seen that for both 99.99% and E4S small additions of zinc result in increased activity. This is then reversed as more zinc is dissolved in the solution. The 5 g/l plots are not as noble as the 0 g/l plots. It was noted that 99.99% aluminium reached a steady-state potential after immersion for 2 minutes. However, E4S did not display a steady-state potential at any time.

The potential-time curves for the degreased only coupons were very similar to those shown except that all plots were slightly more active. The degreased only 99.99% aluminium coupons also displayed some instablity for the first 30 seconds of immersion, but following this settled at potentials in the same order as the cleaned coupons.

EDXA was carried out during examination of the potential-time samples in the SEM. Zinc was not found in any coatings observed.

6.2.6 Effect of metallic contamination of chromate-phosphate solutions on formation of conversion coatings

The result of contamination by zinc of the standard chromate-phosphate solution on the topography of coatings formed are shown in Photo 25 for 2 minutes immersion, and Photo 26 for 5 minutes immersion. The EDXA results are shown in Table 6.2.6.1. Zinc was not detected in the coating until 15 g/l had been added. Photo 25

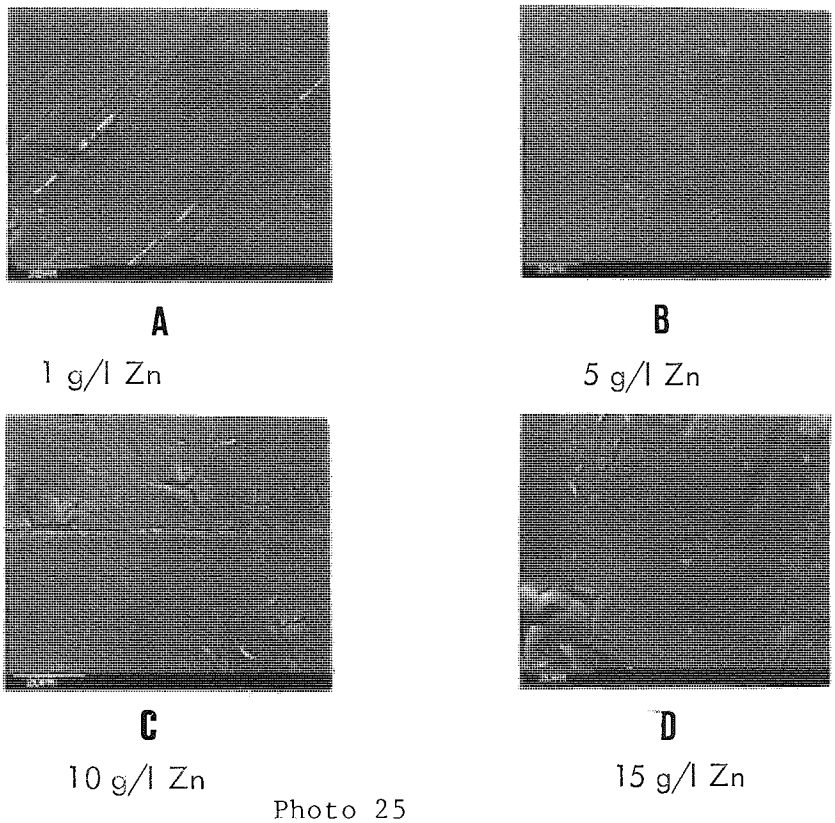

A
1 g/l Zn

B
5 g/l Zn

C
10 g/l Zn

D
15 g/l Zn

Photo 25

Coatings formed in chromate-phosphate solutions with increasing zinc content after 2 minutes immersion.

(Mag = x 1K Ta = 30° for all frames)

Frame A; Shows the topography of a normal coating with few defects or large cracks.

Frame B; The number of pit-type defects has increasesd with increasing zinc additions.

Frame C; Large 'crows-foot' type defects randomly distributed over surface.

Frame D; Large areas of ruptured coating. Mud-cracking has become finer with increasing zinc additions.

and 26 show that the coating formed was markedly affected by zinc additions well below 15 g/l. The coupon weight versus time curves for increasing zinc additions are shown in Figure 6.2.6.1. Additions of zinc greater than 2 g/l cause the rate of coupon weight gain to decrease. Figure 6.2.6.2 shows the potential-time curves corresponding to the weight change versus time plots. Zinc additions lead to a more active substrate surface.

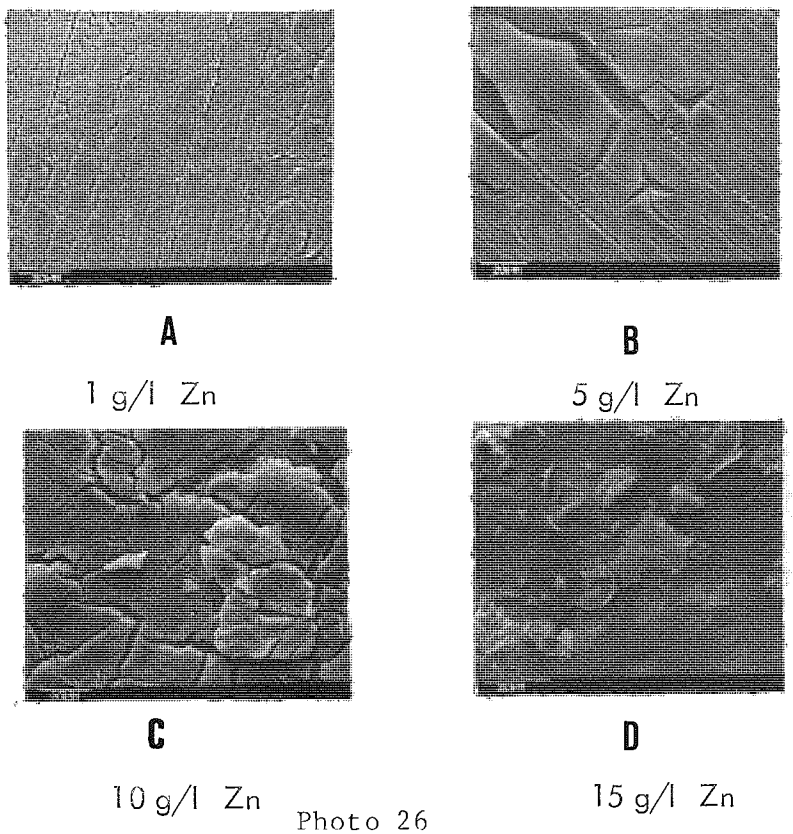

Photo 26

Coating formed in chromate-phosphate solutions with increasing zinc content after 5 minutes immersion.

(Mag = x 1K Ta = 30° for all frames)

Frame A; Optimum coating weight, few coating defects present.

Frame B; Large areas of ruptured coating.

Frame C; Coating has become non-uniform and rough with large open cracks clearly visible.

Frame D; Zinc deposition (bottom left) on substrate. Very little coating remaining (mid frame).

Table 6.2.6.1 EDXA Results for Coatings Produced in Chromate-Phosphate Solutions Contaminated with zinc.

Zinc Content (g/l)	Time of Immersion (minutes)	Major Peaks				P:Cr ratio
		Al (%	P (%)	Cr (%)	Zn (%)	
1	1	92.7	5.1	2.2	-	2.3
1	2	93.9	4.3	1.8	-	2.4
1	5	53.6	33.6	12.8	-	2.6
2	1	94.9	3.3	1.6	0.1	2.1
2	2	81.6	12.7	5.6	trace	2.3
2	5	60.5	27.4	12.1	-	2.3
5	1	95.3	3.2	1.5	trace	2.1
5	2	83.8	11.0	5.2	-	2.1
5	5	58 0	28.3	12.8	-	2.2
10	1	95.7	2.9	1.4	-	2.1
10	2	84.8	10.3	4.9	-	2.1
10	5	74.2	17.7	8.0	-	2.2
15	1	97.6	1.5	0.8	0.1	1.9
15	2	97.6	2.0	1.3	0.1	1.5
15	5	97.5	0.8	0.4	1.3	2.0

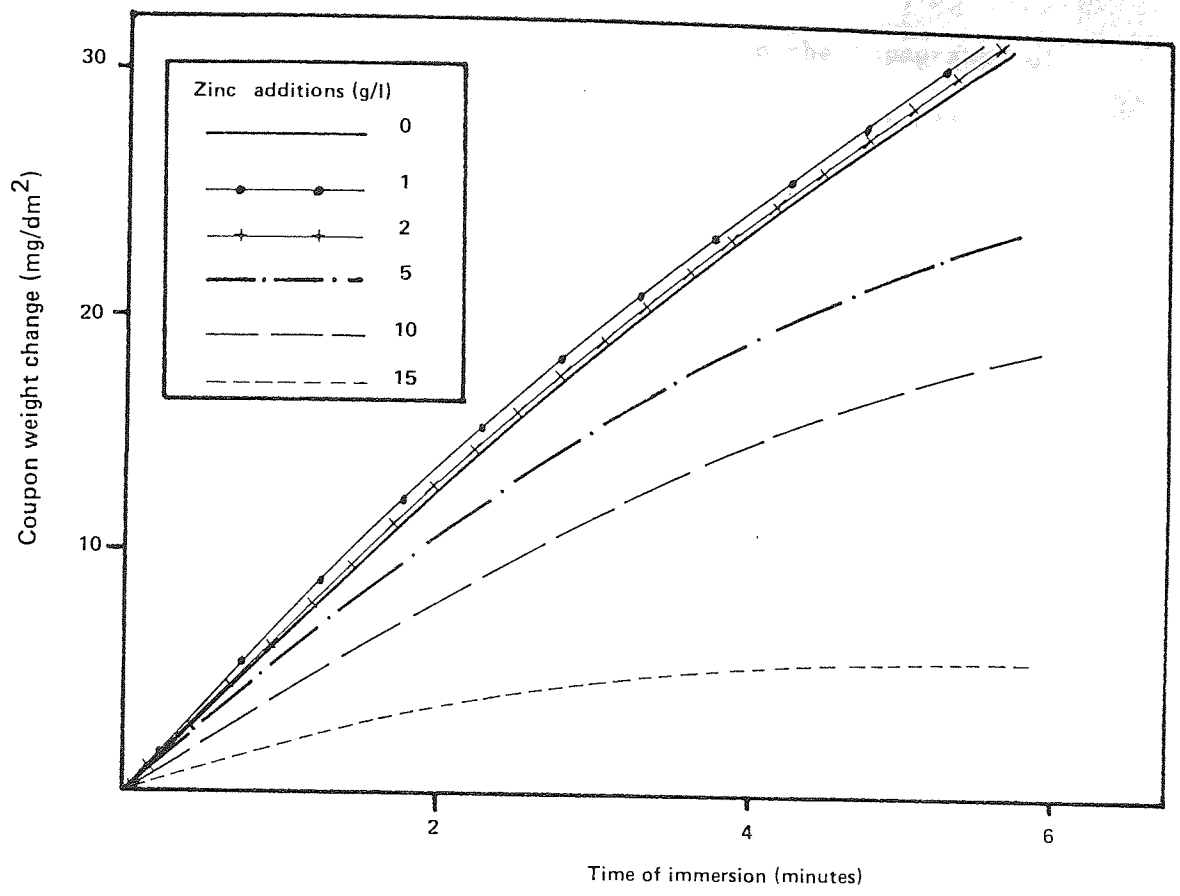

Figure 6.2.6.1 Weight-change against time of immersion for 99.99% aluminium in a chromate-phosphate solution containing various amounts of zinc

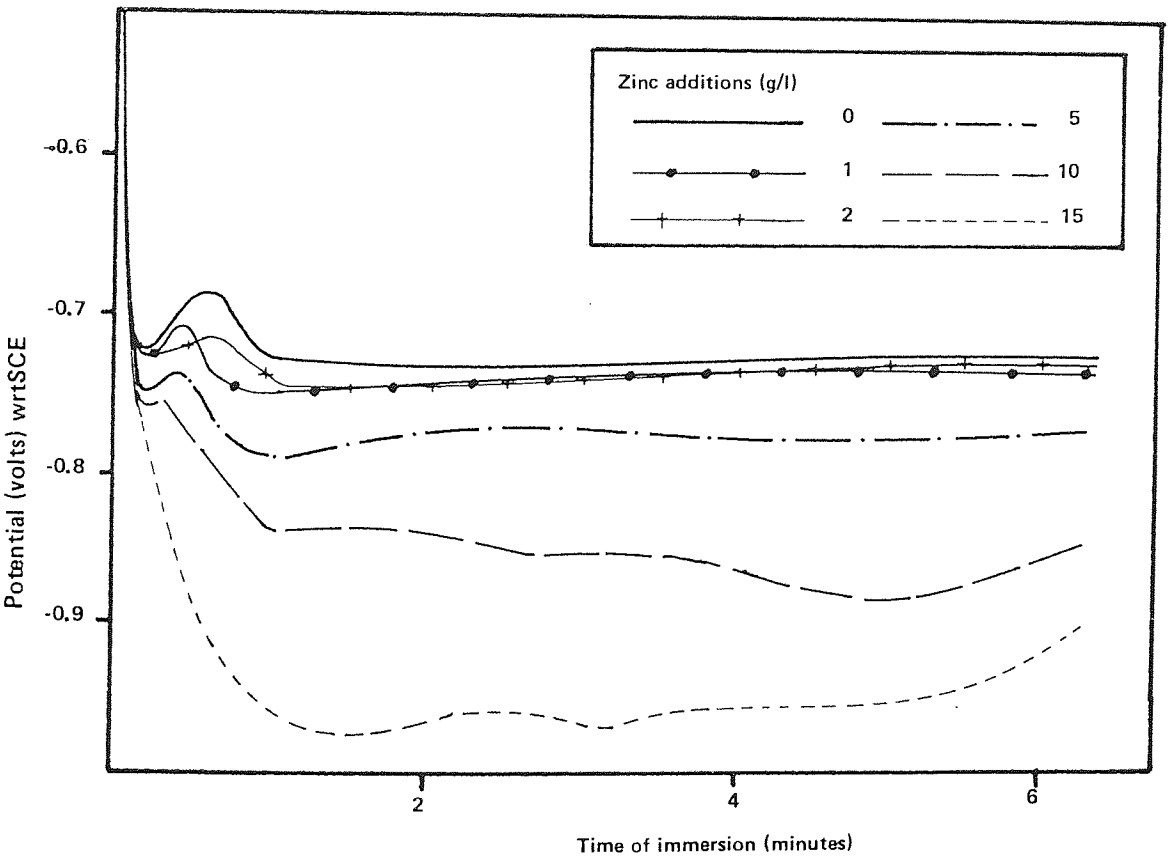

Figure 6.2.6.2 Potential-time curves for 99.99% aluminium in a chromate-phosphate solution containing various additions of zinc

The effect that magnesium contamination had on the topography of coatings formed is shown in Photo 27. 1 g/l magnesium addition had little effect on the coating, but an addition of 3 g/l caused the coating to completely fail (Photo 27C). It was noted that many pit-defects were caused by precipitation of small iron nodules on the substrate (Photo 27D). Contamination of the solution by iron was presumed to be due to impurities within the magnesium oxide. Table 6.2.6.2 show the results of EDXA of the coatings formed. Magnesium was not detected. Figures 6.2.6.3 and 6.2.6.4 show the corresponding weight change versus time and potential-time curves respectively. Both show a similar response to contamination as seen for zinc contamination.

Table 6.2.6.2 EDXA Results for Coatings Produced in Chromate-Phosphate Solutions Contaminated with Magnesium

Magnesium Content (g/l)	Time of Immersion (minutes)	Major Peaks				P:Cr ratio
		Al (%)	P (%)	Cr (%)	Mg (%)	
1	1	90.1	6.3	2.8	-	2.3
	2	83.4	11.7	4.9	-	2.4
	5	40.3	42.2	17.5	-	2.4
	10	5.2	65.7	29.1	-	2.3
2	1	91.5	5.9	2.6	-	2.3
	2	79.1	14.6	6.3	-	2.3
	5	18.6	52.3	29.3	-	1.8
	10	7.6	63.3	29.1	-	2.2
3	1	91.2	6.1	2.7	-	2.3
	2	74.7	17.2	7.8	-	2.2
	5	30.7	46.8	22.3	-	2.1
	10	10.9	61.9	27.2	-	2.3
4	1	89.4	6.8	3.7	-	1.8
	2	83.3	11.1	5.6	-	2.0
	5	37.3	43.6	19.1	-	2.3
	10	6.1	63.9	30.0	-	2.1

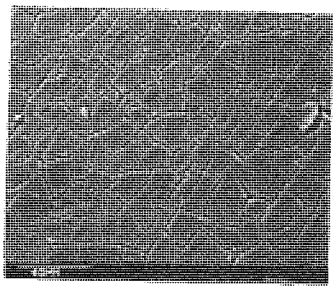

A

1 g/l Mg

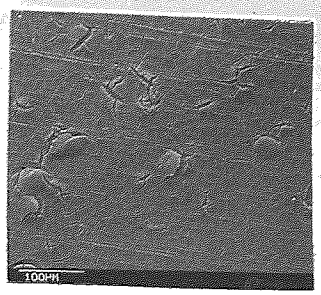

B

2 g/l Mg

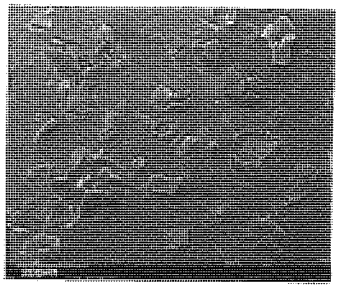

C

3 g/l Mg

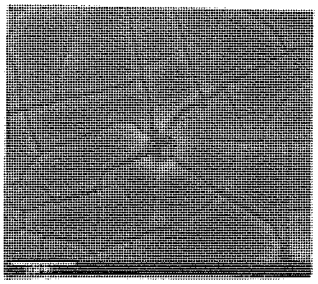

D

4 g/l Mg

Photo 27

Coatings formed in chromate-phosphate solutions with increasing magnesium content after 10 minutes immersion.

(Ta = 30° for all frames)

Frame A; Mag = x 500: Very few defects in coating, uniform crack density.

Frame B; Mag = x 200: Large defects on surface.

Frame C; Mag = x 100: Surface completely covered with defects.

Frame D; Mag = x 2K: Iron particle in centre of frame found to be associated with many defect areas in Mg contaminated solutions.

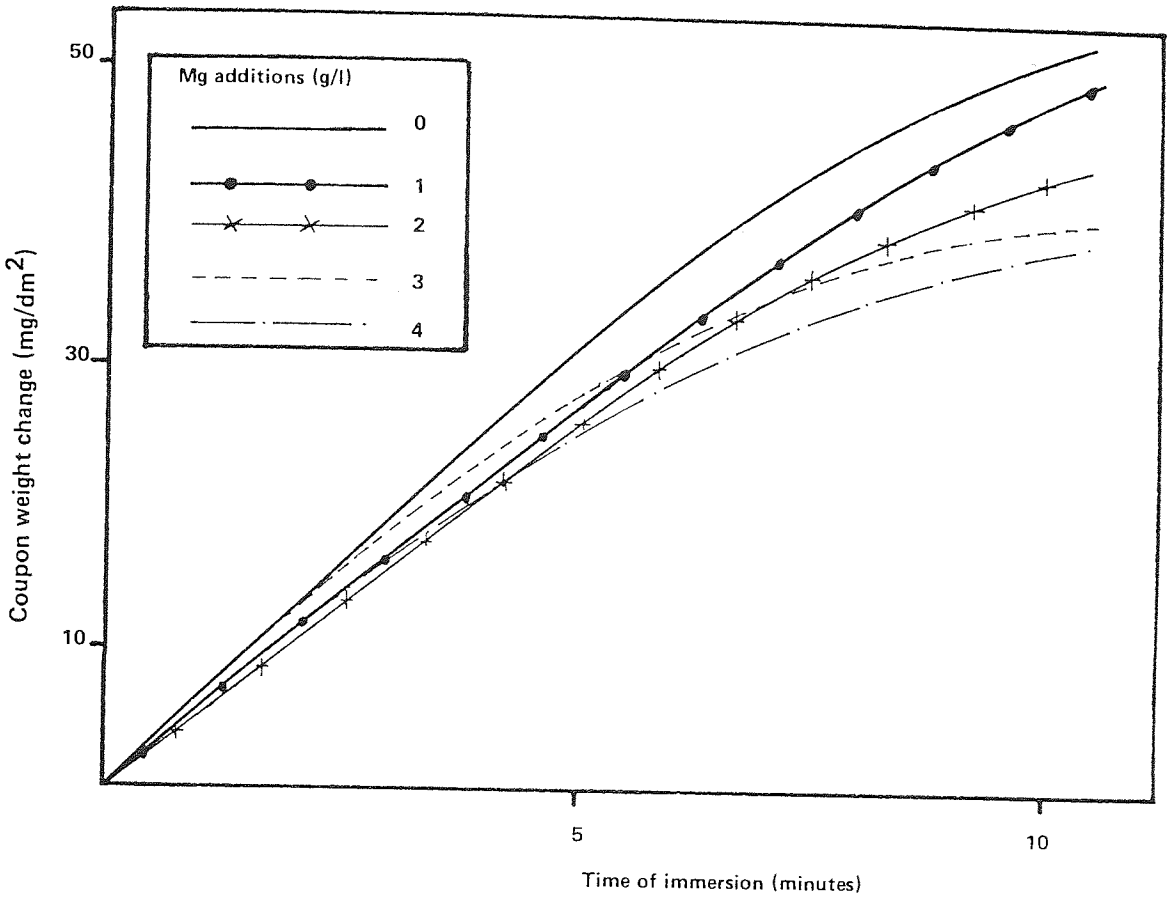

Figure 6.2.6.3 Weight change against time for 99.99% aluminium in a chromate-phosphate solution with various magnesium additions

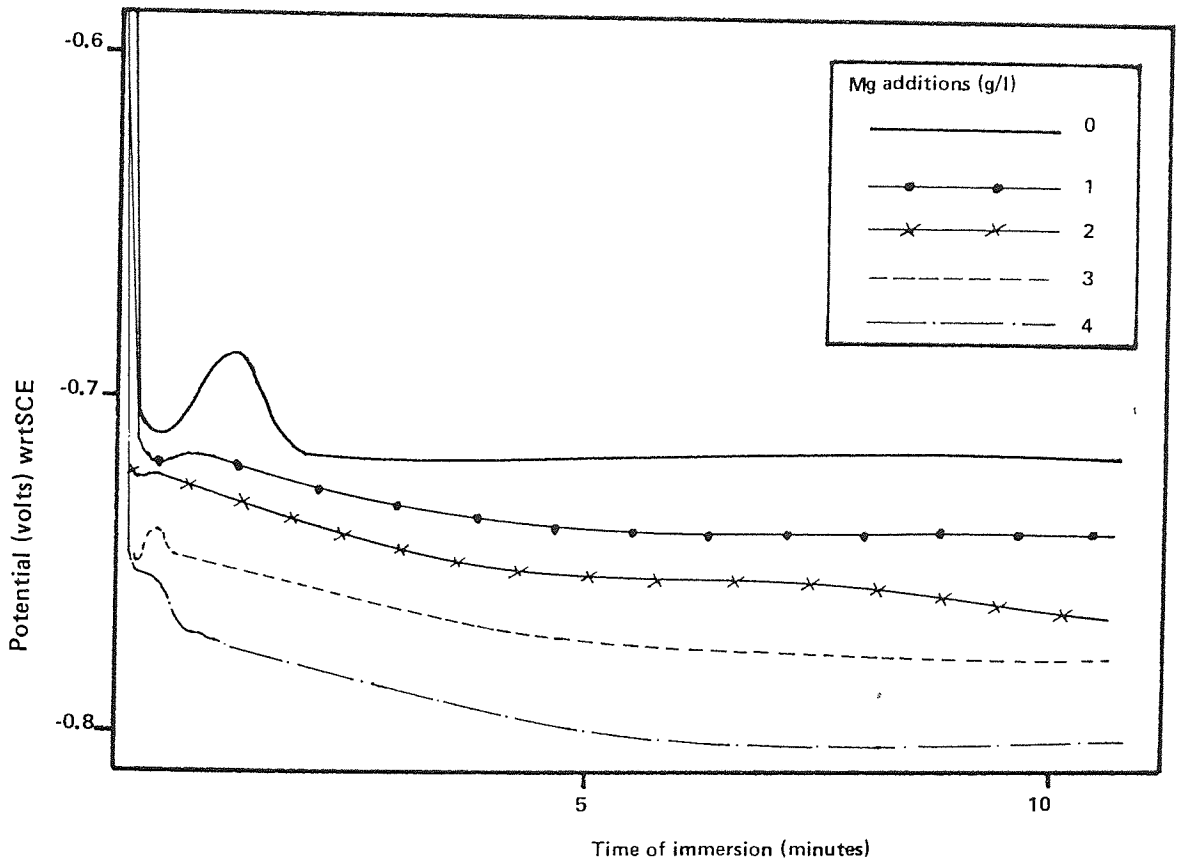

Figure 6.2.6.4 Potential-time curves for 99.99% aluminium in a chromate-phosphate solution with various magnesium additions

The effect of copper additions to the standard chromate-phosphate solution on the coatings formed by 2 and 10 minutes immersion are shown in Photos 28 and 29. Copper particles were found to precipitate on the conversion coating (Photo 28A) between layers of the coating (Photo 29B) and on the substrate (Photo 28B). Copper additions of 5 g/l or more inhibited coating formation. EDXA results (Table 6.2.6.3) show the composition for coatings formed in solutions with up on 3 g/l copper additions. Very little coating could be detected in solutions with greater copper additions.

The coupon weight change versus time curves (Figure 6.2.6.5) show a decrease in the rate of weight gain from increasing copper additions up to 3 g/l. Further additions result in increasing coupon weight gain rates, probably due to the precipitation of large copper nodules (Photo 28 C-D and 29 C-D). Figure 6.2.6.6 showing the corresponding potential-time results show increased surface activity for copper additions up to 2 g/l. Further additions result in less active (or more noble) potentials which is also due to the precipitation of copper on the aluminium substrate. The potential-time curves for the 5 and 10 g/l copper additions show a marked tendency to hunt, probably caused by hydrogen gas evolution on the anodic copper nodules.

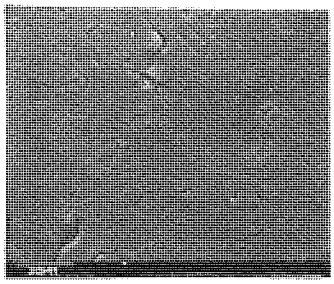

A

2 g/l Cu

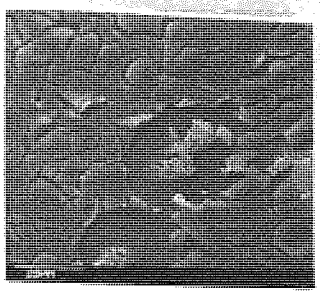

B

3 g/l Cu

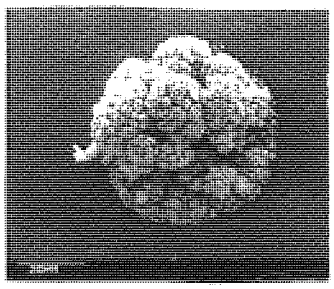

C

5 g/l Cu

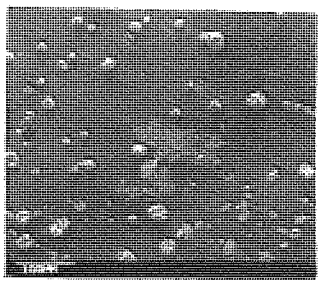

D

10 g/l Cu

Photo 28

Effect of increasing copper content in chromate-phosphate solution on coatings formed by 2 minutes immersion.

(Ta = 30° for all frames)

Frame A; Mag = x 1K: Small copper particles precipitated on to coating surface (mid-frame).

Frame B; Mag = x 1K: Areas with intense copper deposition devoid of coating.

Frame C; Mag = x 1K: Large copper nodules on substrate surface; no coating detected.

Frame D; Mag = x 200: Distribution of copper nodules on surface.

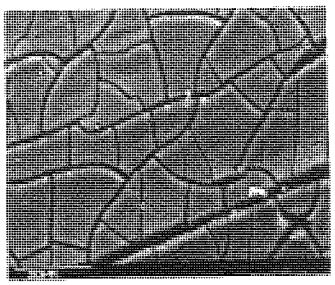

A

1 g/l Cu

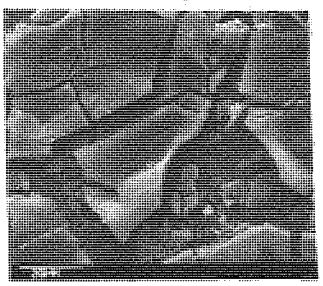

B

2 g/l Cu

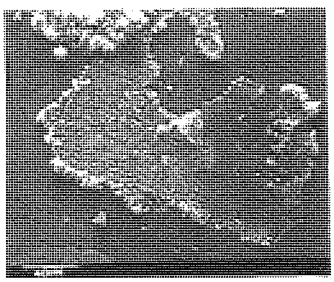

C

3 g/l Cu

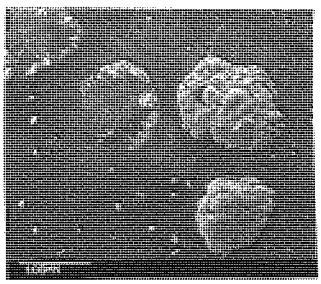

D

5 g/l Cu

Photo 29

Effect of increasing copper content in chromate-phosphate solution on coatings formed by 10 minutes immersion.

(Ta = 30° for all all frames)

Frame A; Mag = 1K: Normal topography for 10 minute chromate-phosphate coating.

Frame B; Mag = x 1K: Copper particles precipitated between upper and lower layers of coating.

Frame C; Mag = x 500: Copper particles precipitated on preferential areas; no coating detected in this area.

Frame D; Mag x 200: Site of four copper nodules; two on the left have fallen or been knocked off.

Table 6.2.6.3 EDXA Results for Coatings Formed in Copper contaminated Chromate-Phosphate Solutions

Copper Content (g/l)	Time of Immersion (minutes)	Major Peaks				P:Cr ratio
		Al (%)	P (%)	Cr (%)	Cu (%)	
1	1	95.3	3.4	1.3	-	2.6
	2	86.3	9.6	4.1	-	2.3
	5	54.4	32.4	13.2	-	2.5
	10	6.3	62.0	31.5	trace	2.0
2	1	93.3	4.6	2.1	trace	2.2
	2	85.4	9.5	4.9	0.1	1.9
	5	54.5	30.9	14.2	0.4	2.2
	10	33.2	40.8	20.7	5.2	2.0
3	1	94.6	3.6	1.6	0.1	2.3
	2	87.5	8.7	3.7	0.1	2.4
	5	69.6	21.1	9.2	0.1	2.3
	10	67.2	21.7	9.8	1.2	2.2

NB Coatings formed beyond 3 g/l copper content had large Cu particles on the surface and very little coating. Therefore EDXA was not appropriate.

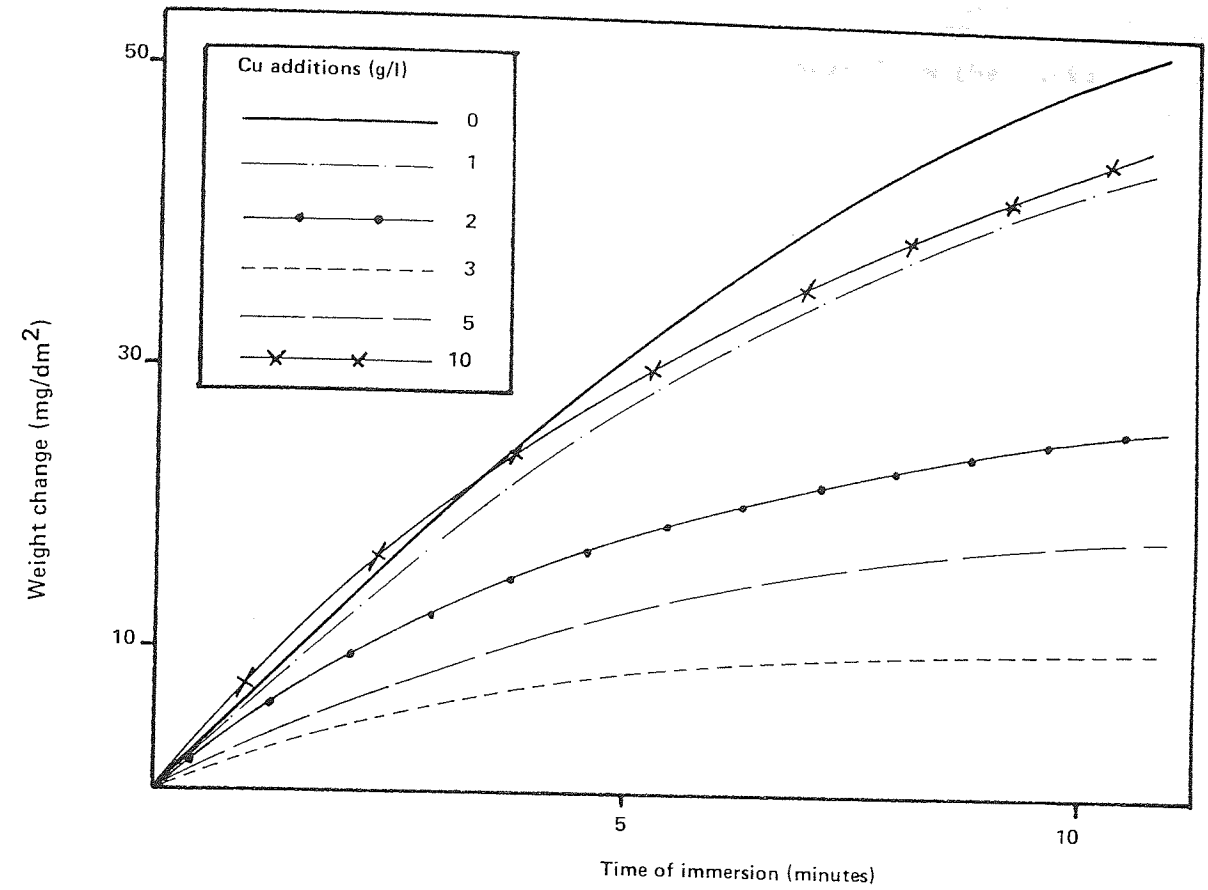

Figure 6.2.6.5 Weight change against time for 99.99% aluminium in a chromate-phosphate solution with various additions of copper

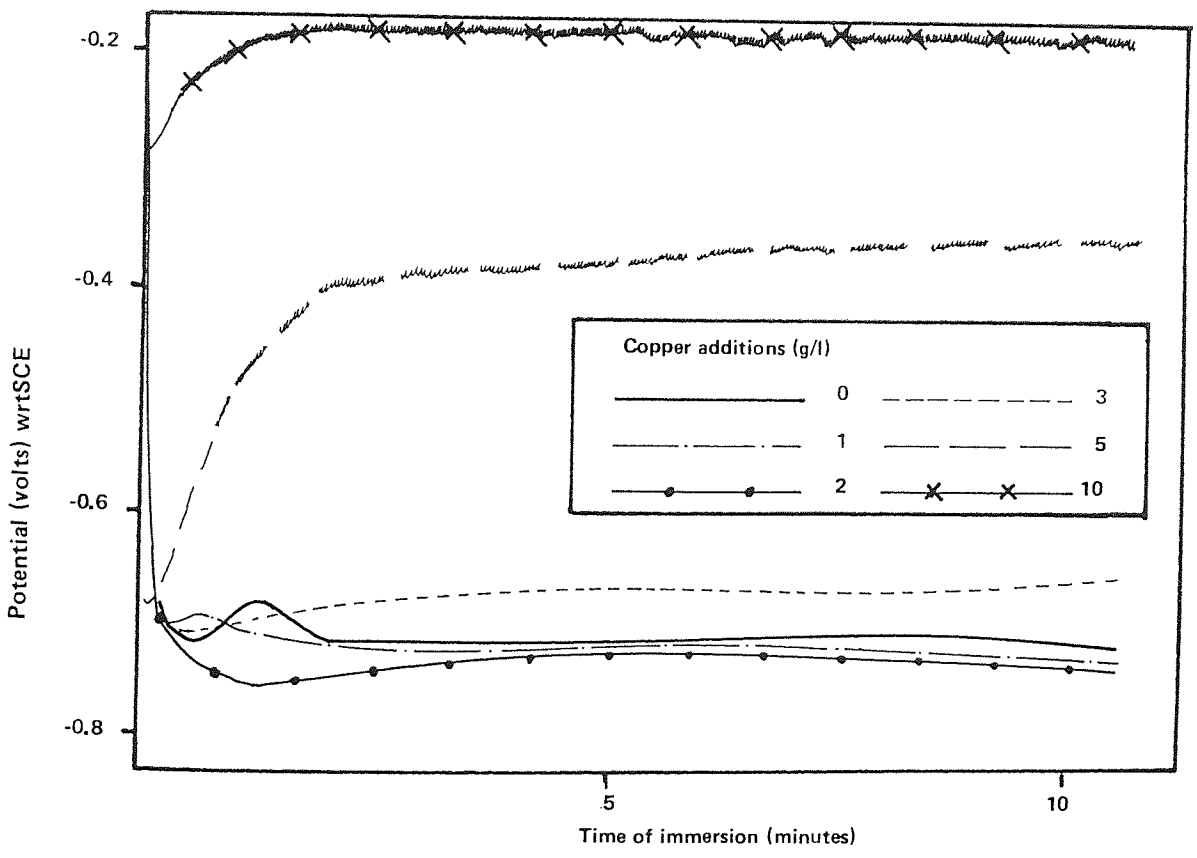

Figure 6.2.6.6 Potential-time curves for 99.99% aluminium in a chromate-phosphate solution with various additions of copper

Finally the samples of AC51 and Alocrom 100 taken from the tanks at Metallic Protectives Ltd, Warwick were found to have aluminium and zinc contents shown in Table 6.2.6.4.

Table 6.2.6.4 Aluminium and Zinc Content in Industrial (used) Solutions of AC51 and Alocrom 100

Analysed Element	AC51	Alocrom 100
Aluminium (g/l)	0.14	0.68
Zinc (g/l)	1.8	5.4

7. EFFECT OF PRETREATMENT ON POWDER COATINGS

7.1 Introduction to Experimental Work

The interaction between an aluminium substrate and an applied powder coating has been studied using powder flow, corrosion resistance and potential-time techniques. Powder flow was examined by Gokemre and Dennis(58,59), who heated powder on various substrates and measured the resultant area covered as a function of surface temperature. A similar technique has been used in the present study to investigate powder flow on various chromate-phosphate conversion coatings. The influence of the powder particle size and state (ie fresh or recycled) has also been studied.

The effect of the surface pretreatment and the final powder coating on corrosion resistance, weathering, and accelerated corrosion resistance was studied alongside the powder flow work in order to find any correlation that may lead to an improved coating system.

7.1.1 Powder flow study

A Cambridge Instruments Quantimet (QMT) with manual control settings was set up in a similar fashion to that described by Whiting(58). The main change was that an external meter source from the QTM was used to provide a direct record of percentage area on a chart recorder.

A twin pen 'Servotec' solid state recorder was used to monitor and record the temperature of the test panel surface in conjunction to a thermocouple, and a line pre-drawn on the chart to correspond with the required temperature gradient. The remaining channel was used to record the percentage area.

A schematic diagram of the equipment is shown in Figure 7.1.1.1. It was found that the most satisfactory illumination was achieved using two lamps focused directly at the spot to be studied and inclined to an angle of approximately 30° to the horizontal position. Lighting was a critical factor as the QTM has been designed to measure the percentage area of white or black under the field of view. By adjusting the threshold level, up to three shades of grey could be distinguished. Therefore illumination conditions must not vary from test to test or during any particular test. This error was avoided by ensuring that the brightest part of the focused beam was visible through the QTM.

Another important variable was the base percentage area (ie the initial % area). This was set at 20% for all flow observations, as this had been found to be a suitable base value in previous work(58,59).

Great care was needed in selecting a representative area on the test panel which satisfied all the test conditions, which were:-

i) 20% initial area covered by powder

ii) particle size distribution representative of the powder under observation

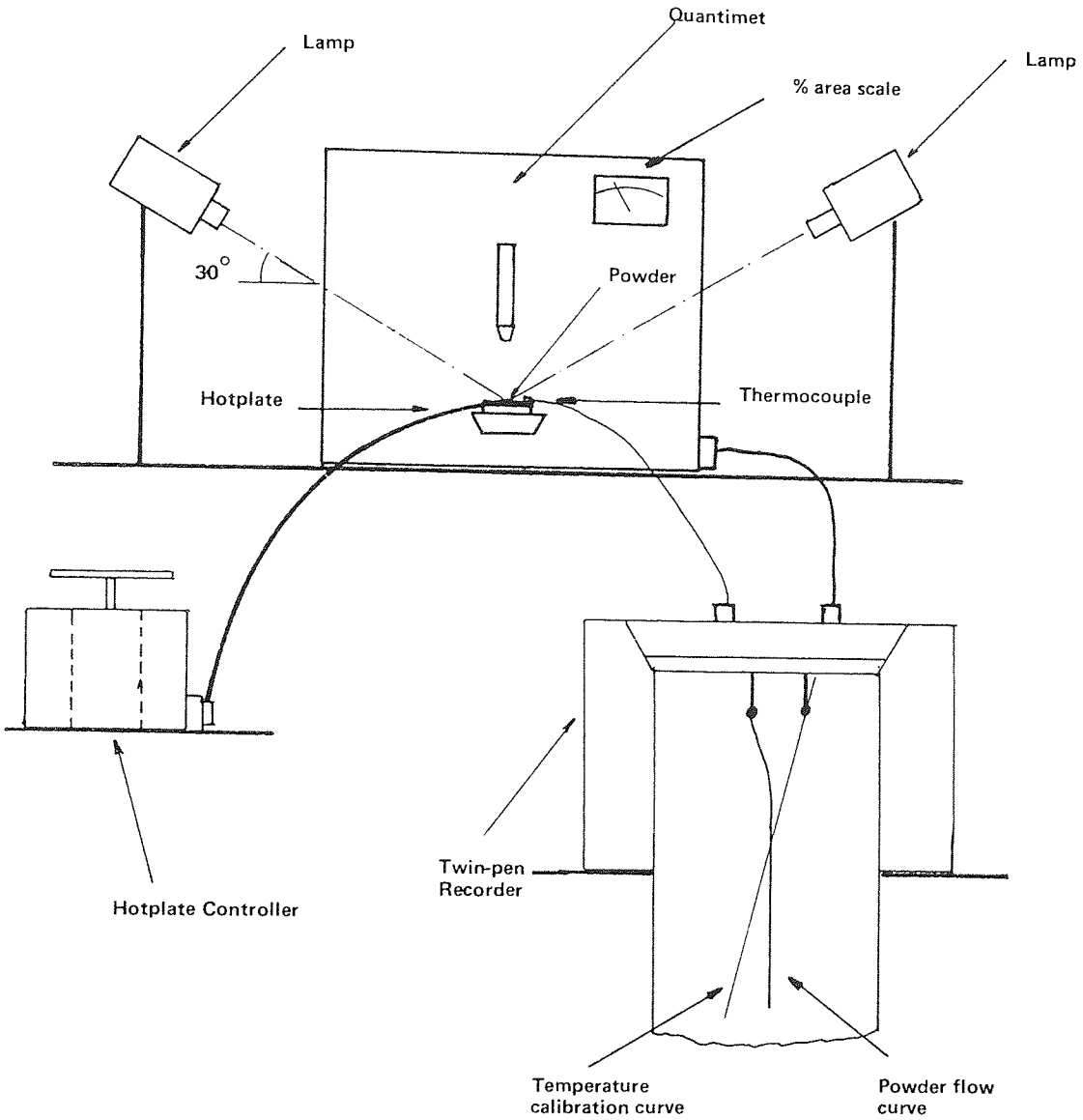

Figure 7.1.1.1 Schematic diagram of the equipment used for powder flow experiments

iii) particles had not "piled-up" on one another giving a false percentage area reading.

A fine artist's brush was used to spread the powder evenly over the test panel surface before the start of the test.

The thermocouple was attached to the test panel by spot welding the bead on to the pretreated panel. Great care was necessary during handling of the test panel after this stage since the thermocouple could be easily detached.

The QTM and chart recorder were allowed to warm up for a period of at least 60 minutes before the start of the first test. During this time the test panel was put into position and a suitable area meeting the requirements stated above was found after having applied some powder with the fine brush and adjusted the lighting.

The stage heater was controlled with a variac, temperature being continuously monitored via the thermocouple and chart recorder. The heater and chart recorder where switched on simultaneously. The voltage applied to the heater was adjusted in order to keep the thermocouple pen (on the chart recorder) on the line previously drawn on the chart.

The powder flow test was carried out on five pretreated surfaces which were supplied by Metallic Protectives Ltd as follows:-

i) Alocrom 100 1.5 mins on E4S aluminium alloy

ii) Alocrom 100 3.0 mins on E4S aluminium alloy

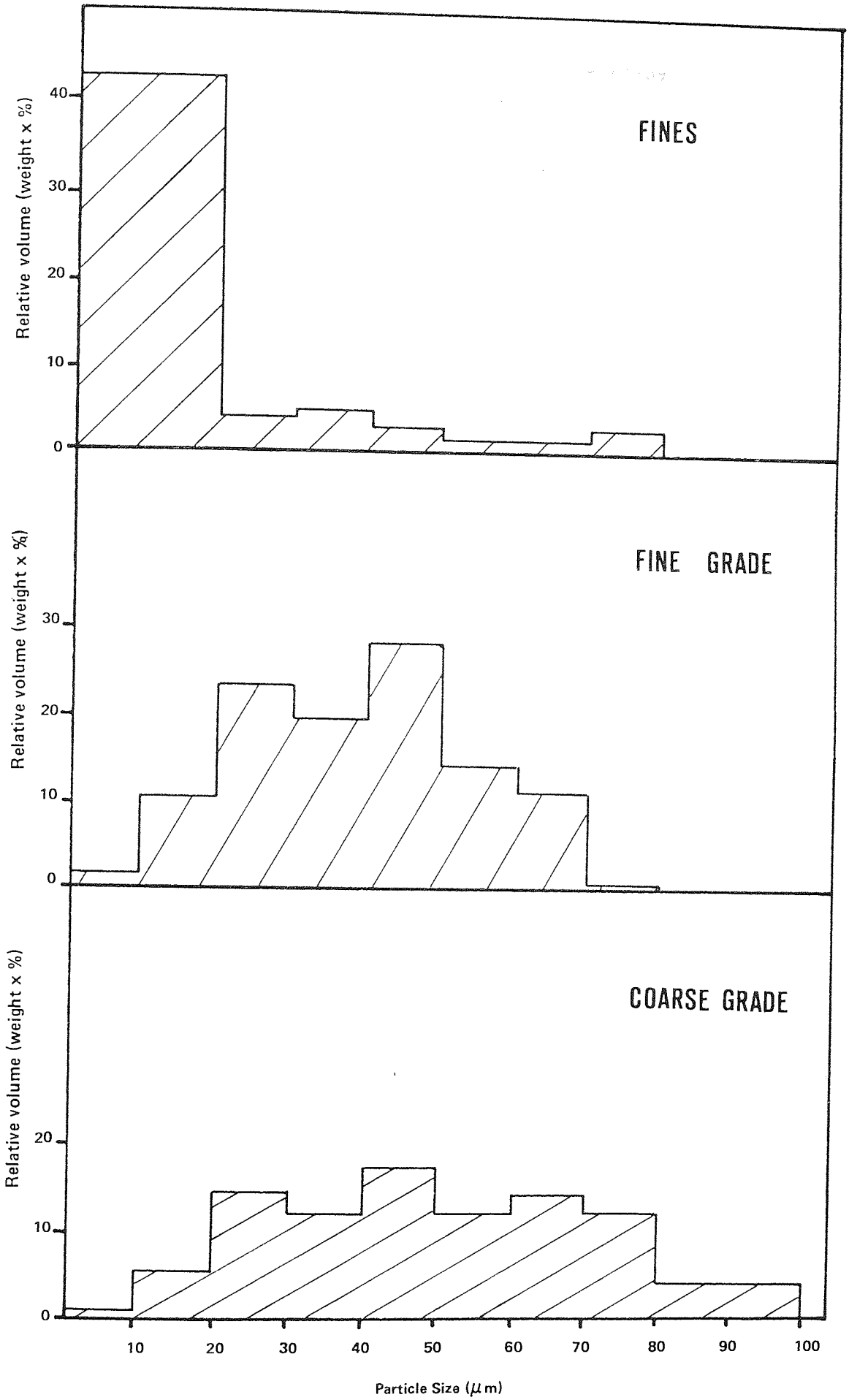

Figure 7.1.1.2 Particle size distribution for the three grades 44S polyester powder supplied by Blundell Permoglaze Ltd

iii) Alocrom 100 5.0 mins on E4S aluminium alloy

iv) Alocrom 100 5.0 mins on hot dipped galvanised steel

v) Alocrom 1200 5.0 mins on E4S aluminium alloy.

Five classfied powders supplied by Blundell-Permoglaze Ltd, Tyseley Division, were studied:-

i) Fine particle size polyester powder (44S)

ii) Standard particle size polyester powder (44S)

iii) Coarse particle size polyester powder (44S)

iv) Recycled polyester powder (44S)

v) 34 NF polydrox polyester powder (German)

Thus a total of 25 tests were conducted, each had a heating rate of 10°C per minute. All supplied powders were stored in air-tight containers and were pigmented white.

The above procedure was also used to find how powder flow was influenced by fresh conversion coatings and freshly made powders. E4S aluminium alloy was cut into coupons measuring 70 x 10mm, degreased in acetone and acid cleaned in aged AC51. These were then immersed in freshly prepared aged Alocrom 100 at room temperature and at 45°C for 90 seconds, followed by thorough rinsing and drying. Fresh standard white polyester powder (44S) was produced and classified into fine, standard and coarse grades by Blundell-Permoglaze for this work. The particle size distribution for each powder is shown in Figure 7.1.1.2. These were very similar to the grades used in the initial work in this section.

Each test was repeated three times in order to ensure that the resultant curves were reproducible. The heating rate was set at 30°C per minute for this work which was close to conditions typically found in industry.

Samples of each powder were studied under the SEM in order to correlate the 'Coulter Counter' results, as seen in Figure 7.1.1.2, with physical appearance.

7.1.2 Corrosion and weathering tests

The effect of pretreatment and use of recycled powder on corrosion resistance was studied. Panels of E4S aluminium alloy measuring 120 x 70mm were treated in Alocrom 100 for times of 1.5, 3.0 and 5.0 minutes, and in Alocrom 1200 for 5 minutes. These panels were subsequently powder coated with standard 44S polyester powder as supplied by Blundell-Permoglaze Ltd. A second set of panels were also powder coated with 44S polyester powder, but this second powder was in the 'recycled' condition and was obtained from a Blundell-Permoglaze customer.

In all, five complete sets of coated panels were produced. Two sets were used for outdoor exposure on the second floor balcony at Aston University (inclined at 30° facing East). Two sets were subjected to 500 hours of neutral salt spray (5%) followed by 300 hours of acetic acid salt spray at a pH of 3.2. In both cases one set of panels was undamaged and the other had a diagonal line scribed through to the substrate on one face.

The last set of panels was used for extended potential-time determinations (100 hours). The potential was measured between a saturated calomel electrode and a panel immersed in an acetic acid - salt solution (pH 3.2). Care was taken to ensure that the solution level in the electrode and the salt solution were the same to avoid contamination of one by the other. The electrode was held as close to the panel as possible and it was placed in the same position relative to the panel in every case. The solution was not stirred. The potential was measured on a chart recorder set to run at 10 mm/hour.

7.1.3 Powder coating in the laboratory

To produce sprayed powder coated panels under laboratory conditions, powder coating equipment was installed in a fume cupboard; the walls of which were lined with polyester sheeting, and the extraction arranged to flow from the bottom, in order to avoid a build up of powder in the cupboard.

The powder coating equipment consisted of three main units:-

i) The generator

ii) The powder spray gun

iii) The powder feed system

which were manufactured and supplied by Controsion Ltd.

'Goldseal' test panels produced by Pyrene Chemicals Ltd were used to test the system and were found to be satisfactorily covered. They were carefully sprayed in order to achieve uniform coverage,

ie allowing for build-up at edges and the effect of gravitation. Coatings were about 70 μm thick after curing, which was carried out for 15 minutes at 200°C.

7.2 Results

7.2.1 Powder flow study

The powder flow curves obtained have been arranged into six figures. Figures 7.2.1.1-3 shows the results for each of the five powders tested on coupons treated in Alocrom 100 for 1.5, 3 and 5 minutes respectively. Figure 7.2.1.4 shows the flow curves obtained using fresh powder with various particle size distributions on coupons treated in Alocrom 100 for 90 seconds at room temperature and at 45°C. The powder flow curves for various powders on aluminium coupons treated in Alocrom 1200 for 5 minutes and galvanised steel coupons treated in Alocrom 100 for 5 minutes are shown in Figures 7.2.1.5-6 respectively. Table 7.2.1 shows the ultimate coverage and flow temperatures for various powders on coupons treated in Alocrom 100 at room temperature.

Table 7.2.1 Tabulated Powder Flow Results for Powders on Alocrom 100 Conversion Coatings (1.5-5 minutes immersion times)

Powder distribution or type	Ultimate Coverage (%)	Flow Temperature Range (°C)	
		Start	Stop
Fine	23-26	45-60	100
Standard	27-34	50-60	110-140
Coarse	32-36	55-65	110-120
Recycled	28-31	55-60	115-125
Polydrox	35-39	50	120

The electron photomicrographs of the powders used in the powder flow study are shown in Photo 30 and Photo 31. Photo 30 shows the fine, standard and coarse distributions of the 44S polyester powder. Photo 31 shows the recycled and polydrox powders.

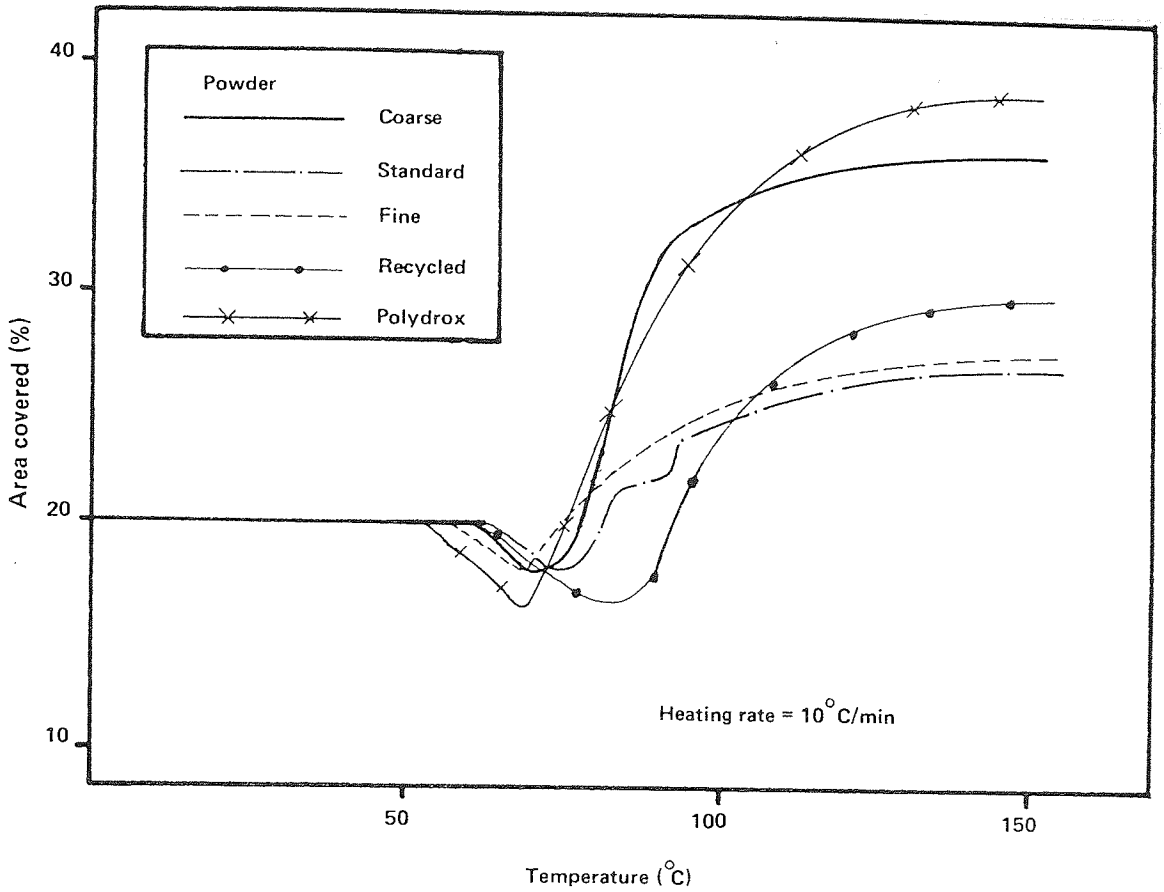

Figure 7.2.1.1 Powder flow curves for various polyester powders on E4S treated in Alocrom 100 for 1.5 minutes at room temperature

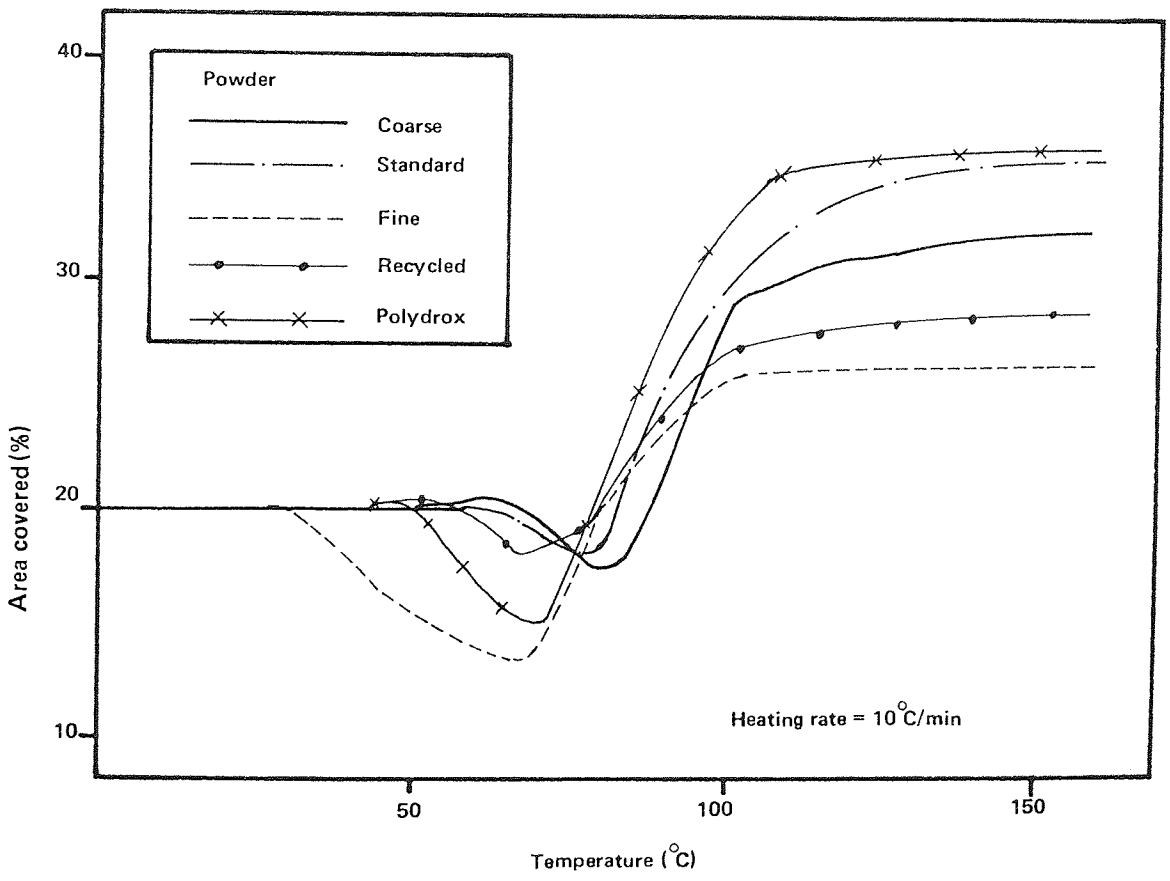

Figure 7.2.1.2 Powder flow curve for various polyester powders on E4S treated in Alocrom 100 for 3 minutes at room temperature

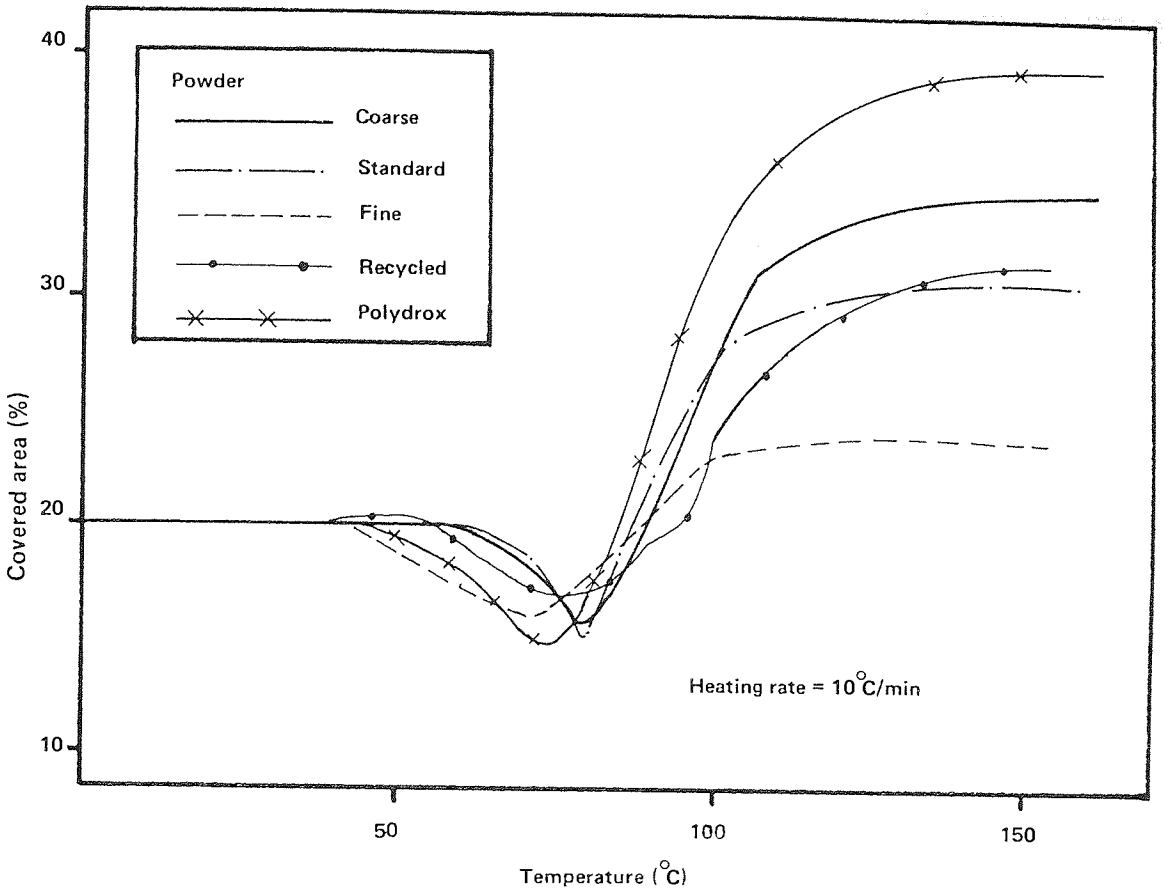

Figure 7.2.1.3 Powder flow curves for various polyester powders on E4S treated in Alocrom 100 for 5 minutes at room temperature

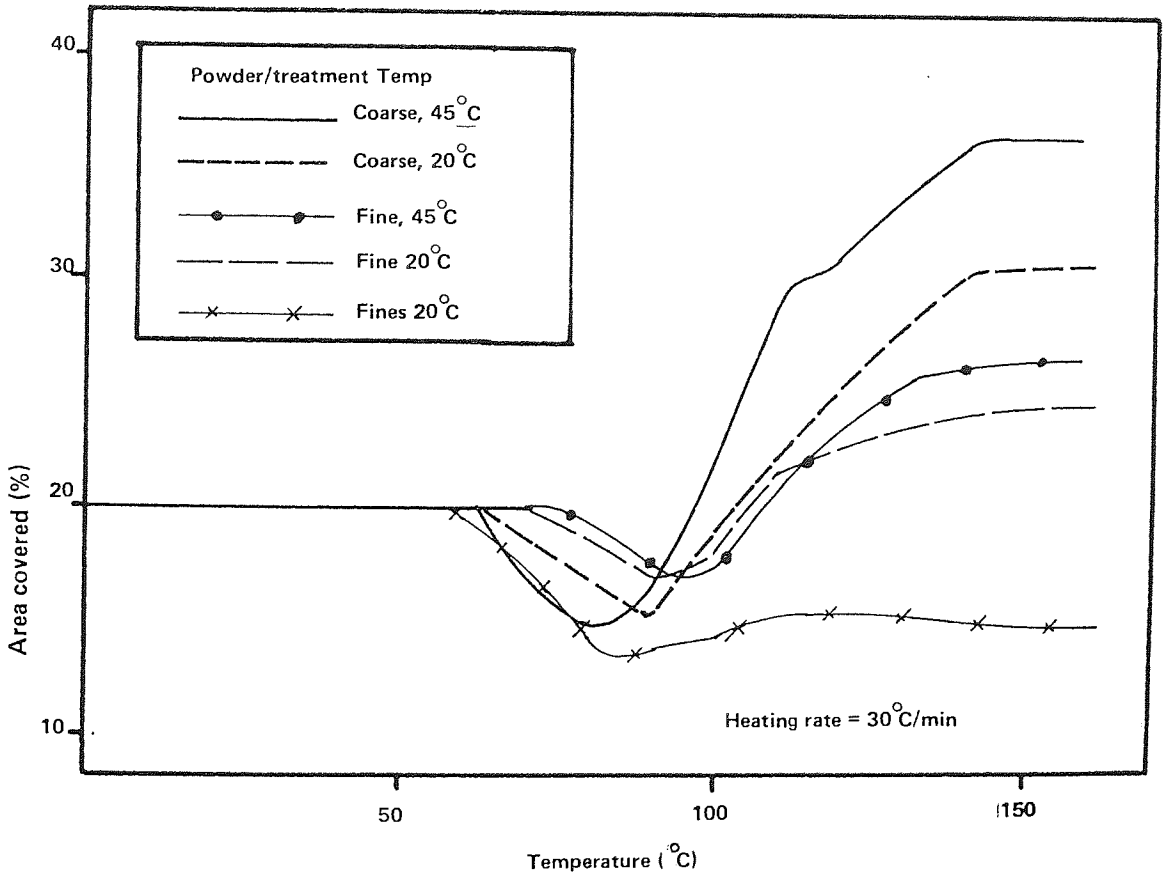

Figure 7.2.1.4 Powder flow curves for various grades of 44S polyester powder on E4S treated in Alocrom 100 at 45 °C and 20C for 90 seconds

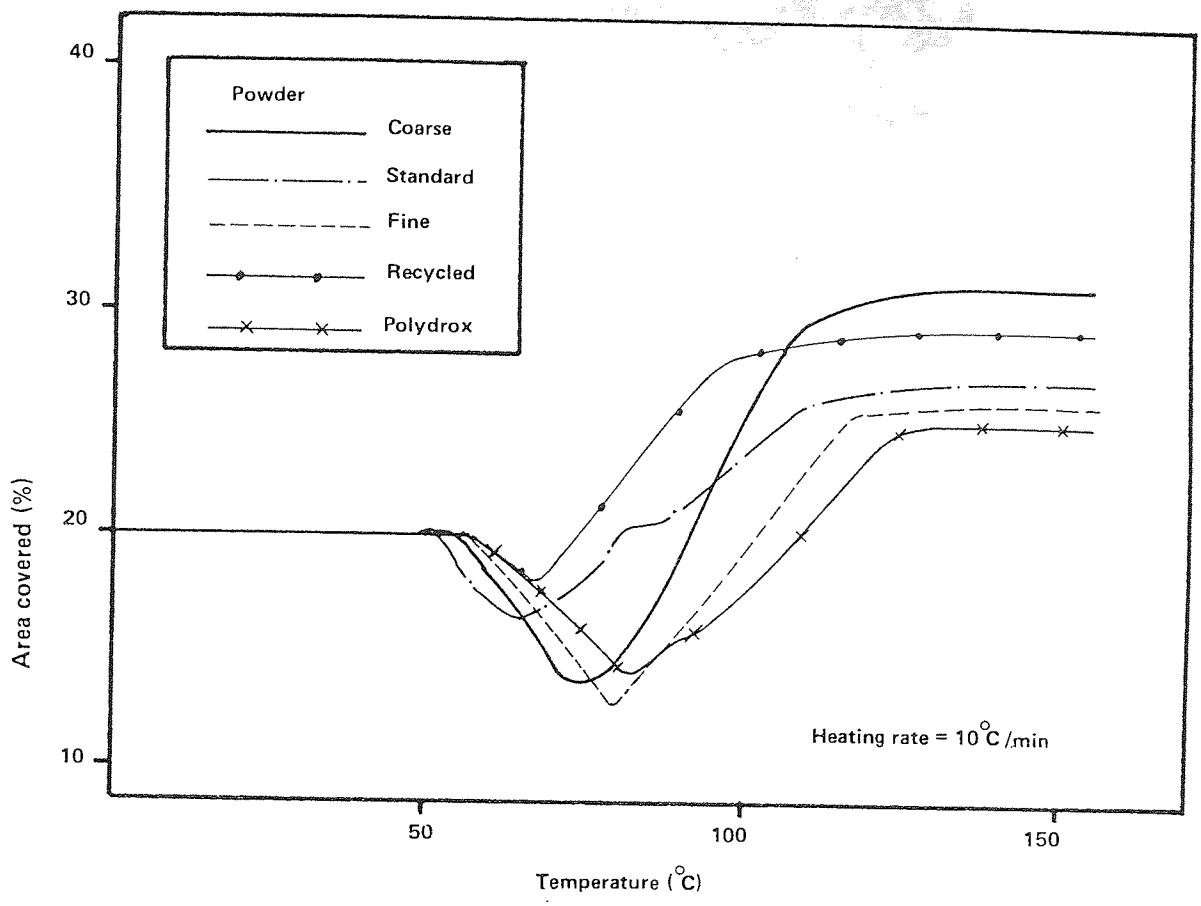

Figure 7.2.1.5 Powder flow curves for various polyester powders on E4S treated in Alocrom 1200 for 5 minutes at room temperature

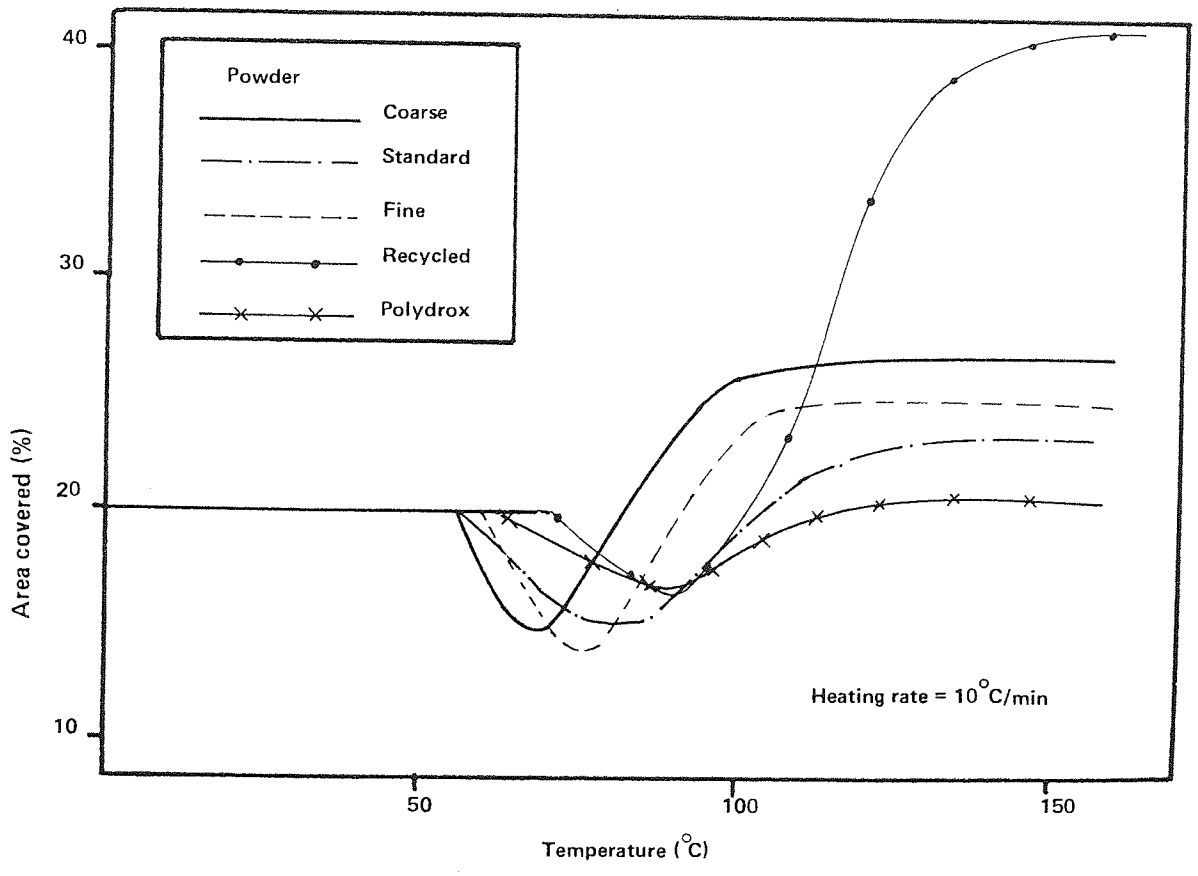

Figure 7.2.1.6 Powder flow curves for various polyester powders on hot dipped galvanised steel treated in Alocrom 100 for 5 minutes

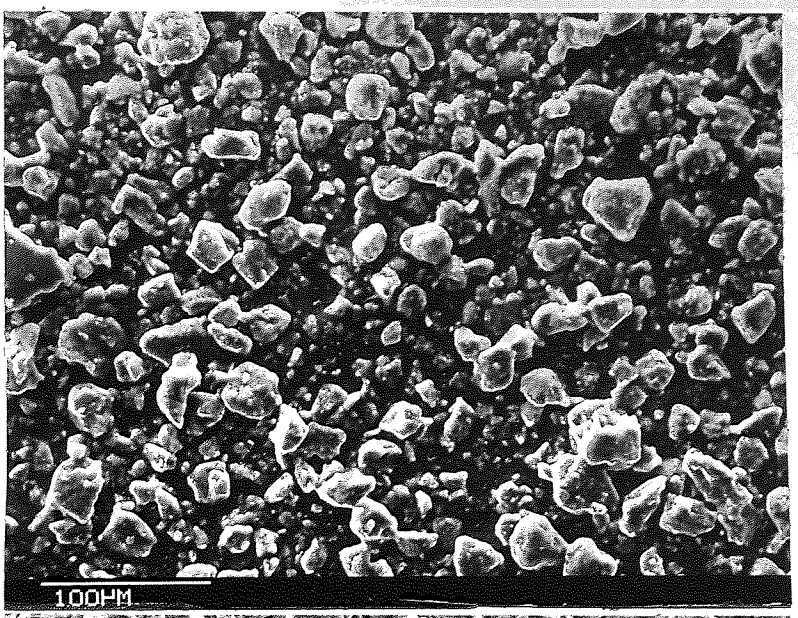

Fine

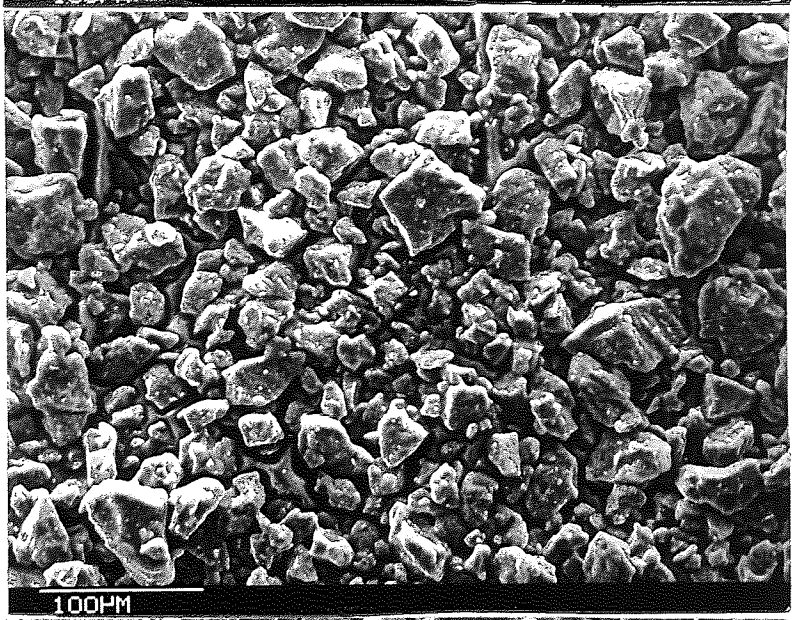

standard

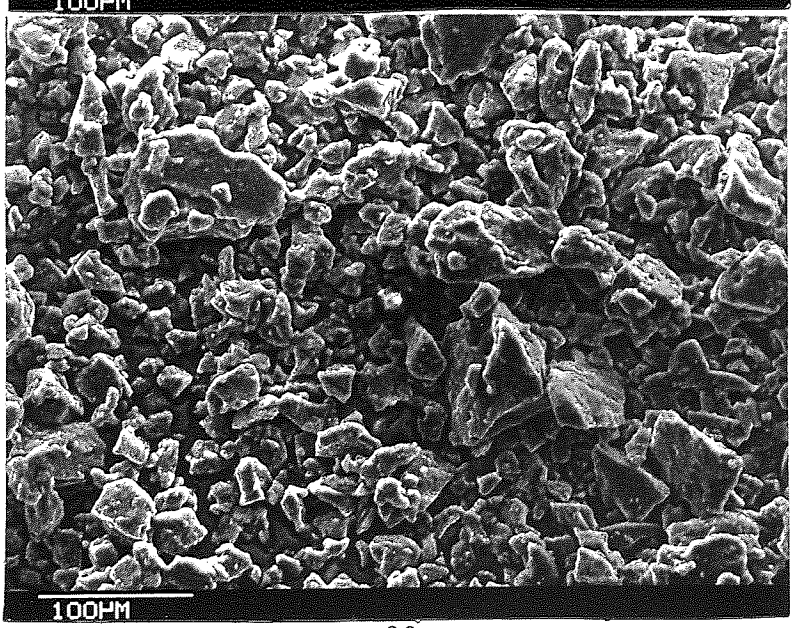

coarse

Photo 30

44S Polyester powder 'as received' in fine, standard and coarse distributions.

(Mag. = x1K Ta = 30°)

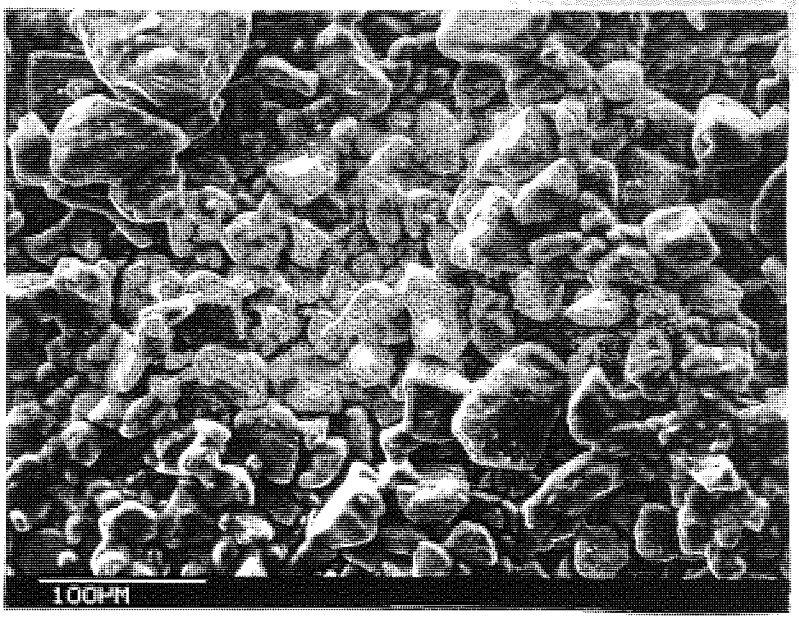

Recycled

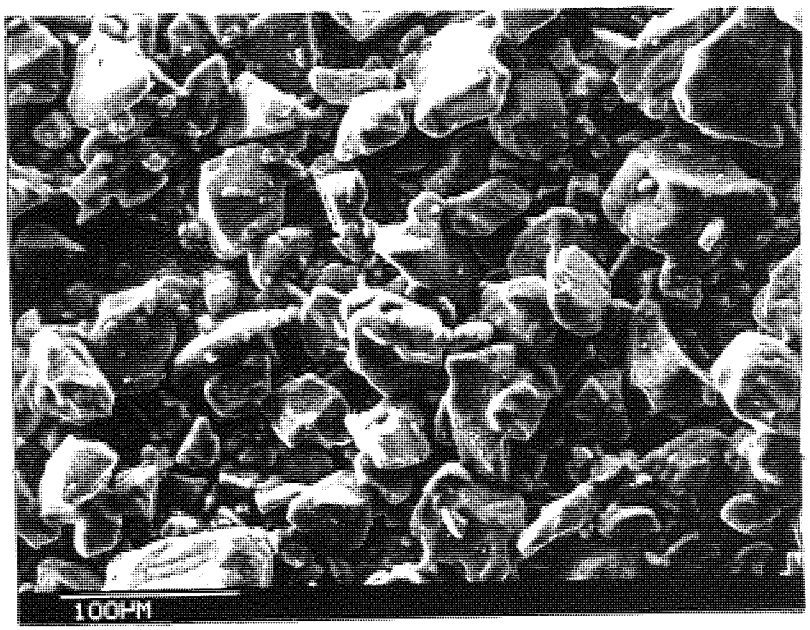

Polydrox

Photo 31

Electron micrographs of recycled 44S polyester powder and 34nF Polydrox powder

(Mag. = x1K Ta = 30°)

7.2.2 Corrosion and weathering tests

The corrosion test results show that polyester powder coatings have very good corrosion resistance when sprayed on panels given short a pretreatment in Alocrom 100. No significant degradation was noted on any panel. Recycled powder coatings were no worse than the fresh powder coatings. The salt-spray test panels survived 800 hours without any blisters or corrosion occurring near the scribed diagonal line. The panels were taken down from the roof and washed after exposure for ten months. No useful information could be gleaned from them. The coatings had not chalked, yellowed, embrittled or blistered.

The results from the extended potential-time determinations showed that all panels tested had a similar behaviour. The powder coating particle distribution (or type) had no appreciable influence on the potential. A measurable potential was not recorded for any of the coatings for up to 24 hours from the start of the test. This was followed by random fluctuations between 0 and -0.7 volts wrt SCE for the following 24 hours. A steady potential of about -0.75 volts wrt SCE was then recorded to the end of the test for all coatings.

It was found that panels with a diagonal line scribed through the coating to the substrate were of no use for the potential-time study. The exposed aluminium masked any changes in potential caused by degradation of the coating.

8. 'LOW BAKE' POLYESTER POWDER STUDY

8.1 Introduction to Experimental Work

The improvement recently claimed by manufacturers of 'low-bake' polyester powder resin was investigated. Powders were manufactured and tested in the Laboratories of Blundell-Permoglaze Ltd, Tysley. Three new 'low-bake' polyester powder resins were chosen. In each case manufacturers claimed full cure took place within ten minutes at 160°C. It is known that pigments and fillers have a direct influence on the behaviour of powder coatings, so a number of these were studied alongside the polyester resins. The effect of the pretreatment given to the aluminium test panels was also studied during this work. A standardised procedure was used to extrude, mill and classify each batch in order to eliminate any variation of coating properties which are known to arise from varying production conditions.

Physical, mechanical, weathering and chemical resistance properties of the cured powder coatings were found for each combination of resin, pigment and filler. In all tests a standard semi-gloss polyester powder was used as a control. British standards were consulted and used where appropriate in all coating tests and examinations, in particular BS 3900 and BS 1391. Finally, the influence of particle size distribution on transfer efficiency (charging efficiency), was studied.

8.1.1 Powder manufacture

Three 'low-bake' polyester resins were made-up with two pigments and two fillers, giving a total of 12 different combinations. Each batch had the same basic formulation; only the resin, filler or pigment differed. The standard formulation used was as follows:-

Resin	1100 g
Pigment	665g
Filler	490g
Tepic	90g
Flow agent PV5	22g
Askawax	17g

An electronic digital gravimetric scale was used throughout and all measurements were to within 0.5 grammes.

A purpose built mixer was used in order to ensure thorough mixing of the ingredients before extrusion. Mixing time was five minutes. Contamination was kept to a practical minimum at this stage by carfully wiping down the blade and cleaning the barrel with the aid of a compressed air line between batches.

The extrusion process is responsible for the balance of properties in the final coating, so it was essential that this critical stage of manufacture be carefully controlled and that extrusion conditions remained constant during production of all powders.

The machine used for this program was a multi-purpose twin screw

extruder. The screws had been specially designed for powder production and consisted of four stages: mixing, melting, chopping and back flow mixing.

The most important factors are cleanliness, % work and temperature. Careful control of these conditions ensure consistent results which effectively eliminate a group of variables which would be difficult to quantify during this program.

Particle size distribution is another important variable in the production of powder paints. Powders must be milled to within specified limits to ensure smooth transportation through application equipment and good flow on curing. A "Pallman" cross flow milling machine was used throughout the program. This allowed milling conditions to be altered, and hence control of particle size distribution. Control was affected in three ways:-
Rotor speed, volume of air-flow, and feed-rate. Volume of air-flow was controlled by various sized disc's situated directly in front of the impeller, thus altering the rate at which the powder travels through the mill.

Finally after having produced a powder with the correct particle size distribution it was sieved to remove any large particles that may have been pulled through the mill. For this purpose a nylon 125 μm mesh sieve was attached to a uni-directional horizontal vibrating frame.

During the final stage of powder production particle size distribution was found using a "Coulter-Counter", a device which measures changes

in resistance as particles suspended in an ultra-pure electrolyte are sucked through an orifice of known size. Accuracy is dependant upon the orifice diameter in relation to the particles, ideally the particles should just pass through; in practice the orifice must be somewhat larger to avoid repeated blocking. For this work, as indeed for most powder coating work, a 150 μm diameter orifice was used. Due to the internal electronics of the device two particles passing though the orifice almost simultaneously could be resolved. Thus once this equipment was calibrated it gave very accurate results. The results are based on samples of powder, so these samples must be carefully selected to be representative of the entire batch.

8.1.2 Production of powder coated test panels

Aluminium panels (E4S) measuring 145 x 75 mm and approximately 0.75 mm thick were used for this study. The bulk of the work was carried out using panels that had been pretreated by immersion in an Alocrom 100 solution for 5 minutes. This was done in a commercial tank which is in continuous use at Metallic Protectives Ltd, Warwick. The remaining panels were treated by immersion in Bonderite 790 for 5 minutes by Pyrene Chemicals Ltd in their development laboratory. Bonderite 790 is a chrome-free pretreatment solution.

The panels were sprayed with an "Areostyle" Manual gun which had been modified by Controsion Ltd to accept a funnel hopper that sits on the top rear part of the barrel and introduces powder to the air-flow by a combination of suction and gravity. When

changing batches only the hopper and barrel needed to be cleaned, which was done with a compressed-air line. High-tension was supplied to the spray gun by a Controsion, Piezo-electric transformer self-regulating field generator module (PET-SRD series 6000). Panels were sprayed in a large earthed extraction booth with automatic self-clean filters. Care was taken to ensure good earthing of the panels, since failure to do so is the main cause for "back-ionisation" and in extreme cases may cause electrical discharge when the panel is picked up. Coatings with a thickness of 75 $\pm$ 5 μm were set as a standard. However, coatings 60-90 μm were used if the variation across a single panel was no more than 10 μm.

Spray panels were cured in a small industrial resistance heated furnace made by Bollard and Sons Ltd of Dudley. This furnace was chosen in preference to smaller laboratory furnaces because temperature stability was better and temperature build-up was quicker (ie when the furnace door was opened for a short time). Panels were placed near the centre of the furnance.

It was known that aluminium alloy panels require 4 minutes in a furnace at 200°C to reach 200°C, therefore all panels were cured for the specified time plus 4 minutes. Resin manufacturers usually quote curing times for substrates at curing temperature. For the purpose of this study this convention will be observed.

8.1.3 Physical and mechanical testing of powder coatings

The physical and mechanical properties of the powder coatings were characterised using a number of destructive tests. Reproducible results

were achieved by strict adherence to the test procedure described in the relavent British Standard, and repetition of tests to ensure consistent results. All tests were callibrated against high performance semi-gloss polyester powder coating (8 PP 044S; Blundell-Permoglaze Ltd).

The following tests and relevant British Standards were used:-

i) Coating thickness (BS 3900: Part C: 1974)
using a 'minitector' eddy-current thickness meter

ii) Gloss (BS 3900: Part E5: 1980)

iii) Scratch resistance (BS 3900: Part E2: 1970)

iv) Impact resistance (BS 3900: Part E7: 1974)

v) Cross-cut adhesion test (BS 3900: Part E6: 1974)

vi) Slow indentation test (BS 3900: Part E4: 1976)
using an 'Erichsen' test rig

vii) Conical bend test (ASTM D522-41)

The bend test described in the British Standard (BS 3900: Part E1: 1970) was not used in this work since tests are conducted using a number of cylindrical mandrels of various diameters (2-32 mm), and so requires a large number of test panels. Owing to the geometry of the conical mandrel (2-40 mm in diameter) coating failure occurs under slightly different conditions. Therefore the two types of bend test should not be compared with each other.

8.1.4 Chemical resistance test

The ability of powder coatings to resist chemical attack cannot be measured directly, therefore the change in hardness after exposure was used to assess chemical resistance.

Coated panels were partially immersed in a chemical solution; the panels arranged so that they were standing upright without touching either the sides of the tank or each other.

The back and edges of all panels were stopped off before immersion to avoid chemical attack on the coating substrate. Immersion was for 48 hours or until the coating blistered. Scratch resistance and gloss measurements were carried out immediately after the panels were rinsed and dried. Measurements were taken from areas which were immersed, and areas immediately above the chemical solution. Some panels were also tested by slow indent (Erichsen) in order to show any changes in ductility after exposure.

The chemical solutions used for this test were:-

i) Di-acetyl alcohol (DAA)

ii) Isopropal alcohol (IPS1)

iii) Potassium hydroxide (35% solution)

iv) Concentrated bleach (household)

v) Nitric acid (50% solution)

Coating resistance to sulphur dioxide was also tested. SO_2 degradation can cause yellowing or blistering of the coating, in some instances this can occur rapidly. The equipment and procedure used for this test is covered by BS 1391. The test was run continuously for 360 hours, and the solution was checked twice daily. Inspection of the exposed panels was carried out in a colour-match cabinet using a set of unexposed panels as a reference. The test panels also had a line scribed diagonally across the panel through to the substrate; this was carefully inspected for any sign of corrosion.

Finally the coatings were tested for permeability resistance. Coated panels were placed on a rack in a pressure cooker containing 500 ml of distilled water, which was set to a pressure of 1 bar (corresponding to a boiling point of 122°C for water). The test was run for periods of 2 hours, excluding warm up time, and stopped when blisters appeared on the test panels.

8.1.5. Weathering resistance tests

The weathering resistance of a powder coating is an important factor, and must be excellent under many different conditions if it is to have any future as a commerical coating. Test sites have ben chosen at Birmingham (severe industrial atmosphere), Warwick (Rural/light industrial), Hull (Coastal/Industrial) and Florida (semi tropical/coastal). The sites were chosen partly due to convenience, but also as seen above, to cover a range of severe conditions and therefore should give a balanced overall result, showing up any particular weakness in the coatings within

a reasonable time.

Accelerated corrosion testing of coated panels was carried out in a salt spray cabinet built to the specifications layed down by BS 3600: Part F4, using a 5% salt solution adjusted to a pH of 3.2 with acetic acid for 1000 hours, or until failure.

Artificial weathering tests were also conducted on panels coated with the various 'low-bake' powders in a weatherometer which conformed to the specification set by BS 3600: part F3 and the MOD specifications in addendum 1 of BS 3600: part F3. The test panels were exposed continuously for 2000 hours before being checked for changes in gloss and colour against a set of unexposed panels.

8.1.6 Change per unit mass measurement

The change per unit mass (Q/M) was found for various powders that had been milled to standard and fine particle distribution sizes. The Q/M ratio is easily obtained using a Faraday cup and grid arrangement shown in Figure 8.1.6. After the gun had been purged with the powder under test it was sprayed into the clean cup for 2 seconds. The charge held by the powder was read from a suitable meter and the weight of the powder was found gravimetrically, so the ratio for Q/M could be calculated. The equipment used for this work was supplied by the 'Wolfon Electrostatic Unit' at Southampton University and gave an extremely accurate measurement of Q/M.

The average surface area for a unit volume of powder particles

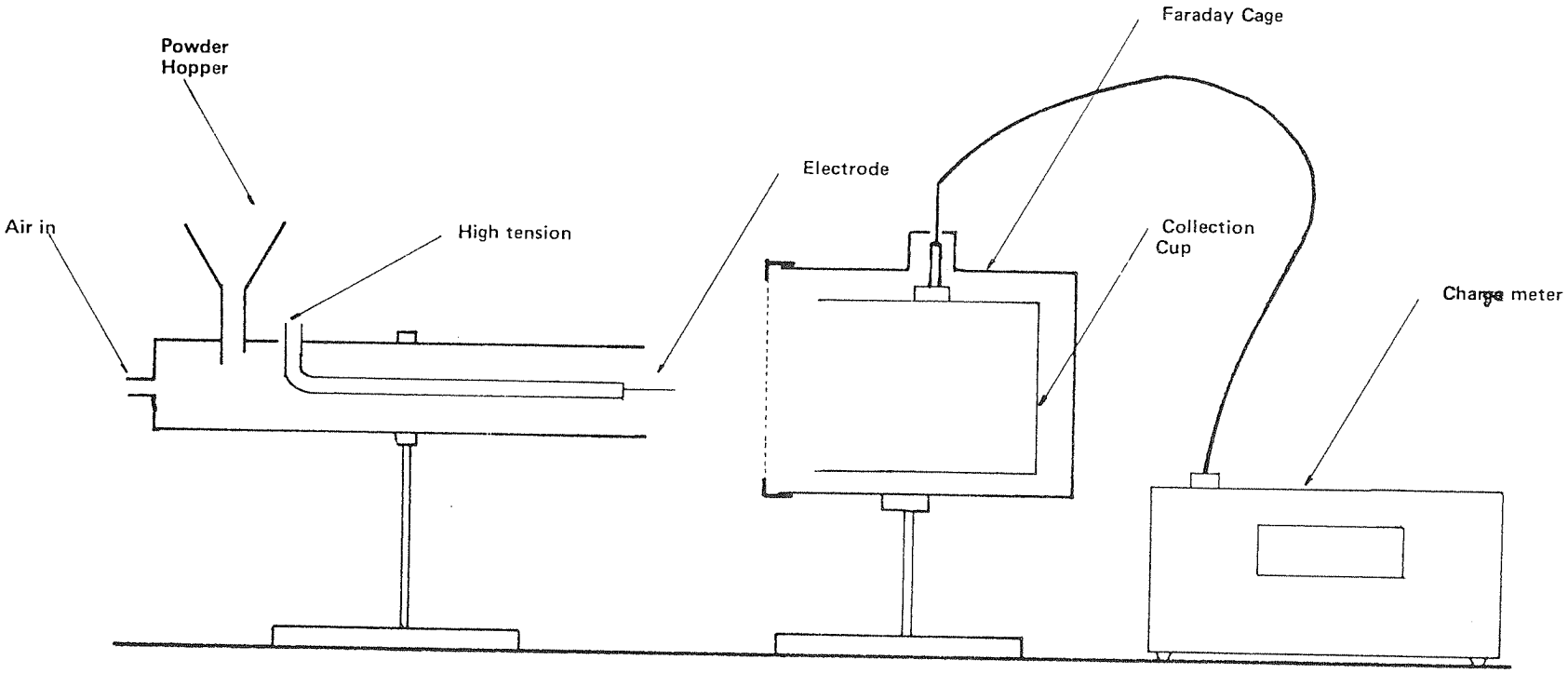

Figure 8.1.6 Diagram showing equipment used for Q/M Measurements

was calculated from Coulter-Counter analysis results for each powder and particle size distriubtion. The ratio of charge to surface area could then be found.

8.2 'Results

Table 8.2 shows the type of resin, pigment and filler in each batch, the most important classifications are batches 1-4 containing resin A, 5-8 resin B, and 9-12 resin C.

TABLE 8.2 Batch Identification

	Resin A		Resin B		Resin C	
	Pigment 1	Pigment 2	Pigment 1	Pigment 2	Pigment 1	Pigment 2
Filler X	1	2	5	6	9	10
Filler Y	3	4	7	9	11	12

Milling and sieving produced powder with a slightly wider particle size distribution than would be expected from full-size production machinery. Typical coulter-counter results for normal and fine distributions are shown in Figures 8.2.1-2 respectively. The fine distribution powder was used for Q/M experiments only.

8.2.1 Physical and mechanical testing of powder coatings

Gloss measurements were found to vary slightly across some panels. Tables 8.2.1-2 show the average and range of gloss values recorded over a number of panels per batch. A visual assessment for flow was also noted.

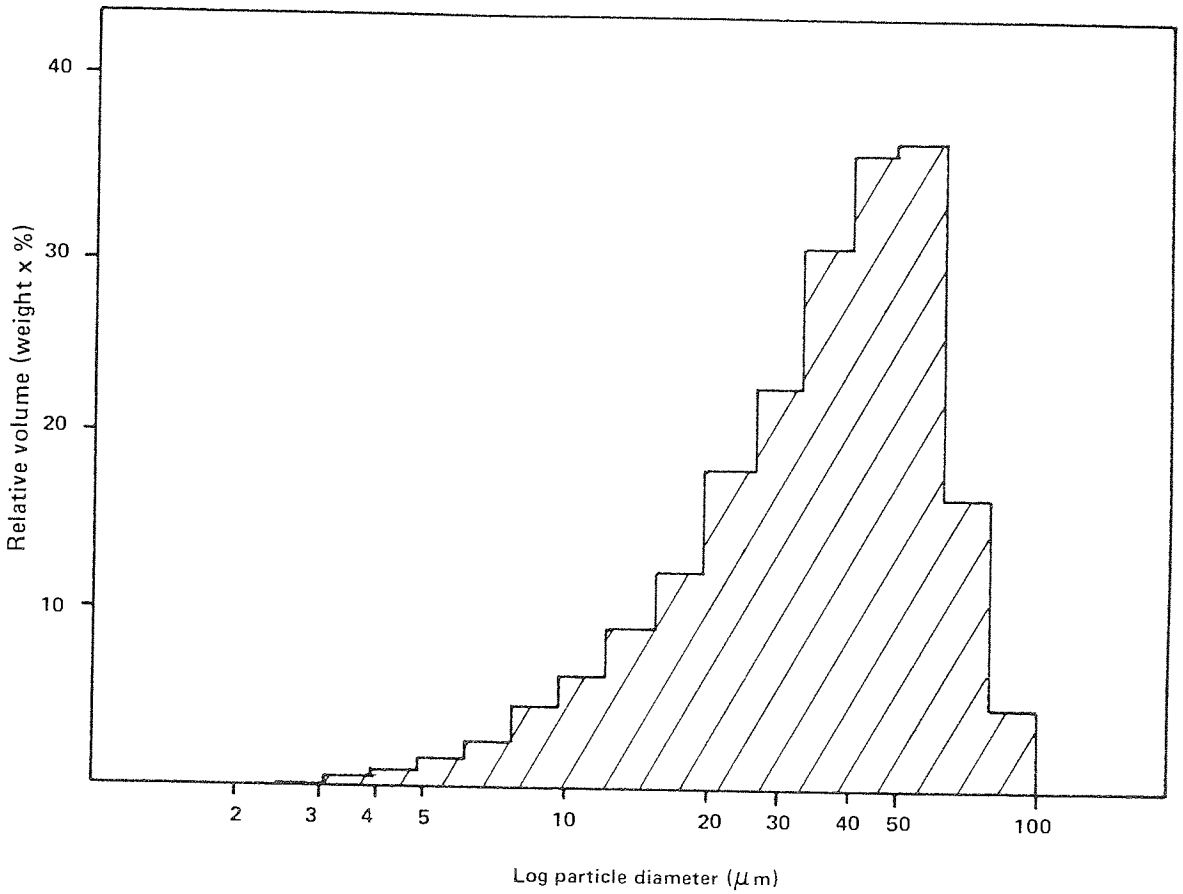

Figure 8.2.1 Particle size distribution for batch 1, standard grind

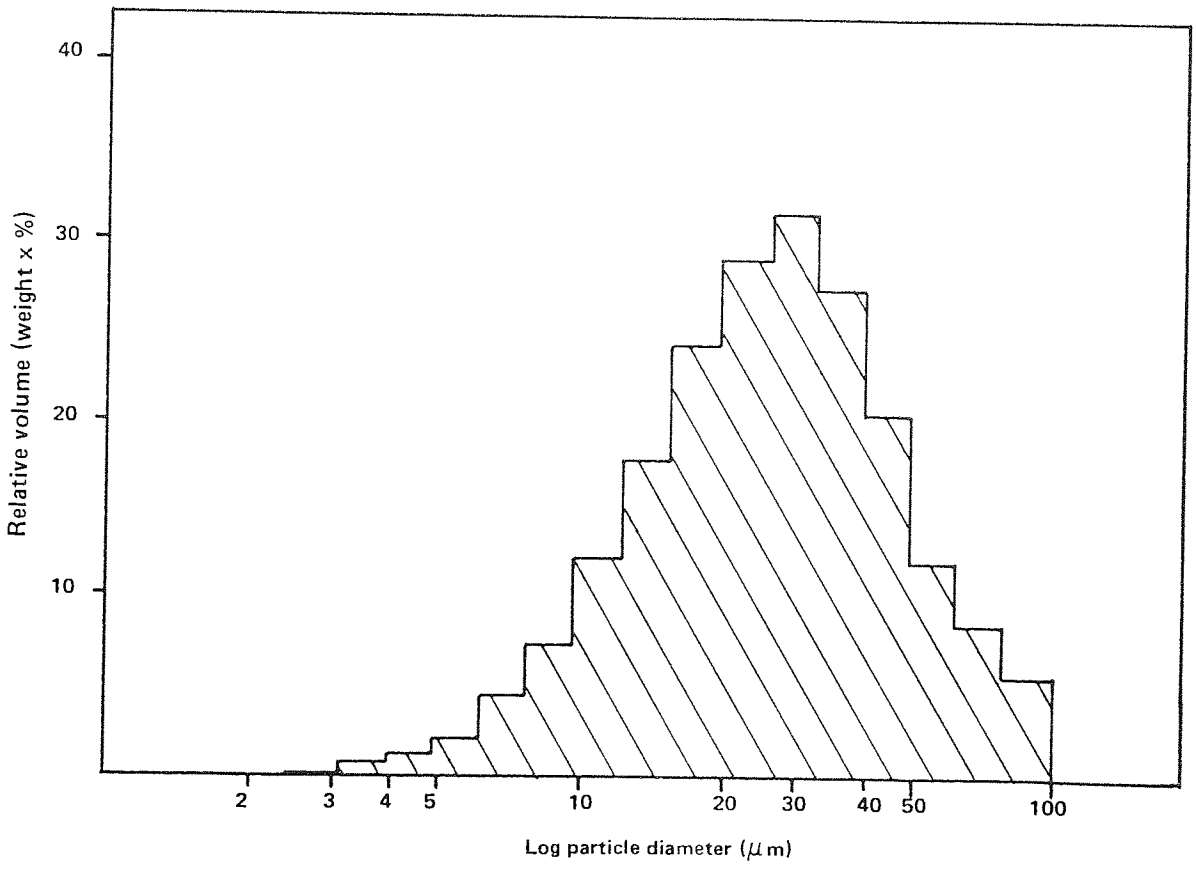

Figure 8.2.2 Particle size distribution for batch 1, fine grind

Table 8.2.1.1 Specular Gloss (60°) and Paint Flow for Various Powders on Pretreated Aluminium Panels Cured at 160°C for 10 Minutes

Pretreatment	Batch No	Gloss			FLOW (Visual Assessment)
		Average (%)	Maximum (%)	Minimum (%)	
Alocrom 100	STANDARD	70	70	70	Excellent
	1	57	69	54	Very good
	2	62	72	48	Very good
	3	65	67	64	Good
	4	66	67	65	Good
	5	34	40	28	Very poor
	9	75	77	73	Good
	10	74	77	69	Good
	11	67	64	69	Good
	12	68	69	66	Good
Bonderite 790	1	48	50	45	Very good
	2	50	63	47	Very good
	9	76	77	75	Good
	12	68	69	67	Good
	STANDARD	70	71	69	Excellent

Table 8.2.1.2 Specular Gloss (60°) and Paint Flow for Various Powders on Pretreated Aluminium Panels Cured at 170°C for 10 Minutes.

Pretreatment	Batch No	Gloss Average (%)	Gloss Maximum (%)	Gloss Minimum (%)	FLOW (Visual Assessment)
Alocrom 100	STANDARD	70	70	70	Excellent
	1	57	65	52	Very good
	2	62	66	57	Very good
	3	45	50	42	Good
	4	64	66	63	Good
	5	35	48	30	Very poor
	9	73	74	72	Good
	10	74	75	72	Good
	11	66	68	64	Good
	12	67	68	65	Good
Bonderite 790	1	71	74	67	Very good
	2	71	72	70	Very good
	9	73	74	71	Good
	12	63	63	62	Good
	STANDARD	70	71	69	Excellent

The first round of scratch resistance tests were carried out as "GO/NO GO" type tests using 4kg as the load on the needle. The loads required to penetrate the coatings were found after this was seen to be insufficient for this work. All results are within 200 grammes to failure.

Table 8.2.1.3 Scratch Resistance Against Pretreatment and Cure Temperature of Various Powders

Pretreatment	Cure Temperature Temperature (°C)	Batch	Scratch resistance (kg)
Alocrom 100	200	Standard	7.6
	160	1	passed at 4 kg
		2	passed at 4 kg
		3	passed at 4 kg
		4	passed at 4 kg
		5	passed at 4 kg
		9	5.0
		10	5.3
		11	5.3
		12	5.6
	170	1	6.8
		2	5.0
		3	9.3
		4	7.2
		5	8.3
		9	5.7
		10	5.0
		11	6.0
		12	8.0
	200	Standard	6.5
Bonderite 790	160	1	4.5
		2	4.0
		9	4.4
		12	4.7
	170	1	5.5
		2	4.4
		9	4.7
		12	4.8

The test rig used for impact resistance had a maximum impact of 1.06 Kg.m. All tested panels were carefully examined by eye; any sign of cracking constituted a failure. Table 8.2.1.4 shows the results for coatings given direct impact. Table 8.2.1.5 shows the rsults for coatings given reverse impact, ie impact from the back of the panel.

Table 8.2.1.4 Direct Impact Resistance Results for Temperature of Cure, Pretreatment and Batch.

Pretreatment	Cure Temperature (°C)	Batch	Impact (kg.m)
Alocrom 100	200	Standard	1.060*
	160	1	0.277
		2	0.922
		3	1.060*
		4	1.060*
		5	1.060*
		9	0.392
		10	0.115
		11	0.115
		12	0.300
	170	1	1.060*
		2	1.060*
		3	1.060*
		4	1.060*
		5	1.060*
		9	1.060*
		10	1.060*
		11	1.060*
		12	1.060*
	180	2	1.060*
		3	1.060*
Bonderite 790	200	Standard	1.060*
	160	1	1.060*
		2	1.060*
		9	0.277
		12	0.691
	170	1	1.060*
		2	1.060*
		9	1.060*
		12	1.060*

Note: 1.060* = did not fail at maximum impact

Table 8.2.1.5 Reverse Impact Resistance Results for Temperature of Cure, Pretreatment and Batch.

Pretreatment	Cure Temperature (°C)	Batch	Impact (kg.m)
Alocrom 100	200	Standard	1.060*
	160	1	0.115
		2	0.576
		3	0.277
		4	0.345
		5	-
		9	-
		10	-
		11	-
		12	-
	170	1	1.060
		2	1.060*
		3	0.737
		4	0.277
		5	0.783
		9	0.507
		10	-
		11	0.046
		12	0.461
	180	2	0.922
		3	0.691
Bonderite 790	200	Standard	0.230
	160	1	0.323
		2	1.014
		9	-
		12	0.092
	170	1	0.691
		2	1.060*
		9	0.369
		12	0.507

Note: 1.060* = did not fail at maximum impact

The cross hatch adhesion test was not expected to provide any positive information for this study, it was used to check that all panels used had been correctly pretreated. Adhesion failure would point to contaminated panel surfaces rather than poor coatings. Every panel used in this study was given a 1 mm cross hatch adhesion test: all passed.

Table 8.2.1.6 shows the results obtained by slow indentation. A low result gives good indication of a brittle failure, whereas a result higher than 8.0 mm is probably due to a substrate failure rather than the coating becoming cracked. All results shown are the point at which cracking was first noted.

Tabee 8.2.1.6 Slow-Indentation Results

Pretreatment	Cure Temperature (°C)	Batch	Indentation (mm)
Alocrom 100	200	Standard 44S	8.1
	160	1	4.1
		2	6.0
		3	4.3
		4	5.5
		5	7.5
		9	2.7
		10	1.4
		11	1.8
		12	3.5
	170	1	7.5
		2	7.7
		3	6.4
		4	6.3
		5	7.5
		9	8.2
		10	8.3
		11	5.8
		12	6.3
	180	2	8.2
		3	7.2
Bonderite 790	200	Standard 44S	6.9
	160	1	6.7
		2	6.3
		9	5.7
		12	5.1
	170	1	6.1
		2	6.1
		9	6.1
		12	6.1

The majority of panels passed the conical bend test at 2 mm diameter, the smallest diameter available on the mandrel. Table 8.2.1.7 gives the results of those panels which failed. The measurement from the 2 mm diameter end of the mandrel to the uncracked region of the panel was noted which can be taken as an indication of the extent of failure.

TABLE 8.2.1.7 Conical Bend Test Failures Showing Length of Cracks from the 2 mm Diameter End of the Mandrel

Pretreatment	Cure Temperature °C	Batch No.	Length of cracks from 2 mm dia. end (mm)
Alocrom 100	160	9	102
		10	76
		11	76
		12	51
	170	10	6
		11	6
Bonderite 790	160	9	127
		12	51

8.2.2 Chemical resistance tests

Chemical resistance was determined after immersion in various chemicals for 48 hours by gloss, scratch resistance and slow indentation. Only half of a panel was immersed so a comparison can be made between submerged areas and areas subjected to the chemical fumes. Coating thickness may have some bearing on these tests therefore these are shown. All panels tested were pretreated in Alocrom 100 and cured at 160°C.

Table 8.2.2.1 Gloss Determination after Exposure To Di-Acetyl Alcohol for 48 hours

Batch	Gloss (%)			Thickness (μm)
	Before	Top	Bottom	
Standard 44S	70	60	37	70
1	57	-	15	85
2	62	-	25	90
3	65	-	15	110
4	66	-	17	55
5	34	-	15	60
9	74	60	40	90
10	75	55	16	120
11	66	57	12	85
12	68	50	19	85

Table 8.2.2.2 Gloss Determination after Exposure to Isopropyl Alcohol for 48 hours

Batch	Gloss(%)			Thickness (μm)
	Before	Top	Bottom	
Standard 44S	70	61	66	60
1	57	-	53	40
2	62	-	56	100
3	65	-	51	110
4	66	-	52	50
5	34	-	21	60
9	74	60	61	80
10	75	60	61	100
11	66	66	42	80
12	68	66	48	85

Table 8.2.2.3 Gloss Determination after Exposure to Bleach for 48 hours

Batch	Gloss (%)			Thickness (μm)
	Before	Top	Bottom	
Standard 44S	70	70	67	70
1	57	-	67	45
2	62	-	70	85
3	65	-	46	140
4	66	-	70	55
5	34	-	29	100
9	74	76	74	100
10	75	74	74	90
11	66	68	66	85
12	68	67	65	85

Table 8.2.2.4 Gloss Determination after Exposure to Potassium Hydroxide (35%) for 48 hours

Batch	Gloss (%)			Thickness (μm)
	Before	Top	Bottom	
Standard 44S	70	68	53	85
1	57	-	-	40
2	62	-	-	85
3	65	-	-	110
4	66	-	-	53
5	34	-	-	100
9	74	72	67	90
10	75	75	69	70
11	66	71	62	80
12	68	67	61	80

Table 8.2.2.5 Gloss Determination after Exposure to 50% Nitric Acid for 48 hours

Batch	Gloss (%)			Thickness (μm)
	Before	Top	Bottom	
Standard 44S	70	17	-	70
1	57	Detached after 26 hrs		65
2	62	" " 42 hrs		100
3	65	" " 42 hrs		110
4	66	" " 26 hrs		50
5	34	" " 42 hrs		60
9	74	19	-	90
10	75	16	-	120
11	66	11	-	110
12	68	9	-	90

Table 8.2.2.6 Scratch Resistance after Exposure to Di Acetyl Alcohol for 48 hours

Batch	Scratch Resistance (kg)			Thickness (μm)
	Before	Top	Bottom	
Standard 44S	7.6	4.6	0.5	70
1	-	3.9	0.4	85
2	-	4.4	0.3	90
3	-	4.7	0.5	110
4	-	4.6	0.2	55
5	-	3.9	0.6	60
9	5.0	5.1	0	90
10	5.3	5.2	0	120
11	5.3	5.0	0	85
12	5.6	4.4	0.5	85

Table 8.2.2.7 Scratch Resistance after Exposure to Isopropyl Alcohol for 48 hours

Batch	Scratch Resistance (kg)			Thickness (μm)
	Before	Top	Bottom	
Standard 44S	7.6	5.5	5.4	80
1	-	1.9	5.0	40
2	-	3.6	5.6	100
3	-	3.4	5.3	110
4	-	3.8	4.8	50
5	-	4.8	5.0	60
9	5.0	5.0	5.0	80
10	5.3	4.4	5.3	100
11	5.3	5.2	5.2	80
12	5.6	4.6	5.2	85

Table 8.2.2.8 Scratch Resistance after Exposure to Bleach for 48 hours

Batch	Scratch Resistance (kg)			Thickness (μm)
	Before	Top	Bottom	
Standard 44S	7.6	5.4	5.0	70
1	-	4.2	4.2	45
2	-	5.9	5.7	85
3	-	5.6	5.3	140
4	-	5.6	5.6	55
5	-	6.1	5.3	100
9	5.0	5.4	4.7	100
10	5.3	5.7	5.4	90
11	5.3	4.5	3.7	85
12	5.6	4.4	4.3	85

Table 8.2.29 Scratch Resistance after Exposure to (35%) Potassium Hydroxide for 48 hours

Batch	Scracth Resistance (kg)			Thickness (μm)
	Before	Top	Bottom	
Standard 44S	7.6	6.7	6.2	70
1	-	5.3	5.3	40
2	-	6.3	6.5	85
3	-	6.1	6.0	110
4	-	5.5	4.3	55
5	-	6.7	6.2	100
9	5.0	4.6	4.9	90
10	5.3	3.8	4.3	70
11	5.3	4.7	3.8	80
12	5.6	4.7	4.7	80

Table 8.2.2.10 Scratch Resistance after Exposure to 50% Nitric Acid for up to 48 hours

Batch	Scratch Resistance (kg)			Thickness (μm)
	Before	Top	Bottom	
Standard 44S	7.6	6.5	0.5	70
1	-	Detached after 26 hours		65
2	-	" "	42 hours	100
3	-	" "	42 hours	110
4	-	" "	26 hours	50
5	-	" "	42 hours	60
9	5.0	6.5	-	90
10	5.3	6.0	1.2	125
11	5.3	6.0	0.9	110
12	5.6	4.0	-	90

Table 8.2.2.11 Slow Indentation Results for Resin C Powders after Exposure to Various Chemicals for 48 hours

Chemcial	Batch	Indent (mm)			Thickness (μm)
		Before	Top	Bottom	
DAA	Standard	8.1	8.3	8.2	70
	9	2.7	2.0	8.2	90
	10	1.4	0.6	8.1	120
	11	1.8	1.6	7.7	85
	12	3.5	2.0	8.2	85
1PS1	Standard	8.1	6.9	4.0	80
	9	2.7	1.2	4.6	80
	10	1.4	0.7	5.3	100
	11	1.8	1.9	6.8	80
	12	3.5	1.4	6.8	85
Bleach	Standard	8.1	8.0	7.7	85
	9	2.7	1.0	1.0	90
	10	1.4	0.6	0.6	100
	11	1.8	1.1	1.0	90
	12	3.5	1.2	0.9	85
KOH (35%)	Standard	8.1	5.8	5.0	85
	9	2.7	1.1	0.9	90
	10	1.4	0.5	0.5	70
	11	1.8	1.4	1.1	80
	12	3.5	1.1	1.2	80
Nitric (50%)	Standard	8.1	7.8	-	80
	9	2.7	1.5	-	90
	10	1.4	2.8	8.5	125
	11	1.8	7.1	7.5	110
	12	3.5	6.1	-	90

All panels given the sulphur dioxide resistance test were pretreated in Alocrom 100 and cured at 160°C for 10 minutes. This type of SO_2 test is not very corrosive and si it is mainly a coating surface test. No panels showed any sign of corrosion along the scored diagonal line. The change in colour was inspected under various controlled light conditions and all panels passed except mix 3 which was found to have severely yellowed by the end of 360 hours under test.

Table 8.2.2.12 shows the time to failure during the permeability test for batches 1,2, and 9 cured at 160°C and 170°C. All panels were given pretreatment in Alocrom 100 prior to powder coating. Batches 1,2 and 9 were chosen for this test as they had the best overall properties at this point.

Table 8.2.2.12 Permeability Results

Batch	Curing Temperature	Time to failure
Standard 44S	200	18-45+
1 2 9	160	18-30 30 30
1 2 9	170	30 38 30

8.2.3 Weathering resistance tests

Outdoor exposure panels at Warwick, Birmingham, Hull and Florida have not shown any sign of degradation in the first 12 months of exposure. Research staff at Blundell-Permoglaze will continue to monitor the progress of these panels in the future.

Salt spray corrosion results showed that the pyrene chromium-free pretreatment Bonderite 790 did not give adequate corrosion resistance to the coating system. No panel pretreated in this solution could withstand more than 700 hours exposure. The panels pretreated in Alocrom 100 were exposed for 1100 hours and were found to have survived much better. The order of superiority for panels pretreated in Alocrom 100 was:

1) (The best) Batch 9 cured at 170°C
2) Batch 1 cured at 170°C
3) Standard 44S
4) Batch 9 cured at 160°C
5) Batch 1 cured at 160°C
6) Batch 2 cured at 160°C
7) Batch 2 cured at 170°C

No panel had completely failed. The worst panel had blistered up to 17mm from the edge of the diagonal score line.

The order of superiority for panels pretreated in Bonderite 790 was:-

1) (the best) Batch 12 cured at 170°C
2) Standard 44S
3) Batch 1 cured at 160°C
4) Batch 9 cured at 170°C
5) Batch 1 cured at 170°C
6) Batch 12 cured at 160°C
7) Batch 2 cured at 170°C

This test was stopped after 651 hours; the last two panels failed completely at this stage.

The panels that had been exposed in the weatherometer at Hull (Blundell-Permoglaze) for 200 hours were all pretreated with Alocrom 100. It was found that panels cured at 160°C had yellowed and lost some gloss (compared by eye only). However all of the panels cured at 170°C were found to have better yellowing and chalking resistance than the standard polyester. No coatings showed any sign of blistering or corrosive failure.

8.2.4 Charge per unit mass measurement

This work was carried out over several days at metallic Protectives Ltd, Warwick. It appeared that despite carefully controlled conditions, slight atmospheric changes lead to widely differing results. The cause of this occurrence could not be pin-pointed. The results presented in this report were all taken on the same day and are therefore assumed to be consistent. Control runs carried out at intervals during the day support this assumption.

Table 8.2.4.1 shows the mass of collected powder, the charge carried by the powder, and the Q/M ratios.

The surface area of a unit volume of particles was calculated for each batch and grind, assuming that

i) particles were spherical

ii) particles had a packing density of 1

iii) particles were collected in the Faraday cage with the same size distribution as found by Coulter Counter analysis.

Table 8.2.4.2 shows the Coulter counter analysis results used for each calculation. The equation used was as follows:-

$$\text{S.a.} = \frac{V}{\Sigma\, 4/3\,\pi\, r^3 N} \times \Sigma 4\pi r^2 N$$

where

r = average particle radius for each size distribution interval

N = proportion of particles in each size distribution interval

V = unit volume

The results for this calculation are shown in Table 8.2.4.3 together with a ratio for the charge carried per unit area in Coulumbs found by dividing the Q/M ratio by the surface area per unit volume for each powder and grind.

Table 8.2.4.1 Showing Q/M Ratios for Batch Numbers 1,2 and 9, with Standard and Fine Grinds

Powder	Grind	Charge (Q) ($C \times 10^{-7}$)	Mass (mg)	Q/M ($C/Kg \times 10^{-4}$)
44S	Standard	0.59	0.117	5.02
	Fine	0.31	0.016	19.57
1	Standard	0.58	0.096	6.09
	Fine	0.46	0.071	6.47
2	Standard	0.75	0.128	5.82
	Fine	0.46	0.062	7.35
9	Standard	0.64	0.128	4.96
	Fine	0.44	0.050	8.75

Table 8.2.4.2 Percentage Distributions for Powders 1,2 and 9, with Fine and Standard Grinds

Average Particle Diameter (μm)	44S	Mix 1		Mix 2		Mix 3	
	Fine	Standard	Fine	Standard	Fine	Standard	Fine
2.7	0	0.1	0.0	0.0	0.0	0.0	0.0
3.5	3.4	0.1	0.2	0.1	0.0	0.1	0.3
4.4	9.4	0.2	0.5	0.1	0.2	0.3	1.0
5.5	7.4	0.6	1.0	0.7	0.7	0.8	1.2
7.0	26.3	1.2	1.6	1.4	1.8	1.2	3.0
9.0	23.9	2.2	3.2	2.2	3.7	1.8	4.0
11.0	9.4	3.3	5.6	3.9	6.5	2.8	6.5
14.0	2.4	4.5	8.5	5.3	10.6	4.1	10.0
18.0	0.9	6.3	12.0	7.4	15.3	0.0	13.2
22.5	0.5	8.5	14.0	10.0	18.0	7.8	16.5
27.5	1.6	11.0	15.7	13.3	18.6	10.9	17.3
35.0	0.5	15.0	13.5	16.2	13.5	16.3	12.0
45.0	2.4	17.8	10.0	19.6	6.2	21.8	8.0
57.0	0.2	17.8	6.7	14.1	3.5	17.5	3.0
70.0	4.2	8.2	5.0	4.0	1.4	6.5	0.0
90.0	0.3	2.2	2.5	2.0	0.0	2.3	4.0

Table 8.2.4.3 Surface Area per unit Volume and Charge Carried per unit Surface Area

Powder	Grind	Surface area per mm^3 volume (mm^2)	Charge carried per m^2 surface area (C)
44S	Fine	107.8	18.2
1	Fine	112.8	5.7
	Standard	108.0	5.7
2	Fine	157.8	4.7
	Standard	114.9	5.1
9	Fine	113.8	7.7
	Standard	110.0	4.5

9. DISCUSSION OF RESULTS

9.1 Introduction

Modern architectural design often depends upon the excellent durability of powder coated aluminium extrusions for many types of outdoor cladding systems. The improved performance of polyester powder coatings has been achieved through better quality control, by using newly formulated resins and crosslinking agents, and by developing highly durable colour fast pigments. However the corrosion resistance of the system also depends on the pretreatment given to the aluminium, and formulations for aluminium pretreatments have hardly changed since the 1940's.

For environmental reasons the use of hexavalent chromium is becoming heavily penalised. Effluent levels are being reduced and strictly monitored and therefore control is more expensive. Chromium-free pretreatments have been developed, but do not meet the high standards set by chromate or mixed chromate-phosphate pretreatments. Progress has been slow due to the complexity of, and difficulty in studying the mechanisms of film-growth and paint bonding of chromate conversion coatings, and developments have been ad hoc.

This discussion is centred on the film forming and paint bonding mechanisms of chromate-phosphate pretreatments. However, work has also been carried out on powder paint coatings including the study of particle flow and the development of a 'low-bake' polyester powder coating. The discussion incorporates this work and relates the topics and their influence upon each other as

shown in Figure 9.1. The discussion covers the topics shown diagrammatically in Figure 9.1 proceeding in an anti-clockwise direction and starting at the top right hand corner. Figure 9.1 is useful in showing the interrelation between the many factors influencing the powder painting of aluminium.

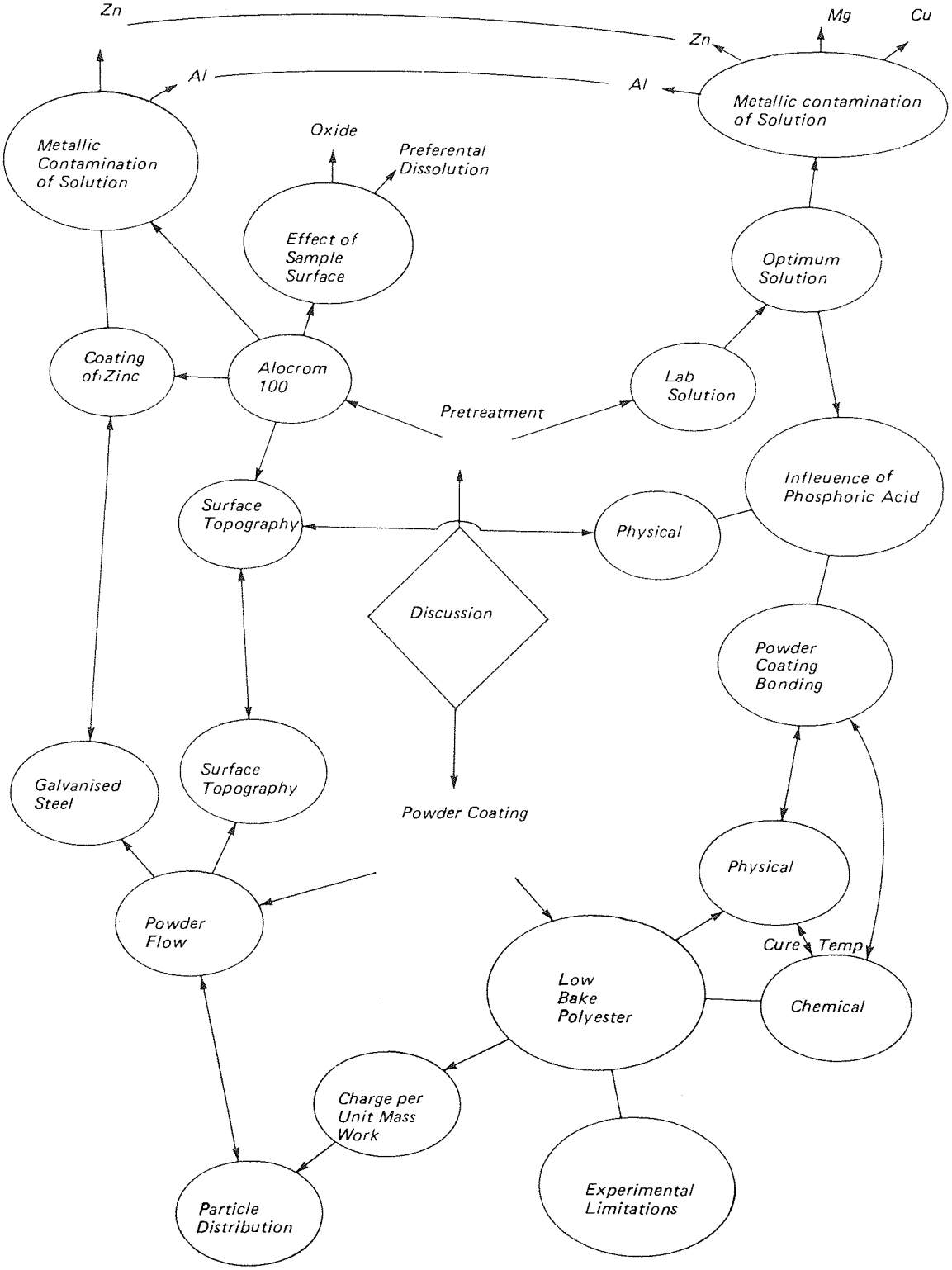

Figure 9.1 *Diagram showing the interrelation of the factors influencing the powder painting of Aluminium.*

9.2 Mechanism of Coating Growth and Adhesion to Organic Coatings

The mechanism of nucleation and growth of conversion coatings has been studied many times[79,94,95,96,97,106]. However, the mechanism of coating formation has not been explained in sufficient detail. Conversion coatings produced by immersion in chromate solutions have been described as amorphous films[79] or as insoluble gels[101,106] with the major component being either hydrated chromium hydroxide or hydrated chromium phosphate depending upon the chromate solution used[97]. Since the introduction of modern electron spectrographic techniques for surface analysis much time has been spent on coating analysis[97,101,103,106] and the detection of any residual hexavalant chromium in the coating[98,99,100,101]. Much of the information gleaned has been useful, such as the role of the fluoride ion in forming the coating. However, many results have been misleading which has added to the confusion concerning not only the mechanisms of film formation, but also the mechanisms of corrosion resistance and of bonding to organic coatings.

Much of the published work was carried out using a proprietary solution, the formulation of which was not known. The original patent by Spruance[93] was therefore studied and an 'optimum' solution composition giving conversion coatings similar to those produced by Alocrom 100 was chosen for the experimental work carried out for this thesis.

9.2.1 Study of coating growth in a phosphate-free solution

The role of the phosphate ion was studied by keeping the composition

of the 'optimum' solution constant except for the phosphoric acid content. Figure 9.2.1 shows the range of compositions studied when plotted on the operating diagram taken from the original patent[93].

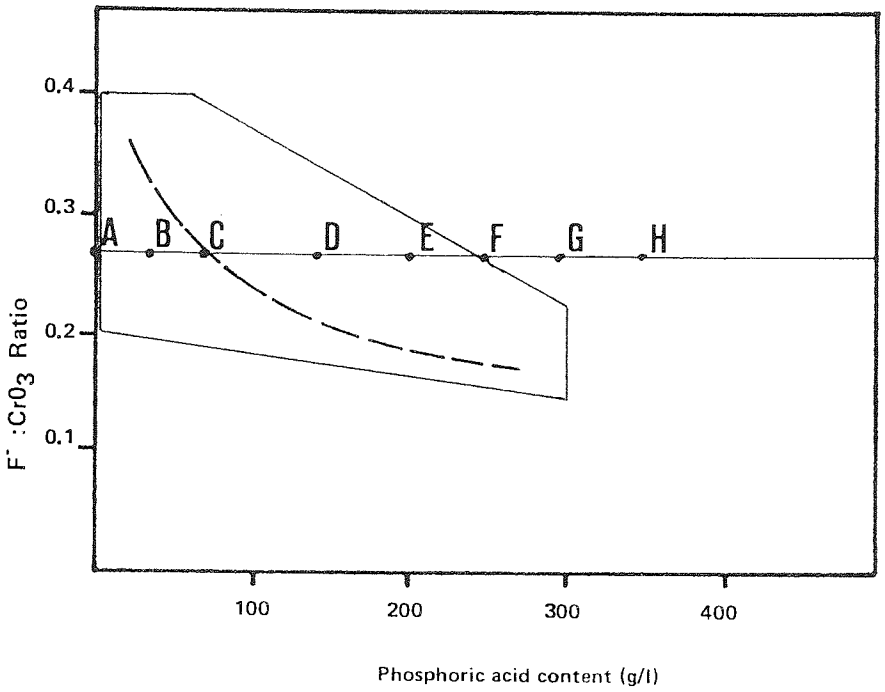

Figure 9.2.1 Operating range of chromate-phosphate solutions showing position of solution A-H

Solution A was phosphate-free and its fluoride ion to chromic acid ratio of 0.27 was much lower than obtained by extrapolating the optimum curve to zero phosphoric acid. Despite the advice in the patent[93] that solutions containing less than 6 g/l phosphoric acid were difficult to control because the solution quickly became unbalanced, a coating was formed which gave an insight into the mechanism of formation of conversion coatings on aluminium.

The main feature observed was the formation of spherical particles which grew up to 4 μm in diameter (Photo 11). Treverton and Amor[104] had previously reported much smaller spherical particles (30-70 nm)

in coatings formed by immersion in Alocrom 1200E (a ferricyanide accelerated commercial chromate solution which contained no phosphoric acid) at 35°C for up to 2 minutes. However, they considered an improvement in the resolution of the microscope was needed for confirmation of the spherical shape of their particles. The formation of spherical particles of aluminium hydroxide and chromium hydroxide has been studied by Matijevic[113] and others[114]. It was found that the conditions for producing spherical particles were specific and only formed in the presence of certain anions. In their absence, different shaped particles (such as rods or ellipsoids) of aluminium hydroxide were precipitated. Electron diffraction patterns of the spherical particles showed they were non-crystalline although the visibly crystalline structure displayed a clearly defined crystal structure.

Bell and Matijevic[115] used transmission electron microscopy to study the growth of spherical amorphous hydrous chromic oxide particles and found that the spheres initiated from a strand-like solid which was presumed to be an inorganic polymer formed by condensation of hydrous chromium-oxide. Condensation polymerisation at the surface caused further growth of the particle to become approximately spherical, with none of the characteristic preferential directionality seen in crystalline growth.

Published work on the composition of chromate conversion coatings has been reviewed by Treverton and Davis[97,102], who themselves used photoelectron spectroscopy in conjunction with ion milling to obtain depth-profiles of chromate coatings. Similar techniques were used by Katzman et al[94]. They found that the coatings

were composed mainly of a form of hydrated chromium oxide (chromium in the trivalent state) with aluminium fluorides and oxides present at the coating/substrate interface. This suggests that the composition of the layers of merged spherical particles obtained in the phosphate-free solution (Solution A) are a hydrated form of chromium oxide.

9.2.2 The role of the fluoride ion during film growth

The role of the fluoride ion has long been thought to be the removal of the initial oxide film present on the aluminium surface[87]. This has recently been confirmed by Treverton[97,107] Katzman et al[94] and others[105,106], who used various techniques to establish that fluoride was present mainly at the coating/substrate interface. Katzman et al[94] transferred specimens from a chromate/fluoride solution to a chromate solution containing no fluoride and found that the growth of the coating stopped, showing that throughout the conversion process fluoride was essential to prevent repassivation.

The conversion process is an electrochemical process, the anodic reaction being the dissolution of aluminium, which proceeds once the initial oxide film has been dissolved. The corresponding cathodic reactions are the evolution of hydrogen which is observed throughout the process and the reduction of hexavalent chromium to form a hydrated trivalent chromium oxide. This redox reaction initiates at cathodic sites on the original oxide surface to form strands of hydrated chromium oxide which then grow into spherical particles as described by Bell and Matijevic[115]. The coupon

weight change study (Figure 5.2.4.1) showed that the specimen weight increased linearly with time for the first few minutes of immersion (in solution A) followed by a gradual slowing down of the rate of weight increase. This result is consistent with the growth mechanism of spherical particles by condensation polymerisation. The constant rate of reaction at the surface of the particle limits growth initially giving a linear weight gain. Once the particles begin to merge (Photo 11C) to form a monolayer, the surface available for reaction becomes limited and so a fall in the rate of growth results. Growth does not stop completely because gaps persist where merging of the spheres is incomplete. Indeed channels are necessary for transport of fresh solution to the metal interface, and of hydrogen outwards into the bulk solution. Chromate coatings have been sectioned by ultramicrotome and examined in the transmission microscope by Furneaux et al[106] and fine randomly sited pathways were observed through the coating. The pathways, channels or gaps between the spheres contain solution during the coating process; thus on subsequent drying aluminium and fluoride remain on the channel walls. Evidence of such a non-uniform distribution of aluminium and fluoride was found by Abd Rabbo et al[105] using secondary ion mass spectroscopy.

9.2.3 Mechanisms of coating adhesion

Spherical particles nucleated, grew and merged to form a strongly adherent monolayer in about two minutes. Prolonged immersion resulted in flakes of the coating becoming detached (Photo 11D) and after 120 minutes the coating was loose and powdery because

of undermining of the coating and roughening of the metal/coating interface by the continuing anodic dissolution of the aluminium.

Matijevic et al[116,117] studied the adhesion of spherical hydrated chromium oxide particles on glass and stainless steel and found that the particles were strongly held in crevices, pits and grooves on the stainless steel. Mechanical keying played a part but in the case of stainless steel the bonding was essentially physical as there was no evidence of the chemical bonding that was found for the adhesion of the particles to glass surfaces.

Mechanical keying contributes to the adhesion between the merging spherical particles (Photo 11B) but condensation reactions between particles can form strong chemical bonds which are further encouraged by oven drying. Baking of chromate conversion coatings is a common industrial practice before application of organic coatings.

The reason for the excellent adhesion of paint coatings to chromate conversion coatings has been under debate for some time. Murphy[118] attributes this property to chromate inhibition of corrosion of the underlying aluminium which would otherwise undermine the paint and give loss of adhesion in service. Treverton and Amor[108] suggest that adhesion between conversion and organic coatings was somehow dependent upon the surface area of the small spherical particles they thought were present in their chromate films. They noted that the surface area of aluminium powder could be increased 300% by relatively short treatment in Alocrom solutions. Zettlemoyer et al[114] found that the surface area of spherical hydrated

chromium oxide particles increased after heating; this was explained by the removal of the water of hydration and the subsequent formation of micropores or gaps between the inorganic polymer chain structure. Pope et al[119] also observed that the spherical particles had relatively high surface areas and were useful absorbents. The gaps between the chains of the inorganic polymer structure of the spherical hydrated chromium oxide particle permit the absorption and diffusion of organic molecules, particularly if the absorbed molecules can chelate chromium ions. Selective absorption was also shown using a range of organic acids.

The application of Matijevic's research may enable the selective absorption of corrosion inhibitors and adhesion promoters from the organic coating into the spherical particles present in the conversion coating, increasing the durability and service performance of painted aluminium.

9.2.4 The role of the phosphate ion during film formation

It is clear that sodium detected in the phosphate-free coating was present in the particles rather than in the channels between them. Spot EDXA on individual spheres showed an increase in sodium content, as well as an increased chromium content (Table 5.2.4.1). This can be explained if sodium ions have been absorbed into the inorganic polymer structure during coating growth.

The introduction of phosphoric acid into the solution (Figure 9.2.1, solution B) results in the disappearance of sodium and the appearance of phosphorus in the coating formed (Table 5.2.4.2). This may be due

to preferential absorption of phosphate ions or by direct formation of hydrated chromium phosphate. SEM examination of this coating (Photo 12) reveals a relatively smooth uniform film that completely covered the surface after only 2 minutes immersion. Spherical particles could not be resolved. The gain in coupon weight roughly followed the parabolic relationship seen for the phosphate-free solution (solution A) after formation of the monolayer (Figure 5.2.4.1). The rate of coating formation was greater at all times. It can be seen from the potential-time curves (Figure 5.2.4.2) that the potential recorded during immersion was lower (more active) in solutions containing phosphoric acid. This was due to attack on the substrate by the more aggresive solution, increasing the rate of aluminium dissolution and reduction of hexavalant chromium. The rate of coating growth by condensation polymerisation is dependent upon the surface area of spherical hydrated chromium oxide particles. So a large number of small particles will grow faster than a smaller number of larger particles. This is supported by the observed behaviour of the growing conversion coatings; increased coupon weight gain despite a faster rate of substrate loss, and the inability to resolve any particles in the coating when observed under the SEM.

9.2.5 Mechanism of coating growth

Particle nucleation must occur on cathodic sites at the metal/coating interface. Since the individual particles are very small the period of growth is short. As particles grow, the previously formed layers are displaced outwards. The growing layer then merges into the bulk of the coating as shown in Figure 9.2.5. As the dissolution of the aluminium substrate proceeds, undermining

of the coating occurs. The nucleation sites are randomly spaced. Fine channels run through the coating allowing transport of fresh solution to the interface and hydrogen gas away into the the bulk solution. Chromium hydroxide is slightly soluble in chromate solutions, so the expected result if the coating grows outwards from the substrate/metal interface is that the outer surface of the coating would become attacked by the solution. This view is supported by the evidence (Photo 12) which shows increased pitting and roughening of the outer surface of the coating with increased immersion time in the solution.

It is concluded therefore that compact conversion coatings form at the metal/coating interface beneath the previously formed layers. Further, as the phosphoric acid content increases, the amount of pitting and roughening of the surface of coatings formed also increases, as is clearly shown by Photos 13C, 14C, 15D, 16D and 17C.

A side effect concerning the removal of water of hydration on drying, apart from increased condensation polymerisation between particles, is that the coating becomes stressed. Prolonged immersion causes the edges of 'islands' of thick coatings to lift away from the substrate (Photo 12D). In very thin coatings the tension caused by drying can be tolerated since the stress is small. However, as thicker coatings dry, the level of tension increases until cracking occurs, relieving the stress. Photo 12C shows a ridge that had formed before cracking took place, suggesting that cracking occurred after coating formation.

Increasing the level of phosphoric acid in the solution results in increasingly active potentials (Figure 5.2.4.2) consistent with aggresive anodic dissolution. There is a corresponding reduction in the coupon weight change rate (Figure 5.2.4.1) until at 200 g/l phosphoric acid (solution E) the coupon weight decreases with time from the moment of immersion. A visual examination of samples produced in this solution showed that a coating was present. Subsequent study under the SEM revealed the formation of spherical particles about 500 nm in diameter (Photo 15A). These particles grew and merged together to form a monolayer with 95% coverage after 10 minutes immersion. However, unlike the solution free of phosphoric acid, a second more compact layer began to form over the initial monolayer (Photo 15C), achieving full coverage by 40 minutes (Photo 15E). This structure is very similar to the structure exhibited by the coating formed from the 'mid-point' solution (Photo 8B) which had double the amount of chromic acid and fluoride but much less phosphoric acid and which achieved full coverage within 90 seconds.

Treverton and Davis[102] suggested that phosphorus acts as an accelerator in a similar way to ferricyanide in accelerated chromate-chromate solutions. The adsorption of ferricyanide on the coating surface prevented the adsorption of chromates on the same sites. This increased the chromate concentration in the solution at the coating/metal interface and the rate of reduction to form the coating. In the case of chromate-phosphate coatings this would lead to an increase in phosphorus concentration in the upper part of the coating and would on further reaction become a hydrated form of chromate-phosphate. Depth profiles obtained by various

workers[94,102] elsewhere and in this work Figure 6.2.2.1 support this theory.

Matijevic[113,114] demonstrated that relatively large spheres of hydrated chromium hydroxide were produced as the result of highly specific conditions. The formation of large spherical particles occurred when phosphoric acid was not present and again when the level of phosphoric acid reached 200 g/l in solutions with the same concentration of chromic acid and fluoride in solution. As particles nucleate and grow on the aluminium surface phosphate ions become absorbed, progressively reducing the rate of growth of the particles.

Rapid dissolution of aluminium shown by coupon weight loss (Figure 5.2.4.1) makes particle nucleation on the substrate surface difficult thus favouring nucleation of particles on the surface of previously formed particles.

Once particles have become established on the substrate, local solution conditions may be different from those in the bulk solution since the effect of agitation becomes reduced at the coupon surface. In particular, the local phosphate ion concentration falls as it becomes absorbed by an increasing number of hydrated chromium hydroxide particles. The specific conditions required for the growth of large spherical particles are lost and smaller particles result. Photo 15B shows very small particles forming over larger particles beneath them along areas of high activity (scratches or rolling lines) after 2 minutes of immersion. Growth of this 'upper layer' continues to spread outwards along the coupon surface until

after 40 minutes the 'upper layer' has achieved full coverage (Photo 15E).

A similar sequence of coating growth can account for the coating structure seen for the 'mid-point' solution (Photo 8 A-C). The higher level of chromic acid and fluoride in the solution leads to an increased rate of reduction of hexavalent chromium and increased coating formation rate. Spherical particles 0.25 μm in diameter cover the surface within 45 seconds of immersion. Local solution and precipitation conditions change slightly, encouraging the growth of columnar particles and a further decrease in local phosphate ion concentration. This change from the specific conditions required for large spherical particle growth, and rapid aluminium dissolution due to the high level of both fluoride and phosphoric acid, promote the growth of small particles (which cannot be resolved) on the existing particles. After 90 seconds immersion these small particles have completely covered the initial layer of large particles (Photo 8B). At this point the solution conditions immediately above the 'upper layer' approach that of the bulk solution and so large spherical particles are again formed (Photo 8C). These results suggest that under certain conditions coating growth takes place at the solution/coating interface on top of previously formed layers.

A further increase in the level of phosphoric acid takes the solution out of the operating range (Figure 9.2.1). The time taken for the coating to achieve full coverage increases. This is probably due to the increased rate of aluminium dissolution as shown by the coupon weight loss (Figure 5.2.4.1). At 300 g/l phosphoric acid,

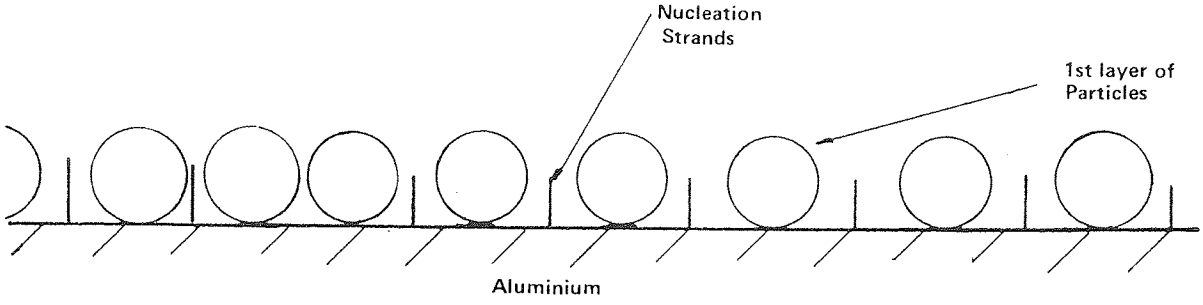

a) The first layer of particles have formed and the next layer begins nucleation by forming strands

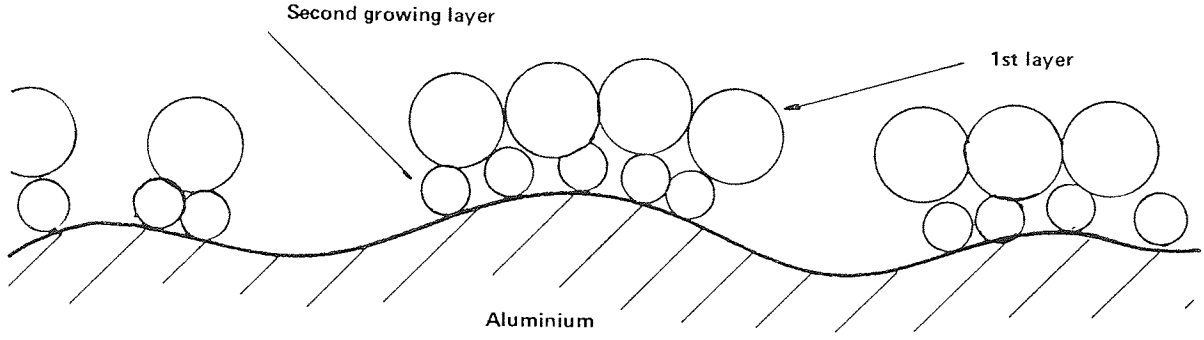

b) Second layer of particles grow pushing the upper layer outwards. Aluminium dissolution of the substrate causes roughening

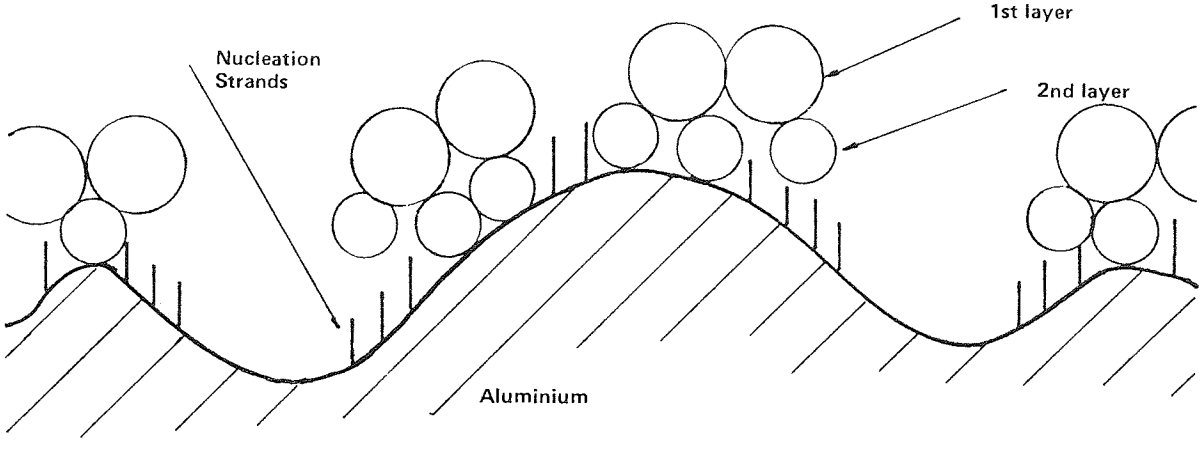

c) The second layer of particles have grown and nucleation of the next layer begins. Aluminium dissolution continues causing undermining of the growing coating.

Figure 9.2.5 Schematic diagram showing various stages of nucleation and growth of the coating as spherical particles

patches of coating can be detected after 60 minutes immersion (Photo 17C,D). The patches seem to correspond to the underlying grain structure of the 99.99% aluminium substrate (Photo 17D), perhaps showing preferential growth dependent on crystallographic orientation. After 20 minutes immersion, whiskers or 'rod-like' particles were found growing on the surface (Photo 17 A-B). Matijevic's(113,114,115) work has shown that spherical particles of hydrated chromium hydroxide were formed under specific conditions but in their absence different shaped particles grew, such as rods or ellipsoids which were crystalline. Still higher levels of phosphoric acid in the solution prevent any further coating formation. The rate of aluminium dissolution increases until the phosphoric acid concentration exceeds 560 g/l (33% v/v) when the rate falls (Figure 5.2.4.1) with a corresponding drop in potential (Figure 5.2.4.2). SEM examination has shown that these phosphoric acid contents are high enough to produce chemical polishing of the substrate (Photo 19).

Thus the role of phosphoric acid in chromate conversion coating solutions can now be explained. Firstly it increases the rate of anodic dissolution of aluminium. There is a corresponding increase in the rate of the cathodic reduction of hexavalent chromium. Secondly, the absorption of phosphate ions into the freshly formed hydrated chromium oxide particles reduces the rate of growth of individual particles and encourages nucleation of new particles at the metal/coating interface.

9.3 The Influence of Metallic Contamination

9.3.1 The influence of dissolved aluminium

The influence of solution contamination by various metallic anions has been briefly studied by Treverton(107). It was found that increased aluminium content of accelerated chromate solutions resulted in changes in the composition of the films rather than their thickness. However, the operating instructions(111) for Alocrom 100 (a chromate-phosphate solution) state that freshly prepared solutions should be aged by immersion of aluminium with a surface area of 0.5 dm^2 per litre of solution for between 30 minutes to 1 hour in order to produce adequate quality conversion coatings. Failure to do so may result in the formation of thin, powdery coatings.

Atomic absorption spectroscopy revealed that fresh Alocrom 100 solution had an aluminium content of 0.16 g/l. Isolation and analysis of an insoluble sludge found at the bottom of tanks of freshly-made Alocrom 100 showed that this aluminium was present as K_2NaAlF_6. Wernick and Pinner(75) state that this insoluble compound precipitates in order to control the aluminium content arising from aluminium dissolution during use. Its occurrence in freshly-made Alocrom 100 may be due to contamination of the solution components during production but more probably it has been added as an anti-caking agent to aid the flow of the powdered ingredients in bulk transportation and mixing.

Aluminium additions of 0.3 g/l to Alocrom 100 have shown that the

rate of coating growth increases by 33%. However further additions decrease the rate of growth, until at 1 g/l the coating weight after 5 minutes immersion is only 13% of the coating weight obtained after a similar immersion time in the solution giving the maximum growth rate (Figure 6.2.1.5). The potential-time curves (Figure 6.2.1.4) show that for increasing aluminium additions up to 0.5 g/l, the potential reaches a steady state at increasingly more noble potentials.

The dissolution of aluminium is rapid in fresh aluminium-free solutions and decreases as the aluminium content of the solution increases. The rate of anodic reaction decreases with increasing aluminium content. The reduction of hexavalent chromium to trivalent chromium, the major constitutent required *for coating formation*, is cathodic. Thus the rate at which trivalent chromium is produced is influenced by the rate of the anodic dissolution of aluminium. Therefore, as the aluminium content in the solution increases so the rate of coating growth decreases.

The curves showing the change of weight with time show that the rate of coating weight gain increases both with time, and with increasing aluminium in solutions up to 0.3 g/l. This shows that the weight gain increases despite decreasing anodic and cathodic activity, and correspondingly slower coating formation. This can be explained by considering the effect of decreasing aluminium dissolution upon the weight of the coupon. The weight loss due to dissolution rapidly slows down as the aluminium content in solution builds up. The true rate of coating formation also decreases, but since the true surface area of the metal/solution

interface increases as the natural oxide is dissolved by the hydrogen fluoride in solution, the actual rate of coating formation increases, resulting in the observed weight-change versus time relationship. It was noted that the potential decreases (becoming more active) after 5 minutes immersion in solutions with 0.3-0.5 g/l aluminium additons. This can be attributed to fluoride undermining the coating around anodic areas during formation of thick conversion coatings after prolonged immersion.

Increasing the aluminium content of Alocrom 100 solutions beyond 0.3 g/l results in a reduction in the rate of coupon weight gain. Since the rate of aluminium dissolution is also reduced this shift in the weight-change versus time trend cannot be caused by attack on the substrate by the solution. Therefore it must be due to a reduction in the rate of coating formation. SEM observations (Photos 20 and 21) and EDXA (Figure 6.2.1.1-3) have confirmed that the reduced rate of coating weight gain was caused by slower coating formation and growth rather than by less dense or porous coatings. This suggests that the anodic dissolution of aluminium is the controlling factor governing the rate of coating formation.

The potential recorded within the first minute of immersion drops to an active potential, then rises slightly, before either settling at a steady potential or becoming more active, depending upon the amount of aluminium in solution. The slight rise after the first drop is probably due to the formation of gas bubbles on the substrate surface. However the first drop is due to hydrogen fluoride dissolving away part of the natural oxide film from the substrate surface. The reduction of aluminium dissolution against

increasing aluminium content in the solution is further shown by the less active potential reached by the first drop (Figure 6.2.1.4), which corresponds to the reduction in the initial coupon weight loss (Figure 6.2.1.5) seen during the first minute.

Aluminium additions greater than 0.5 g/l reduce the rate of coating growth and increase the activity of recorded potentials. The potential remains active after a coating has formed because of continuous undermining of the coating as it grows (and repairs) by hydrogen fluoride.

Depth profiles obtained by electron spectroscopy in conjunction with ion beam milling, clearly show a reduction in the conversion coating film thickness with increasing aluminium content in solution (Figures 6.2.2.1-4). The profile showing the coating for 0.1 g/l additions is very similar to the result shown by Treverton[102]. However, careful examination of the remaining profiles reveals that the position of the fluoride trace moves away from coating/substrate interface as the amount of aluminium in the solution increases.

Katzman et al[94] have suggested that the coating precipitates as mixed hydrated chromium and aluminium oxides and that the fluoride ion is required at all stages of coating formation in order to remove the soluble aluminium hydroxide which is replaced by more corrosion resistant chromium hydroxide. In this way thick corrosion resistant coatings can be formed with few weak spots in the coating itself.

The observed depth profiles can be explained by considering the role of the fluoride ion in relation to the removal of any aluminium oxide trapped beneath the growing conversion coating. As the coatings become thinner and less protective the trapped aluminium oxide is dissolved by hydrogen fluoride leaving a thin layer of chromium hydroxide with no fluoride present. It has been shown that compact coatings nucleate and grow from the coating/metal substrate outward (Section 9.2.5). The lack of fluoride at the coating/metal interface indicates that precipitation of aluminium hydroxide mixed with chromium hydroxide is unlikely. If aluminium hydroxide were precipitated with chromium hydroxide at the growing interface, fluoride ions would be found within this region since they aggresively attack aluminium hydroxide. The presence of fluoride ions above the coating/metal interface is probably due to solution trapped in fine channels; undercutting of the coating would not have begun since depth-profiles were obtained from 30 second coatings. This was enough time to produce a thin coating but not thick enough to promote any undercutting. Fluoride ions were not detected at the coating surface probably because they were removed from this region by rinsing.

The ability of the coating to absorb aluminium ions has been studied by atomic absorption (Figure 5.2.4.3-4). The phosphoric acid content in the solution promotes aluminium dissolution from the substrate. Aluminium ions therefore continuously enter the bulk solution unless they precipitate out or become trapped or absorbed by the coating. The atomic absorption results show that the aluminium content in solutions containing phosphoric acid follow a parabolic relationship directly dependent upon the rate of aluminium dissolution (Figure 5.2.4.4). Some aluminium ions do become trapped or absorbed

in the coating however, and this is shown by Solution A (Figure 5.2.4.3) which has a low rate of aluminium dissolution but shows no increase in aluminium content after 20 minutes.

The aluminium content of chromate-phosphate conversion coating solutions has a dramatic effect on the coatings formed. Since aluminium is not 'mopped-up' significantly by the coatings as they grow some other form of control is required. Industrially, control is achieved by a combination of drag-out and induced aluminium precipitation in solution to form a sludge at the bottom of the tank. Further work is required in order to ascertain the efficiency of such solution control and to find its effect on the uniformity of coatings produced.

9.3.2 The influence of dissolved zinc and magnesium

Metallic contamination of the solution by zinc is quite common in industry as galvanised steel is often pretreated in chromate solutions before being powder painted. Analysis of a typical commercial chromate-phosphate bath showed that the aluminium content was 0.68 g/l; enough to adversely affect coatings produced, but the zinc content was several times higher than this at 5.36 g/l without apparently causing any problems or loss of quality.

Potential-time studies show that in general, increasing metallic additions leads to more negative potentials, or increased surface activity (Figures 6.2.5.2, 6.2.6.2, 6.2.6.4). However the corresponding weight change results and SEM observations show decreasing rates of coating growth and thinner, less protective

films which would result in the more active potentials seen.

SEM observations show that at higher levels of zinc contamination the coating becomes increasingly defective resulting in areas of complete coating detachment (Photo 26B). This may be caused by either loss of adhesion between the substrate and the coating or increased stress within the coating as it dries. It was found by Energy Dispersive X-Ray Microanalysis that zinc was not absorbed into the coating in any significant amount (Table 6.2.6.1). The presence of metallic ions in the solution can affect the rate of coating growth by reducing the rate of aluminium dissolution from the substrate depending on the species and number of ions present.

The weight change results of both zinc and magnesium contamination solutions are fairly similar up to an addition of about 5 g/l (the limit of magnesium added). Further zinc additions resulted in a decreasing rate of film growth. At 15 g/l, zinc nodules were deposited on the surface (Photo 26D).

9.3.3 The influence of dissolved copper

Copper additions of up to 3 g/l were found to markedly decrease the coating growth rate (Figure 6.2.6.5). The potential-time curves obtained from solutions with copper additions (Figure 6.2.6.6) are more readily interpreted than the potential-time curves for additions of zinc or magnesium. Initially the addition of copper caused a decrease in measured potential, probably due to increased solution ion conductivity. At 3 g/l the potential became more noble as copper nodules were deposited on the aluminium surface, becoming

the dominant feature (Photo 29C). Further copper additions lead to a corresponding increase in potential, the curve becoming erratic due to gassing at the large cathodic copper nodules (Photo 29D). As copper deposition begins to dominate the cathodic activity on the substrate, the deceasing rate in gain of coupon weight is reversed (Figure 6.2.6.5).

The effect of metallic contamination on the rate of coating formation can therefore be explained in terms of a reduction in anodic dissolution of aluminium. The results for zinc contamination of Alocrom 100 cannot be fully explained by this mechanism. The 5 g/l zinc addition result on both 99.99% aluminium and E45 aluminium alloy showed a higher coating growth rate (Figure 6.2.5.1) and a reduced activity (Figure 6.2.5.2) than for zero and 1 g/l zinc additions.

It is possible that this inconsistent result occurred as a consequence of the experimental technique used for preparing the solutions. The 1 g/l of zinc granules did not take too long to dissolve in the Alocrom 100 solution but, the 5 g/l zinc took several weeks to dissolve, and it was found necessary to adjust the solution strength and water content before carrying out any experimental work with this solution. It would therefore appear that in this case like was not compared with like, the readjusted solution being chemically more active and so able to produce an acceptable coating.

It would seem that the industrial bath analysed containing 0.68 g/l of aluminium and 5.36 g/l of zinc should be producing poor, light coatings. This was not found to be the case. It must

therefore be assumed that this solution is being run in such a way as to reduce the effect of metallic contamination. It is known that for practical reasons this particular bath is run at 1/3 of the strength recommended by ICI[111]. One consequence of this will be that this bath requires more control and attention than normal. However, it has also been shown that up to a point, reduced solution concentration increases the rate of coating formation (Figure 5.2.2), so it is possible that in this case, by good fortune, the two opposing influences effecting the coating weight have balanced out to give acceptable conversion coatings in 5 minutes immersion, the standard treatment time for this bath.

9.4. The Influence of the Cleaner and the Initial Oxide Film on the Conversion Coating Process

The manufacturers* describe AC51, the acidic cleaner used throughout this work, as a non-etch acidic aluminium cleaner. However, it was noticed that the aluminium surface became pitted on immersion in freshly prepared AC51 (Photo 7D). Analysis of a sample of AC51 taken from a vat in commercial use showed that it contained 0.14 g/l aluminium and 1.8 g/l zinc. The zinc in the solution came from galvanised steel processed through the same cleaner used for aluminium components. The influence of the aluminium content of the cleaner on the subsequent conversion coating was studied.

The rate at which aluminium dissolved in AC51 (Figure 4.2.4.1) followed a parabolic relationship whose rate constant depended on the surface area of aluminium per unit volume. Potential-time curves showed that the time taken for the initial fall of potential is increased greatly with increased aluminium content. An aged cleaning solution with a relatively high metallic ion concentration slows down the rate of oxide removal and minimises intense pitting attack of the substrate.

These results show the importance of using aged solutions in the laboratory when studying industrial solutions designed to have a long life. Fresh AC51 leaves the substrate surface pitted and highly active; aged solutions reproduce industrial conditions more realistically.

* Robertson's Chemical Ltd., Wattisfield, Norfolk

The experimental work carried out to investigate the influence of the aluminium surface oxide film thickness on the efficiency of the acidic cleaner showed that the 'solution usage' had a greater effect than the oxide film thickeness (Figures 4.2.2.2-5).

When much thicker oxide films were formed anodically at $-8°C$ and at ambient temperature, it was found that the initial fall in potential, seen when recording the potential-time curves (Figures 4.2.2.6-7), was related to the oxide film thickness. The potential then became erratic until some time later a steady-state potential was reached. The cause for this erratic behaviour was probably due to the oxide structure becoming undermined and gassing blocking pores and cracks.

Manson and Shinder[112] found that increasing anodising solution temperature lead to increased ion mobility, the rate of aluminium dissolution increased and the anodic film structure became more porous with a larger pore size. It was noted that the samples anodised at ambient temperature displayed a tendency to deviate in potential to a greater extent than the samples anodised at $-8°C$ when immersed in AC51 (Figures 4.2.2.6-7).

The larger pore size leads to a higher degree of undermining and gassing (giving the erratic pontential recorded), and consequently leads to more effective removal by the cleaner, giving the more consistent most active potential. Figure 4.2.2.8 shows the relationship between the anodic oxide thickness and the time taken to reach the most active potential. This shows that the higher anodising temperature samples reached the most active state more quickly than the $-8°C$ samples, pointing to quicker removal of the oxide film.

Increased air-formed oxide films were removed by fresh Alocrom 100 solutions within 30 seconds of immersion (Figure 4.2.3). This finding is of industrial significance because it shows that variations from batch to batch in the thickness of the oxide on aluminium do not affect chromate phosphate conversion coatings or their subsequent service performance when painted because all oxide films are removed within the first 30 seconds of immersion.

9.5 The Effect of Substrate Pretreatment and Particle Distribution of Thermoset Polyester Powder on Powder Flow Measurements

The technique used by Gokemre and Dennis[58] to study powder flow was modified and improved by arranging direct curve plotting of specimen temperature and powder flow.

Flow curves were obtained for pigmented (white) thermosetting polyester powder classified into various particle size distributions (Figure 7.2.1.1-6). The ultimate coverage, flow start temperatures and flow stop temperatures were found for powder flow on E4S aluminium alloy pretreated in Alocrom 100 for 1.5 to 5 minutes at room temperature (Table 7.2.1). These results show that powder size has a marked effect on the ultimate coverage. Increasing powder size lead to an increased ultimate coverage. Nix and Dodge[57] studied the causes of 'orange-peel' in powder coatings and reported that smaller particles flow better than large particles. A possible explanation of their observation is that Nix and Dodge were describing the flow required to produce smooth, level coatings rather than the flow of individual particles measured in the current work.

If it is assumed that the flow of an individual particle is dependent upon the viscosity and surface tension of the melted particle then the size of the particle does not influence its final thickness after cure. The volume of a large particle is greater than the total volume of several smaller particles having the same total surface area as the large particle. Therefore the large particle will cover a greater area than the corresponding number of smaller particles after curing.

Table 7.2.1 also shows that fine particles begin and stop flowing at lower temperatures than standard or coarse particles. The longer time for large particles to start flowing is probably caused by poor thermal conductivity within the particle. At lower heating rates, particles of different sizes would melt nearer the same temperature. In industry where heating rates of 30°C/ minute are not unusual, small particles on the outside of the coating may melt and gel before large particles do so. This contributes to orange peel. The recycled powder had very similar flow characteristics to the standard powder showing that recycling does not markedly affect powder flow of the particular powder studied. Polydrox, a commercial polyester powder produced in Germany, had particularly high flow characteristics on Alocrom 100. However, the flow characteristics of Polydrox on galvanised steel and on aluminium pretreated in Alocrom 1200E, were very poor (Figure 7.2.1.5-6). The good flow on Alocrom 100 coatings is therefore due to better wettability, or reduced surface tension rather than lower viscosity. This view was supported by the observation that the flow temperature and the gelation temperature of Polydox were not affect by the substrate pretreatment used.

In general, powder particles of whatever size flowed more readily on substrate with shorter pretreatment times (Figure 7.2.1.1-3). Longer pretreatment times led to rougher surface coatings with deeper mud-cracks (Photo 3 and 5). Molten particles flow over smooth surfaces with hair-line cracks better than over a rough, deeply cracked surface. It is not known how the topography of the pretreated surfaces affects paint adhesion but Treverton(107) found that paint bonding was as good after 3 seconds treatment in

a chromate solution as after 30 seconds treatment. Thick chromate-phosphate coatings are mechanically weak and prone to cracking and flaking so it is likely that powder flow can give a good indication of the mechanical or physical characteristics of the combined pretreatment and powder coating.

The powder flow curves show that the results with the standard and coarse distributions were not always consistent. SEM examination of the classified powders shows a significant visible difference between the particle size of the fine and standard distributions (Photo 30), but the coarse powder distributions contain a large proportion of particles less than 20 μm in diameter. The inconsistent behaviour of the standard and coarse powders can now be explained. The distribution of particles within the field of view of the Quantimet at the start of a powder flow test depends on the particle distribution of the parent sample. The standard and coarse powders both have large and small particles with a large scatter in the samples examined on the Quantiment.

Gokemre and Dennis[58] reported that stale powders did not flow as well as either fresh powders or vacuum treated stale powders. Figure 7.2.1.4 shows that the flow of fresh coarse and fine powders was not significantly different from that of the stale or old powder used previously (Figure 7.2.1.3). This shows that fresh powders age very rapidly unless they are kept in air-tight and refrigerated conditions. The powder flow curves produced with old or stale powder may therefore be more representative of industrial conditions.

Experiments were undertaken to assess the use of Alocrom 100 as a pretreatment for galvanised steel prior to powder coating. Galvanised sheet was pretreated in Alocrom 100 for 5 minutes before powder flow studies were carried out. In general, powder flow was markedly reduced (Figure 7.2.1.6). Since the viscosity of the molten particles is an intrinsic property unaffected by the substrate, reduced flow must be the result of increased surface tension. The initial zinc dissolution in Alocrom 100 is rapid. Figure 6.2.4.1 shows that the coating formed on zinc stopped growing after 10 minutes. SEM observations showed that the film formed was discontinuous (Photo 22) and that the surface topography was dominated by crystallographic etching of the zinc. It is clear that Alocrom 100 is not a suitable pretreatment for zinc or galvanised sheet prior to powder coating. Reduced flow is a result of the forces of cohesion between the polymer chains being greater than the forces of adhesion between the molten particle and the zinc surface, pointing to poorly bonded coatings on galvanised sheet products.

9.6 The Development and Testing of 'Low-Bake' Polyester Powder Coatings

Production costs of powder coated products can be reduced by using resins capable of becoming fully cured at reduced temperatures and curing times. Until recently the cost of 'low-bake' resins prohibited their use. However, the higher production cost of new high-quality low-bake polyester resins(92) has been offset by energy savings at curing(7).

Production problems have arisen in the past with low-bake resins as they often contain a higher proportion of accelerators, or cross-linking agents, which increase the possibility of partial curing during the extrusion process. Down-time is a costly occurrence for any production line, and partial curing during powder manufacture is particularly expensive as it involves stripping the extrusion equipment and dislodging the partially cured thermoset material. This is a difficult labour intensive and time consuming process. The new economic low-bake resins therefore had to satisfy the following requirements:-

i) Economic viability

ii) Stability during transportation and storage

iii) Production process compatibility

iv) Final coating durability (mechanical, physical and chemical).

Three 'low-bake' polyester resins which satisfy the first two requirements were chosen for a detailed study of production process compatibility and final coating durability. It was known that the

pigment and filler combined with the resin could have a dramatic effect upon both the strength and weathering characteristics of the final coating(57,71). Therefore two fillers were tested with each resin and two white pigments were tested with each resin/filler combination. The precise chemical make up and process route for each ingredient were not divulged by the manufacturers for commercial reasons. However, it can be said that the two fillers were of different quality and that the pigment was titanium oxide in both cases. Pigment 1 was coated with a hydrous oxide in order to reduce photocatalytic activity of the titanium dioxide and minimize degradation of the powder coating when exposed to outdoor environments. Pigment 2 was uncoated titanium dioxide.

9.6.1 Physical properties of powder coatings

Experiments on one of the resins (Resin B) were abandoned. Suitable extrusion conditions could not be found for this resin. It was found to have a high melt viscosity which resulted in a rapid increase in process temperature during extrusion. The other two resins, A and C, were found to be compatible with the production process using any combination of filler or pigment. Mechanical hardness and strength tests on the baked coatings showed that the optimum curing temperature was 170°C for 10 minutes in all cases (Table 8.2.1.3-7). Coatings cured at 160°C for 10 minutes were hard and had high scratch resistance (Table 8.2.1.3) but were brittle with poor impact and slow indentation results (Tables 8.2.1.4-6). Increasing the curing temperature to 180°C for 10 minutes reduced the shock resistance of the coatings tested (Table 8.2.1.5) and increased the ductility (Table 8.2.1.6) it was also

noted that the coatings had become slightly yellow in colour.

These results show that at 160°C the cross-linking reactions had not been completed within 10 minutes. Whereas at 180°C the maximum cross-linking density had been passed within 10 minutes and degradation had begun. This is in agreement with work by Williams(49) who studied the influence of the degree of cure on the physical and mechanical properties of thermoset powder coatings.

The influence of the filler and pigment in the various resins could only be distinguished by mechanical testing when the optimum cure had been achieved. Table 9.5 shows the mechanical performance of the experimental low-bake formulations expressed as a percentge of that of standard 44S. Blundell-Permoglaze 44S is a white semi-gloss polyester. The mechanical performance was assessed from the combined mechanical tests. It can be seen (Table 9.5) that although the pigment and filler had an influence on the mechanical properties of the coatings, no general trend was evident.

Table 9.5 Mechanical Performance of Low-Bake Polyester Powders

Resin	Filler	Pigment	Rating %	Comments
Standard (44S)			100	200°c @ 10 mins cure
A	X	1	95.5	
A	Y	1	91.4	Failed SO_2 test
A	Y	2	88.5	
A	Y	2	66.6	Brittle coating
B	X	1	95.5	Unsuitable resin
C	Y	2	76.2	
C	X	1	75.4	
C	X	2	56.1	Failed reverse impact
C	Y	1	51.7	Failed conical bend

Clearly, resin A performed better than resin C and the coated pigment appeared to improve its strength and toughness. Filler Y may be responsible for reducing the toughness and the sulphur dioxide resistance of resin A. However the influence of the pigment and filler on resin C does not show the same trend, or any other. This result may be due to testing brittle coatings which can form hair-line cracks long before detection, and make the test end-point difficult to judge.

9.6.2 Chemical resistance properties of powder coatings

Chemical resistance was measured by immersing powder coated aluminium panels in various chemicals for 48 hours followed by gloss measurements and mechanical testing. Chemical resistance was about equal for all resins and additions. Gloss retention and hardness were equal to,

if not better than those of the standard polyester. In general, coatings had good resistance to high molecular weight solvents, bleach and alkali, but poor resistance to low molecular weight solvents and strong acids. The artificial weathering tests showed that the pretreatment and pigment both played an important role. Aluminium panels pretreated with 'Bonderite 790', a chrome-free pretreatment under development by Pyrene chemicals limited, prior to being powder coated and exposed to a salt spray failed within 700 hours. Panels pretreated with Alocrom 100 survived over 1000 hours and in all cases had little corrosion damage. The salt-spray corrosion tests also revealed that pigment 1, the coated pigment, improves the corrosion resistance of the coating. The weatherometer results show that low-bake polyester coatings are as colour fast and chalking resistant as the standard polyester coating when properly cured. Therefore the accelerated weathering tests suggest that low-bake polyester resins are as corrosion and weather resistant as standard coatings when mixed with the right additions and given optimum cure.

9.6.3 Limitations of procedures used to test powder coatings

Most of the tests used to assess the mechanical performance of the coatings were originally quality control tests. The British Standards which apply to each test method were written with quality control in mind. As such, these tests are adequate, as poor batches of powder can be quickly identified and withdrawn. However, they are not sensitive, reliable or reproducible enough for development work.

The conical bend and cross-hatch adhesion tests were used as pass/fail type tests. Failure of a coating would eliminate it from further consideration. Scratch resistance, slow indentation, impact testing and permeability all had a definite point of coating failure which in many cases was difficult to detect or correctly interpret. Scratch resistance results could be high or low depending upon the condition of the steel ball on the scribe. If metal pick-up had occurred on the scribe, (from the substrate) subsequent results would be low. On the other hand should the scribe become contaminated by the coating itself, the steel ball skated across the coating giving a high result. Slow indentation and impact testing were more consistent. However, brittle coatings produce fine hair-line cracks which are hard to detect, and soft coatings display ductile failure and so it can be difficult to define the point of failure. These problems were partly overcome by repeated testing of suspect results. However it is clear that no satisfactory simple coating test for mechanical performance is available which may be used both in a quality control laboratory and as a development tool.

Chemical resistance of coatings could not be measured directly but were dependent upon changing mechanical properties and gloss of the coating. The test devised in which panels were partially immersed in various chemicals has shown an important result that was not fully appreciated previously. Fumes from the chemical solutions can effect coatings in a completely different way from the chemical attack on coatings below the solutions surface.

In general it was found that all coatings had better resistance to isopropyl alcohol than to di acetyl alcohol (Tables 8.2.2.6-7).

The former has a higher molecular weight and so cannot penetrate the polymer coating as readily as the di acetyl alcohol. However the scratch resistance of coatings just above the solutions surface show that the fumes from isopropyl alcohol soften the coatings more than di acetyl alcohol. This may occur because the fumes from di acetyl alcohol are swept away from the vicinity by denser air, so protecting the exposed part of the panel. The heavier fumes from isopropyl alcohol, which are not as easily dispersed by air currents, penetrate the adjacent coating. Table 8.2.2.10 shows the slow indentation results of coatings after exposure to various chemicals. Nitric acid fumes soften the coatings, whereas bleach and potassium hydroxide cause embrittlement. This was not shown up by the scratch resistance results and so demonstrates the importance of having a test of mechanical performance that can measure the strength as well as hardness of a coating.

The chemical resistance tests show that in terms of hardness and gloss retention, all of the 'low-bake' coatings have similar properties to the standard. However, the ductility of the standard polyester coating was not as adversely affected by chemical attack as the ductility of resin C coatings. This suggests that the slow indentation test is more sensitive to chemical attack of powder coatings than scratch resistance, since attack leads to changing ductility rather than changing hardness.

9.7 Powder Charging Characteristics

The powder charging characteristics of any system can be measured by collecting the powder sprayed over a given length of time, measuring the total electrostatic charge contained by the collected particles and dividing this by the weight of the particles, giving a charge per unit mass.

The transfer efficiency of a powder coating system can be defined as the proportion of the sprayed powder that becomes sufficiently charged to be attracted to an earthed substrate during application.

Little is known about the charging mechanisms involved as powders pass through a corona discharge or the effect particle size has on transfer efficiency. Masuda and Akutsa[34] found agreement with Pauthenier's equation describing the charging of spherical particles by ion bombardment[32] for non-conductive spherical particles. Since the electronic resistance of powders is very high it is likely that the applied charge is held on the surface of the particles. The assumptions used for work conducted at Southampton[34] can be tested by studying the Q/M ratio for powders with different particle distributions. Q/M measurements show that the fine distribution particles collect more charge than the standard size particles (Table 8.2.4.1). Coulter Count analysis was used to calculate the surface area of a unit volume of particles for each distribution (assuming a packing density of 1.0), and a ratio was found between charge and surface area (Table 8.2.4.3). If charge were held uniformly over the surface the charge per unit area ratio would be equal for standard and fine distributions. Very

good agreement was found for batch 1, and reasonable agreement for batch 2.

The results for batch 9 do not show such good agreement. The fine distribution had a higher charge to surface area ratio than the standard distribution. It was also noted that the standard polyester fines produced a high result (Table 8.2.4.3). Inspection of the Q/M results show that very little powder was collected in both of these cases. Experimental error may have been caused by a reduced flow of particles. In practice this is difficult to avoid since operating conditions were fixed and on wetting, fine powders do not flow as well as coarser powders in dry transportation systems. A further cause of error may have arisen from the assumption that the particles are spherical. SEM observations have shown that this is not the case (Photo 30). Charge will not be spread evenly over the surface of the particles but will collect at sharp points, and could partially discharge before becoming attracted to the earthed work piece.

Reducing the particle size distribution has been seen to increase transfer efficiency. This would result in less recycled powder being generated and re-used improving the finished quality of powder coatings. However powder flow studies have shown that particles with a fine size distribution do not melt and flow as well as particles with a large size distribution. A compromise must be found between particle flow, levelling characteristics and transfer efficiency, in order to minimise 'orange-peel', and reduce contamination from recycling.

Finally, the influence on transfer efficiency of various additions to the resin can be measured using this technique. The charge held per unit area for batch 2 is lower than for batch 1, suggesting that the coated pigment improves the transfer efficiency of the powder. Fundamental research using this technique could help explain the mechanisms of particle charging, and the influence of the filler, pigments, and resins on charge retention.

10. CONCLUSION

The main conclusions that have been reached during this work are:

1) The major component found in chromate-phosphate conversion coatings is hydrated chromium hydroxide. This forms from hexavalant chromium which has been reduced via a redox reaction at the metal/coating interface. The hydrated chromium hydroxide forms an ionic polymer by condensation polymerisation which promotes the growth of small spherical particles.

2) Phosphoric acid accelerates the growth of chromate-phosphate conversion coatings in two ways. Firstly, by increasing the rate of aluminium dissolution from the substrate (an anodic reaction) there is a corresponding increase in the rate of reduction of hexavalant chromium (a cathodic reaction), and so increases the availability of the film forming material. Secondly, the phosphate ion becomes adsorbed into the growing chromium hydroxide particles blocking further growth and encouraging the formation of many more smaller particles. This increases the total actual area of growing particles which is the rate controlling factor for the growth of chromium hydroxide by condensation polymerisation.

3) A balance must be achieved between oxide film attacking agents (HF), coating formation agents (CrO_3) and the accelerator (H_3PO_4) in order to produce compact, dense and

uniform chromate-phosphate conversion coatings. There must be enough fluoride present to remove the initial oxide film from the surface of the aluminium substrate and ensure continued contact between the metal and solution. There must be a balance of hexavalant chromium in solution to enable reduction and formation of hydrated chromium hydroxide particles. And, there must be enough phosphate ions present to control the size of the growing particles. However, too much phosphoric acid will inhibit coating growth, due to intense anodic dissolution.

4. The typical mud-cracked appearance of chromate-phosphate conversion coatings occurs as a result of water loss during drying after coating formation. Internal stress build up of heavy conversion coatings can also result in lateral cracking and flake off of relatively large areas.

5. Dissolved metallic ions in chromate-phosphate solutions influence the compactness of the conversion coatings formed. There is an optimum aluminium content, found to be about 0.5 g/l Al under the conditions used. Dissolved magnesium and zinc, at and above the 1 g/l level, both increase the flaking and number of defects in the conversion coating. Dissolved copper is particularly harmful because it deposits as small nodules surrounded by a small ring of uncoated material giving potential sites for the subsequent initiation of corrosion.

6. Air formed oxide films on aluminium substrate are quickly removed by balanced chromate-phosphate solutions and do not significantly affect coating formation.

7. The melting characteristics of powder particles as they are heated can be described in three stages:- melting, flow and gelation. The powder particle size has a significant influence over the melting and gelation temperature; smaller powder particles lead to reduced temperatures in both cases. The ultimate flow achieved depended on both the powder particle size and the topography of the substrate surface. Large particles flow better than small particles and rough surfaces (ie longer pretreatment times), inhibit particle flow.

8) The optimum curing conditions for the 'low-bake' polyester powder coatings are 10 minutes at 170°C, this is 10°C higher than claimed by the resin manufacturers. Under curing (10 minutes at 160°C) lead to brittle paint coatings with poor mechanical properties. When the low-bake polyester powder coating was cured under optimum conditions the mechanical, physical and accelerated weathering properties could match the standard polyester powder coating. However, it was not possible to attain the very high degree of chemical resistance, for which the standard polyester powder coating is renowned with the 'low-bake' polyester powder.

9. The charge applied to powder paints during application by electrostatic spraying is carried on the surface of the powder particles. The transfer efficiency can be increased by reducing the particle size distribution. However, this is limited by the application systems ability to transport a fine powder without becoming blocked.

FURTHER WORK

This work has shown that chromate-phosphate conversion coatings are formed by nucleation and growth of spherical chromium hydroxide. Mechanisms have been suggested to explain the observed topographical features of the coatings, which were related to the phosphoric acid content of the solution. Further work is necessary to find the conditions and factors which favour growth from the outside of the coating rather than at the metal/coating interface. A greater understanding of this may lead to finding conditions at which compact coating growth could be increased still further making this process (or a similar chromium free process) suitable for coil-coating techniques currently used in industry.

The excellent properties obtained by chromate-phosphate pretreatment, has been suggested, are due to the formation of hydrated chromium hydroxide as an ionic polymer by condensation polymerisation. New chromium-free processes are required and may now be developed using ionic polymer technology and optimising the mechanisms promoting growth and paint bonding, particularly the application of Matijevic's research[113,115,116,117] on preferential adsorption of adhesion promoting agents.

Metallic contamination of the solution has been shown to be a major cause of defects and flaking in conversion coatings. Industrially, metallic contamination caused by dissolution of alloying elements in the substrate is controlled by precipitation. This suggests that the level of metallic contamination in conversion

coating baths continuously changes. Work is required to find the effect of such changes on the appearance, mechanical properties and corrosion resistance of the coating produced.

Alocrom 100 had been developed for aluminium pretreatment and is not a suitable pretreatment for zinc, probably because of the high rate of zinc dissolution. Further work is necessary to find the reason for incomplete coverage and to produce a conversion coating solution suitable for processing both zinc and aluminium, and other common substrates.

It was noted that charge acceptance of powders may be partially dependent upon the resin and additions, it could therefore be of great benefit to the design of future application systems and powder formulations to study the mechanisms of charge acceptance and the effect of the particle composition. A greater understanding and application of this technology may lead to 100% powder transfer making quick colour change possible, and therefore improving the commercial viability of powder coating.

Finally, transfer efficiency can be improved by reducing the particle size distribution of the powder (since the surface area holding charge is increased). Manufacture and application technologies are not suited to production and use of fine particles. Further work is necessary to find the effect fine particles have on the levelling of coatings, and if this has a positive result, development of fine powder production and application techniques is necessary to take advantage of the increased transfer efficiency.

ACKNOWLEDGEMENTS

The author gratefully acknowledges the support of the SERC in the form of a CASE award granted for this work. Thanks and appreciation also goes to all the staff of the collaborating firms:-

Alcan Laboratories Ltd, Banbury
Blundell-Permoglaze Ltd, Tyseley Division
Metallic Protectives Ltd of Warwick

and in particular:- Mr J Mitchell (Chief Chemist BPL)
Mr R Groom (Director MPL)
Mr A Bowmer (Section Leader BPL)
Mr C Matthews (Development Chemist BPL)
Dr G Stanford (Consultant MPL)

all of who have given valuable time and help without hesitation.

Special thanks goes to Dr J K Dennis and Dr D J Arrowsmith who supervised this work and gave great encouragement throughout. Finally I wish to thank my wife Paula for typing this thesis (and many other reports) and for supporting me when the grant ran out!

REFERENCES

1. D.D. Taft and F.E. Pegg: Product Finishing 1979 32 (1) 64; 1979 32 (2) 46
2. R.P. Franiau: Powder Coatings 1980 3 (1) 15
3. E.F. Gormley: Plating and Surface Finishing 1982 69 (5) 78
4. Anon.: Polymers Paint Colour Journal (Redhill) 1980 179 761
5. Anon.: Paint Manufacture and Resin News 1980 50 (8) 1
6. P.H. Pettit and T. Kaltenbach: Product Finishing 1981 34 (8) 12
7. E.F. Law: Product Finishing 1982 35 (8) 12
8. P. Ribnitz: Powder Coatings 1981 4 (2) 6
9. D. Howell: Product Finishing 1981 34 (8) 44
10. Anon.: Powder Metallurgy 1981 24 (4) 223
11. Private Communication: Alan Bowmer, Blundell-Permoglaze Jan. 1983
12. P. Franz and A. Bolt: Powder Coatings 1981 4 (1) 3
13. S.T. Harris: Powder Coatings 1981 4 (2) 2
14. J. Cartwright: Powder Coatings 1981 4 (2) 12
15. K. McIntyre: Modern Paint and Coatings 1982 (11) 63
16. S.T. Harris: "The Technology of Powder Coatings" 1976: Portcullis Press, London
17. K.A. Pai Panandiker and C. Danick: Powder Coatings 1979 2 (2) 12
18. D.D. Taft: Powder Coatings 1979 2 (3) 5
19. Technical Service Report No. D 9165 GC Tioxide Titanium Pigments
20. G.F. Hardy: Journal of Paint Technology 1974 46 (599) 73
21. J. Szasz: Industrial Finishing 1970 22 (270) 4
22. W.J. Richardson: Surfacing Journal 1974 5 (3) 10
23. G. Friberg: Powder Coatings 1981 4 (3) 2
24. J.D. Toff: Product Finishing 1976 29 (3) 14
25. M.J. Drury: Product Finishing 1974 27 (11) 37

26. M. Cowley: Product Finishing 1975 28 (5) 22

27. Private communication: S. Singh, Southampton University, June 1983

28. J.F. Hughes: Finishing 1982 6 (11) 17

29. Anon.: Modern Plastics International 1979 9 (2) 8

30. R.C. Lever: Powder Coatings 1979 2 (3) 2

31. Anon.: Finishing 1982 6 (12) 21

32. H.J. White: Trans AIEE 1951 70 1186

33. M.M. Pauthenier and M. Moreau Hanot: J. Phys Radium (Series 7) 1932, 590

34. S. Musuda and K. Akutsu: Proc Conf IEE, 1975 (p 909) JAPAN

35. R.P. Corbett: Dechema Monographics 1973, MR pp 1370-1409, Band 72, pp 261-272

36. A.W. Bright and R.P. Corbett: Conference of Electrical Machines, Forming and Coating 1975.

37. S. Singh and A.W. Bright: 3rd International Congress on Static Electricity European Federation of Chemical Engineering 1977 (Grenoble)

38. J.A. Cross and J.D. Bassett: Trans IMF 1974 52 112

39. R.P. Corbett, J.A. Cross, J.D. Bassett: Proc Conf I Phys 1975 (Series 27) 221

40. J.A. Cross: Proc Conf I Phys 1975 (Series 27) 202

41. H. Krupp: Advances in Colloid and Interface Science 1967 1 111

42. A.W. Bright: JOCCA 1976 60 23

43. S. Masuda, A. Mizuno and K. Akutsu: Journal of Electrostatics, 1976 2

44. S. Masuda, A. Mizuno and K. Akutsu: IEEE/IAS 12th Annual Meeting 1977 Los Angeles

45. G.F. Hardy: Journal of Paint Technology 1974 46 599

46. S. Masuda, K. Akutsu and T. Saito: Proc Conf IEE 1967 (p 470)

47. J.F. Hughes and Y.C. Ting: IEEE/IAS 12th Annual Meeting 1977 (p 906) Los Angeles

48. S. Singh, B.C. O'Neill and A.W. Bright: Journal of Electrostatics 1978 4 325

49. J.F. Williams: Materials Protection and Performance 1974 10 (9) 15

50. S. T. Harris: JOCCA 1981 64 (9) 364

51. C. Klaren and A. Ghijsels: Proceedings of the XIIth FATIPEC Congress Garmisch - Partenkirchen, May 1974

52. S. Gabriel: JOCCA 1976 59 52

53. E.W. Drew: Paint Manuf 1977 47 11

54. O.W. Smith and J.V. Koleoske: Journal of Paint Technology 1976 48 (621) 42

55. M.J. Hannon et al.: Journal of Coatings Technology 1973 45 (582) 42

56. M. Brugger and M. Gempeler: Double Liaison 1975 22 171

57. V.G. Nix and J.S. Dodge: Journal of Paint Technology 1973 45 (586) 59

58. B. Gokemre and J.K. Dennis: Trans IMF 1980 58 15

59. B. Whiting and J.K. Dennis: Trans IMF 1978 56 32

60. D.C. Freshwater: Proceedings of the International Symposium on Powder Coating, 13-15 Feb., 1965

61. C.L. Brett: Journal of Applied Polymer Science 1976 20 1431

62. T.J. Nakamichi: J Japan Soc Colour Mater 1978 51 528

63. Z.S. Aleksandara, N.E. Kharitinych and M.T. Bryk: Continental Paint and Resin News 1981 19 No.4, 153

64. J.B. Enns, J.K. Gillham and M.J. Doyle: ACS; Div of ORPL paper 1980 43 669

65. L.A. Simpson: Proceedings of the XVIIth FATIPEC Congress, Lugano, September 1984

66. S.Y. Pusatcioglu, A.L. Frickle and J.C. Hassler: Journal of Applied Polymer Science 1979 24 937

67. H. Kubota: J Appl Polym Sci 1975 19 2279

68. S.Y. Pusatcioglu, A.L. Frickle and J.C. Hassler: J Appl Polym Sci 1979 24 947

69. G.K. Martin and R.I. Tilley: British Polymer Journal 1971 3 36

70. P.D. Gabriele, J.R. Geib, R.M. Iannuci and W.J. Reid: ACS; ORPL papers 1982 47 Sept. 359

71. T.J. Bickerton: Australian OCCA Proceedings and News 1982 June, 17

72. E.R. Hoffman: JOCCA 1969 52 113

73. W. Berger: Paint Manufacture 1972 (11) 30

74. M.L. Ellinger: Paint Technology 1963 27 (12) 40

75. S. Wernick and R. Pinner: "Surface Treatment and Finishing of Aluminium and its Alloys" Robert Draper Ltd, England, 4th Ed, 1972

76. R.F. Ayres: Metal Progress 1960 78 (9) 101

77. C. Ries: Aluminium Rev 1975 51 393

78. S.J. Ketchem: "The Finishing of Aluminum", ed. G.H. Kissin Chapter 6, Reinhold 1963

79. N.J. Newhard: Metal Finishing 1972 76 No.7, 49: Metal Finishing 1972 76 No.8, 66

80. J.D. Edwards: Metal Industry 1942 61 103-5, 119-120

81. C.A. Kumins: Offic Dig Federation Soc Paint Technol 1962 34 843

82. J.D. Plumkett: NASA SP-5014 "Contributions to the Technology of Inorganic coatings" p.47, Washington DC 1964

84. O. Bauer and O. Vogel: German Patent 423,758 (1923)

83. H. Buff: Liebigs Ann Chem 1857 102 No.3, 265

85. G. Eckert: Wasser ü Abwasser 1932 29 282

86. G. Eckert: Aluminium 1937 19 606

87. F.J. Murphy: Tech proc Am Electroplaters Soc 1961 48 60

88. M. Schenk: "Werkstoff Aluminium ü Seine Anodische Oxidation" A. Francke AG, Berne 1948, 546-7

89. W. Helling and H. Neunzig: Chem Fabrik 1937 10 431

90. W. Helling and H. Neunzig: Aluminium 1938 20 536

91. Vereinigte Aluminium Werke A.G.: German Patent 691,903 (1937)

92. Vereinigte Aluminium Werke A.G.: German Patent 678,119 (1937)

93. F.P. Spruance and American Chemical Paint Company: US patent 2,438,877 (1945)

94. H.A. Katzman, G.M. Malouf, R. Bauer and G.W. Stupian: Application of Surface Science 1979 2 416

95. D.B. Freeman and A.M. Triggle: Trans IMF 1958 1960 37 56

96. L.A. Nimon and G.K. Korpi: Plating 1972 59 421

97. J.A. Treverton and N.C. Davies: Metals Technology 1977 4 480

98. W.G. Zelley: "Development of Improved Conversion Coatings for Aluminium Alloys" Final Report NAS8-11226, July 1966

99. H. Shapiro: "Restrictions on the use of chromate" Product Finishing 1968

100. A. Gallacio, F. Pearlstein and M. D'Ambrosio: Metal Finishing 1966 64 (8) 50

101. R.J. Sunderland: 6th Proc Int Vac Cong; Jap J Appl Phys 1974, Suppl 2, Pt 1, 347

102. J.A. Treverton and N.C. Davies: Surface and Interface Analysis 1981 3 194

103. R.F. Reeves and N.J. Newhard: Ind Heating 1969 36 705

104. M. Pourbaix: "Atlas of Electrochemical Equilibra in Aqueous Solutions" Translation from French by J.A. Franklin, Pergamon, 1966

105. M.F. Abd Rabbo, J.A. Richardson and G.C. Wood: Corrosion Science 1978 18 117

106. R.C. Furneaux, G.E. Thompson and G.C. Wood: Corrosion Science 1979 19 63

107. J.A. Treverton: Proc Int Conf "Production and Use of Coil-Coated Strip" 1981, The Metals Society

108. J.A. Treverton and M.P. Amor: Trans IMF 1982 60 92

109. T. Valand and G. Nilsson: Corrosion Science 1977 17 449

110. J.D. Venables, D.K. Macnamara, J.M. Chen, T.S. Sun, R.L Hopping: Application of Surface Science 1979 3 88

111. "Pretreatment for Metal" Alocrom 100; Information Sheet No. 4/1; ICI Paints Division

112. R.B. Mason and C.J. Shinder: Metal Finishing 1948 p65

113. E. Matijevic: Progress of Colloid & Polymer Science 1976 61 24

114. A.C. Zettlemoyer, M. Siddiq and F.J Micale: Journal of Colloid & Interface Science 1978 66 173

115. A. Bell and E. Matijevic: Journal of Physical Chemistry 1974 78 2621

116. J.E. Kolakowski and E. Matijevic: J Chem Soc Faraday Trans I. 1979 75 65

117. R.J. Kuo and E. Matijevic: J Chem Soc Faraday Trans I. 1979 75 2014

118. J.F. Murphy: The Finishing of Aluminum" Ed. G.H Kissin, Reinhold 1963, pp 68-90

119. G. Pope, E. Matijevic and C. Patel: Journal of Colloid and Interface Science 1981 80 74

120. G. Tolley: Metal Industry 1950 Dec 12th pg 255